

DEVELOPMENT OF NOVEL 3D *IN VITRO*
CELL MODELS FOR GENOTOXICITY
ASSESSMENT

Martina Štampar

Doctoral Dissertation
Jožef Stefan International Postgraduate School
Ljubljana, Slovenia

Supervisor:

Assist. Prof. Dr. Bojana Žegura, National Institute of Biology, Ljubljana, Slovenia

Evaluation Board:

Prof. Dr. Metka Filipič, Chair, Jožef Stefan International Postgraduate School and National Institute of Biology, Ljubljana, Slovenia

Prof. Dr. Lucija Peterlin Mašič, Member, Faculty of Pharmacy, University of Ljubljana, Ljubljana, Slovenia

Assist. Prof. Dr. Špela Baebler, Member, National Institute of Biology, Ljubljana, Slovenia

MEDNARODNA PODIPLOMSKA ŠOLA JOŽEFA STEFANA
JOŽEF STEFAN INTERNATIONAL POSTGRADUATE SCHOOL



Martina Štampar

DEVELOPMENT OF NOVEL 3D *IN VITRO* CELL
MODELS FOR GENOTOXICITY ASSESSMENT

Doctoral Dissertation

RAZVOJ NOVIH *IN VITRO* 3D CELIČNIH MODELOV
ZA DOLOČANJE GENOTOKSIČNOSTI

Doktorska disertacija

Supervisor: Assist. Prof. Dr. Bojana Žegura

Ljubljana, Slovenia, January 2021

To my beloved HepG2 cells, which have always grown diligently.

Acknowledgments

First, I would like to thank my supervisor, Assist. Prof. Dr. Bojana Žegura, for giving me the opportunity to be a part of the research group at the Department of Genetic Toxicology and Cancer Biology at the National Institute of Biology in Ljubljana. I am thankful for her valuable advice, professional lectures, discussions and support, as well as the motivation provided during my PhD training. Moreover, I would like to thank her for revising and correcting this thesis and all of my other manuscripts. I enjoyed being your student.

I would like to thank Prof. Dr. Metka Filipič, who is the head of the Department of Genetic Toxicology and Cancer Biology, for giving me the opportunity to work with her research group, for all the encouraging, positive advice, discussions, and financial support, as well as all the manuscript revisions she helped with during my PhD studies.

I would like to thank my GENious co-workers, especially Klara, Barbara B., Matjaž, Alja, Karmen, Tina, Jana, Bernarda, Mateja, Metka N., Katja, Barbara Ž. B., and Sonja, for their daily effort in creating a pleasant and friendly atmosphere in the office. They supported me with their great knowledge and skills, ideas, advice, motivational words, coffee time, laughs, and much more. I would also like to thank the FITO team for their support with their infallible knowledge and advice.

I am grateful to the members of the evaluation board, Prof. Dr. Metka Filipič, Assist. Prof. Dr. Špela Baebler, and Prof. Dr. Lucija Peterlin Mašič, for the revision of this doctoral dissertation.

I would also like to thank the research group from the Department of Biochemistry and Molecular Biology at the University of Southern Denmark, Odense, Denmark: Helle, Prof. Dr. Adelina Rogowska-Wrzesinska and Prof. Dr. Krzysztof Wrzesinski, who gave me the opportunity to work in their laboratory and made great contributions to the results published in this thesis.

The biggest thanks goes to my family for all the love and support you have shown me throughout these years, and to Miha – thank you for all your support, without which I would have stopped these studies a long time ago. You have been amazing, and I will now clear all the papers off the kitchen table as I promised.

Last but not least, I would like to thank my friends and all others who in one way or another shared their support and were a source of inspiration.

This doctoral dissertation was funded by the Slovenian Research Agency, the J1-2465 project, the ARRS Young Researcher Grant to MR-MStampar and by COST Action CA16119 (*In vitro* 3-D total cell guidance and fitness).

Abstract

The determination of genotoxicity is an important element in the safety assessment of various substances, with the purpose of preventing a number of chemicals from affecting human health. Genotoxicity testing is required for all classes of chemicals, drugs and biological agents, which can lead to a wide range of diseases, cancer included. In the last decades, there has been an ongoing shift towards developing new effective testing methods, since a single test is not sufficient for the detection of all relevant genotoxic aspects; consequently, a variety of complementary testing techniques and methodologies have to be used. In addition, increasing emphasis is given to alternative *in vitro* models, which focus on the genotoxic effects of chemicals and environmental contaminants, thereby contributing to the reduction of animals used in preclinical testing.

In toxicology, hepatocellular two-dimensional (2D) cell models are being conventionally used for determining the damaging effects of chemicals *in vitro*. Nevertheless, there is a demand for new approaches as currently existing models often yield misleading results because they lack expressions of important metabolic enzymes. In this respect, newly developed *in vitro* three-dimensional (3D) cell-based models are gaining importance as they more realistically imitate the *in vivo* cell behavior. In the *in vitro* conditions 3D models give more accurate results compared to 2D cultures; as such, they offer an attractive alternative to animal testing. Even though 3D cell models are better than 2D cell models, they lack standardization, in particular in terms of cultivation protocols and adequate characterization, which prevent their general use in the field of genotoxicity.

This thesis aims to validate and optimize an approach for testing the genotoxic activity of chemicals on a hepatocellular *in vitro* 3D cell model (spheroid) developed from a human hepatocellular carcinoma (HepG2 and HepG2/C3A) cell line by the forced floating method and cultured in a dynamic bioreactor (CelVivo BAM/bioreactor) system. We showed that the newly developed 3D cell models better illustrate *in vivo* conditions than traditional monolayer cell cultures, since they have improved cell-matrix and cell-cell interactions, as well as preserved *in vivo* cell phenotypes. Moreover, we showed decreased proliferation over the cultivation period and a higher expression of liver-specific functions and genes encoding phase I and II metabolic enzymes in 3D models compared to 2D models.

In the present study, we applied novel hepatocellular *in vitro* 3D models cultured under static and dynamic conditions for the assessment of cytotoxicity and genotoxicity of xenobiotic compounds. Compared to 2D cell models the applied *in vitro* 3D cell models showed increased stability and viability, thus enabling long-term exposures, which is particularly important in studying genotoxic compounds at lower concentrations, to which humans are exposed in everyday life. Moreover, transcriptomic analyses revealed that 3D cell models express genes related to metabolism and characteristic of hepatic cells to a higher extent than 2D models, showing a higher sensitivity to the detection of indirect-acting genotoxic compounds.

We believe that the newly developed hepatocellular 3D cell models, due to their more complex structure and improved metabolic capacity, provide a suitable experimental model for genotoxicity studies as well as the regulatory testing of new chemicals and products.

Despite that, 3D cell models must be further characterized and validated in terms of cell division and response to genotoxic stress in order to better know their behavior and properties. The 3D models have the potential to bridge the gap between *in vitro* and animal studies.

Povzetek

Ocena genotoksičnosti je pomemben element pri določanju varnosti najrazličnejših snovi, in sicer z namenom, da bi preprečili vpliv številnih kemikalij na zdravje ljudi. Zato je testiranje genotoksičnosti potrebno za vse razrede kemikalij, zdravil in bioloških dejavnikov, ki lahko privedejo do številnih bolezni, vključno z rakom. Posledično se v zadnjih desetletjih vedno bolj spodbuja razvoj novih učinkovitih metod testiranja, saj en sam test ne zadostuje za odkrivanje vseh pomembnih genotoksičnih učinkov; zato je torej za testiranje potrebno uporabiti različne komplementarne tehnike in metodologije. Poleg tega je vse večji poudarek na alternativnih *in vitro* modelih, ki se osredotočajo na genotoksične učinke kemikalij in onesnaževalcev okolja ter tako znatno prispevajo k zmanjšanju števila živali, ki se uporabljajo v predkliničnih testiranjih.

Trenutno se za ugotavljanje škodljivih učinkov kemikalij uporabljajo tradicionalni *in vitro* dvodimenzionalni (2D) modeli jetrnih celic. Pojavlja pa se vedno večje povpraševanje po novih pristopih, kar pomeni, da je treba trenutno obstoječe modele izboljšati in nadgraditi, saj pogosto dajejo lažno pozitivne rezultate, kar je posledica manjka pomembnih presnovnih encimov v celicah teh modelov. Zaradi tega se povečuje pomembnost novo razvitih *in vitro* tridimenzionalnih (3D) celičnih modelov, ki bolj realistično posnemajo vedenje celic *in vivo* in dajejo natančnejše rezultate v pogojih *in vitro* v primerjavi z 2D kulturami. Tako novo razviti 3D celični modeli predstavljajo privlačno alternativo poskusom na živalih. Čeprav imajo 3D celični modeli veliko boljših lastnosti od tradicionalnih 2D celičnih modelov, jih je za nadaljnjo uporabo treba standardizirati. Predvsem je treba prilagoditi protokole gojenja in jih ustrezno okarakterizirati, kar bo omogočilo njihovo vsesplošno uporabo na področju genetske toksikologije.

Cilj doktorske disertacije je validirati in optimizirati metodo za testiranje genotoksične aktivnosti kemikalij na jetrnem *in vitro* 3D celičnem modelu (sferoid), ki smo ga razvili iz dveh človeških hepatocelularnih karcinogenih celičnih linij (HepG2 in HepG2/C3A) z metodo, ki uporablja centrifugalno silo za nastanek sferoidov ter gojenjem sferoidov v statičnem sistemu in v dinamičnem biorektorskem (CelVivo BAM/bioreaktor) sistemu. Pokazali smo, da novo razviti 3D celični modeli boljše posnemajo pogoje *in vivo* kot tradicionalne 2D celične kulture, saj imajo tako izboljšane povezave med celicami in matriksom ter med samimi celicami kot tudi ohranjen *in vivo* fenotip celic. Pokazali smo, da se v novih jetrnih 3D modelih proliferacija celic zmanjšuje s časom gojenja, v primerjavi z 2D modeli pa je povečano izražanje jetrno specifičnih funkcij in genov, ki kodirajo presnovne encime faze I in II.

V doktorski disertaciji smo nove jetrne *in vitro* 3D modele, gojene v statičnih in dinamičnih pogojih, uporabili za oceno citotoksičnosti in genotoksičnosti modelnih telesu tujih spojin. V primerjavi z 2D modeli so 3D modeli pokazali večjo stabilnost in živost celic. Z izraženimi lastnostmi 3D modeli omogočajo proučevanje dolgodobne izpostavljenosti različnim spojinam. Pomembnost tega se kaže pri preučevanju genotoksičnih spojin pri nižjih koncentracijah, ki smo jim ljudje vsakodnevno izpostavljeni. Poleg tega so analize na transkriptomski ravni pokazale, da 3D celični modeli izražajo gene,

ki so povezani z metabolizmom in lastnostmi jetrnih celic, v večji meri kot 2D modeli, kar kaže na večjo občutljivost za odkrivanje posredno delujočih genotoksičnih spojin.

Z raziskavami smo pokazali, da novo razviti 3D modeli jetrnih celic zaradi svoje bolj zapletene strukture in izboljšane presnovne sposobnosti zagotavljajo primeren eksperimentalni model za študije genotoksičnosti in regulatorno testiranje novih kemikalij in izdelkov. Kljub temu pa je potrebno 3D celične modele nadalje opredeliti in preveriti obnašanje glede delitev celic in odziva na genotoksični stres, da bi bolje poznali vedenje in lastnosti celic v 3D modelu. Novi jetrni 3D modeli nakazujejo možnost premostitve vrzeli med raziskavami *in vitro* in študijami na živalih.

Contents

List of Figures	xv
List of Tables	xvii
Abbreviations	xix
1 Introduction	1
1.1 Genotoxicity Risk Assessment to Protect Human and Animal Health	1
1.2 Xenobiotics	2
1.3 Hepatocellular Cell Models in Genotoxicity Studies	2
1.3.1 Two-dimensional (2D) cell models.....	2
1.3.1.1 Primary human hepatocytes (PHH).....	3
1.3.1.2 Hepatocarcinoma-derived cell lines.....	4
1.3.2 Three-dimensional (3D) cell cultures.....	5
1.3.2.1 A systematic overview of the field.....	5
1.3.2.2 Hepatocellular 3D cell models – spheroids.....	7
1.3.2.3 Techniques for forming spheroids	9
1.3.2.4 Hepatocellular 3D models in toxicology.....	9
1.4 Scientific Problems and Aims of the Thesis.....	10
1.5 Research Hypotheses.....	12
1.6 Publications Included and the Candidate's Contributions.....	13
2 Scientific Publications	15
2.1 Characterization of In Vitro 3D Cell Model Developed from Human Hepatocellular Carcinoma (HepG2) Cell Line.....	15
2.2 Development of In Vitro 3D Cell Model from Hepatocellular Carcinoma (HepG2) Cell Line and its Application for Genotoxicity Testing	36
2.3 HepG2 Spheroids as a Biosensor-Like Cell Based System for (Geno)toxicity Assessment (Submitted)	50
2.4 Application of Advanced HepG2 3D Cell Model for Studying Genotoxic Activity of Cyanobacterial Toxin Cylindrospermopsin	72
2.5 A Toolbox for Separation of Spheroids into Core and Rim Fractions or Viable Single Cell Suspension and their Downstream Applications	84
2.6 Hepatocellular Carcinoma (HepG2/C3A) Cell-Based 3D Model for Genotoxicity Testing of Chemicals.....	110
3 Discussion and Conclusions	123
Appendix A Supplementary Material of Included Publications	125
A.1 Supplementary Material of Publication 2.1.....	125
A.2 Supplementary Material of Publication 2.2.....	126
A.3 Supplementary Material of Publication 2.3.....	127

References	131
Bibliography	141
Biography	143

List of Figures

Figure 1.1: The effect of changing the cells grown into an <i>in vitro</i> 2D (monolayer) cell model. Over the time of cultivation, the cells adopt a flattened morphology.....	3
Figure 1.2: The number of publications (left) and the number of citations per year (right) on 3D models, showing an increased interest in applying hepatocellular 3D cell models....	6
Figure 1.3: Groups of journals in the field of hepatocellular 3D cell cultures. The results were obtained using bibliometric coupling (VOSviewer). Each colour assigned by the VOSviewer software represents a different cluster. The blue cluster represents journals that are focused on the biochemical engineering and the engineering of organs and tissues from a hepatocellular source. The green cluster represents journals focused on biomaterials, while red cluster represents journals concerning cancer biology and stem cell applications and yellow cluster stands for journals focused on (geno)toxicology research, pharmaceutical applications and the metabolism of xenobiotics.....	7
Figure 1.4: The effect of changing the cells grown in an <i>in vitro</i> 3D (spheroid) model. The presence of an ECM allows the cells to maintain a 3D structure and organization.....	8
Figure 1.5: A map of the usual zones of cell proliferation in a three-dimensional spheroid, where the models of oxygenation, nutrition, and CO ₂ removal are shown.....	8
Figure 1.6: Clusters of publications using hepatocellular 3D cell models in the field of toxicology. Each colour assigned by the VOSviewer software represents a different cluster. The blue cluster represents publications describing hepatocellular 3D cell models in ecotoxicological and environmental studies and pharmacological studies. The green cluster represents publications describing the application and use of new 3D models for accurate risk assessment and environmental health, for (geno)toxicity assessment as an alternative to monolayer culture. The red cluster represent publications describing the <i>in vitro</i> drug-induced responses, long-term induced hepatotoxicity, xenobiotic metabolism, and repeated dose toxicity.....	10

List of Tables

Table 1.1: Properties/characteristics of hepatocarcinoma-derived cell lines presented as advantages and disadvantages.....	4
--	---

Abbreviations

2D	...	Two-dimensional
3D	...	Three-dimensional
3R	...	Strategy which supports the Replacement, Reduction and Refinement of animal models in preclinical testing
AFB1	...	Aflatoxin B1
ATP	...	High-sensitivity Adenosine Triphosphate
B(a)P	...	Benzo(a)pyrene
CYN	...	Cylindrospermopsin
CYP 450	...	Cytochromes P450
DNA	...	Deoxyribonucleic acid
EFSA	...	European Food Safety Authority
ET	...	Etoposide
HepG2, C3A, HepaRG, HuH6	...	Hepatocellular carcinoma-derived human cell lines
IQ	...	2-amino-3-methylimidazo[4,5-f]quinoline
mRNA	...	Messenger ribonucleic acid
MTS	...	3-(4,5-dimethylthiazol-2-yl)-5-(3-carboxymethoxyphenyl)-2-(4-sulfophenyl)-2Htetrazolium
OECD	...	The Organisation for Economic Co-operation and Development
PHH	...	Human primary hepatocytes
PhIP	...	2-Amino-1-methyl-6-phenylimidazo[4,5-b]pyridine
qRT-PCR	...	Quantitative real-time polymerase chain reaction
REACH	...	Registration, Evaluation, Authorisation and Restriction of Chemicals
ROS	...	Intracellular reactive oxygen species
γ H2AX	...	Histone H2A variant X phosphorylated at Serine 139

Chapter 1

Introduction

1.1 Genotoxicity Risk Assessment to Protect Human and Animal Health

The determination of genotoxicity is an important part of the safety assessment of multiple types of products, including industrial chemicals, pesticides, pharmaceuticals, food additives, cosmetics and veterinary drugs, with the purpose to protect human, animal and environmental health (Corvi & Madia, 2017; Jacobs et al., 2020). This is particularly important due to the increased number of chemicals with limited toxicological data to which humans are potentially exposed (Claxton et al., 2010). A very important toxicity mechanism is damage to the genetic material, particularly when considering the carcinogenicity of chemical substances (Guo et al., 2019). The induced DNA damage when not repaired, lead to irreversible damage, such as gene mutations and chromosome aberrations that can be transmitted to the next generation when it occurs in germ cells.

For a sufficient assessment of genotoxic effects, three important endpoints need to be evaluated (structural chromosome aberrations, gene mutation and numerical chromosome aberrations) and the following procedure is estimated stepwise, starting with a cascade of short-term *in vitro* genotoxicity tests endorsed by several international organizations (OECD, IHC etc.) (Corvi et al., 2013). If a compound is positive in one or more of these basic tests, further *in vitro* mechanistic studies are performed, followed in specific cases by *in vivo* testing (Corvi & Madia, 2017; Kirkland et al., 2007) to determine the health risk for humans (Kirkland et al., 2005). At this time, genotoxicity assays are conducted on metabolically non-competent rodent or human cell lines (human lymphoblast cells (TK6), mouse lymphoma cells (L5178Y) or Chinese hamster lung cells (V79)), meaning that an increased number of compounds is subject to earlier and often unnecessary *in vivo* genotoxicity testing (Fowler et al., 2012; Watson et al., 2014).

Although many of these *in vitro* assays are being used successfully to predict genotoxicity, they cannot fully replace animal tests, which are currently used to assess the safety of substances (Corvi et al., 2013). Furthermore, Kirkland et al. (2005, 2006; Kirkland and Speit, 2008) questioned the specificity of these tests in a series of articles. The above-mentioned limitations and misleading positive results signal the necessity to develop improved three-dimensional (3D) human models that are more relevant in regards to *in vivo* conditions and could be considered as a practical alternative (Saleh & Genever, 2011). Moreover, the 3R strategy (reduce, replace, refine) employed by EU REACH (Registration, Evaluation, Authorization and restriction of Chemicals) focuses on the reduction and optimization of the use of animals for *in vivo* testing (Corvi & Madia, 2017; Pfuhler et al.,

2009) and highlights the need for the development of new cell-based *in vitro* models that can more realistically mimic *in vivo* cell behavior and can provide more reliable results compared to 2D conditions.

1.2 Xenobiotics

Xenobiotics are chemical compounds (plant ingredients, drugs, pesticides, cosmetics, flavorings, food additives, industrial chemicals and environmental pollutants) present in living organisms but foreign to them, meaning that they do not appear within the normal metabolic pathways (Park et al., 2014). The majority of these chemical compounds enter the body through one's diet, drinking water, air, and drug administration, they are usually present in higher-than-normal concentrations and later encounter a large set of detoxification processes (Patterson et al., 2010). Drug metabolism or xenobiotic metabolism is a biochemical modification of xenobiotics supported by metabolic enzymes to enable excretion hydrophilic products in living organisms. The process has three phases: i) Phase I, enzymes (cytochrome P450 oxidases) introduce reactive or polar groups into xenobiotics; ii) Phase II, the modified compounds are conjugated to polar compounds catalyzed by transferase enzymes; iii) Phase III, the conjugated xenobiotics are further processed, and in the next step recognized by efflux transporters and pumped out of cells (Patel & Jyoti Sen, 2013). Organic xenobiotics that induce a damaging effect or toxicity can be classified into two types, i.e. direct-acting and indirect-acting compounds (Mackowiak & Wang, 2016; Patel & Jyoti Sen, 2013). Direct-acting xenobiotics are electrophilic and can directly react with a biomolecules to produce toxic effect. On the other hand, indirect-acting chemicals are not primarily reactive, so they require an activation step into reactive electrophilic intermediate. In general, the majority of environmental pollutants are indirect-acting (Park et al., 2014).

1.3 Hepatocellular Cell Models in Genotoxicity Studies

1.3.1 Two-dimensional (2D) cell models

Harrison developed the cell culturing process in 1907 during his investigation into the source of nerve fibres (Harrison et al., 1907). Later on, major improvements were made to the 2D cell culture technique, such as the development of culture flasks, blood plasma as the source of nutrition was supplemented by a synthetic medium and the development of antibiotics and antifungals that are appropriate for cell cultures (Breslin & O'Driscoll, 2013).

The standard toxicological approach to evaluating toxicity requires complex *in vivo* studies. Due to concerns about animal wellbeing and the recommendations of the 3R strategy, the development of suitable *in vitro* culture systems has become a priority in toxicology research (Soldatow et al., 2013). The liver is the main organ involved in the metabolism of various xenobiotics in which the detoxification process usually takes place, meaning that some nontoxic compounds might be converted into toxic intermediates (Hinson et al., 2010). The main function of a hepatocellular *in vitro* model is to be able to

detect relevant endpoints, in particular assessing the toxicity of novel xenobiotic compounds (Kyffin et al., 2018).

Traditionally, *in vitro* cell cultures are typically grown as a monolayer (2D) on a flat surface, most frequently in culture flasks or, occasionally, in Petri-dishes, which enables cell-to-cell contact only at their periphery. As a result, cells are forced into a monolayer morphology rather than piling on top of one another, which allows the cells to receive a homogenous amount of nutrients and growth factors from the medium (Antoni et al., 2015; Edmondson et al., 2014; Wrzesinski & Fey, 2015). The cells cultured in 2D systems can often proliferate more rapidly than in the *in vivo* conditions, and more cells are synchronized in the same point of the cell cycle, as necrotic cells are usually detached from the surfaces and can be easily removed through a change of the medium (Antoni et al., 2015; Edmondson et al., 2014; Fey & Wrzesinski, 2012; Hoffman, 1993; Kyffin et al., 2018). Cells grown in monolayer conditions are generally flattened and stretched, which would not appear *in vivo* (Figure 1.1) (Tibbitt & Anseth, 2009). Moreover, many cellular processes, including cell differentiation, proliferation, apoptosis, as well as gene and protein expression, can be affected by the unnatural cell morphology in the 2D culture compared to *in vivo* models (Kyffin et al., 2018; Smith et al., 2012). Consequently, 2D cultured cells may not adequately mimic the *in vivo* microenvironment and can therefore unmorally respond to toxic insult, which then lead to misleading results.



Figure 1.1: The effect of changing the cells grown into an *in vitro* 2D (monolayer) cell model. Over the time of cultivation, the cells adopt a flattened morphology (Reprocell USA, 2020).

1.3.1.1 Primary human hepatocytes (PHH)

It is generally accepted that human primary hepatocytes (PHH) serve as the gold standard for metabolic and toxicity studies. This is due to their human origin and the expression of phase I and II metabolic enzymes relevant to the human metabolism of xenobiotic and other characteristics, such as the expression of liver-specific transporters, ammonia detoxification, glucose metabolism, as well as albumin production and urea secretion (Fey & Wrzesinski, 2012; Godoy et al., 2013; Harris et al., 2004; Kyffin et al., 2018; LeCluyse, 2001).

Nevertheless, there are serious drawbacks related to the application of isolated PHH *in vitro*. These include: complex isolation and culturing of cells, inability to expand, rapid dedifferentiation and loss of the hepatic phenotype, genetic and metabolic differences due to the polymorphism of donors often present in the metabolic enzymes, limited availability and high costs related to the performance of the experiments. As a consequence of these limitations, PHH are not suitable for routine use for genotoxicity testing, so a lot of research has shifted towards using hepatocellular-derived cell lines and other alternatives (Drewitz et al., 2011; Dvorak, 2016; Kyffin et al., 2018; Otto et al., 2008).

1.3.1.2 Hepatocarcinoma-derived cell lines

In recent decades, test systems with hepatocellular carcinoma-derived human cell lines, such as HepG2, C3A, HepaRG, HuH6, and many others (Table 1.1), which are easily assessable, have a high reproducibility of results, and the preserved activity of certain metabolic enzymes *in vitro*, have been introduced to routine genotoxicity testing (Donato et al., 2015; Guillouzo et al., 2007; Shah et al., 2018; Waldherr et al., 2018; Wrzesinski & Fey, 2013). The aforementioned cells are a good compromise between ease of culturing and the expression of several important enzymes involved in xenobiotic metabolism (Bazou et al., 2008; Nakamura et al., 2011; Wilkening et al., 2003) as they possess several phenotypic characteristics and the nuclear transcription factor (Nrf2) expression. This is of great importance for drug metabolism and toxicity response, as well as some functional properties of hepatocellular cells (Duret et al., 2007; Hurrell et al., 2019).

Nonetheless, the crucial limitations while using these cell lines cultured in 2D are the low expression of CYP450 enzymes, xenobiotic receptors, and phase II enzymes (Chang & Hughes-Fulford, 2009; Kyffin et al., 2018). As a result, liver cell functions *in vivo* are not adequately expressed. Therefore, such cell models may produce misleading toxicological data which leads to unnecessary follow-up animal testing (Gerets et al., 2012). The above-mentioned limitations have led to the development and optimization of new alternative three-dimensional (3D) cell models, which more closely mimic *in vivo* conditions and give more promising results regarding human exposure, although 3D models have still not replaced two-dimensional (2D) models on a large scale.

Table 1.1: Properties/characteristics of hepatocarcinoma-derived cell lines presented as advantages and disadvantages.

Cell lines (2D models)	Properties/characteristics
HepG2	<ul style="list-style-type: none"> -Nuclear transcription factor (Nrf2) expression (Ishikawa et al., 2013); -Wild-type tumor suppressor TP53 expression (Lee & Park, 2015); -Availability (Castell et al., 2006); -Growth without limitation and the lack of inter-donor variation ensuring reproducible results (Castell et al., 2006); -Simple handling with easy culture protocols (Jennen et al., 2010). <hr/> <ul style="list-style-type: none"> -The phenotype of <i>in vivo</i> hepatocytes is not completely represent; -Many phase I and II enzymes are not sufficiently expressed (Jennen et al., 2010); -The assessment of many genotoxic compounds utilizing the HepG2 cell line is inaccurate (Castell et al., 2006).
HepG2/C3A (a subclone)	<ul style="list-style-type: none"> -More advantageous characteristics are demonstrated compared to the parent HepG2 cells (Fey & Wrzesinski, 2012); -Express wild-type tumor suppressor TP53 (Lee & Park, 2015); -A more reflective model for hepatotoxicity studies (Fey & Wrzesinski, 2012); -Contact-inhibited growth characteristics: increased alpha-fetoprotein and albumin production, ability to proliferate and thrive in glucose-deficient media (Fey & Wrzesinski, 2012); -More differentiated and have a more metabolically active hepatocellular phenotype in comparison with the parent HepG2 cell line (Nelson et al., 2017).

HepaRG

-
- When grown as 2D, they showed low functionality and an altered phenotype compared to human hepatocytes *in vivo* (Gaskell et al., 2016);
 - Low CYP activity and poor sustainability (Nelson et al., 2017).
-
- Hepatocellular carcinoma-derived cell line;
 - Express wild-type tumor suppressor TP53 (Jennen et al., 2010);
 - Several phase II enzymes and membrane transporters are expressed which are comparable to freshly isolated or cultured primary human hepatocytes (Jennen et al., 2010),
 - An undifferentiated morphology acquires when seeded at a low density (Mandon et al., 2019);
 - Improved CYP450 expression together with a better liver-specific functionality (Mandon et al., 2019);
 - More sensitive to expression of phase I and II enzymes when compared with HepG2 cells (Kyffin et al., 2018).
-
- Require long culture procedure (cost and time consuming) (Kyffin et al., 2018);
 - Availability to all researchers is limited (Mandon et al., 2019);
 - Derived from an individual with poor alleles for CYP2D6, CYP3A5 and CYP2C9 (Kammerer & Küpper, 2018);
 - 2D cultures of HepaRG cells do not have urea production pathway (Lübberstedt et al., 2011);
 - The liver metabolizing function are represent of only one single donor (Kammerer & Küpper, 2018).
-

1.3.2 Three-dimensional (3D) cell cultures

1.3.2.1 A systematic overview of the field

When culturing the cells in 3D systems, they form aggregates and spheroids (Figure 1.4) (Mehta et al., 2012). The use of 3D models has significantly increased over the past decade, as novel preclinical test systems and as alternatives to animal testing due to a growing desire to implement the 3R strategy in research (Augustyniak et al., 2019; Bahinski et al., 2014; Pfuhler et al., 2020). The relevance of developing new advanced *in vitro* models is also highlighted in the European chemical safety legislation's REACH program (Registration, Evaluation, Authorisation and Restriction of Chemical substances (2007/2006)), as they decrease both the cost and the time for hazard characterization and risk assessment.

In order to provide a quantitative systematic review of research on hepatocellular 3D models, and specifically hepatocellular 3D models in human toxicology, we conducted a bibliometric analysis, which allowed us to identify the most significant publications, authors, journals and countries in the field of 3D models. To do so, we first collected bibliographic and citation data from the Web of Science core collection using the appropriate operators OR and AND, as well as the following search terms: "3D cell model," "3D cell culture," "three-dimensional cell model," "three-dimensional cell culture," "spheroid," "hepatocyte," "liver," "HepG2," and "*in vitro*". Our search yielded 1535 publications analyzing hepatocellular 3D models.

A quick overview of the dataset reveals that the three oldest published papers stem from 1991. The number of publications gradually increased from 3 in 1991 to 41 in 2008. In the last couple of years, the field started growing exponentially, from 97 published articles in 2015 to 178 and 166 published articles in 2018 and 2019, respectively (Figure 1.2). These results suggest that the research field studying hepatocellular 3D models is relatively young. Furthermore, the number of citations increased even more, from 3109 in 2014 to 6050 citations in 2018. This exponential increase in research activity shows the importance of and interest in applying and developing hepatocellular 3D cell models. In the last 5 years, the research field has also become substantially globalized. A map of countries publishing articles on hepatocellular 3D models reveals that research is conducted on nearly all continents in the world. The main leader in the research field is the USA with 508 published articles, followed by China (286), Japan (266) and Germany (179).

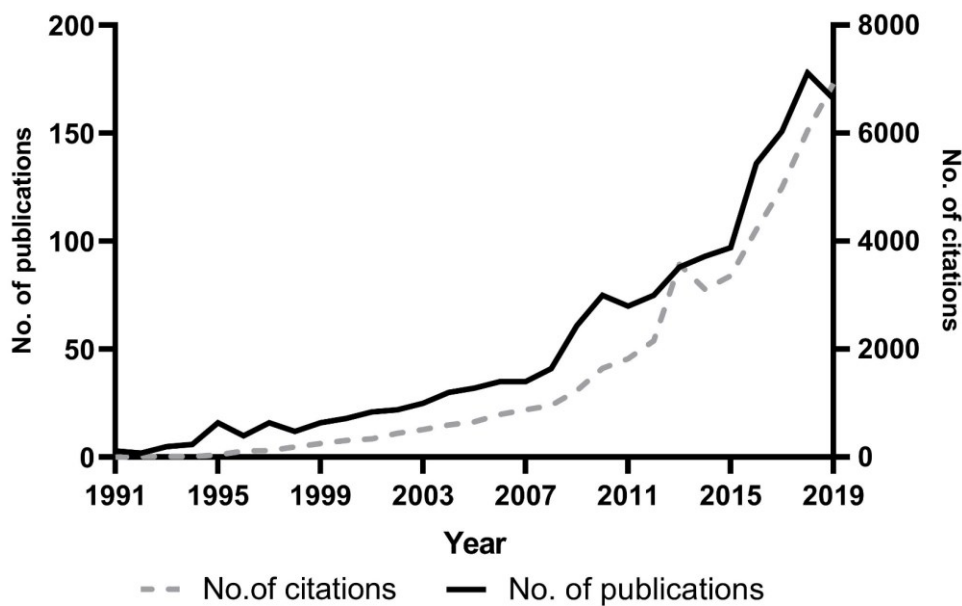


Figure 1.2: The number of publications (left) and the number of citations per year (right) on 3D models, showing an increased interest in applying hepatocellular 3D cell models.

To get a better grasp of the structure of the research field we used bibliographic coupling, which was introduced by Kessler in 1963 and connects authors, publications and journals based on the number of citations they share (Dominko & Verbič, 2019). Using this approach, we utilized the VOSviewer software package to form and visualize clusters (for a thorough discussion see Eck and Waltman (2010)). VOSviewer forms a map in three steps. First, it requires a similarity matrix as input and uses the proximity index to normalize it. Second, it uses the similarity matrix obtained in the first step to construct a map. Items with a higher degree of similarity are located closer to one another by minimizing the weighted sum of the squared Euclidean distances between all item pairs. Third, it performs three different types of transformations, specifically translation, rotation and reflection, in order to produce consistent results.

The map of the most important journals (Figure 1.3) allows us to disentangle the structure of the research field on hepatocellular 3D models. We see four different clusters of journals. The blue cluster generally represents journals that are focused on the biochemical engineering of hepatocellular 3D cell models and the engineering of organs and tissues from a hepatocellular source. The green cluster is strongly connected with the blue

cluster and contains journals that deal with biomaterials. The red cluster of journals is interested in topics that concern cancer biology and stem cell applications and development. The smaller yellow cluster of journals addresses the connection between (geno)toxicology research, pharmaceutical applications and the metabolism of xenobiotics. The leading journals in the “engineering” cluster are *Biotechnology and Bioengineering*, *Tissue Engineering Part A*, *Artificial Organs* and *Tissue Engineering*. Furthermore, the leading journals in the “biomaterials” cluster are *Biomaterials*, *Scientific Reports* and *Acta Biomaterialia*. In the “cancer biology” cluster, the leading journals are *PLOS One* and *Cell Biology*, while in the “(geno)toxicology” cluster, *Toxicology in Vitro* and *Archives of Toxicology* are the leading ones. We can observe numerous connections between the journals indicating a higher degree of interactions between clusters, meaning that there are some strong connections, most notably between journals in the “engineering” cluster and journals in the “biomaterials” cluster, as well as journals in the “biomaterials” and “(geno)toxicology” clusters. We can also observe that hepatocellular 3D models are gaining importance in journals concerned with toxicology.

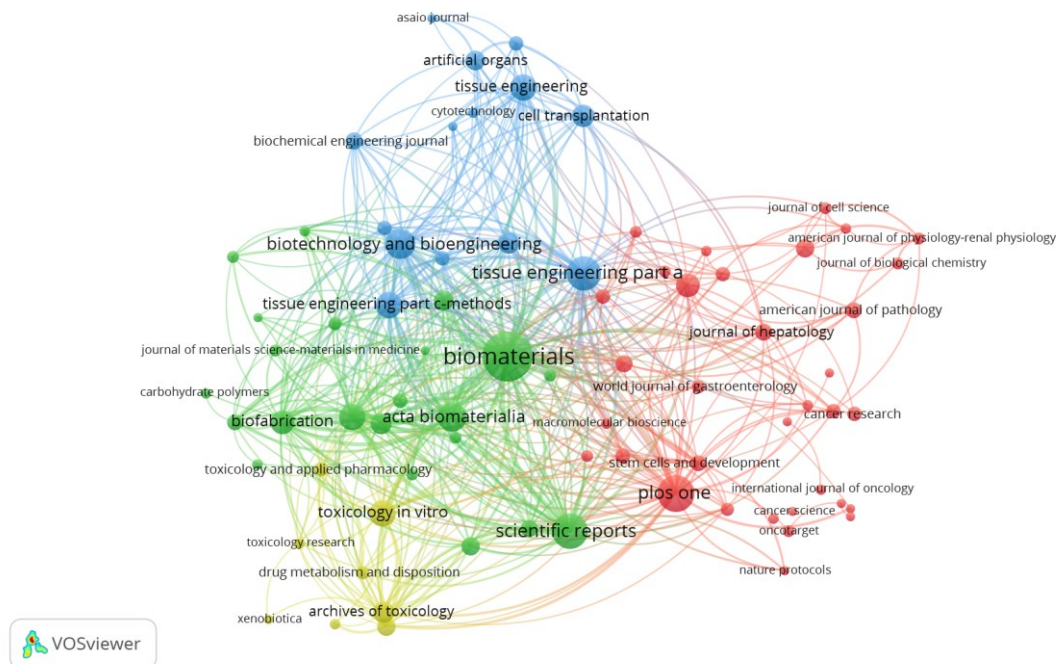


Figure 1.3: Groups of journals in the field of hepatocellular 3D cell cultures. The results were obtained using bibliometric coupling (VOSviewer). Each colour assigned by the VOSviewer software represents a different cluster. The blue cluster represents journals that are focused on the biochemical engineering and the engineering of organs and tissues from a hepatocellular source. The green cluster represents journals focused on biomaterials, while red cluster represents journals concerning cancer biology and stem cell applications and yellow cluster stands for journals focused on (geno)toxicology research, pharmaceutical applications and the metabolism of xenobiotics.

1.3.2.2 Hepatocellular 3D cell models – spheroids

Spheroids are 3D spherical cellular structures representing one of the most common way to culture cells in 3D (Figure 1.4) (Mehta et al. 2012). Spheroids contain cells in different

stages, which often comprises proliferating, quiescent, apoptotic, hypoxic, and necrotic cells (Kim, 2005). Because of the more natural 3D shape, cell-cell interactions and cell-extracellular matrix interactions that appear in spheroids more accurately imitate the natural *in vivo* environment and create a complex microenvironment (Elje et al. 2019; Godoy et al. 2013; Mandon et al. 2019; Pfuhler et al. 2020; Shah et al. 2018; Štampar et al. 2019; Wrzesinski and Fey 2013). Due to the 3D environment, cell growth is undisturbed in comparison to 2D models, as regular trypsinization is not needed (Wrzesinski et al., 2014; Wrzesinski & Fey, 2013).

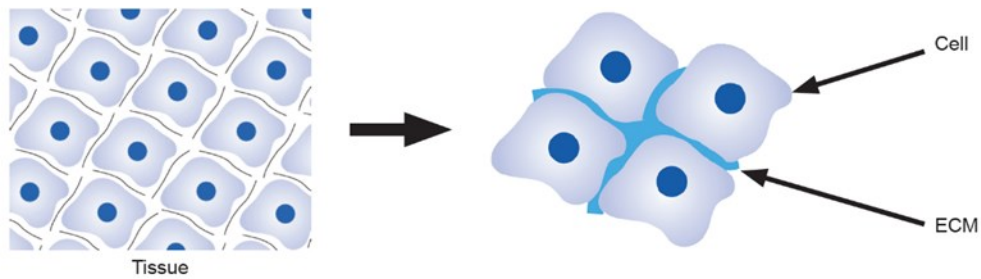


Figure 1.4: The effect of changing the cells grown in an *in vitro* 3D (spheroid) model. The presence of an ECM allows the cells to maintain a 3D structure and organization (Reprocell USA, 2020).

Spheroids provide a closer depiction of cell polarization, while in a two-dimensional form (monolayer) the cells are only partially polarized (Breslin & O’Driscoll, 2013). Spheroids are usually comprised of three main zones: i) an outer proliferating rim, ii) an inactive viable zone, and iii) an inner necrotic core, which can occur because of the lower diffusion of nutrients and oxygen creating hypoxic conditions (Asthana & Kisaalita, 2012; Mehta et al., 2012; Wrzesinski et al., 2014) (Figure 1.5). This kind of cellular heterogeneity is remarkably similar to *in vivo* tissues (Mehta et al., 2012).

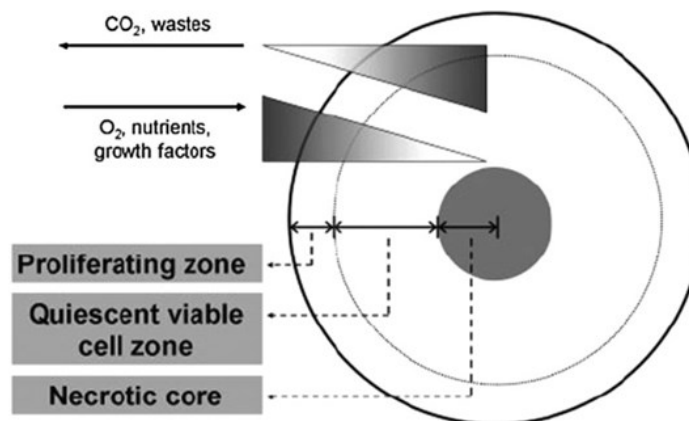


Figure 1.5: A map of the usual zones of cell proliferation in a three-dimensional spheroid, where the models of oxygenation, nutrition, and CO₂ removal are shown (Edmondson et al., 2014).

An additional important advantage of hepatocellular 3D cell models compared to 2D cell models is that they enable prolonged exposures due to their increased stability since they retain a high cell viability and stable morphology over several weeks (Bell et al., 2016). Finally, through an analysis of gene expression, microRNA abundance and metabolic profiles, it has been demonstrated that spheroids have a phenotype significantly more

relevant to *in vivo* as compared to 2D monolayer cultures (Smith et al., 2012; Štampar et al., 2019; Wrzesinski et al., 2014).

1.3.2.3 Techniques for forming spheroids

In order to produce *in vivo*-like structures, several static and perfusion techniques for culturing 3D cell models (spheroids) have been studied. These include non-adhesive surfaces, spinner flasks, hanging drop cultures, bioreactors, and micro-moulding (Breslin & O'Driscoll, 2013; Fey & Wrzesinski, 2012; Ravi et al., 2015). Although these techniques, which we detail below, offer several advantages, many of them are expensive, technically challenging, and require appropriate facilities (Shah et al. 2018). Two relatively simple methods for generating 3D spheroids are the forced floating method (Ivascu & Kubbies, 2006) and the hanging drop method (Kelm et al., 2003). The advantages of both methods are that they are easy to handle, are generally reproducible, the produced spheroids are densely packed rather than loose cell aggregates, and they show low variability in size (Breslin & O'Driscoll, 2013). Particularly when using the forced floating method, the generated spheroids are easily accessible for experimentation on single spheroids. In addition, the method is compatible with high-throughput drug testing since these spheroids are usually generated in a 96- or 384- well plate, which facilitates the production of large numbers of morphologically homogenous spheroids (Ivascu & Kubbies, 2006). The more advanced techniques are dynamic-based approaches for the creation of spheroids, which can be split into two categories: (i) spinner flask bioreactors (Jong, 2005) and (ii) rotating bioreactors (Fey & Wrzesinski, 2012; Goodwin et al., 1993). In general, the formed spheroids are placed into a bioreactor and the content is kept in motion, that is, either gently stirred or the container is rotated. The rotation creates a flow of media around the spheroids, resulting in a higher diffusion of nutrients and oxygen into the spheroids and preventing the formation of a necrotic core (Breslin & O'Driscoll, 2013; Fey & Wrzesinski, 2012; Gong et al., 2015).

1.3.2.4 Hepatocellular 3D models in toxicology

The branch of research concerning the use of hepatocellular *in vitro* 3D models in the field of genotoxicity is still relatively young. While at first hepatocellular 3D cell models were mostly used for drug development, extensive improvement has recently been made to the development of 3D cell models used for studying genotoxic effects, for instance chromosomal instability (Shah et al. 2018) and DNA damage (Elje et al. 2019; Mandon et al. 2019; Štampar et al. 2019) induced by chemicals and environmental samples (Hercog et al., 2020). For this purpose, progress in the establishment of robust protocols has been made for skin, airway and liver tissue equivalents (Basu et al., 2020; Pfuhler et al., 2020). Even so, the integration of *in vitro* 3D cell culture models is prevented by the lack of protocol standardization and insufficient characterization of the spheroids. An analysis of publications describing the application of 3D models in toxicology using bibliographic coupling confirms that their use for the purpose of toxicity testing is fairly new. Furthermore, Figure 1.6 shows that these publications can be found in three distinct clusters, each of which investigates different aspects of using hepatocellular 3D models.

The blue cluster can be divided into two smaller parts. The first part mainly represents publications describing hepatocellular 3D cell models for application in ecotoxicological and environmental studies, and the second part concerns pharmacological studies. The majority of the publications can be found in the red cluster. These publications concern the following

topics: *in vitro* drug-induced responses, long-term induced hepatotoxicity, xenobiotic metabolism, and repeated dose toxicity. The green cluster can be further split into three sub-clusters of publications. The first sub-cluster of publications concerns the application of new 3D models for accurate risk assessment and environmental health, the second sub-cluster concerns the use of 3D models for (geno)toxicity assessment as an alternative to monolayer culture, and the last sub-cluster consists of publications investigating key physiological functions of hepatocellular 3D models.

Before concluding, we would like to mention some of the limitations of this study. These concern primarily the fact that all our data was selected exclusively from Web of Science. As a result, we could not systematically assess the selection bias or, more specifically, we were unable to verify whether our analysis included all the relevant publications.

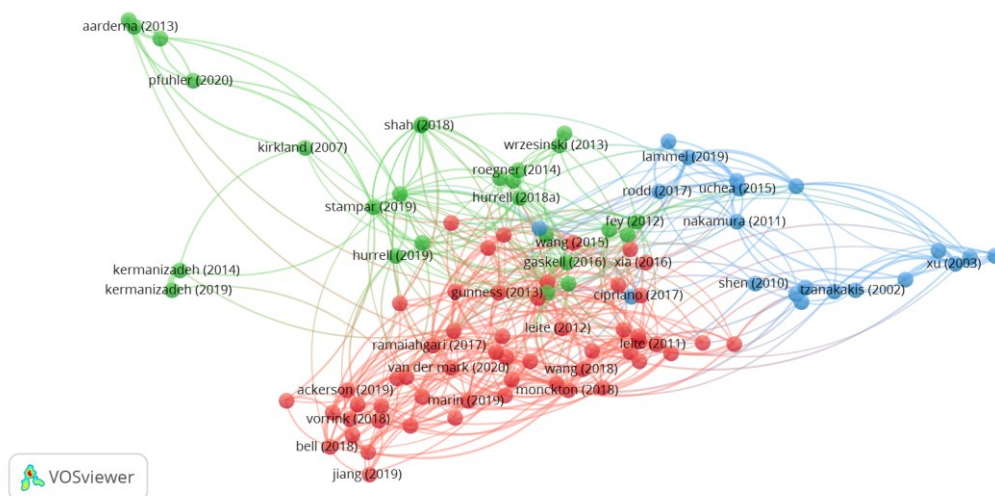


Figure 1.6: Clusters of publications using hepatocellular 3D cell models in the field of toxicology. Each colour assigned by the VOSviewer software represents a different cluster. The blue cluster represents publications describing hepatocellular 3D cell models in ecotoxicological and environmental studies and pharmacological studies. The green cluster represents publications describing the application and use of new 3D models for accurate risk assessment and environmental health, for (geno)toxicity assessment as an alternative to monolayer culture. The red cluster represent publications describing the *in vitro* drug-induced responses, long-term induced hepatotoxicity, xenobiotic metabolism, and repeated dose toxicity.

1.4 Scientific Problems and Aims of the Thesis

Liver cell lines cultured in 2D conditions are the most commonly used system for investigating the damaging effects of xenobiotic compounds *in vitro* (Soldatow et al., 2013). Nevertheless, most hepatocellular cells grown in monolayer (2D) conditions lack the relevant characteristic of hepatic cells, mostly due to the limited expression of drug-metabolizing enzymes (Kirkland et al. 2007; Shah et al. 2018; Wrzesinski and Fey 2013). These shortcomings can lead to misleading results and can make interpretation of the outcomes questionable (Guo et al., 2019). Therefore, a demand for establishing improved experimental models in toxicological studies has arisen (Corvi et al., 2013). In genetic toxicology, the 3R strategy strongly encourages taking advantage of alternative *in vitro*

models to assess the genotoxic effects of chemicals and environmental contaminants in order to reduce the use of animals in preclinical testing (Pfuhler et al., 2009). Recent three-dimensional (3D) cultures, which better reflect *in vivo* conditions, are considered an effective model for drug development and toxicological studies. They also have improved cell-cell and cell-matrix interactions, as well as preserved complex *in vivo* cell phenotypes (Aucamp et al., 2017; Loessner et al., 2010). Especially hepatocellular 3D models generally exhibit a higher level of liver-specific functions, including metabolic enzymes, in comparison to 2D cell models (Elje et al. 2019; Mandon et al. 2019; Štampar et al. 2019).

The determination of the genotoxic potential is the critical element of safety assessment for all sorts of substances, such as chemicals, food additives, pharmaceuticals, cosmetics ingredients, etc. (Corvi et al., 2013). Currently, there is an ongoing trend to develop standardized and robust *in vitro* 3D models, which better imitate the *in vivo* environment for the toxicity assessment of critical endpoints of the above-mentioned substances (chemicals, food additives, pharmaceuticals, etc.) (Elje et al., 2020; Guo et al., 2019; Hurrell et al., 2019; Mandon et al., 2019; Pfuhler et al., 2020). Therefore, **the first aim** of the doctoral thesis was to develop, optimize, validate, and characterize the technique and culture conditions for obtaining viable HepG2 3D cell models (spheroids) with enhanced characteristics of hepatic cells. For this purpose, we tested different initial densities of cells for the development of spheroids, which were cultivated for different periods of time. Furthermore, we performed an expression profile of selected genes that code for cell proliferation, drug-metabolizing enzymes, transporters, and liver-specific factors.

In the next part, we focused on the genotoxic effects of selected model compounds representing different classes of genotoxic carcinogens which require metabolic activation to electrophilic intermediates: polycyclic aromatic hydrocarbon benzo(a)pyrene (B(a)P), mycotoxin aflatoxin B1 (AFB1), two heterocyclic aromatic amines (PhIP and IQ), and direct-acting compound etoposide (ET). All selected compounds are known to cause DNA damage; therefore, **the second aim** was to determine whether there are differences in the assessment of genotoxic effects between 2D and 3D cell models.

We developed and optimized a novel approach for studying genotoxic effects and processes related to genotoxicity using multi-labelling with antibodies and detection by flow cytometry, which allows high-throughput analyses. Therefore, **the third aim** was to show that the newly developed HepG2 3D model can be used for genotoxicity assessment by applying the flow cytometric analysis and microscopy, and to show that the developed model is more sensitive for the detection of adverse genotoxic effects of various compounds compared to 2D cultures. Furthermore, we evaluated the testing approach by applying the developed methodologies to the evaluation of the (geno)toxic effects of an environmental natural pollutant, the cyanobacterial toxin cylindrospermopsin (CYN). **The fourth aim** was to successfully assess the influence of CYN on cell proliferation, DNA damage induction and the expression of genes involved in cell proliferation, cell death, metabolism, and response to DNA damage.

In the last part of the PhD thesis, the spheroids developed from hepatocellular HepG2/C3A cells were cultured for 21-days using the advanced dynamic clinostat micro-tissue culturing technique. Here, the spheroids are cultured in rotating bioreactors, where the rotation causes growth media to flow around the spheroids. These conditions enable a higher diffusion of oxygen and nutrients to the inner part of the spheroids and prevent the formation of a necrotic core (Fey & Wrzesinski, 2012; Gong et al., 2015; Lin et al., 2008). As bioreactors enable prolonged culturing of spheroids (several weeks), which results in the development of structures with tissue-like characteristics and stable physiological functions, such as bile canaliculi-like structures and sinusoid-like channels we wanted to evaluate the appropriateness of the model for genotoxicity assessment. Thus, **the fifth aim** was to determine the influence of non-cytotoxic concentrations of BaP and PhIP after 24 h and

96 h of exposure on the formation of DNA damage in 21-day-old C3A spheroids. **The sixth aim** was to show that the 3D model utilizing HepG2/C3A spheroids grown under dynamic clinostat conditions can represent a promising *in vitro* model, which can be applied in genotoxicity studies and can contribute to a more reliable assessment of the genotoxic activity of pure chemicals as well as complex mixtures.

1.5 Research Hypotheses

1. The static *in vitro* HepG2 3D cell model better reflects *in vivo* conditions compared to traditional 2D cell models. Specifically, it is hypothesized that:

- the time of cultivation and initial density of cells in the spheroids influence the outcome and sensitivity of the 3D cell model;

- the hepatocellular 3D cell model has improved cell-cell and cell-matrix interactions, preserved *in vivo* cell phenotypes, and that it is capable of creating a more complex microenvironment compared to the 2D monolayer;

- the proliferation of cells is decreased in the 3D cell model, which is more similar to *in vivo* conditions;

- the hepatocellular 3D cell model has a higher expression of liver-specific functions compared to 2D models.

2. The HepG2 *in vitro* 3D cell model differs in liver-specific properties and the gene expression of metabolic enzymes compared to traditional 2D monolayer HepG2 cultures. Specifically, it is hypothesized that:

- hepatic characteristic (morphologic and functional) are more strongly expressed in a 3D cell system compared to a 2D system;

- the expression of genes encoding phase I and II metabolic enzymes is higher in the 3D cell model compared to the 2D cell model.

3. Dynamic culturing conditions in bioreactors enable the formation of reproducible and uniform HepG2/C3A spheroids suitable for prolonged exposure studies. Specifically, it is hypothesized that:

- the constant flow of media results in a higher diffusion of nutrients and oxygen into the inner parts of the spheroids and a concomitant diffusion of waste products out of the spheroids, which maintains high cell viability;

- the genes encoding hepatic markers are expressed in the dynamic 3D cell model.

4. The hepatocellular *in vitro* 3D cell model (grown under static and dynamic conditions) is suitable for the evaluation of the (geno)toxic

effects of direct and indirect-acting genotoxic compounds. Specifically, it is hypothesized that:

- the higher stability and viability of hepatocellular 3D cell models allows long-term exposures to genotoxic compounds at lower concentrations compared to 2D cell model;
- the 3D cell model is more sensitive for the detection of indirect-acting genotoxic compounds due to a higher gene expression of metabolic enzymes

1.6 Publications Included and the Candidate's Contributions

The first manuscript, titled 'Characterization of an *in vitro* 3D cell model developed from human hepatocellular carcinoma (HepG2) cell line,' provides important data on the characterization, optimization and validation of the hepatocellular *in vitro* 3D cell model. The influence of spheroidal age on cell proliferation and metabolic status was studied over a 17-day cultivation period, gaining greater insight into the morphological and physiological characteristics of HepG2 spheroids. I am the first author of this publication. Together with the co-authors, I designed and performed the experiments for the validation of the 3D cell model. I also performed the analysis, conducted an interpretation of the obtained data, and drafted the manuscript.

In the second manuscript, entitled 'Development of *in vitro* 3D cell model from hepatocellular carcinoma (HepG2) cell line and its application for genotoxicity testing,' the formed spheroids were compared to a 2D monolayer. The results showed a higher sensitivity of the 3D model for detecting DNA damage induced by indirect-acting genotoxic compounds and improved metabolic capacity, which may contribute to a more reliable genotoxicity assessment of chemicals. I am the first author of this publication. Together with the co-authors, I designed the study, prepared the spheroids, performed all the *in vitro* experiments, and conducted the analysis and interpretation of the data. I collaborated in the design and validation of the applied flow cytometry method for the simultaneous analysis of proliferation, cell cycle distribution, and γ H2AX formation. I also prepared the manuscript.

The third manuscript, 'HepG2 spheroids as a biosensor-like cell based system for (geno)toxicity assessment,' is focused on the hepatocellular 3D spheroid model and the application of flow cytometric methodologies for the assessment of DNA damage and related pathways. The approach was validated by a detection of the cytotoxic and genotoxic activities of the indirect-acting compounds B(a)P and PhIP, studied by the MTS assay and flow cytometry by measuring the γ H2AX foci, respectively. I am the first author of this publication. In collaboration with the co-authors, I designed and performed all the experiments using well-established techniques – the MTS assay, flow cytometry, confocal microscopy, and qPCR. I analyzed and interpreted the data, and I supervised the work of an MSc student, a co-author who performed the MTS assays and prepared the cells for the flow cytometry. I also prepared the manuscript.

The fourth manuscript, 'Application of an advanced HepG2 3D cell model for studying genotoxicity of cylindrospermopsin,' focuses on the effect of cylindrospermopsin exposure on HepG2 cells in 3D spheroids. I am the co-author of the study. Together with the other authors, I designed and performed the experiments for the formation of spheroids and the qPCR experiments. I also collaborated in the design and validation of the applied

flow cytometry method for the simultaneous analysis of proliferation, cell cycle progression, and γ H2AX formation.

The fifth manuscript, ‘Method for spheroids disassemble into core and rim for downstream applications such as flow cytometry, comet assay, transcriptomics, proteomics and lipidomics,’ highlights the protocol for disassembling 21-day old spheroids into the core and the rim. In addition, the manuscript shows the widespread use of spheroids for measuring various endpoints. I am the co-author of the study. Together with the other authors, I designed the protocol for the disassembly of the spheroids and prepared part of the manuscript.

In the sixth manuscript, ‘Hepatocellular carcinoma (HepG2/C3A) cell-based 3D model for genotoxicity testing of chemicals,’ we aimed to develop an approach for the genotoxicity testing of chemicals using 21-day old spheroids formed from HepG2/C3A cells utilizing the dynamic bioreactor system. The genotoxic effects were assessed in spheroids exposed to model genotoxic compounds BaP and PhIP for a short and prolonged period of time. Cytotoxicity was evaluated with the ATP assay, genotoxicity with the comet assay, and the deregulation of selected genes was assessed using nanolitre-scale q-PCR. I am the first author of this publication. Together with the co-authors, I designed and performed all the experiments as well as analyzed the results and prepared the manuscript.

Chapter 2

Scientific Publications

2.1 Characterization of In Vitro 3D Cell Model Developed from Human Hepatocellular Carcinoma (HepG2) Cell Line

Martina ŠTAMPAR, Barbara BREZNIK, Metka FILIPIČ and Bojana ŽEGURA

Cells 2020, 9(12), 2557. DOI: 10.3390/cells9122557



Article

Characterization of In Vitro 3D Cell Model Developed from Human Hepatocellular Carcinoma (HepG2) Cell Line

Martina Štampar ^{1,2}, Barbara Breznik ¹, Metka Filipič ^{1,2} and Bojana Žegura ^{1,2,*}

¹ Department of Genetic Toxicology and Cancer Biology, National Institute of Biology, 1000 Ljubljana, Slovenia; martina.stampar@nib.si (M.Š.); barbara.breznik@nib.si (B.B.); metka.filipic@nib.si (M.F.)

² Jozef Stefan International Postgraduate School, 1000 Ljubljana, Slovenia

* Correspondence: Bojana.zegura@nib.si; Tel.: +386-5-923-28-62

Received: 23 October 2020; Accepted: 26 November 2020; Published: 28 November 2020

Abstract: In genetic toxicology, there is a trend against the increased use of in vivo models as highlighted by the 3R strategy, thus encouraging the development and implementation of alternative models. Two-dimensional (2D) hepatic cell models, which are generally used for studying the adverse effects of chemicals and consumer products, are prone to giving misleading results. On the other hand, newly developed hepatic three-dimensional (3D) cell models provide an attractive alternative, which, due to improved cell interactions and a higher level of liver-specific functions, including metabolic enzymes, reflect in vivo conditions more accurately. We developed an in vitro 3D cell model from the human hepatocellular carcinoma (HepG2) cell line. The spheroids were cultured under static conditions and characterised by monitoring their growth, morphology, and cell viability during the time of cultivation. A time-dependent suppression of cell division was observed. Cell cycle analysis showed time-dependent accumulation of cells in the G0/G1 phase. Moreover, time-dependent downregulation of proliferation markers was shown at the mRNA level. Genes encoding hepatic markers, metabolic phase I/II enzymes, were time-dependently deregulated compared to monolayers. New knowledge on the characteristics of the 3D cell model is of great importance for its further development and application in the safety assessment of chemicals, food products, and complex mixtures.

Keywords: 3D cell model; HepG2; cell proliferation; cell cycle; gene expression

1. Introduction

In recent years, considerable efforts have been made to develop hepatic in vitro 3D cell models with higher predictability for detecting the genotoxic effects of chemicals and environmental particular liver, which is the main target organ of chemical activation and detoxification processes [1,2]. In toxicology, it is nowadays recommended to use alternative in vitro models for the implementation of the 3R (reduce, refine, and replace) strategy as well as considering the inaccurate prediction of animal models due to inter-species variability. This demands an urgent need for advanced, robust, cost, and time-efficient in vitro models for the safety assessment [3,4]. It is widely recognised that human primary hepatocytes (PHH) are the golden standard for studying metabolism and toxicity, as they are of human origin and express metabolic enzymes that are relevant for human metabolism of xenobiotics [5–9]. However, there are several shortcomings related to the application of PHH such as limited availability, the complexity of isolation and culturing of cells as their expansion in culture is not possible, short life span, rapid dedifferentiation, loss of many hepatocyte functions and hepatic phenotype when cultured in monolayer cultures, high costs associated with

the performance of the experiments, and the most important—genetic and metabolic differences due to polymorphism of donors. Due to the above-mentioned facts, PHH are not suitable for routine use for genotoxicity testing [5,10–12]. Alternatively, hepatic carcinoma-derived cell lines, such as HepG2, C3A, HepaRG, HuH6, and many others, are frequently used in genotoxicity studies, due to their unlimited growth, availability, and high reproducibility of results. These cell lines [13–16] have several phenotypic characteristics and some functional properties of liver cells [17,18] and therefore, represent an effective compromise between the ease of culturing and the expression of several key enzymes involved in xenobiotic metabolism [19–21]. However, the major limitations of hepatic cells cultured in two (2D) dimensions are the low expression of CYP450 enzymes, xenobiotic receptors, and phase II enzymes [5,22] and thus, inadequate expression of liver cell function *in vivo*. Consequently, it is highly plausible that such cell models give inaccurate and false-positive results [23].

In drug development and hepatotoxicity research, there is a high demand for establishing new, reliable, and uniformed models [24] with higher predictability for the consequences of human exposure. The report from the Workshop on Genotoxicity Testing (IWGT) recommends focusing on the development of 3D models, which better reflect the *in vivo* conditions and are capable of creating the complex microenvironment with the purpose of advancing our understanding of complex biological phenomena [4]. Another important advantage of 3D cell models compared to 2D cell models is that they enable prolonged exposures, due to their increased stability as they retain high cell viability and morphology over the period of several weeks [25]. Many static and perfused techniques for culturing 3D cell models (spheroids) are available, such as non-adhesive surfaces, hanging drop cultures, spinner flasks, bioreactors, and micro-moulding [9,26,27]. Each of these techniques offers various advantages; however, many are technically challenging, expensive, and need appropriate facilities [28]. The most important advantages of culturing cells in the form of 3D are increased cell–cell and cell–matrix interactions and higher expression of liver-specific functions (albumin content, urea synthesis, and expression of cytochromes), thus providing a physiologically more relevant model *in vivo* [29–35]. In recent years, hepatic 3D cell models are, in addition to being used for drug development, also applied for studying genotoxic effects, such as chromosomal instability [28] and DNA damage [32,35,36] induced by various chemicals and environmental samples [37]. Although 3D cell models are superior to 2D cell models, the lack of standardisation of 3D cell culture protocols and insufficient characterisation of the spheroids prevent the integration of 3D cell culture models into the field of toxicology research, particularly due to variability in structure and composition of the formed spheroids [38,39].

The aim of the present study was to characterise the HepG2 cells grown in 3D conformation in terms of hepatic properties and the mRNA expression profile of selected genes coding for cell proliferation, drug-metabolising enzymes, transporters, and liver-specific factors. The HepG2 spheroids were formed by the forced floating method from an initial cell density of 6000 and 3000 cells/spheroid. As the age of the spheroids can influence the outcome and sensitivity of the cell model [40], spheroid growth, quality parameters (surface area and perimeter), and viability of cells were monitored over a period of 6 days and 12 days, respectively. The viability of cells in spheroids was determined by the Live/Dead staining using confocal microscopy, while the proliferation of cells (KI67 marker) in spheroids of different age and cell cycle analysis was assessed with flow cytometry. The mRNA expression of selected hepatic markers, genes involved in cell proliferation, and those involved in phase I/II metabolism in spheroids with an initial density of 3000 cells/spheroid was assessed using real-time quantitative PCR (Fluidigm).

2. Materials and Methods

2.1. Chemicals

Minimum essential medium eagle (MEME), penicillin/streptomycin, Na-pyruvate, non-essential amino acids (NEAA), L-glutamine, NaHCO₃, dimethylsulphoxide (DMSO), methylcellulose, propidium iodide (PI), and fluorescein diacetate (FDA) were purchased from Sigma (St. Louis, MO,

USA). Trypsin-EDTA (0.25%), foetal bovine serum (FBS), and TRIzol® reagent were obtained from Gibco (Praisley, Scotland, UK). Hoechst 33258 dye was obtained from Invitrogen (Waltham, MA, USA). Phosphate-buffered saline (PBS), methanol, and ethanol were purchased from PAA Laboratories (Dartmouth, NH, USA). Triton X-100 was obtained from Fisher Sciences (Massachusetts, NJ, USA), while the high capacity cDNA archive kit, TaqMan Universal PCR Master Mix (4440038), and TaqMan Gene Expression Assays were from Applied Biosystems (Massachusetts, NJ, USA). The PreAmp GrandMasterMix (TA05-50) was obtained from TATAA Biocenter AB (Göteborg, Sweden). GE 48.48 Dynamic Array Sample & Assay loading Reagent Kit—10 IFCs (85000821) and 48.48 Dynamic Array: Gene expression chip were obtained from Fluidigm (South San Francisco). Anti-Ki-67-FITC (130-107-586) antibodies and REA Control (I)-FITC (131-104-611) were obtained from Miltenyi Biotec (Bergisch Gladbach, Germany).

2.2. Cell Culture and Formation of 3D Spheroids

The HepG2 cell line was obtained from the ATCC cell bank (HB-8065™) and was grown in MEME media supplemented with 10% FBS, 1% NEAA, 100 IU/mL pen/strep, 0.1 g/mL NaHCO₃, 0.1 g/mL Na-pyruvate, and 2 mM L-glutamine at 37 °C in 5% CO₂ atmosphere. The spheroids were developed by the forced floating method described in Štampar et al. (2019) [35] using a growth medium supplemented with 4% methylcellulose [41]. Two culture conditions for spheroids formation were used. The spheroids with an initial density of 3000 cells/spheroid and 6000 cells/spheroid were seeded and grown for 12 and 4 days, respectively, depending on the specific endpoint measured. The culture media was changed every 2–3 days to obtain the optimal growth of spheroids.

2.3. Monitoring the Growth and Morphology of Spheroids

The surface area of at least 10 spheroids with the initial density of 3000 cells/spheroid and 6000 cells/spheroid was monitored during the time of cultivation (up to 12 and 4 days, respectively). The surface area (mm²) of each spheroid was monitored microscopically every day and determined by planimetry at 40× magnification using the NIS elements software 4.13 v (Nikon Instruments, Melville, NY, USA) connected with the Ti Eclipse inverted microscope (Nikon, Japan). Evaluation of the spheroid growth was determined three times independently.

2.4. Quantification and Viability Determination of the Whole Spheroid by Live/Dead Staining

At least three spheroids for each condition (3000 and 6000 cells/spheroid) were stained and monitored during the time of cultivation. The culture media were replaced with FBS-free media supplemented with FDA (8 µg/mL) and incubated for 1 h in darkness at 37 °C in a 5% CO₂ atmosphere. After staining, the cells were washed with PBS. Subsequently, PI (20 µg/mL) was added and incubated in the dark for an additional 5 min. Following the incubation, the staining mixture was washed with PBS and substituted with fresh serum-free MEME media (100 µL). The staining was performed according to [37] with modifications. The Z-stacks images of single spheroids were captured using the confocal laser scanning microscope Leica TCS SP8 at 100× magnification. Z-stacks of optical sections were captured across the entire spheroid thickness using excitation and emission (PI: 493/636 nm, FDA: 488/530 nm) settings for simultaneous dual-channel recordings; approximately 50 Z-stacks per spheroid were taken. Z-stacks were processed and analysed using the Leica confocal software and presented as a “maximum intensity projection image” gallery. Three independent experiments were performed (N = 3). The quantification of Z-stacks was proceeded in the program Image-Pro 10 (Media Cybernetics, Inc., Rockville, MD, USA), where at least 20 Z-stacks per spheroid were quantified. The percentage of dead cells in the spheroid was calculated as a ratio between the spheroid area and the number of dead cells.

2.5. Analyses of Cell Cycle and Cell Proliferation by Flow Cytometry

The analyses of cell cycle and cell proliferation in spheroids were performed with flow cytometry. The cells from spheroids with an initial density of 3000 and 6000/cells were collected during the time of cultivation for 18 and 4 days, respectively. For the analysis, 30 spheroids per sample were collected and dissociated with enzymatic digestion and mechanical degradation, as described by Štampar et al. (2019). The obtained single-cell suspension was washed (1x PBS), fixed in ethanol, and kept at -20°C until the analysis (for details see Hercog et al. (2019 [42]; 2020 [37])). After the fixation step, the cells were washed in cold PBS, centrifuged, and labelled with anti-KI67-FITC (50-fold diluted antibodies in 1% BSA). Subsequently, the cells were washed with BSA and PBS and afterwards stained with Hoechst 33258 dye (diluted in 0.1% Triton X-100 1:500). The cell analyses were performed on a MACSQuant Analyzer 10 (Miltenyi Biotec, Bergisch Gladbach, Germany), where the FITC intensity, corresponding to the proliferation marker KI67+, was detected in the B1 (525/550 nm) channel and the analysis of the cell cycle was proceeded in the V1 (450/550 nm) channel. Rea-FITC control (Miltenyi Biotec, Bergisch Gladbach, Germany) was used to exclude unspecific binding. The experiments were repeated in three independent biological repetitions, where each time, 2.5×10^4 single cells per experimental point were recorded. The obtained data were analysed and the graphics were prepared in FlowJo software V10 (Becton Dickinson, Franklin Lakes, NJ, USA). The cell cycle distribution of the solvent control and treated samples and KI67-positive cells for each day was compared to the first day of the measurements. The statistical analysis for cell cycle was performed by the two-way ANOVA with Bonferroni's multiple comparisons test, α 0.05%, while the statistical significance of KI67-positive cells was assessed by one-way ANOVA with Dunnett's multiple comparisons test, α 0.05, both using GraphPad Prism V6 (GraphPad Software, San Diego, CA, USA).

2.6. The qPCR Analyses of the Expression of Selected Genes

For the gene expression analysis, only spheroids with a density of 3000 cells/spheroid were collected during the time of cultivation (every two to three days, starting with day three of cultivation). The basal expression of the selected genes was determined in HepG2 monolayer cultures (2D) cultured for 2 days (this is usually the time when in 2D, the gene expression is evaluated after the exposure to various compounds; 24 h for cells to attach to the surface of the plastic and 24 h of subsequent exposure) and in spheroids (3D) cultured for 3, 5, 7, 10, 12, 14, and 17 days. Total mRNA was isolated from one T25 plate in the case of 2D and from a pool of 25 spheroids per sample in the case of 3D, using the TRIzol reagent. The quality and the concentration of total mRNA were measured with a NanoDrop 1000 spectrophotometer (Thermo Fischer Scientific, Wilmington, DE, USA), while degradation was checked by gel-electrophoresis (BioRad Power PAC 3000 and UVP Chem Studio PLUS, Analytik Jena AG, Upland, CA, USA). The cDNA High Capacity Archive Kit was applied for the reverse transcription of 1 μg of total mRNA per sample. The expression of selected genes was quantified by the qPCR on 48.48 Dynamic ArrayTM IFC method, where TaqMan Universal PCR Master Mix and the pre-amplified (TATAA PreAmp GrandMasterMix, Tataa Biocenter, Gothenburg, Sweden) Taqman Gene Expression Assays were used. To eliminate the effects of inhibition and to assess the performance of a primer set, a series of 5-fold dilutions of each target gene was analysed. The qPCR experiments were performed on 48.48 Dynamic ArrayTM IFC chips for gene expression on the BioMark HD machine system (Fluidigm, UK) and data were analysed with an open web program QuantGenious [43]. Experiments were repeated three times independently, each time in two replicates. The difference (2D versus 3D) in gene expression greater than 1.5-fold was considered as up/downregulation (relative expression >1.5 or <0.66 , respectively).

The selected genes: *ALB* (albumin, Hs00910225_m1); *AFP* (α -fetoprotein), Hs00173490_m1; *ALDH3A1* (aldehyde dehydrogenase 3 family member A1), Hs00964880_m1; *TOP2A* (topoisomerase 2- α), Hs01032137_m1; *PCNA* (Proliferating cell nuclear antigen), Hs00427214_g1; *KI67* (cellular marker for proliferation), Hs01032443_m1; *CCND1* (encodes the cyclin D1 protein), Hs00765553_m1; *CDKN1A* (Cyclin Dependent Kinase Inhibitor 1A), Hs00355782_m1; *CYP1A2* (cytochrome P450 family 1 subfamily A member 2), Hs00167927_m1; *CYP1A1* (cytochrome P450 family 1 subfamily A

member 1), Hs01054797_g1; *CYP3A4* (cytochrome P450 family 3 subfamily A member 4), Hs02514989_s1; *AHR* (aryl hydrocarbon receptor), Hs00169233_m1; *UGT2B7* (UDP glucuronosyltransferase family 2 member B7), Hs00426592_m1; *UGT1A1* (UDP glucuronosyltransferase 1 family, polypeptide A1), Hs02511055_s1; *SULT1C2* (sulfotransferase family 1C member 2), Hs00602560_m1; *SULT1B1* (sulfotransferase family 1B member 1), Hs00234899_m1; *NAT1* (N-acetyltransferase 1), Hs02511243_s1; *NAT2* (N-acetyltransferase 2), Hs01854954_s1; *HIF1α* (Hypoxia-inducible factor 1-alpha), Hs00153153_m1; *BBC3* (p53 upregulated modulator of apoptosis), Hs00248075_m1 were pre-amplified. In all experiments, *GAPDH* (Human Endogenous Control, Hs9999905_m1) and *HPRT1* (Hypoxanthine phosphoribosyltransferase 1), Hs02800695_m1) were used as reference genes.

The different tests were performed between the 2 days old monolayer and spheroids on day 3 and all subsequent days with the two-way ANOVA (Dunnnett's test) by multiple unpaired t-test analysis using the Sidak–Bonferroni method ($^+ p < 0.05$, $^* p < 0.05$, respectively). The statistical significance within days was conducted by the two-way ANOVA, considering Tukey's multiple comparisons test ($† p < 0.05$).

3. Results and Discussion

The 2D cultures traditionally used for studying the genotoxic effects of chemicals have several limitations, which consequently lead to misleading results. This has become even more evident with the development of in vitro models that enable the growth of cells in three dimensions (3D), which is physiologically more similar to in vivo conditions [44]. However, before 3D cell models can be integrated for genotoxicity testing research, there is a need for the development and subsequent standardisation of robust models that accurately predict the possible effects of studied compounds [45].

To our knowledge, the present study is the first where a comprehensive characterisation of the HepG2 3D cell model was performed. Based on previous results, two initial cell densities of 3000 and 6000 cells per spheroid were selected for the development of 3D cell models [35]. The HepG2 spheroids were formed by the forced floating method and cultured under static conditions for several days. During the time of cultivation, the spheroids were characterised by measuring the surface area, and viability of cells in spheroids. The characterisation is a very important step in the development of 3D cell models as the obtained data provide the information on whether the model is comparable to the liver in vivo conditions and is thus, more accurate than traditional monolayer culture.

3.1. The Effects on Growth and Morphological Changes over Time

The growth of at least 10 spheroids with the initial density of 3000 cells/spheroid (Figure S1A,B) and 6000 cells/spheroid (Figure S1C,D) was daily measured from 24 h to 7 days. The surface area was monitored by light microscopy and planimetry. The size of the spheroids varied according to the number of cells seeded in each well and increased with time of incubation. The spheroids with an initial density of 3000 cells/spheroid (Figure S1A) grew time-dependently from the first day of seeding. At the end of the cultivation (7 days), the surface area ($0.39 \pm 0.01 \text{ mm}^2$) increased 95% compared to the surface area at 24 h ($0.2 \pm 0.02 \text{ mm}^2$) (Figure S1B). In contrast to this, the spheroids with an initial density of 6000 cells/spheroid (Figure S1C) grew slower and the surface area after 7 days of cultivation increased for only 20% ($0.56 \pm 0.03 \text{ mm}^2$) compared to 24 h ($0.45 \pm 0.05 \text{ mm}^2$) (Figure S1D). At both initial densities, the spheroids maintained uniform spherical shape over the course of the culturing. These results show a steady growth of spheroids during the time of culture, which is in line with other studies on HepG2 spheroids [18,32]. The increase in the average surface area was higher at the lower initial cell density, meaning that the cells proliferated at a higher rate compared to spheroids with higher initial density, which was also reported by Lee et al. (2009) [46]. Based on these results, we concluded that 3000 cells per well was the more optimal density for the formation of spheroids that could be used for long-term exposures; therefore, this density was selected for further characterisation of the spheroids.

3.2. Determination of Live/Dead Cells in Spheroids over Cultivation Time

Live/Dead staining enabled us to investigate at which initial density and time of cultivation the viability of cells started to decrease and consequently, form the necrotic core. A very well-known limitation of aged spheroids is the formation of a necrotic core, which results from the accumulation of metabolic waste products and insufficient diffusion of oxygen/nutrients into the centre of the spheroid starting at a diameter above 200 to 500 μm , as reported by Nath and Devi (2016) [47]. The visual analysis of HepG2 spheroids by confocal microscopy verified the time-resolved viability of the cells in a 3D culture, which was more or less stable over the cultivation time. In Figure 1A,B, representative spheroids from day 3 until day 12 and day 6 in the case of 3000 and 6000 cells/spheroid, respectively, stained with FDA (live) and PI (dead) are shown. Although the percentage of PI-positive cells in spheroids with an initial density of 3000 cells/spheroid increased from 10 days of cultivation onwards, we noticed that only a few dead cells were observed in the centre of the spheroids, meaning that no necrotic core was formed. The quantification of PI-positive cells representing dead cells confirmed a time-dependent increase in non-viable cells that was significant after 10 and 12 days, reaching 14.5% and 18.9% on average (Figure 1C,D), respectively. In spheroids with an initial density of 6000 cells/spheroid, a higher percentage of dead cells compared to 3000 cells/spheroid was observed already after 3 days of cultivation that was 8.4% and 4.0% on average, respectively. Correlating these results with the spheroid growth data, the spheroids with an initial density of 3000 cells/spheroid gradually increased in size and stayed uniformly spherical with limited degrees of necrosis up to day 12. However, in larger spheroids, small patches of death cells started to occur approximately on day 4 and by day 6, reached 16.5% dead cells on average with the visible formation of a necrotic core. Spheroids usually consist of three main zones—an outer proliferating rim, a quiescent viable zone, and an inner necrotic core that can develop due to lower diffusion of nutrients and oxygen forming hypoxic conditions [48–50]. In cancer research, the zones in larger tumour spheroids with a necrotic core resemble the cellular heterogeneity of solid *in vivo* tumours [51] and the necrosis occurring in the centre of the spheroid is a desirable characteristic as it mimics *in vivo* conditions. However, in genetic toxicology, where a model has to recapitulate an *in vivo*-like liver microenvironment, this is an undesirable characteristic. There are only a few studies so far that specifically determined the size or time at which hepatic spheroids develop necrosis that is associated with the cell type, cell number, and culture conditions [32,52]; therefore, the present study contributes new knowledge on the formation of a necrotic core in spheroids with time of cultivation. Previously, in encapsulated 3D HepG2 aggregates, no necrotic core was observed up to three days of culturing, while with prolonged cultivation, the thickness of aggregates disabled the determination of necrotic cells in the centre of the 3D cell model [19]. Elje et al. reported [32] a small necrotic core in HepG2 3D spheroids developed in hanging drops after 1 day of culturing, which was more represented as separate dead cells; however, the viability was stable over time and the cells were cultured for up to 21 days. Furthermore, in hepatic C3A spheroids with initial density of 2500 cells/spheroid, small patches of cell death started to occur approximately at day 14 and, by day 18, a necrotic core was formed [52]. Altogether, these studies, including ours, show that necrosis occurs in the core of the spheroid with time of cultivation and depends on the cell type and 3D conformation.

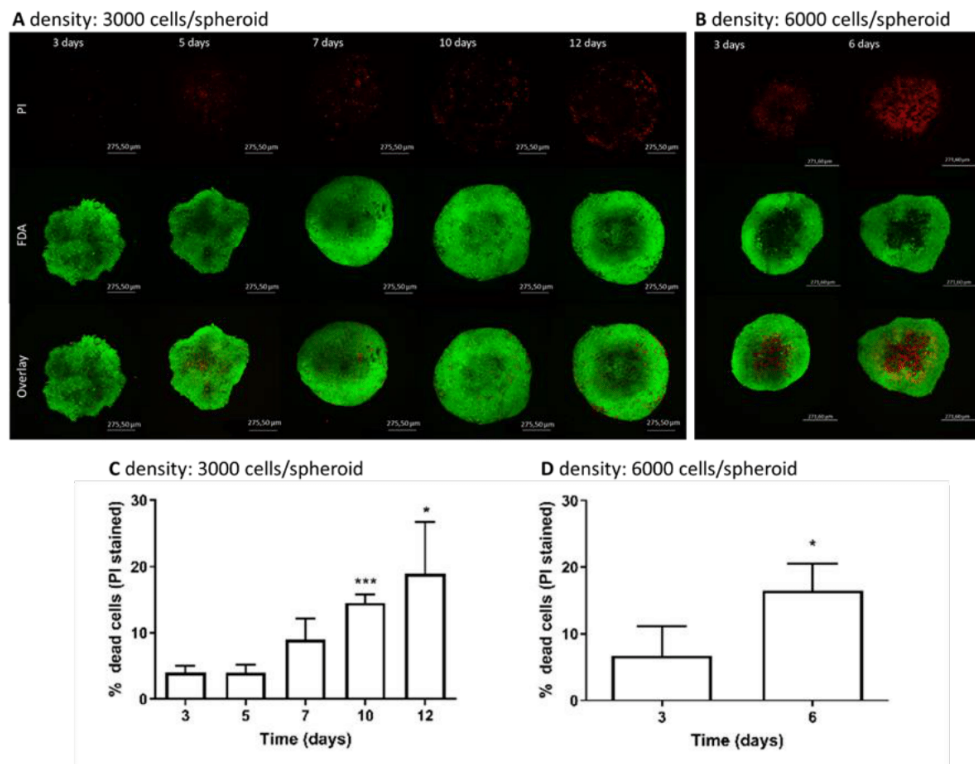


Figure 1. Images of Live/Dead-stained spheroids(A,B) and the quantification of the percentage of PI-positive cells in images of spheroids (C,D) captured over the period of cultivation at different densities (A–C) 3000 cells/spheroid and (B–D) 6000 cells/spheroid. The cells in spheroids were stained with FDA (green, live cells) and PI (red, dead cells). The Z-stacks were obtained using a confocal microscope at 100× magnification (N = 3). A “maximum intensity projection image” of the spheroid was generated from 50 Z-stacks images (A,B). Z-stacks were quantified with the Image-Pro 10 software (C,D) where at least 20 Z-stacks per spheroid were measured and the percentage of dead cells in the spheroid was calculated (N = 3). The statistical significance was calculated with the Student t-test, with alpha 0.05, * $p < 0.05$, ** $p < 0.01$, *** $p < 0.001$, **** $p < 0.0001$.

3.3. Distribution of Cells within the Cell Cycle and Cell Proliferation during the Time of Cultivation

Previous studies on HepG2 3D models reported a strong decrease in cell proliferation, which is associated with a time-dependent cell differentiation process [32,53]. In our study, the proliferation of cells and their distribution within the cell cycle of spheroids with the initial density of 3000 and 6000 cells/spheroid were determined by flow cytometry over the time of cultivation, with simultaneous detection of the fluorescent signals of FITC corresponding to the proliferation marker KI67 and Hoechst 33258 corresponding to the cell cycle distribution. It is well known that KI67 protein is present during all active phases of the cell cycle (G1, S, G2, and M), and it is absent from the resting cells (G0) [54,55]. Therefore, the novel approach of simultaneous staining allowed us to further distinguish the distribution of cells in the G0 (non-proliferating) and G1 (proliferating) phase. The results showed that the overall number of proliferating cells and the number of proliferating cells within the G0/G1 phase decreased over the time of cultivation, which is clearly the consequence of the time-dependent increase in non-proliferating cells (G0) within the G0/G1 peak (Figure 2A–C). The percentage of proliferating cells gradually declined with the time reaching 50% decrease after approximately 7 and 2 days of cultivation at an initial density of 3000 (Figure 2A) and 6000 (Figure 2B) cells/spheroid, respectively. At higher cell density, we noticed that already after 24 h, only 65.5% of cells proliferated and by day 4, only 28% of cells expressed KI67 protein, meaning that at day 4,

the majority of cells did not proliferate. On the contrary, at lower initial cell density, the decrease in cell proliferation was slower. After 3 days of spheroid cultivation, 82% of cells proliferated, while with further cultivation, the proliferation rate decreased to approximately 68%, 54%, and 13% after 5, 7, and 18 days, respectively. The same trend was observed for proliferating cells within the G0/G1 phase. Similarly, a decrease in the number of proliferating cells in HepG2 spheroids and spheroids cultured in hydrogels was reported by Ramaiahgari et al. (2014) [31] and Lee et al. (2009) [46]. Our results clearly showed that spheroids with lower initial density maintain the proliferation of cells at a higher rate and over the longer period compared to the spheroids with higher initial density, meaning that spheroids with lower initial density are more suitable for long-term exposures.

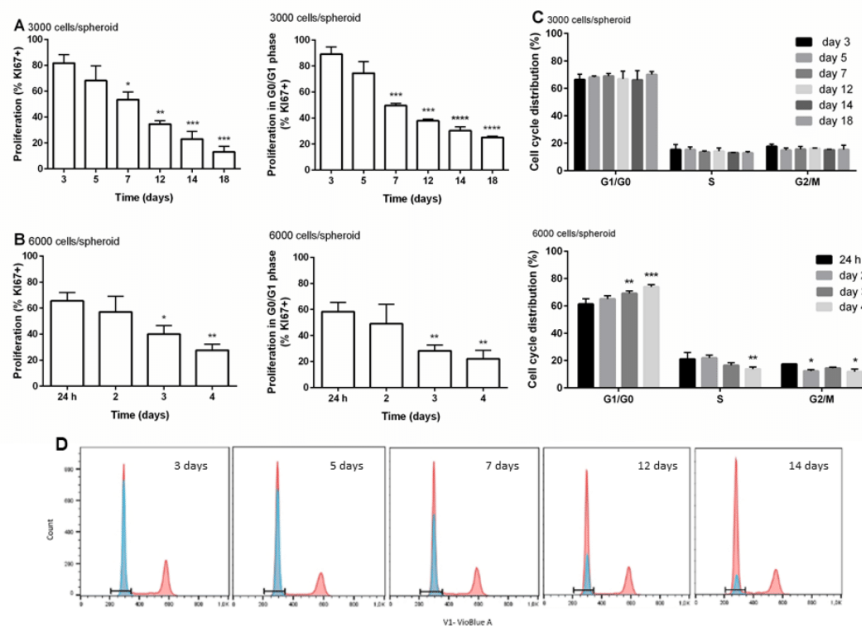


Figure 2. The proliferation of cells and the distribution of cells in different phases of the cell cycle during the time of cultivation. Percentage of KI67-positive cells and the percentage of KI67-positive cells within the G0/G1 phase of cell cycle overtime at density 6000 cells/spheroid (A). Percentage of KI67-positive cells and the percentage of KI67-positive cells within the G0/G1 phase of cell cycle overtime at density 3000 cells/spheroid (B). Distribution of cells in different phases of the cell cycle over the period of cultivation (C). Representative overlays of simultaneous staining with Hoechst for the cell cycle (red) and anti-KI67 antibody (blue) (D). The results are presented as the mean \pm SD (N = 3). The statistical analysis was conducted in GraphPad Prism 6, by the two-way ANOVA using the Bonferroni multiple comparisons test, * $p < 0.05$, ** $p < 0.01$, *** $p < 0.001$, **** $p < 0.0001$.

The cell cycle duration determines the unique doubling time of the cells [26] that is coordinately controlled by cyclin-dependent kinases and their cyclin partners, whose levels fluctuate throughout the phases of the cell cycle [56] (Figure 2C). In the G1 phase of the cell cycle, crucial decisions on DNA replication and completion of the cell division are made [57]. From the obtained results, we can see that at the initial density of 3000 cells/spheroid, the distribution of cells by phases does not change over time of cultivation. At all measured time points during the time of cultivation, approximately $67.7 \pm 3.4\%$ of proliferating cells were in the G1 phase, $14 \pm 1.8\%$ of cells were in the S phase, and $15.8 \pm 1.7\%$ were in the G2 phase, meaning that the cell cycle was not disturbed during 18 days, only the ratio of proliferating/non-proliferating cells in G0/G1 cells changed. On the contrary, in spheroids with the initial density of 6000 cells/spheroid, a slight increase in proliferating cells in the G1 phase

over the time of cultivation was observed, with 61.3% of cells in G1 after 24 h reaching up to 73.9% after 4 days, with a concurrent decrease in cells in the S and G2 phase from 21% and 17% after 24 h to 13.8% and 11.77% after 4 days, respectively (Figure 2D), suggesting cell cycle arrest and thus, the accumulation of cells in the G0/G1 phase with a time of spheroid cultivation. The cell cycle arrest can lead to the inhibition of cell proliferation and/or apoptosis [56], which is in line with the obtained data of the KI67 proliferation marker. These results again show that spheroids with lower initial density maintain a higher rate of cell proliferation compared to spheroids with higher initial density.

3.4. Gene Expression in Spheroids

For the first time, analysis of the expression of genes involved in the proliferation (*TOP2A*, *PCNA*, *KI67*, *CCND1*, and *CDKN1A*), apoptosis (*BBC3*), genes of hepatic markers (*AFP* and *ALB*), and gene a transcription factor encoding aryl hydrocarbon receptor (*AHR*), phase I (*CYP1A1*, *CYP1A2*, and *CYP3A4*), and phase II (*UGT1A1*, *UGT2B7*, *SULT1B1*, *SULT1C2*, *NAT1*, and *NAT2*) xenobiotic-metabolising enzymes was studied in HepG2 spheroids. Gene expression was evaluated in spheroids formed from the lower initial density, namely 3000 cells/spheroid that were cultured for 3, 5, 7, 10, 12, 14, and 17 days. Data for the individual genes were compared to the expression of genes from the monolayer culture at the age of 2 days and are presented as the ratio between 2D (at 2 days of culturing) and 3D at the corresponding time point.

3.4.1. Expression of Genes Involved in Cell Proliferation

Cell proliferation can be regulated by several factors, such as mitogens, growth factors, and survival factors [58]. We studied the genes *PCNA*, *KI67*, and *TOP2A* over the time of culturing, as the expression of the genes involved in the process of cell proliferation may be affected by the time the cells are in culture. A proliferating cell nuclear antigen (*PCNA*), a protein with an important role in DNA replication, has many cell cycle-dependent properties and its absence leads to cell cycle arrest in the S and G2/M phase [59]. Another important proliferation marker *KI67* encodes a nuclear antigen during the G1, S, and G2–M phases of proliferating cells, meaning that it is present during all active phases of the cell cycle, except the G0 phase [60,61]. The expression of *TOP2 α* is cell cycle-dependent and encodes DNA topoisomerase, which is an enzyme that controls and alters the topologic states of DNA during transcription [60,62]. The results showed that all three studied genes, *TOP2A*, *PCNA*, and *KI67*, were time-dependently downregulated compared to 2 days old monolayer culture (Figure 3A). The major shift in the downregulation of the proliferation markers occurred approximately at day seven.

The changes in *KI67* on the mRNA level showed the same trend as the data obtained with flow cytometry, where a decrease in *KI67*-positive cells over the time of cultivation, with approximately 50% of proliferating cells, was detected at day seven. As described before, HepG2 cells accumulated in the G1/G0 phase, due to arrested division in the G0 phase, which is especially noticeable at the initial density of 6000 cells/spheroid. The low proliferation rate in the 3D model can therefore be effectively utilised for studying the effects of long term exposure to various compounds, which is not feasible in a 2D model as the confluence limits the duration of culturing [31,63]. A decrease in cell proliferation in different 3D cell models overtime was reported in several studies with HepG2, using extra-cellular matrix-based hydrogel [31] and spheroids prepared by the hanging drop method [32], and HepG2/C3A, culturing in rotating bioreactors [30]. The occurrence of reduced proliferation over the time of cultivation may also have an impact on the decreased expression of cyclin protein coding genes that control cell cycle progression [64]. In our study, the expression of cyclin protein coding gene *CCND1* was downregulated and a decrease in the first seven days was noticed from a –4.76-fold change after 3 days of cultivation to –8.33-fold change after 7 days of cultivation (Figure 3B). The *CCND1* encodes the cyclin D1 protein, whose elevated expression has been reported in many human tumours and correlates with increased cell proliferation and differentiation due to the reduced G1/S transition [65]. The expression of *CDKN1A*, which is the cell cycle-related gene responsible for the G2/M checkpoint [66], was downregulated (–9.09-fold at day 3) compared to monolayer culture. We noticed a slight increase in *CDKN1A* expression with time of incubation reaching the maximal level

at day 7 (−7.14-fold) (Figure 3B). After the seventh day, the expression of both cyclin protein coding genes remained unchanged, which, compared to 2D monolayer culture, indicates the non-proliferating differentiated phenotype of HepG2 spheroids as described by Hiemstra et al. (2019) [67] and by Ramaiahgari et al. (2014) [31].

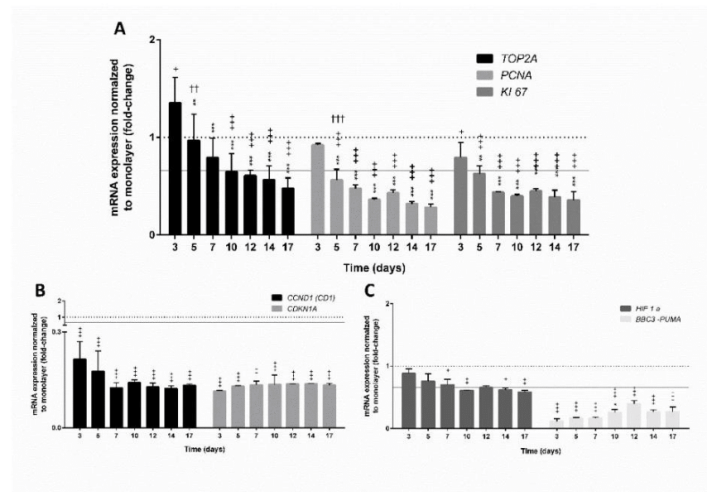


Figure 3. Relative expression of genes involved in the proliferation process (A,B) and apoptosis (C) over time from 3 to 17 days. The significant difference between (i) the monolayer culture (2D) and the spheroids (3D) ($+ p < 0.05$, $++ p < 0.01$, $+++ p < 0.001$); (ii) the first day (at day 3) of measurement and all subsequent days ($* p < 0.05$, $** p < 0.01$, $*** p < 0.001$); and (iii) within days ($† p < 0.01$, $†† p < 0.001$) was calculated in GraphPad Prism 6, by two-way ANOVA considering Dunnett’s multiple comparisons test. Results are presented as the mean \pm SD ($N = 3$). The dotted line denotes the expression of the corresponding gene in monolayer culture (1-fold change), the grey line indicates up- or downregulation of genes with the threshold set at 1.5-fold, which is more than 1.5 or less than 0.66 relative expression, respectively.

Altogether, the results suggest that the expression of gene markers related to the proliferation and division of cells decreased over time. Similarly, the expression of *BBC3*, a gene related to apoptosis, was downregulated in spheroids at the age of 3 days (−8.7-fold) compared to monolayer culture; however, with further incubation, the expression of *BBC3* increased, reaching the highest level after day 12 (−2.56-fold change) and then, declining again (Figure 3C). The pro-apoptotic protein *BBC3* interacts with anti-apoptotic Bcl-2 family members, resulting in mitochondria-induced apoptosis and cell death through the caspase cascade [68]. It was reported that the diffusion of oxygen into the centre of spheroids is difficult if a diameter is larger than 200 μm (larger spheroids), which consequently causes hypoxia in the core [49]. Live/Dead stained spheroids (density 3000 cells/spheroid) showed no signs of necrosis in the centre; however, in spheroids with a higher initial density (6000 cells/spheroid), necrosis was observed at day 6. This could be related to the hypoxia as reported by Ramaiahgari et al. (2014) [31] (Figure 3). We further investigated the transcription level of the *HIF1 α* gene, one of the hypoxia-inducible factors, which mediates cellular adaptation to hypoxic conditions [69]. The obtained results showed that at lower initial density (3000 cells/spheroid) during 17-day cultivation, the *HIF1 α* was downregulated compared to monolayer culture and the changes were significantly different from day 7 onwards with no further time-dependent deregulations (Figure 3C), which indicates that no excessive hypoxia was present in HepG2 spheroids up to 17 days.

3.4.2. Expression of Genes Encoding Hepatic Markers

Long-term cultivation of HepG2 cells in 3D conformation led to the enhancement of the expression of liver-specific markers, as shown for alpha-fetoprotein (*AFP*) and albumin (*ALB*) compared to monolayer culture (Figure 4). Alpha-fetoprotein is involved in pleiotropic activities affecting the processes of cell differentiation and growth regulation [70]. Compared to 2D, *AFP* expression in spheroids was 4.57-fold higher, which was statistically significant, at the age of 3 days and reached the maximal mRNA level at day 7 (6.84-fold). With further cultivation, the expression of *AFP* did not change much. Similarly, the expression of *ALB* in 3D significantly differed from the expression in 2D and was 4.95-fold upregulated at day 7. The *ALB* expression gradually increased and reached the maximal level at day 10 (9.56-fold) with a slightly decrease after 12 and 17 days (7.67-fold and 8.03-fold, respectively). Albumin is a stable protein and has a serum half-life of 20 days. Its synthesis is typically regulated on the transcriptional level [71]. Previously, the elevated expression of albumin in HepG2 spheroids compared to monolayer cultures was reported at mRNA [22,35] and protein [31] levels. Altogether, these studies show that hepatic functions are strongly enhanced in 3D systems compared to the 2D monolayer cultures [15,18,19,25,38,53].

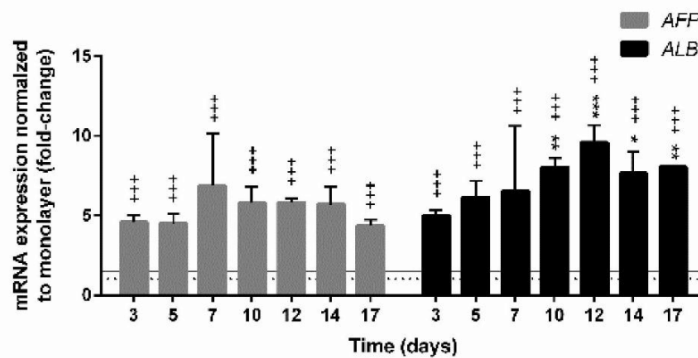


Figure 4. Monitoring the mRNA expression of hepatic markers over time. The significant difference between (i) the monolayer culture (2D) and the spheroids (3D) (+++ $p < 0.001$) and (ii) the first day (at day 3) of measurement and all subsequent days (* $p < 0.05$, ** $p < 0.01$, *** $p < 0.001$); was calculated in GraphPad Prism 6, by the two-way ANOVA considering Dunnett's multiple comparisons test. Results are presented as the mean \pm SD (N = 3). The dotted line denotes the expression of the corresponding gene in monolayer culture (1-fold change); the grey line indicates up- or downregulation of genes with the threshold set at 1.5-fold, which is more than 1.5 or less than 0.66 relative expression, respectively.

3.4.3. Expression of Genes Involved in the Xenobiotic Metabolism

Biotransformation of xenobiotic substances is divided into phase I and II reactions, where phase I reactions include the transformation of a parent compound to more polar metabolite(s), while phase II biotransformation results in metabolic inactivation by conjugating reactions including glucuronidation, sulfation, acetylation, methylation, glutathione, and amino acid conjugation. In general, the respective conjugates are more hydrophilic than the parent compounds and are excreted from the organism [72,73]. The most important enzymes from phase I reactions belong to the superfamily CYP450 and play an important role in cellular metabolism and homeostasis, and detoxification and metabolic activation of xenobiotic compounds into reactive metabolites [74,75]. In general, hepatocellular carcinoma monolayer cell cultures exhibit low expression of drug-

metabolising enzymes including CYPs and therefore, do not represent ideal alternative systems to human hepatocytes for drug metabolism and hepatotoxicity testing [76]. Recently, several published studies have described the higher expression of CYP enzymes in hepatic cells cultured in 3D conformation [6,18,21,25,28,31,35,77]. Moreover, it has been reported that HepG2 spheroids developed by the forced floating method are metabolically competent, thus expressing various CYP450 enzymes, and are sensitive for detecting the genotoxic effects of indirect-acting genotoxic compounds [35]. In the present study, we evaluated the gene expression of *CYP1A1*, *CYP1A2*, *CYP3A4*, *AHR*, and *ALDH3A1* in 3D spheroids at the age of 3, 5, 7, 10, 12, 14, and 17 days, and compared to the expression of monolayer culture at the age of 2 days (Figure 5). The results revealed that all studied CYPs were clearly upregulated in a 3D model compared to 2D (Figure 5A). The basal mRNA level of *CYP1A1* was approximately 2-fold higher than in monolayer culture and remained at the same level throughout the whole duration of the spheroid cultivation. Similarly, the expression of *CYP1A2* remained constant from day 5 onwards. *CYP3A4*, the major hepatic CYP contributing to the metabolism of more than 50% of xenobiotic substances [76], was reported not to be expressed in HepG2 cells grown in monolayer [20], which strongly limits the use of HepG2 cells for the assessment of the drug metabolism. As already previously shown [35,67,78], the results of the present study confirmed the significant upregulation of *CYP3A4* from day 3 onwards (2.16-fold) with a gradual increase in the mRNA level, reaching the highest level at day 12 (5.76-fold). Altogether, these results demonstrate that HepG2 cells grown in 3D conformation show differentiation into more metabolically competent cells when compared to monolayer cultures. The expression pattern of metabolic genes closer to primary hepatocytes has also been reported for several hepatocellular carcinoma cell lines grown under certain prolonged culturing conditions. For instance, the confluent growth of Huh7 cells resulted in a cell phenotype change and an increase in the *CYP3A4* mRNA level, protein content, and activity after 4 weeks in confluent culture [79], while differentiated HepaRG cells expressed higher levels of CYPs compared to non-differentiated [80,81]. Additionally, HepG2 cells grown in 3D conformation expressed an increased level of *CYP1A1*, *CYP1A2*, and *CYP3A4* genes [35], while HepG2/C3A cells grown in 3D under dynamic conditions for 3 weeks showed elevated expression of *CYP1A1* and *CYP3A4* [77] compared to 2D cultures.

Another phase I enzyme *ALDH3A1* (Figure 5C), a member of aldehyde dehydrogenase 3 family that catalyses the aliphatic and aromatic aldehydes to the corresponding acids [82,83], was downregulated already in 3 days old spheroids (−3.45-fold) and with further cultivation, the expression of *ALDH3A1* dropped sharply (−12.8-fold and −20-fold at 10 and 14 days, respectively). Low basal expression of *ALDH3A1* in the normal liver was reported by Muzio et al. (2012) [84], while induced levels were determined in liver, colon, bladder, and lung [82,85,86]. The results showing low gene expression are in line with the decreased proliferation of HepG2 cells in spheroids, as it is known that the activation of *ALDH3A1* stimulates the proliferation [84], thus the low mRNA level of *ALDH3A1* corroborates decreased cell proliferation and arrested cell cycle determined by the flow cytometry. The expression of drug-metabolising enzymes including *CYP1A1*, *CYP1A2*, and *ALDH3A1* is regulated by the activation of nuclear factors such as aryl hydrocarbon receptors (AhR) [87]. The basal expression of the *AHR* gene in HepG2 spheroids at the age of 3 days did not significantly differ from the expression in monolayer culture; however, with further incubation, it slowly increased over the time of incubation, reaching the maximal level (1.41-fold) at 17 days. Altogether, the obtained results are in line with the findings of Ramaiahgari et al. (2014) [31], Shah et al. (2018) [28], and Štampar et al. (2019 [35]; 2020 [77]), who described that HepG2 spheroids express higher mRNA levels of phase I metabolic enzymes, which is an important physiological function of hepatic cells in vivo [88].

The enzymes from phase II drug metabolism represent the detoxification step of xenobiotic compounds with the main pathway by the formation of glucuronide conjugates by glucuronosyltransferases (UGTs). In HepG2 spheroids (Figure 5B), the basal mRNA level of *UGT1A1* compared to monolayer culture showed great upregulation from day 3 onwards that was time-dependent, reaching a maximal level at day 12 (5.74-fold). Subsequently, the *UGT1A1* mRNA level decreased (4.13-fold at day 14) and remained constant during further cultivation. Time-dependent

elevation of *UGT1A1* expression in HepG2 spheroids was already previously reported by Ramaiahgari et al. (2014) [31] and Štampar et al. (2019) [35]. For the gene *UGT2B7*, slight but not significant upregulation was detected at day 3 (1.49-fold); however, its expression did not increase with time. Previously, it has been demonstrated that dynamic HepG2/C3A spheroids expressed an increased mRNA level of *UGT2B7* after three weeks of culturing [77]. In addition to glucuronidation, sulfonation is very important in the biotransformation of xenobiotics [89], where sulfotransferases (SULTs) catalyse the sulfate conjugation of a variety of exogenous chemicals and endobiotics using 3'-phosphoadenosine-5'-phosphosulfate as the donor [90]. On the other hand, in the reaction, pro-carcinogens are converted into highly reactive intermediates that can act as chemical mutagens and carcinogens by covalently binding to DNA [91]. The results showed that the mRNA level of *SULT1B1* was significantly upregulated (2.89-fold) already after 3 days of culturing; however, the expression was downregulated after prolonged cultivation (−2.13 fold and −3.33-fold at 12 and 17 days, respectively). On the contrary, *SULT1C2* was significantly elevated already at day 3 (3.09-fold) and the expression sharply increased with time (6.16-fold by day 17). Another important group of phase II enzymes is *N*-acetyltransferases (NAT) that catalyse the activation of aromatic and heterocyclic amines via *O*-acetylation, while *N*-acetylation of the parent amines is considered a detoxification step [73]. The gene encoding *NAT1* was not importantly deregulated in HepG2 spheroids—at most, it was slightly downregulated (−1.5-fold at day 17). In contrast, the expression of *NAT2* was significantly elevated with the highest expression observed at day 12 (3.95-fold). Transcriptomic analyses revealed that in dynamic HepG2/C3A spheroids, *NAT1* was not importantly deregulated when compared to 2D culture, while *NAT2* was significantly downregulated in 25 days old culture [77]. NATs are substrate-specific and have distinct tissue distribution, where *NAT1* has a ubiquitous tissue distribution and its expression is related to cancers, while *NAT2* activity has been described in the liver, colon, and intestinal epithelium [73]. In the present study, many crucial genes that are involved in the activation and detoxification of xenobiotic substances and are in HepG2 monolayer cultures expressed at a very low rate, or are even not detectable, were clearly expressed in HepG2 3D spheroids.

In a study on HepG2 spheroids, Elenberger et al. (2018), based on ultrastructural and organotypic functional investigations, identified clearly different phases of HepG2 spheroids, including an early phase (day 3 to 6), mid-stage phase (day 6 to 12), and late phase (day 15 to 18), all showing significant differences in cell-to-cell interactions, specialised microstructures such as the formation of bile canaliculi, and metabolic activities including albumin and urea secretion. Similarly, the results of the present study suggested three stages of spheroid formation; the early stage at the age of 3–6 days, mid-stage at the age of 7–12 days, and the late stage at the age of >14 days. In HepG2 spheroids, the expression of hepatic markers and metabolic genes from phases I and II changed over time of cultivation with important changes observed by day 7. The highest mRNA levels for the majority of metabolic genes were noticeable at 10 to 12 days, which, with further cultivation, gradually declined, suggesting that the aforementioned cultivation time is long enough for HepG2 cell differentiation and the development of a metabolically competent cell model with the quantitative and qualitative expression of phase I and II metabolic enzymes compared to a 2D cell model. In addition to metabolic activity, we noticed an important change in cell proliferation at day 7 with a slight increase in cell death, which turned out to be significant after 10 days of cultivation. Taken together, our study demonstrated that the spheroidal age needs to be considered as an important parameter in the development of spheroid-based in vitro models.

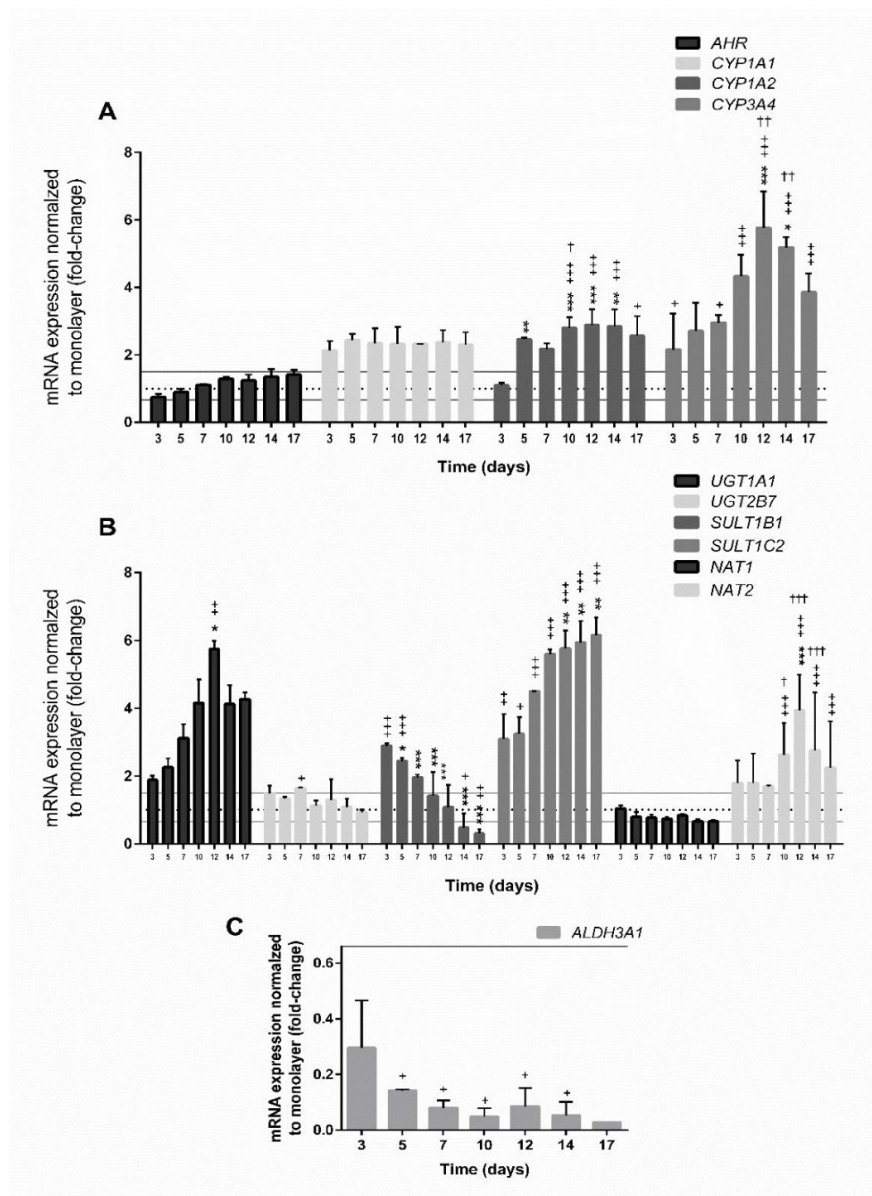


Figure 5. The mRNA expression of selected genes involved in the I (A) and II (B-C) phase of metabolism over time from day 3 to day 17. The significant difference between (i) the monolayer culture (2D) and the spheroids (3D) (+ $p < 0.05$, ++ $p < 0.01$, +++ $p < 0.001$); (ii) the first day (at day 3) of measurement and all subsequent days (* $p < 0.05$, ** $p < 0.01$, *** $p < 0.001$); and (iii) within days (+ $p < 0.05$, ++ $p < 0.01$, +++ $p < 0.001$) was calculated in GraphPad Prism 6, by two-way ANOVA considering Dunnett's multiple comparisons test. Results are presented as the mean \pm SD (N = 3). The dotted line denotes the expression of the corresponding gene in monolayer culture (1-fold change), the grey line indicates up- or downregulation of genes with the threshold set at 1.5-fold, which is more than 1.5 or less than 0.66 relative expression, respectively.

4. Conclusions

In vitro, 3D cell models compared to traditional monolayer cultures better resemble the cell organisation of tissues and organs and thus, more accurately mimic the in vivo microenvironment. In recent years, they have also become a promising tool in the field of genetic toxicology in order to reduce, replace, and refine animal experiments. Nevertheless, before 3D models can be routinely used for genotoxicity assessment, they have to be comprehensively characterised and growth conditions need to be optimised to allow for the reproducibility and comparability of the results. Furthermore, systematic characterisation allows us to identify all the crucial advantages and disadvantages, which is of high importance for the further use of the new 3D models. To our knowledge, the present study is the first where a 3D HepG2 cell model was systematically characterised and standardised including advanced cell cycle and proliferation analysis by flow cytometry, and gene expressions. In the present work, we developed uniform 3D HepG2 spheroids of similar size and shape grown under static conditions. The influence of spheroidal age on cell proliferation and metabolic status was studied over a 17-day cultivation period to gain a deeper understanding of the morphological and physiological characteristics of HepG2 spheroids. Based on new knowledge obtained within our study, we can conclude that the initial cell density for the formation of spheroids is very important in order to obtain spheroids with viable dividing cells, which is a prerequisite for studying the adverse geno-/toxic effects, as a division of cells is necessary for damage to be incorporated into DNA. Compared to the 2D monolayer cultures, HepG2 spheroids showed a time-dependent reduction in cell proliferation with cell division arrested in the G0/G1 phase of the cell cycle. Moreover, the spheroids revealed increased liver-specific functions and demonstrated strong physiological relevance concerning gene expression of hepatic markers and metabolic enzymes, in particular for sulfotransferases in phase II, thus indicating differentiation into more metabolically competent cells; this, however, has to be further confirmed at the protein level. We believe that the 3D HepG2 cell model with characterised cell growth and proliferation, as well as known expression of hepatic markers and metabolic enzymes, will contribute to a more reliable assessment of genotoxic activity of chemicals, due to its higher physiological relevance for human exposure and may, therefore, provide an alternative to animal models, which comply with the 3Rs policy to reduce in vivo testing.

Supplementary Materials: The following are available online at www.mdpi.com/2073-4409/9/12/2557/s1, Figure S1: The growth and morphology of spheroids (planimetry) monitored during 7 days of cultivation. The surface area of spheroid size was measured every 24 h (A–B: initial density of 3000 cells/spheroid and C–D: initial density of 6000 cells/spheroid). The images were taken using an inverted microscope at 40× magnification (N = 3). Results are presented as the mean ± SD (N = 10). The statistical analysis was performed in GraphPad Prism 6, by the one-way ANOVA using the Dunnett's multiple comparisons tests, ** $p < 0.01$, *** $p < 0.001$.

Author Contributions: Conceptualization: B.Ž., M.Š.; methodology: M.Š., B.B., B.Ž.; software: M.Š., B.B.; validation: M.Š., B.Ž., B.B.; formal analysis: M.Š., B.Ž., B.B.; investigation: M.Š., B.B., B.Ž.; resources: M.F., B.Ž.; data curation: M.Š., B.Ž.; writing—original draft: M.Š., B.Ž.; writing—review and editing: M.F., B.B.; visualization: M.Š., B.B., B.Ž.; supervision: B.Ž.; project administration: B.Ž., M.F.; funding acquisition: M.F., B.Ž. All authors have read and agreed to the published version of the manuscript.

Funding: The authors acknowledge the financial support from the Slovenian Research Agency [J1-2465, P1-0245 and MR-MStampar, postdoctoral project Z3-1870-BBreznik], and COST Action CA16119 (In vitro 3-D total cell guidance and fitness).

Conflicts of Interest: The authors declare no conflict of interest.

References

1. Thummel, K. Factors influencing drug metabolism. In *xPharm: The Comprehensive Pharmacology Reference*; Elsevier: Amsterdam, The Netherlands, 2007; pp. 1–18, ISBN 9780080552323.
2. Croom, E. Metabolism of xenobiotics of human environments. In *Progress in Molecular Biology and Translational Science*; Elsevier: Amsterdam, The Netherlands, 2012; Volume 112, pp. 31–88.
3. Corvi, R.; Madia, F. In vitro genotoxicity testing—Can the performance be enhanced? *Food Chem. Toxicol.* **2017**, *106*, 600–608, doi:10.1016/j.fct.2016.08.024.

4. Pfuhler, S.; Van Benthem, J.; Curren, R.; Doak, S.H.; Dusinska, M.; Hayashi, M.; Heflich, R.H.; Kidd, D.; Kirkland, D.; Luan, Y.; et al. Use of in vitro 3D tissue models in genotoxicity testing: Strategic fit, validation status and way forward. Report of the working group from the 7th International Workshop on Genotoxicity Testing (IWGT). *Mutat. Res. Genet. Toxicol. Environ. Mutagen.* **2020**, *850–851*, 503135, doi:10.1016/j.mrgentox.2020.503135.
5. Kyffin, J.A.; Sharma, P.; Leedale, J.A.; Colley, H.; Murdoch, C.; Mistry, P.; Webb, S.D. Impact of cell types and culture methods on the functionality of in vitro liver systems – A review of cell systems for hepatotoxicity assessment. *Toxicol. In Vitro.* **2018**, *48*, 262–275, doi:10.1016/j.tiv.2018.01.023.
6. Godoy, P.; Hewitt, N.J.; Albrecht, U.; Andersen, M.E.; Ansari, N.; Bhattacharya, S.; Bode, J.G.; Bolleyn, J.; Borner, C.; Böttger, J.; et al. Recent advances in 2D and 3D in vitro systems using primary hepatocytes, alternative hepatocyte sources and non-parenchymal liver cells and their use in investigating mechanisms of hepatotoxicity, cell signaling and ADME. *Arch. Toxicol.* **2013**, *87*, 1315–1530, doi:10.1007/s00204-013-1078-5.
7. Harris, A.J.; Dial, S.L.; A Casciano, D. Comparison of basal gene expression profiles and effects of hepatocarcinogens on gene expression in cultured primary human hepatocytes and HepG2 cells. *Mutat. Res. Mol. Mech. Mutagen.* **2004**, *549*, 79–99, doi:10.1016/j.mrfmmm.2003.11.014.
8. Lecluyse, E.L. Human hepatocyte culture systems for the in vitro evaluation of cytochrome P450 expression and regulation. *Eur. J. Pharm. Sci.* **2001**, *13*, 343–368, doi:10.1016/s0928-0987(01)00135-x.
9. Fey, S.J.; Wrzesinski, K. Determination of Drug Toxicity Using 3D Spheroids Constructed From an Immortal Human Hepatocyte Cell Line. *Toxicol. Sci.* **2012**, *127*, 403–411, doi:10.1093/toxsci/kfs122.
10. Wang, Z.; Luo, X.; Anene-Nzelu, C.; Yu, Y.; Hong, X.; Singh, N.H.; Xia, L.; Liu, S.; Yu, H. HepaRG culture in tethered spheroids as an in vitro three-dimensional model for drug safety screening. *J. Appl. Toxicol.* **2015**, *35*, 909–917, doi:10.1002/jat.3090.
11. Otto, M.; Hansen, S.H.; Dalgaard, L.; Dubois, J.; Badolo, L. Development of an in vitro assay for the investigation of metabolism-induced drug hepatotoxicity. *Cell Biol. Toxicol.* **2008**, *24*, 87–99, doi:10.1007/s10565-007-9018-x.
12. Drewitz, M.; Helbling, M.; Fried, N.; Bieri, M.; Moritz, W.; Lichtenberg, J.; Kelm, J.M. Towards automated production and drug sensitivity testing using scaffold-free spherical tumor microtissues. *Biotechnol. J.* **2011**, *6*, 1488–1496, doi:10.1002/biot.201100290.
13. Guillouzo, A.; Corlu, A.; Aninat, C.; Glaise, D.; Morel, F.; Guguen-Guillouzo, C. The human hepatoma HepaRG cells: A highly differentiated model for studies of liver metabolism and toxicity of xenobiotics. *Chem. Biol. Interact.* **2007**, *168*, 66–73, doi:10.1016/j.cbi.2006.12.003.
14. Donato, M.; Tolosa, L.; Gómez-Lechón, M.J. Culture and Functional Characterization of Human Hepatoma HepG2 Cells. In *Protocols in In Vitro Hepatocyte Research*; Springer: New York, NY, USA, 2015; pp. 77–93, ISBN 9781493920747.
15. Wrzesinski, K.; Fey, S.J. After trypsinisation, 3D spheroids of C3A hepatocytes need 18 days to re-establish similar levels of key physiological functions to those seen in the liver. *Toxicol. Res.* **2013**, *2*, 123–135, doi:10.1039/c2tx20060k.
16. Waldherr, M.; Lundt, N.; Klaas, M.; Betzold, S.; Wurdack, M.; Baumann, V.; Estrecho, E.; Nalotov, A.; Cherotchenko, E.; Cai, H.; et al. Observation of bosonic condensation in a hybrid monolayer MoSe₂-GaAs microcavity. *Nat. Commun.* **2018**, *9*, 1–6, doi:10.1038/s41467-018-05532-7.
17. Duret, C.; Gerbal-Chaloin, S.; Ramos, J.; Fabre, J.-M.; Jacquet, E.; Navarro, F.; Blanc, P.; Cunha, A.S.; Maurel, P.; Daujat-Chavanieu, M.; et al. Isolation, Characterization, and Differentiation to Hepatocyte-Like Cells of Nonparenchymal Epithelial Cells from Adult Human Liver. *STEM CELLS* **2007**, *25*, 1779–1790, doi:10.1634/stemcells.2006-0664.
18. Hurrell, T.; Lilley, K.S.; Cromarty, A.D. Proteomic responses of HepG2 cell monolayers and 3D spheroids to selected hepatotoxins. *Toxicol. Lett.* **2019**, *300*, 40–50, doi:10.1016/j.toxlet.2018.10.030.
19. Bazou, D.; Coakley, W.; Hayes, A.; Jackson, S. Long-term viability and proliferation of alginate-encapsulated 3-D HepG2 aggregates formed in an ultrasound trap. *Toxicol. Vitro.* **2008**, *22*, 1321–1331, doi:10.1016/j.tiv.2008.03.014.
20. Wilkening, S.; Stahl, F.; Bader, A. Comparison of primary human hepatocytes and hepatoma cell line HepG2 with regard to their biotransformation properties. *Drug Metab. Dispos.* **2003**, *31*, 1035–1042, doi:10.1124/dmd.31.8.1035.

21. Nakamura, K.; Kato, N.; Aizawa, K.; Mizutani, R.; Yamauchi, J.; Tanoue, A. Expression of albumin and cytochrome P450 enzymes in HepG2 cells cultured with a nanotechnology-based culture plate with microfabricated scaffold. *J. Toxicol. Sci.* **2011**, *36*, 625–633, doi:10.2131/jts.36.625.
22. Chang, T.T.; Hughes-Fulford, M. Monolayer and Spheroid Culture of Human Liver Hepatocellular Carcinoma Cell Line Cells Demonstrate Distinct Global Gene Expression Patterns and Functional Phenotypes. *Tissue Eng. Part A* **2009**, *15*, 559–567, doi:10.1089/ten.tea.2007.0434.
23. Gerets, H.H.J.; Tilmant, K.; Gerin, B.; Chanteux, H.; Depelchin, B.O.; Dhalluin, S.; Atienzar, F.A. Characterization of primary human hepatocytes, HepG2 cells, and HepaRG cells at the mRNA level and CYP activity in response to inducers and their predictivity for the detection of human hepatotoxins. *Cell Biol. Toxicol.* **2012**, *28*, 69–87, doi:10.1007/s10565-011-9208-4.
24. Hughes, B. Industry concern over EU hepatotoxicity guidance. *Nat. Rev. Drug Discov.* **2008**, *7*, 719, doi:10.1038/nrd2677.
25. Bell, C.C.; Hendriks, D.F.G.; Moro, S.M.L.; Ellis, E.; Walsh, J.; Renblom, A.; Puigvert, L.F.; Dankers, A.C.A.; Jacobs, F.; Snoeys, J.; et al. Characterization of primary human hepatocyte spheroids as a model system for drug-induced liver injury, liver function and disease. *Sci. Rep.* **2016**, *6*, 25187, doi:10.1038/srep25187.
26. Ravi, M.; Paramesh, V.; Kaviya, S.; Anuradha, E.; Solomon, F.P. 3D Cell Culture Systems: Advantages and Applications. *J. Cell. Physiol.* **2015**, *230*, 16–26, doi:10.1002/jcp.24683.
27. Breslin, S.; O'Driscoll, L. Three-dimensional cell culture: the missing link in drug discovery. *Drug Discov. Today* **2013**, *18*, 240–249, doi:10.1016/j.drudis.2012.10.003.
28. Shah, U.-K.; Mallia, J.D.O.; Singh, N.; Chapman, K.E.; Doak, S.H.; Jenkins, G. A three-dimensional in vitro HepG2 cells liver spheroid model for genotoxicity studies. *Mutat. Res. Genet. Toxicol. Environ. Mutagen.* **2018**, *825*, 51–58, doi:10.1016/j.mrgentox.2017.12.005.
29. Li; Guo, Y.-H.; Li, C.-L.; Tian, T.; Nan, K.-J.; Zhao, N.; Cui, J.; Wang, J.; Zhang, W. Survival advantages of multicellular spheroids vs. monolayers of HepG2 cells in vitro. *Oncol. Rep.* **2008**, *20*, 1465–1471, doi:10.3892/or_00000167.
30. Aucamp, J.; Calitz, C.; Bronkhorst, A.J.; Wrzesinski, K.; Hamman, J.; Gouws, C.; Pretorius, P.J. Cell-free DNA in a three-dimensional spheroid cell culture model: A preliminary study. *Int. J. Biochem. Cell Biol.* **2017**, *89*, 182–192, doi:10.1016/j.biocel.2017.06.014.
31. Ramaiahgari, S.C.; Braver, M.W.D.; Herpers, B.; Terpstra, V.; Commandeur, J.N.; Van De Water, B.; Price, L.S. A 3D in vitro model of differentiated HepG2 cell spheroids with improved liver-like properties for repeated dose high-throughput toxicity studies. *Arch. Toxicol.* **2014**, *88*, 1083–1095, doi:10.1007/s00204-014-1215-9.
32. Elje, E.; Hesler, M.; Rundén-Pran, E.; Mann, P.; Mariussen, E.; Wagner, S.; Dusinska, M.; Kohl, Y. The comet assay applied to HepG2 liver spheroids. *Mutat. Res. Genet. Toxicol. Environ. Mutagen.* **2019**, *845*, 403033, doi:10.1016/j.mrgentox.2019.03.006.
33. Loessner, D.; Stok, K.S.; Lutolf, M.P.; Huttmacher, D.W.; Clements, J.A.; Rizzi, S.C. Bioengineered 3D platform to explore cell–ECM interactions and drug resistance of epithelial ovarian cancer cells. *Biomaterials* **2010**, *31*, 8494–8506, doi:10.1016/j.biomaterials.2010.07.064.
34. Wrzesinski, K. From 2D to 3D—A New Dimension for Modelling the Effect of Natural Products on Human Tissue. *Curr. Pharm. Des.* **2015**, *21*, 5605–5616, doi:10.2174/1381612821666151002114227.
35. Štampar, M.; Tomc, J.; Filipič, M.; Žegura, B. Development of in vitro 3D cell model from hepatocellular carcinoma (HepG2) cell line and its application for genotoxicity testing. *Arch. Toxicol.* **2019**, *93*, 3321–3333, doi:10.1007/s00204-019-02576-6.
36. Mandon, M.; Huet, S.; Dubreil, E.; Fessard, V.; Le Hégarat, L. Three-dimensional HepaRG spheroids as a liver model to study human genotoxicity in vitro with the single cell gel electrophoresis assay. *Sci. Rep.* **2019**, *9*, 10548, doi:10.1038/s41598-019-47114-7.
37. Hercog, K.; Štampar, M.; Štern, A.; Filipič, M.; Žegura, B. Application of advanced HepG2 3D cell model for studying genotoxic activity of cyanobacterial toxin cylindrospermopsin. *Environ. Pollut.* **2020**, *265*, 114965, doi:10.1016/j.envpol.2020.114965.
38. Eilenberger, C.; Rothbauer, M.; Ehmoser, E.-K.; Ertl, P.; Küpcü, S. Effect of Spheroidal Age on Sorafenib Diffusivity and Toxicity in a 3D HepG2 Spheroid Model. *Sci. Rep.* **2019**, *9*, 4863, doi:10.1038/s41598-019-41273-3.
39. Vinken, M.; Hengstler, J.G. Characterization of hepatocyte-based in vitro systems for reliable toxicity testing. *Arch. Toxicol.* **2018**, *92*, 2981–2986, doi:10.1007/s00204-018-2297-6.

40. Gong, X.; Lin, C.; Cheng, J.; Su, J.; Zhao, H.; Liu, T.; Wen, X.; Zhao, P. Generation of Multicellular Tumor Spheroids with Microwell-Based Agarose Scaffolds for Drug Testing. *PLoS ONE* **2015**, *10*, e0130348, doi:10.1371/journal.pone.0130348.
41. Breznik, B.; Motaln, H.; Vittori, M.; Rotter, A.; Turnšek, T.L. Mesenchymal stem cells differentially affect the invasion of distinct glioblastoma cell lines. *Oncotarget* **2017**, *8*, 25482–25499, doi:10.18632/oncotarget.16041.
42. Hercog, K.; Maisanaba, S.; Filipič, M.; Sollner-Dolenc, M.; Kač, L.; Zegura, B. Genotoxic activity of bisphenol A and its analogues bisphenol S, bisphenol F and bisphenol AF and their mixtures in human hepatocellular carcinoma (HepG2) cells. *Sci. Total Environ.* **2019**, *687*, 267–276, doi:10.1016/j.scitotenv.2019.05.486.
43. Baebler, Š.; Svalina, M.; Petek, M.; Stare, K.; Rotter, A.; Pompe-Novak, M.; Gruden, K. quantGenius: Implementation of a decision support system for qPCR-based gene quantification. *BMC Bioinform.* **2017**, *18*, 276, doi:10.1186/s12859-017-1688-7.
44. Witte, R.P.; Kao, W.J. Keratinocyte-fibroblast paracrine interaction: The effects of substrate and culture condition. *Biomaterials* **2005**, *26*, 3673–3682, doi:10.1016/j.biomaterials.2004.09.054.
45. Bokhari, M.; Carnachan, R.J.; Cameron, N.R.; Przyborski, S.A. Culture of HepG2 liver cells on three dimensional polystyrene scaffolds enhances cell structure and function during toxicological challenge. *J. Anat.* **2007**, *211*, 567–576, doi:10.1111/j.1469-7580.2007.00778.x.
46. Lee, C.-M.; Pohl, J.; Morgan, E.T. Dual Mechanisms of CYP3A Protein Regulation by Proinflammatory Cytokine Stimulation in Primary Hepatocyte Cultures. *Drug Metab. Dispos.* **2009**, *37*, 865–872, doi:10.1124/dmd.108.026187.
47. Nath, S.; Devi, G.R. Three-dimensional culture systems in cancer research: Focus on tumor spheroid model. *Pharmacol. Ther.* **2016**, *163*, 94–108, doi:10.1016/j.pharmthera.2016.03.013.
48. Mehta, G.; Hsiao, A.Y.; Ingram, M.; Luker, G.D.; Takayama, S. Opportunities and challenges for use of tumor spheroids as models to test drug delivery and efficacy. *J. Control. Release* **2012**, *164*, 192–204, doi:10.1016/j.jconrel.2012.04.045.
49. Asthana, A.; Kisaalita, W.S. Microtissue size and hypoxia in HTS with 3D cultures. *Drug Discov. Today* **2012**, *17*, 810–817, doi:10.1016/j.drudis.2012.03.004.
50. Wrzesinski, K.; Rogowska-Wrzesinska, A.; Kanlaya, R.; Borkowski, K.; Schwämmle, V.; Dai, J.; Joensen, K.E.; Wojdyla, K.; Carvalho, V.B.; Fey, S.J. The Cultural Divide: Exponential Growth in Classical 2D and Metabolic Equilibrium in 3D Environments. *PLoS ONE* **2014**, *9*, e106973, doi:10.1371/journal.pone.0106973.
51. Zaroni, M.; Piccinini, F.; Arienti, C.; Zamagni, A.; Santi, S.; Polico, R.; Bevilacqua, A.; Tesei, A. 3D tumor spheroid models for in vitro therapeutic screening: A systematic approach to enhance the biological relevance of data obtained. *Sci. Rep.* **2016**, *6*, 19103, doi:10.1038/srep19103.
52. Gaskell, H.; Sharma, P.; Colley, H.E.; Murdoch, C.; Williams, D.P.; Webb, S.D. Characterization of a functional C3A liver spheroid model. *Toxicol. Res.* **2016**, *5*, 1053–1065, doi:10.1039/c6tx00101g.
53. Luckert, C.; Schulz, C.; Lehmann, N.; Thomas, M.; Hofmann, U.; Hammad, S.; Hengstler, J.G.; Braeuning, A.; Lampen, A.; Hessel, S. Comparative analysis of 3D culture methods on human HepG2 cells. *Arch. Toxicol.* **2017**, *91*, 393–406, doi:10.1007/s00204-016-1677-z.
54. Li, L.T.; Jiang, G.; Chen, Q.; Zheng, J.N. Ki67 is a promising molecular target in the diagnosis of cancer (Review). *Mol. Med. Rep.* **2015**, *11*, 1566–1572, doi:10.3892/mmr.2014.2914.
55. Gerlach, C.; Sakkab, D.Y.; Scholzen, T.; Daßler, R.; Alison, M.R.; Gerdes, J. Ki-67 expression during rat liver regeneration after partial hepatectomy. *Hepatology* **1997**, *26*, 573–578, doi:10.1002/hep.510260307.
56. Wang, W.; Heideman, L.; Chung, C.S.; Pelling, J.C.; Koehler, K.J.; Birt, D.F. Cell-cycle arrest at G2/M and growth inhibition by apigenin in human colon carcinoma cell lines. *Mol. Carcinog.* **2000**, *28*, 102–110.
57. Bartek, J.; Lukas, J. Mammalian G1- and S-phase checkpoints in response to DNA damage. *Curr. Opin. Cell Biol.* **2001**, *13*, 738–747, doi:10.1016/s0955-0674(00)00280-5.
58. Alberts, B.; Johnson, A.; Lewis, J.; Raff, M.; Roberts, K.; Walter, P. Extracellular Control of Cell Division, Cell Growth, and Apoptosis. *Mol. Biol. Cell* **2002**, *91*, 40–53.
59. Dillehay, K.L.; Seibel, W.L.; Zhao, D.; Lu, S.; Dong, Z. Target validation and structure–activity analysis of a series of novel PCNA inhibitors. *Pharmacol. Res. Perspect.* **2015**, *3*, e00115, doi:10.1002/prp2.115.
60. Yang, C.; Su, H.; Liao, X.; Han, C.; Yu, T.; Zhu, G.; Wang, X.; Winkler, C.A.; O'Brien, S.J.; Peng, T. Marker of proliferation Ki-67 expression is associated with transforming growth factor beta 1 and can predict the prognosis of patients with hepatic B virus-related hepatocellular carcinoma. *Cancer Manag. Res.* **2018**, *10*, 679–696, doi:10.2147/cmar.s162595.

61. Zhang, D.; Liu, E.; Kang, J.; Yang, X.; Liu, H. MiR-3613-3p affects cell proliferation and cell cycle in hepatocellular carcinoma. *Oncotarget* **2017**, *8*, 93014–93028, doi:10.18632/oncotarget.21745.
62. Neubauer, E.; Wirtz, R.M.; Kaemmerer, D.; Athelou, M.; Schmidt, L.; Sanger, J.; Lupp, A. Comparative evaluation of three proliferation markers, Ki-67, TOP2A, and RacGAP1, in bronchopulmonary neuroendocrine neoplasms: Issues and prospects. *Oncotarget* **2016**, *7*, 41959–41973, doi:10.18632/oncotarget.9747.
63. Ramaiahgari, S.C.; Waidyanatha, S.; Dixon, D.; DeVito, M.J.; Paules, R.S.; Ferguson, S.S. From the Cover: Three-Dimensional (3D) HepaRG Spheroid Model With Physiologically Relevant Xenobiotic Metabolism Competence and Hepatocyte Functionality for Liver Toxicity Screening. *Toxicol. Sci.* **2017**, *159*, 124–136, doi:10.1093/toxsci/kfx122.
64. Duronio, R.J.; Xiong, Y. Signaling Pathways that Control Cell Proliferation. *Cold Spring Harb. Perspect. Biol.* **2013**, *5*, a008904, doi:10.1101/cshperspect.a008904.
65. Snoj, N.; Dinh, P.; Bedard, P.; Sotiriou, C. Molecular Biology of Breast Cancer. In *Molecular Pathology: The Molecular Basis of Human Disease*; Elsevier Inc.: Amsterdam, The Netherlands: 2009; pp. 501–517, ISBN 9780123744197.
66. Tamura, R.E.; De Vasconcellos, J.F.; Sarkar, D.; Libermann, A.T.; Fisher, P.B.; Zerbini, L.F. GADD45 Proteins: Central Players in Tumorigenesis. *Curr. Mol. Med.* **2012**, *12*, 634–651, doi:10.2174/156652412800619978.
67. Hiemstra, S.; Ramaiahgari, S.C.; Wink, S.; Callegaro, G.; Coonen, M.; Meerman, J.; Jennen, D.; Van Den Nieuwendijk, K.; Dankers, A.; Snoeys, J.; et al. High-throughput confocal imaging of differentiated 3D liver-like spheroid cellular stress response reporters for identification of drug-induced liver injury liability. *Arch. Toxicol.* **2019**, *93*, 2895–2911, doi:10.1007/s00204-019-02552-0.
68. Nakano, K.; Vousden, K.H. PUMA, a Novel Proapoptotic Gene, Is Induced by p53. *Mol. Cell* **2001**, *7*, 683–694, doi:10.1016/s1097-2765(01)00214-3.
69. Mathieu, J.; Zhou, W.; Xing, Y.; Sperber, H.; Ferreccio, A.; Agoston, Z.; Kuppusamy, K.T.; Moon, R.T.; Ruohola-Baker, H. Hypoxia-Inducible Factors Have Distinct and Stage-Specific Roles during Reprogramming of Human Cells to Pluripotency. *Cell Stem Cell* **2014**, *14*, 592–605, doi:10.1016/j.stem.2014.02.012.
70. Li, M.; Li, H.; Li, C.; Wang, S.; Jiang, W.; Liu, Z.; Zhou, S.; Liu, X.; McNutt, M.A.; Li, G. Alpha-fetoprotein: A new member of intracellular signal molecules in regulation of the PI3K/AKT signaling in human hepatoma cell lines. *Int. J. Cancer* **2011**, *128*, 524–532, doi:10.1002/ijc.25373.
71. Friedrichs, B. Th. Peters, Jr.: All about Albumin. Biochemistry, Genetics, and Medical Applications. XX and 432 pages, numerous figures and tables. Academic Press, Inc., San Diego, California, 1996. Price: 85.00 US \$. *Food/Nahrung* **1997**, *41*, 382, doi:10.1002/food.19970410631.
72. Anzenbacher, P.; Anzenbacherova, E. Cytochromes P450 and metabolism of xenobiotics. *Cell. Mol. Life Sci.* **2001**, *58*, 737–747, doi:10.1007/pl00000897.
73. Jancova, P.; Anzenbacher, P.; Anzenbacherova, E. Phase II drug metabolizing enzymes Activity and expression of detoxification enzymes: Effect of age, obesity induction and administration of plant extracts View project microflora View project PHASE II DRUG METABOLIZING ENZYMES. *Biomed. Pap. Med. Fac. Univ. Palacky Olomouc Czech Repub.* **2010**, *154*, 103–116, doi:10.5507/bp.2010.017.
74. Watkins, P.B. Role of Cytochromes P450 in Drug Metabolism and Hepatotoxicity. *Semin. Liver Dis.* **1990**, *10*, 235–250, doi:10.1055/s-2008-1040480.
75. Manikandan, P.; Nagini, S. Cytochrome P450 Structure, Function and Clinical Significance: A Review. *Curr. Drug Targets* **2018**, *19*, 38–54, doi:10.2174/1389450118666170125144557.
76. Donato, M.; Jover, R.; Gomez-Lechon, M. Hepatic Cell Lines for Drug Hepatotoxicity Testing: Limitations and Strategies to Upgrade their Metabolic Competence by Gene Engineering. *Curr. Drug Metab.* **2013**, *14*, 946–968, doi:10.2174/1389200211314090002.
77. Štampar, M.; Frandsen, H.S.; Rogowska-Wrzesinska, A.; Wrzesinski, K.; Filipic, M.; Žegura, B. Hepatocellular carcinoma (HepG2/C3A) cell-based 3D model for genotoxicity testing of chemicals. *Sci. Total. Environ.* **2020**, 143255, doi:10.1016/j.scitotenv.2020.143255.
78. Takahashi, Y.; Hori, Y.; Yamamoto, T.; Urashima, T.; Ohara, Y.; Tanaka, H. 3D spheroid cultures improve the metabolic gene expression profiles of HepaRG cells. *Biosci. Rep.* **2015**, *35*, e00208, doi:10.1042/bsr20150034.

79. Sivertsson, L.; Ek, M.; Darnell, M.; Edebert, I.; Ingelman-Sundberg, M.; Neve, E.P.A. CYP3A4 Catalytic Activity Is Induced in Confluent Huh7 Hepatoma Cells. *Drug Metab. Dispos.* **2010**, *38*, 995–1002, doi:10.1124/dmd.110.032367.
80. Kanebratt, K.P.; Andersson, T.B. Evaluation of HepaRG Cells as an in Vitro Model for Human Drug Metabolism Studies. *Drug Metab. Dispos.* **2008**, *36*, 1444–1452, doi:10.1124/dmd.107.020016.
81. Gunness, P.; Mueller, D.; Shevchenko, V.; Heinzle, E.; Ingelman-Sundberg, M.; Noor, F. 3D Organotypic Cultures of Human HepaRG Cells: A Tool for In Vitro Toxicity Studies. *Toxicol. Sci.* **2013**, *133*, 67–78, doi:10.1093/toxsci/kft021.
82. Sotiropoulou, M.; Pappas, P.; Marselos, M. Effects of 3-methylcholanthrene and aspirin co-administration on ALDH3A1 in HepG2 cells. *Chem. Biol. Interact.* **2001**, *130–132*, 235–245, doi:10.1016/s0009-2797(00)00268-4.
83. Lindahl, R. Aldehyde Dehydrogenases and Their Role in Carcinogenesis. *Crit. Rev. Biochem. Mol. Biol.* **1992**, *27*, 283–335, doi:10.3109/10409239209082565.
84. Muzio, G.; Maggiora, M.; Paiuzzi, E.; Oraldi, M.; Canuto, R. Aldehyde dehydrogenases and cell proliferation. *Free Radic. Biol. Med.* **2012**, *52*, 735–746, doi:10.1016/j.freeradbiomed.2011.11.033.
85. Holmes, R.S.; Hempel, J. Comparative studies of vertebrate aldehyde dehydrogenase 3: Sequences, structures, phylogeny and evolution. Evidence for a mammalian origin for the ALDH3A1 gene. *Chem. Biol. Interact.* **2011**, *191*, 113–121, doi:10.1016/j.cbi.2011.01.014.
86. Liu, H.; Cui, B.; Xu, Y.; Hu, C.; Liu, Y.; Qu, G.; Li, D.; Wu, Y.; Zhang, D.; Quan, S.; et al. Ethyl carbamate induces cell death through its effects on multiple metabolic pathways. *Chem. Biol. Interact.* **2017**, *277*, 21–32, doi:10.1016/j.cbi.2017.08.008.
87. Hahn, M.E. The aryl hydrocarbon receptor: A comparative perspective. *Comp. Biochem. Physiol. Part C Pharmacol. Toxicol. Endocrinol.* **1998**, *121*, 23–53, doi:10.1016/s0742-8413(98)10028-2.
88. Snykers, S.; De Kock, J.; Rogiers, V.; Vanhaecke, T. In Vitro Differentiation of Embryonic and Adult Stem Cells into Hepatocytes: State of the Art. *STEM CELLS* **2009**, *27*, 577–605, doi:10.1634/stemcells.2008-0963.
89. Gamage, N.; Barnett, A.; Hempel, N.; Duggleby, R.G.; Windmill, K.F.; Martin, J.L.; McManus, M.E. Human Sulfotransferases and Their Role in Chemical Metabolism. *Toxicol. Sci.* **2006**, *90*, 5–22, doi:10.1093/toxsci/kfj061.
90. Altmann, B.; Ahrens, R.; Welle, A.; Dinglreiter, H.; Schneider, M.; Schober, A. Microstructuring of multiwell plates for three-dimensional cell culture applications by ultrasonic embossing. *Biomed. Microdevices* **2012**, *14*, 291–301, doi:10.1007/s10544-011-9605-8.
91. Song, N.R. Bioactivation of benzylic and allylic alcohols via sulfo-conjugation. *Chem. Biol. Interact.* **1998**, *109*, 221–235, doi:10.1016/s0009-2797(97)00134-8.

Publisher’s Note: MDPI stays neutral with regard to jurisdictional claims in published maps and institutional affiliations.



© 2020 by the authors. Licensee MDPI, Basel, Switzerland. This article is an open access article distributed under the terms and conditions of the Creative Commons Attribution (CC BY) license (<http://creativecommons.org/licenses/by/4.0/>).

2.2 Development of In Vitro 3D Cell Model from Hepatocellular Carcinoma (HepG2) Cell Line and its Application for Genotoxicity Testing

Martina ŠTAMPAR, Jana TOMC, Metka FILIPIČ and Bojana ŽEGURA

Archives of Toxicology 2019; 93(11): 3321-3333. DOI: 10.1007/s00204-019-02576-6.



Development of in vitro 3D cell model from hepatocellular carcinoma (HepG2) cell line and its application for genotoxicity testing

Martina Štampar^{1,2} · Jana Tomc^{1,2} · Metka Filipič¹ · Bojana Žegura¹

Received: 3 July 2019 / Accepted: 17 September 2019
© Springer-Verlag GmbH Germany, part of Springer Nature 2019

Abstract

The evaluation of genotoxicity plays an important role within hazard identification and risk assessment of chemicals and consumer products. For genotoxicity assessment, in vitro hepatic cells are often used as they have retained certain level of xenobiotic metabolic activity. However, current protocols are designed for the use on 2D monolayer models that are associated with several limitations due to the lack of numerous biological functions, which results in the loss of many hepatic properties. In this respect, an attractive alternative are three-dimensional (3D) models. The aim of our study was to develop physiologically more relevant 3D cell model (spheroids) from the human hepatocellular carcinoma (HepG2) cell line for genotoxicity testing. The spheroids were prepared by the forced floating method, which had been optimized for the production of a large number of uniform spheroids. The sensitivity of the spheroids to detect genotoxicity was determined by the comet assay after the exposure of spheroids to non-cytotoxic concentrations of model indirect acting genotoxic compounds, namely polycyclic aromatic hydrocarbon (B(a)P), mycotoxin (AFB1), two heterocyclic aromatic amines (PhIP and IQ) and a direct acting etoposide (ET). All five tested compounds concentration dependently induced DNA damage. Higher sensitivity of 3D cell model compared to 2D monolayer culture was noticed particularly for detection of the genotoxicity of the heterocyclic aromatic amines and BaP. Deregulation of mRNA expression (qPCR) by genotoxic compounds revealed that HepG2 cells in 3D express important genes encoding phase I and II metabolic enzymes, as well as DNA damage responsive genes in an inducible form. The newly developed HepG2 3D model shows improved sensitivity for detecting genotoxic compounds compared to 2D cultures and can provide a suitable experimental model for genotoxicity assessment.

Keywords In vitro 3D cell model · Genotoxic · Comet assay · Gene expression

Introduction

Human exposure to genotoxic chemicals is of particular concern as they induce DNA-damage that is considered to play a crucial role in the etiology of diseases including cancer, infertility, malformation in the offspring, arthritis and other human disorders (Altindag et al. 2007; Hoeijmakers 2009). Therefore, for human hazard and risk assessment genotoxicity data are obligatory for newly developed chemicals and products such as drugs, cosmetics, food and feed additives, pesticides etc. (Corvi and Madia 2017). The guidelines for genotoxicity testing require in the first stage a battery of in vitro tests with bacteria and mammalian cells, and when positive results are obtained, follow-up experiments with rodents are conducted. However, evidence is accumulating that currently used in vitro genotoxicity test systems are not sufficiently reliable since the indicator cells do not reflect

Electronic supplementary material The online version of this article (<https://doi.org/10.1007/s00204-019-02576-6>) contains supplementary material, which is available to authorized users.

✉ Bojana Žegura
bojana.zegura@nib.si
Martina Štampar
martina.stampar@nib.si
Jana Tomc
jana.tomc@gmail.com
Metka Filipič
metka.filipic@nib.si

¹ Department of Genetic Toxicology and Cancer Biology, National Institute of Biology, Večna pot 111, 1000 Ljubljana, Slovenia

² Jozef Stefan International Postgraduate School, Ljubljana, Slovenia

the metabolism of chemicals in human body and often the obtained results are misleading. Consequently, *in vivo* experiments have to be performed, which are in addition to being costly associated with ethical issues. Nowadays, EU legislation regulates the use of laboratory animals in order to protect their wellbeing and welfare [Directive on the protection of animals used for scientific purposes (2010/63)].

Human primary hepatocytes are generally considered as the gold standard for chemical metabolism and toxicity studies (LeCluyse 2001); however, their limited availability, short life span, genetic and metabolic inter-donor differences, rapid dedifferentiation, loss of hepatocyte functions and hepatic phenotype in two-dimensional (2D) cultivation as well as relatively high cost represent a significant limitation for routine *in vitro* genotoxicity testing (Gomez-Lechon et al. 2004; den Braver-Sewradj et al. 2016). In the attempts to develop more predictive *in vitro* genotoxicity models several human hepatic tumor cell lines including HepG2 (Majer et al. 2004), C3A (Fey and Wrzesinski 2012), HepaRG (Le Hégarat et al. 2014), Huh6 (Waldherr et al. 2018) and others, have been demonstrated to express certain xenobiotic metabolizing enzymes and are able to detect genotoxic effects of certain genotoxic compounds that require enzymatic activation when tested *in vitro*. However, compared to normal liver cells the expression levels of key metabolic enzymes are generally much lower in these cell lines (Wilkening et al. 2003; Guo et al. 2011; Gerets et al. 2012). Traditionally, these *in vitro* cell based assays are performed using two-dimensional (2D) monolayer cells cultures, which poorly reflect *in vivo* conditions. In 2D monolayer cultures the cells lack numerous biological functions like cell–cell and cell–matrix contacts, which results in decreased cell differentiation, flattened morphology of cells with altered cytoskeleton, reduced viability, and altered cell signalling pathways and most importantly reduction or loss of many hepatic enzymes involved in metabolism of xenobiotic substances (Edmondson et al. 2014; Wrzesinski and Fey 2015). It is increasingly recognized that cells grown in a three dimensional (3D) environment more closely represent normal cellular functions due to the improved cell-to-cell and cell-to-matrix interactions, and by mimicking the *in vivo* architecture of natural tissues and organs (Zhang and Yang 2011; Fey and Wrzesinski 2012; Gunness et al. 2013). Moreover, 3D cell cultures can be grown undisturbed over a longer period of time compared to monolayer cultures, which makes them an appropriate model for long-term repeated dose studies (Wong et al. 2011). Therefore, tremendous effort has been put into the development of a variety of 3D cell models, which hold the promise for applications in drug discovery, cancer cell biology, stem cell research, safety studies and many other cell-based analyses to bridge the traditional 2D monolayer cell culture models and whole-animal systems.

The aim of the present study was to develop and optimize the technique and culture conditions for obtaining a viable hepatic 3D cell culture model (spheroid) using HepG2 cells for genotoxicity testing. The spheroids were prepared by the forced floating method. The basal gene expression of selected xenobiotic metabolic enzymes in spheroids was compared to the expression in 2D monolayer cultures. The response of 3D spheroids to model genotoxic compounds was evaluated by the comet assay that detects DNA damage and compared to the response of 2D monolayer HepG2 culture. The selected model compounds represent different classes of genotoxic carcinogens that require metabolic activation to electrophilic intermediates: polycyclic aromatic hydrocarbon benzo(a)pyrene (B(a)P), mycotoxin aflatoxin B1 (AFB1), two heterocyclic aromatic amines (PhIP and IQ) and etoposide (ET). Additionally, in 3D spheroids modulation of the expression of selected genes involved in xenobiotic metabolism and DNA damage response upon exposure to model genotoxic compounds was evaluated using the real-time quantitative PCR.

Materials and methods

Chemicals

Minimum essential medium eagle (MEME), Na-pyruvat, L-glutamine, non-essential amino acids (NEAA), NaHCO₃, penicillin/streptomycin, methylcellulose, dimethylsulphoxide (DMSO), phenazine methosulfate (PMS), benzo(a)pyrene (B(a)P, CAS-No. 50-32-8) and aflatoxin B1 (AFB1, CAS-No. 1162-65-8) were obtained from Sigma (St. Louis, MO, USA), amino-1-methyl-6-phenylimidazo[4,5-b]pyridine (PhIP, CAS-No. 105650-23-5) and 2-Amino-3-methyl-3H-imidazo[4,5-f]quinoline (IQ, CAS-No. 76180-96-6) were obtained from Toronto Research Chemicals Inc. (Canada), while etoposide (ET) was from Santa Cruz Biotechnology (St. Cruz, USA). Foetal bovine serum (FBS), trypsin–EDTA (0.25%), low melting point agarose (LMP), normal melting point agarose (NMP) and TRIzol[®] reagent were purchased from Gibco (Praisley, Scotland, UK), and CellTiter 96[®] AQueous cell proliferation assay [3-(4,5-dimethylthiazol-2-yl)-2,5-diphenyltetrazolium bromide; MTS] was from Promega, Madison, WI, USA. Ethanol, methanol and phosphate buffered saline (PBS) were obtained from PAA Laboratories (Dartmouth, NH, USA). Triton X-100 was obtained from Fisher Sciences (New Jersey, USA) and GelRed solution from Biotium (Fremont, CA), while the high capacity cDNA archive kit, TaqMan Gene Expression Assays, TaqMan PreAmp Master Mix Kit and TaqMan Universal PCR Master Mix were obtained from Applied Biosystems (New Jersey, USA). The stock solutions of B(a)P (9.9 mM), AFB1 (3.2 mM), PhIP (20 mM), IQ (100 mM), and ET

(25 mg/mL) were prepared in dimethylsulphoxide (DMSO) and were stored at -20°C .

Cell culture

HepG2 cells were obtained from the Cell bank—ATCC, HB-8065TM and were grown in MEME supplemented with 10% FBS, 100 IU/ml pen/strep, 1% NEAA, 0.1 g/mL N-pyruvate, 0.1 g/mL NaHCO₃ and 2 mM L-glutamine at 37°C in a 5% CO₂ atmosphere. Cells were routinely checked for mycoplasma using the MycoAlertTM kit from Lonza (Walkersville, MD, USA).

Generation of 3D spheroids

The spheroids were prepared with the forced floating method in 96-well U-bottom low attachment plates (Falcon, Corning Corporation, New York, USA) using growth medium supplemented with 4% methylcellulose. In each well 500–6000 cells/well were seeded and the plates were subsequently centrifuged for 1.5 h at 28°C and 850g for cells to aggregate and form spheroids that were incubated for 0–96 h at 37°C in a humidified atmosphere with 5% CO₂. The images of spheroids were taken daily for 4 days by light microscopy using a camera attached to the Ti Eclipse inverted microscope (Nikon, Japan) and NIS elements software 4.13 v (Nikon Instruments, Melville, NY, USA).

Treatment of HepG2 monolayer cultures and spheroids with model genotoxic compounds

Cells grown in a monolayer (2D) culture were prior to the treatment seeded onto 96 well plates (Corning Costar Corporation, New York, USA) at the density of 10,000 cells/well for the MTS assay and to 12 well tissue culture treated plates (Corning Costar Corporation, New York, USA) at the density of 80,000 cells/well for the comet assay. The exposure of 3-day old spheroids to tested compounds was performed in 96-well plates with one spheroid per well at the density 6000 cells/well. The monolayers and spheroids were exposed to indirect/direct acting genotoxic compounds: polycyclic aromatic hydrocarbon (B(a)P; 10, 20 and 40 μM); mycotoxin aflatoxin B1 (AFB1; 10, 20 and 40 μM); two heterocyclic aromatic amines (PhIP; 50, 100, 200 μM and IQ; 50, 100, 250 μM); and etoposide (ET; 0.17, 1.7, 17 μM) for 24 h. The concentrations of the model genotoxic compounds were selected based on our previous studies and are in the range of concentrations that did not reduce the viability of HepG2 cells in monolayer cultures by more than 30% (Pezdiric et al. 2013; Gajski et al. 2016), which is the recommended cytotoxicity limit value for testing the induction of DNA damage with the comet assay (Tice et al. 2000). In all experiments, the negative control (growth medium) and the

solvent control (medium containing DMSO) were included. The final concentration of the solvent in the solvent control medium was for each exposure adjusted according to the solvent concentration in exposure conditions.

Cell viability test

Cell viability of monolayers and spheroids after 24-h exposure to model genotoxic compounds was determined with the MTS assay according to the manufacturer's instructions (Promega) with minor modifications (Hercog et al. 2017). Briefly, after the exposure the freshly prepared mixture of MTS: PMS solution (20:1) was added to each well and incubated for additional 3 h. Afterwards, the cell viability was measured using the spectrofluorimeter (Synergy MX, BioTek, Winooski, VT, USA) at 490 nm. Three independent experiments were performed each time in 4–5 replicates where each replicate represented one well or one spheroid, respectively. Statistical significance between treated groups and the solvent control was determined by the One-way ANOVA, and $p < 0.05$ was considered as statistically significant (GraphPad Software, La Jolla, CA, USA).

Comet assay

The induction of DNA strand breaks after the exposure to model genotoxic compounds was evaluated with the comet assay according to Singh et al. (1988) with minor modifications (Waldherr et al. 2018) for the monolayer cell culture and for spheroids. Prior to performing the comet assay on spheroids the procedure for obtaining single cell suspension was optimized by mechanical degradation and enzymatic digestion. After the exposure, each spheroid was left in trypsin–EDTA (0.25%, Gibco) for 3 min and subsequently using a cut tips the spheroid was split into a single cell suspension. The viability of cells in the suspension was checked with trypan blue staining. The following steps were performed as for the monolayer cell culture. Briefly, 30 μL of cell suspension was mixed with 70 μL of 1% LMP agarose and added to the fully frosted slides that had been covered with a layer of 1% NMP agarose. The slides were lysed (0.1 M EDTA, 2.5 M NaOH, pH 10, 0.01 M Tris and 1% Triton X-100) for 1 h at 4°C , unwound and electrophoresed (300 mM NaOH, 1 mM EDTA, pH 13) for 20 min at 25 V and 300 mA (0.5–1 V/cm). The slides were then neutralized (0.4 M Tris buffer; pH 7.5) and the gels were stained with Gelred (Biotium, Fremont CA). The images were captured and analyzed using a fluorescence microscope (Eclipse 800, Nikon, Japan) equipped with a Basler camera and the image analysis software Comet IV (Perceptive Instruments, UK). One spheroid represented one unit and at least two spheroids per experimental point were analysed. Five to six independent experiments were performed wherein 50 randomly

selected nuclei were analyzed per experimental point. The results are expressed as % of tail DNA. One-way ANOVA and Dunnett's Multiple Comparison test were used to analyse the differences in the percentage of tail DNA between treatments and control and for comparing the exposed groups to the control group ($p < 0.01$ was considered as statistically significant).

The gene expression analysis

The expression of *ALBUMIN*, and selected genes involved in the xenobiotic metabolism and DNA damage response was analysed by quantitative real time PCR (qPCR). The expression of *ALBUMIN* and the basal expression of selected metabolic genes were determined in HepG2 monolayer cultures and in spheroids. Further, the induction of genes involved in the xenobiotic metabolism and DNA damage response was determined in spheroids exposed to the highest concentrations of model compounds used in this study (B(a)P: 40 μ M, AFB1: 40 μ M, PhIP: 200 μ M, IQ: 250 μ M and ET: 17 μ M). Total mRNA was isolated from a pool of 30 spheroids for each studied compound and control, using TRIzol Gibco BRL (Paisley, Scotland). Purity and concentration of isolated mRNA were determined using NanoDrop 1000 Spectrophotometer (Thermo Fischer Scientific, Wilmington, USA). The cDNA High Capacity Archive Kit was used for the reverse transcription of 1 μ g of total mRNA per sample. Quantification of selected genes was performed by using the qPCR method where TaqMan Universal PCR Master Mix and the following Taqman Gene Expression Assays were used: *ALB* (*ALBUMIN*, Hs00910225_m1), *MDM2* (oncogene, E3 ubiquitin protein ligase), Hs00234753_m1; *TP53* (tumor protein P53), Hs00153349_m1; *GADD45a* ('growth arrest and DNA damage-inducible gene, alpha'), Hs00169255_m1; *ERCC4* (excision repair cross-complementing rodent repair deficiency, complementation group 4), Hs00193342_m1; *CDKN1A* (cyclindependent kinase inhibitor 1A0), Hs00355782_m1; *UGT1A1* (UDP glucuronosyltransferase 1 family, polypeptide A1), Hs02511055_s1; *CYP1A1* (cytochrome P450 family 1 subfamily A member 1), Hs01054797_g1; *CYP1A2* (cytochrome P450 family 1 subfamily A member 2), Hs00167927_m1; *CYP3A4* (cytochrome P450 family 3 subfamily A member 4), Hs02514989_s1; *GAPDH* (Human Endogenous Controls, Cat. No: 4310884E, Applied Biosystems, USA). *GAPDH* was used as a reference gene in all experiments. To evaluate the performance of a primer set and to eliminate the effect of the inhibition, a serial of tenfold dilutions of each target gene was analysed in the control sample. The qPCR experiments were performed on VIA Real-Time PCR System machine (The Applied Biosystems™). Data were analyzed using the relative quantification according to the solvent control with an open web program quantGenius (Baebler et al. 2017).

Difference greater than 1.5-fold was considered as up/down-regulation (relative expression > 1.5 or < 0.66 , respectively). To obtain fold change from relative expression for down-regulated genes ($RE < 1$) we calculated the inverse value of the relative expression ($1/RE$). Three independent experiments were performed each time in duplicates prepared from a pool of 30 spheroids. The statistical analysis was performed by unpaired parametric *t* test analysis using the Welch's correction, without assuming an equal SD ($*p < 0.05$).

Protein expression

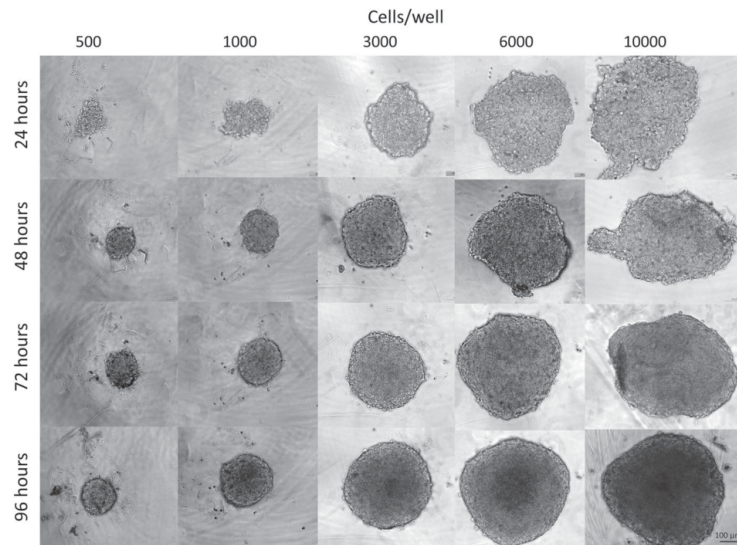
The expression of the selected proteins in spheroids was determined by western blot. The proteins were isolated from a pool of 60 spheroids for each studied compound (BaP: 40 μ M, AFB1: 40 μ M, PhIP: 200 μ M, IQ: 250 μ M and ET: 17 μ M) and control in three independent experiments. Ten μ g of total protein were applied to SDS/PAGE electrophoresis with 40% polyacrylamide gel. After the electrophoresis the gel with the resolved proteins was transferred to immune-Blot®PVDF-Membrane (162-0218, Bio-Rad). The membrane was probed with the rabbit monoclonal primary antibody against UGT1A1 (1:1000, ab170858, Abcam, UK), rabbit polyclonal primary antibody against CYP1A1 (1:500, ab79819, Abcam, UK), rabbit polyclonal primary antibody against CYP1A2 (1:1000, ab3569, Abcam, UK), rabbit polyclonal primary antibody against CYP3A4 (1:500, ab176310, Abcam, UK), rabbit polyclonal primary antibody against SULT1A1 (1:500, ab38411, Abcam, UK), mouse polyclonal primary antibody against NAT2 (1:500, 88443, Abcam, UK), and mouse monoclonal primary antibody against P53 (1:500, ab1101, Abcam, UK). GAPDH rabbit polyclonal primary antibody (1:2000, ab9485, Abcam, UK) represented the control for equal loading. The membrane was incubated with anti-rabbit (1:2500, W401B, Promega, USA) or anti-mouse (1:2500, W402, Promega, USA) secondary antibody conjugated to horseradish peroxidase. Chemiluminescence was developed by Amersham ECL detection reagent (GE Healthcare, UK) according to the manufacturer's protocol and detected with BioSpectrum Imaging System (UVP, Cambridge, UK).

Results

Characterization of spheroids

To determine the optimal condition for producing the spheroids the initial seeding cell densities were set at 500, 1000, 3000, 6000 and 10,000 cells per well. The growth of spheroids was monitored over 96 h of cultivation. At all initial seeding densities uniform spheroids were formed already after 24 h of cultivation (Fig. 1). The measurements of spheroid surface area demonstrated linear increase in the

Fig. 1 Influence of initial cell density on growth and morphology of spheroids. The HepG2 spheroids (3D) were formed from single cell suspension with different starting cell densities/well by using the forced floating method. Microscope images of spheroids taken at 24, 48, 72 and 96 h of cultivation (scale bar = 100 μ m/0.01 cm)



growth of spheroids with slightly higher growth rate at initial cell densities > 3000 cells/well (Supporting information Table S1). Based on these data spheroids produced with the starting cell density of 6000 cells/well and 72 h of cultivation were selected for further experiments.

The basal mRNA expression of *ALBUMIN* and metabolic enzymes *CYP1A1*, *CYP1A2*, *CYP3A4* was significantly higher in HepG2 cells cultivated in 3D cultures compared to 2D cultures, while the mRNA expression of *UGT1A1* was higher in 3D cultures compared to 2D, but the difference was not statistically significant (Fig. 2). In spheroids,

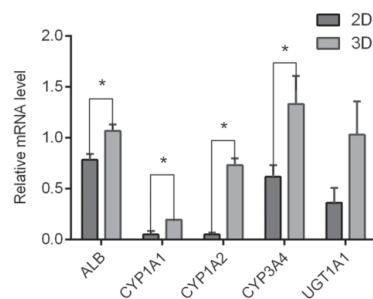


Fig. 2 Basal mRNA expression of *albumin* and genes encoding xenobiotic metabolic enzymes *CYP1A1*, *CYP1A2*, *CYP3A4* and *UGT1A1* in monolayer (2D) and spheroid (3D) HepG2 cell cultures. Results are presented as mean \pm SD of three independent biological and two technical replicates prepared. Significant difference in mRNA expression in 3D cultures compared to 2D cultures was determined with the unpaired parametric *t* test analysis using the Welch's correction, without assuming an equal SD (* $p < 0.05$)

the expression of *CYP1A1* and *CYP1A2* was more than 5 and 15-fold higher, respectively, whereas the expressions of *CYP3A4* and *UGT1A1* were approximately 2-fold higher in spheroids than in 2D monolayer cultures.

Response of 2D and 3D HepG2 cell cultures to the exposure to model genotoxic compounds

The viability of HepG2 cells grown in monolayer (2D) and spheroid (3D) culture was determined after 24 h exposure to four indirect acting model genotoxic compounds B(a)P, AFB1, PhIP and IQ and a direct ET with the MTS assay. The results of the MTS assay showed that at the applied exposure conditions the sensitivity of 2D and 3D HepG2 cell cultures towards cytotoxicity of the tested compounds is comparable (Fig. 3). In neither of the two models the cell viability was reduced by more than 30%, therefore, the same concentrations of the tested compounds were used in further experiments.

The induction of DNA strand breaks was determined with the comet assay in HepG2 cell spheroids after 24-h exposure to model genotoxic compounds, AFB1, B(a)P, PhIP, IQ and ET and was compared to the induction of DNA damage in monolayer culture under the same exposure conditions (Fig. 4). The cells in the single cell suspension were obtained from spheroids by enzymatic digestion and mechanical degradation and showed > 80% viability determined by trypan blue staining (data not shown). In the comet assay, the background level of DNA strand breaks (control) was consistently lower in 3D compared to 2D cell model. Exposure to

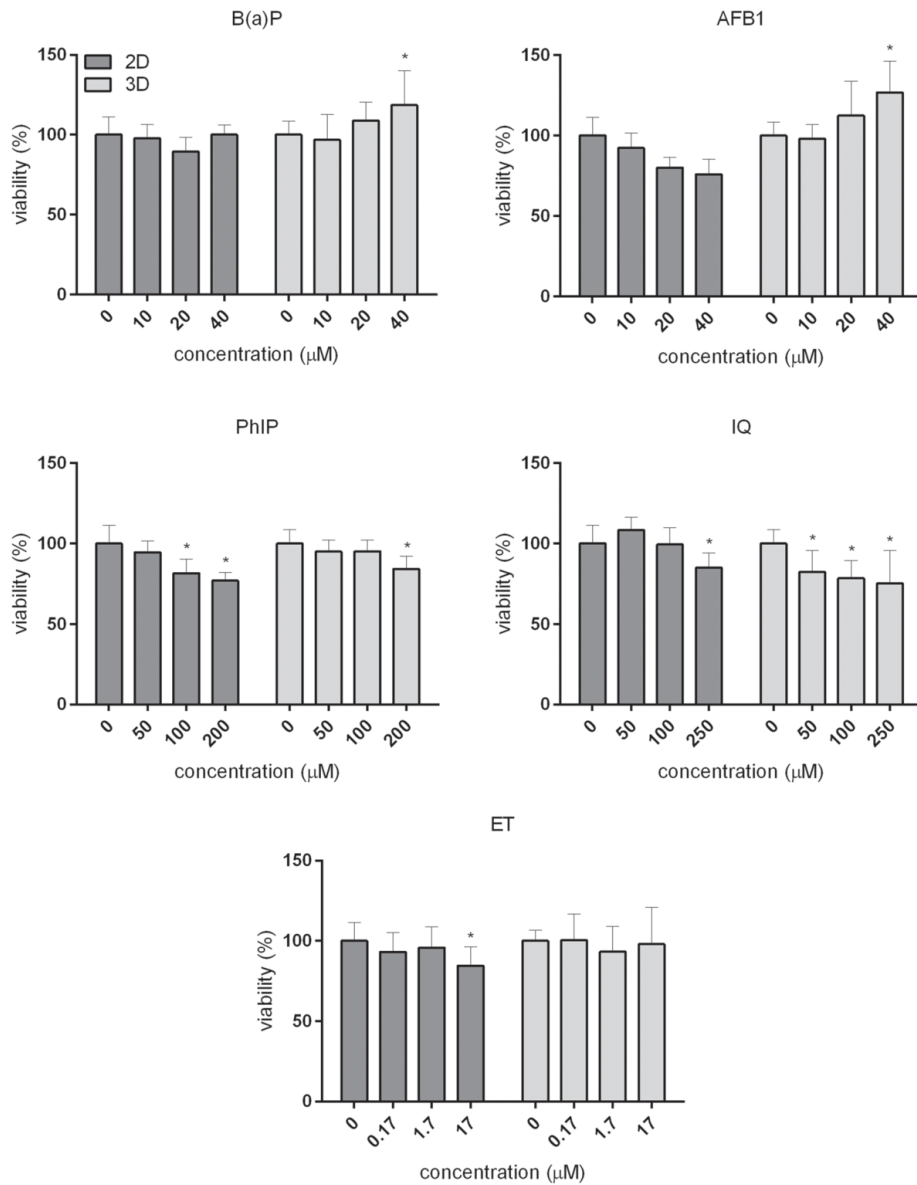


Fig. 3 The viability of HepG2 cells in monolayer (2D) culture and in spheroids (3D) after 24-h exposure to direct/indirect genotoxic compounds determined with the MTS assay. Results are presented as % viable cells \pm SD normalized to the solvent control and performed in

three independent biological with 4–5 technical replicates. The statistical analysis was performed by the one way analysis of variance—ANOVA (* $p < 0.05$, ** $p < 0.01$, *** $p < 0.001$ and **** $p < 0.0001$)

B(a)P and AFB1 induced concentration dependent increase in DNA damage in 2D and 3D models. In the 3D model, B(a)P induced significant increase in DNA damage at lower

concentration than in the 2D model ($\geq 10 \mu\text{g/mL}$ vs $\geq 20 \mu\text{g/mL}$, respectively). AFB1 induced DNA damage was in both cell models observed at $\geq 20 \mu\text{g/mL}$. The heterocyclic

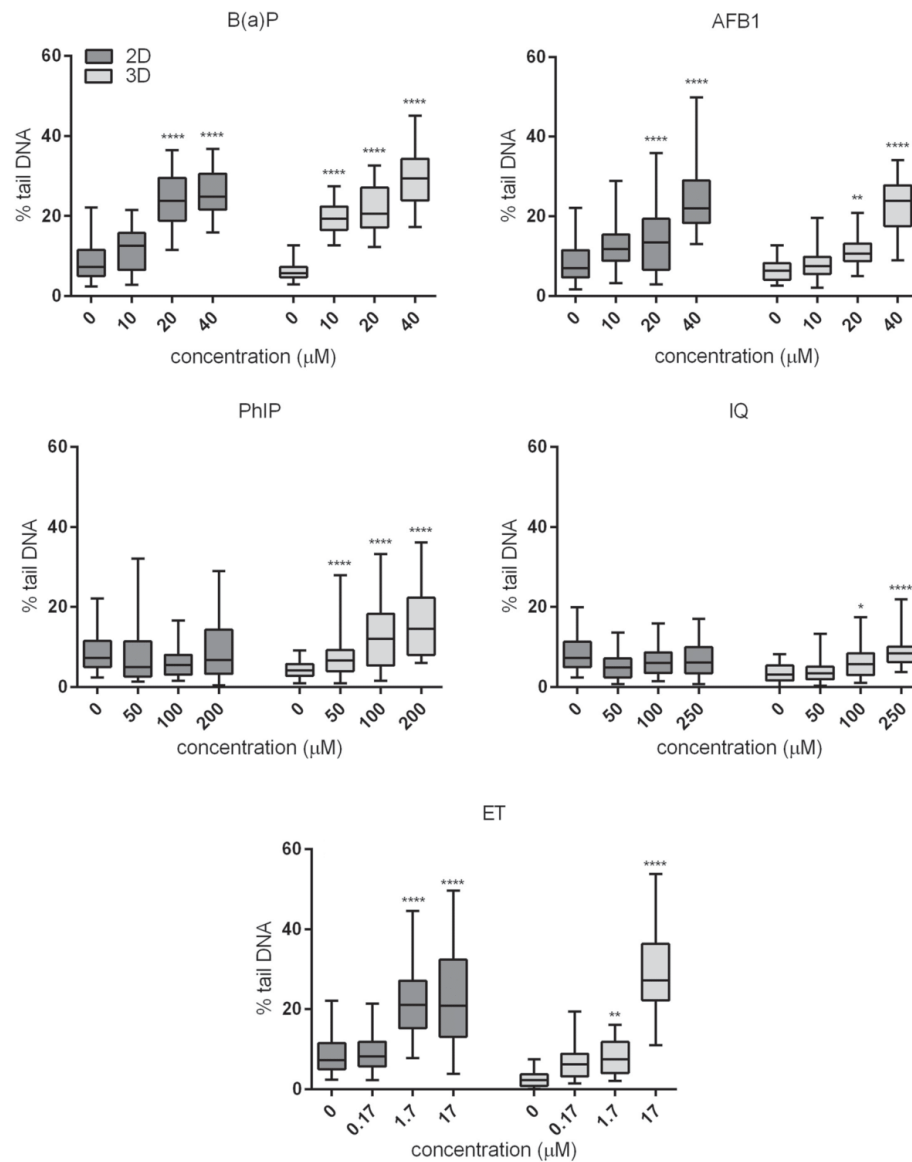


Fig. 4 The induction of DNA damage in HepG2 cell monolayer (2D) cultures and spheroids (3D) after the exposure to indirect model genotoxic compounds B(a)P, AFB1, PhIP, IQ, and direct acting ET. The cell models were exposed to graded doses of genotoxic compounds for 24 h and solvent control (0). DNA damage was determined with the comet assay and is expressed as % tail DNA. Fifty cells were ana-

lyzed per experimental point in each of the 5–6 independent experiments. The distribution of the data is presented in box-plots. Significant difference (One-way ANOVA, Dunett's test) between treated cells and the solvent control is indicated with * $p < 0.05$, ** $p < 0.01$, *** $p < 0.001$ and **** $p < 0.0001$

amines IQ and PhIP induced no increase in DNA damage in the 2D culture model, while in spheroids both compounds concentration dependently increased the amount of DNA strand breaks at concentrations $\geq 100 \mu\text{M}$ and $\geq 50 \mu\text{M}$, respectively. Etoposide, a direct acting genotoxic compound, induced DNA damage in both cell models at concentration $\geq 1.7 \mu\text{M}$. Higher level of DNA damage was observed in the 2D model compared to the 3D model; however, at the same time the background level of DNA damage was much lower in 3D cell model.

Influence of model genotoxic compounds on gene expression in HepG2 spheroids

The mRNA expression of selected genes encoding phase I and II metabolic enzymes and genes involved in DNA damage response was analyzed after 24 h of exposure of spheroids to the highest tested concentration of the model genotoxic compounds B(a)P (40 μM), AFB1 (40 μM), PhIP (200 μM), IQ (250 μM) and ET (17 μM) with qPCR. Relative quantities of mRNA of the selected genes in exposed groups compared to the solvent controls are presented in Figs. 5 and 6.

Expression of genes involved in the xenobiotic metabolism

After 24 h of exposure of spheroids to B(a)P (40 μM) the expression of *CYP1A1* (13.8-fold), *CYP1A2* (2.0-fold), *UGT1A1* (3.61-fold), *NAT1* (2.5-fold) and *SULT1B1* (1.8-fold) were up-regulated compared to control. AFB1 (40 μM) did not significantly affect the expression of genes encoding phase I enzymes (*CYP1A1*, *CYP1A2* and

Fig. 5 The mRNA expression of selected genes involved in the metabolism after 24 h exposure to model genotoxic compounds. Three independent experiments were performed each time in duplicates prepared from a pool of 30 spheroids. An up-regulation and down-regulation of ≥ 1.5 and ≤ 0.66 -fold change, respectively, compared to control was considered as positive response. The statistical analysis between cells treated with BaP, AFB1, PhIP, IQ, ET and the solvent control group was performed by the Student's *t* test ($*p < 0.05$)

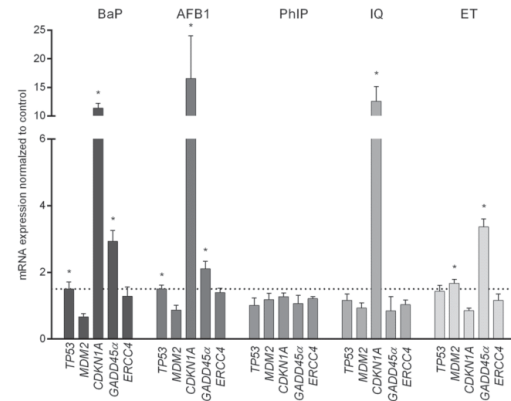
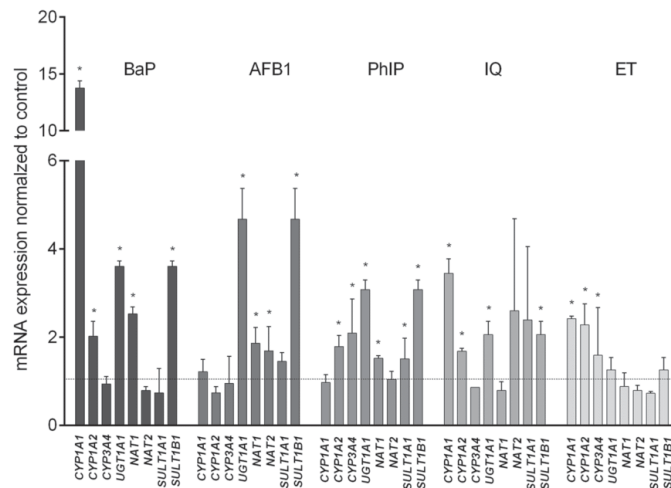


Fig. 6 The mRNA expression of selected genes involved in DNA damage response after 24 h exposure to model genotoxic compounds. Three independent experiments were performed each time in duplicates prepared from a pool of 30 spheroids. The statistical analysis was performed by Student's *t* test analysis ($*p < 0.05$). An up-regulation and down-regulation of ≥ 1.5 and ≤ 0.66 -fold change, respectively, compared to the control was considered as positive response

CYP3A4), while it significantly up-regulated the expression of genes encoding phase II enzymes: *UGT1A1* (4.7-fold), *NAT1* (1.9-fold), *NAT2* (1.7-fold) and *SULT1B1* (1.8-fold). The exposure to IQ (250 μM) up-regulated the expression of phase I metabolic genes *CYP1A1* (3.5-fold), *CYP1A2* (1.7-fold) and *CYP3A4* (2.3-fold), and phase II metabolic genes *UGT1A1* (2.1-fold), *NAT2* (2.6-fold), *SULT1A1* (2.4-fold) and *SULT1B1* (2.1-fold); however, the expressions of *CYP3A4*, *NAT2* and *SULT1A1* were not significantly different from the control. PhIP (200 μM) up-regulated the

mRNA expression of phase I metabolic genes *CYP1A2* (1.8-fold) and *CYP3A4* (2.0-fold) and phase II metabolic genes *UGT1A1* (3.0-fold), *NAT1* (1.5-fold), *SULT1A1* (1.5-fold) and *SULT1B1* (1.9-fold). The direct acting genotoxic compound ET (17 µg/mL) up-regulated studied genes encoding phase I enzymes (*CYP1A1* for 2.4-fold and *CYP1A2* for 2.3-fold). The expression of *CYP3A4* was also increased; however, difference from the control was not significant, while ET did not affect the genes encoding phase II metabolic enzymes (Fig. 5).

The protein expression was further confirmed with the Western blot analysis at the same exposure conditions (Supporting information Figure S1).

Expression of genes involved in DNA damage response

The exposure of spheroids to B(a)P and AFB1 significantly up-regulated the expression of *TP53* (1.5-fold both compounds), *CDKN1A* (11.4-fold and 16.6-fold, respectively) and *GADD45α* (2.93-fold and 2.1-fold, respectively), while the expression of *MDM2* and *ERCC4* was not affected. The heterocyclic amine IQ upregulated only the expression of *CDKN1A* (12.6-fold), while PhIP, deregulated none of the studied genes involved in DNA damage response at applied conditions. ET significantly up-regulated only *MDM2* (1.7-fold) and *GADD45α* (3.4-fold) compared to control. The mRNA expression of *ERCC4* was not affected by the exposure to any of the studied model genotoxic compounds (Fig. 6).

Discussion

Currently, the assessment of genotoxic activity of chemicals mainly relies on in vitro 2D cell models, which however, have many limitations and poor predictability for in vivo conditions (Mazzoleni et al. 2009; Soldatow et al. 2013). Thus, improved in vitro cell-based systems that will more realistically mimic in vivo cell behaviours and provide more predictive results for in vivo conditions are needed. In the present study, we developed a hepatic in vitro 3D cell model (spheroids) from HepG2 cells for the assessment of genotoxic activity of chemicals.

First, the protocol for obtaining uniform, reproducible and viable spheroids using the forced floating method with centrifugation was developed and optimized. Spheroids developed from the initial culture consisting of 6000 cells/well showed uniformity in shape and size, slow steady growth as well as high cell viability after 96 h of growth. Previously, it has been shown that cell contact inhibition in 3D cell models leads to low cell proliferation (Li et al. 2008; Shah et al. 2018), which was also observed in our newly

developed model. The forced floating method proved to be simple, easy to manipulate for experimental purposes and a low cost method that offers the advantage of obtaining a high number of uniform spheroids in a very short time. Compared to monolayer cultures the spheroids expressed higher levels of mRNA of *albumin* a typical functional characteristic of hepatocytes and xenobiotic metabolizing enzymes *CYP1A1*, *CYP1A2* and *CYP3A4* (Fig. 2), the production of which is an important physiological function of hepatocytes in vivo (Snykers et al. 2009). The result is in line with previous studies, which showed that HepG2 3D spheroids developed by the hanging-drop method exhibit higher levels of expression of genes encoding phase I and II drug metabolizing enzymes as well as xenobiotic transcription factors, and transporters compared to 2D systems (Ramaiahgari et al. 2014; Takahashi et al. 2015; Shah et al. 2018; Hurrell et al. 2019). Ramaiahgari et al. (2014) demonstrated time dependent elevation of *albumin* mRNA expression in HepG2 cell spheroids that was significantly higher than in 2D cultures after 7 days of cultivation.

The response of HepG2 spheroids to the exposure of indirect (B(a)P, AFB1, PhIP and IQ) and direct (ET) acting model compounds was determined by measuring the induction of DNA damage by the comet assay. In spheroids, after 24 h exposure to non-cytotoxic concentrations, all tested compounds induced significant, concentration dependent increase in DNA damage. Under the same exposure conditions in HepG2 monolayer cultures PhIP and IQ were inactive as has been reported before (Wilkening et al. 2003; Tomc et al. 2018) and the lowest concentration at which B(a)P induced significant increase in DNA damage was higher in 2D culture than in spheroids. The sensitivity of spheroids for the detection of genotoxic activity of AFB1 and the direct acting genotoxic ET was comparable to that of the monolayer culture. These data clearly indicate higher sensitivity of HepG2 spheroids for detecting genotoxic activity of heterocyclic aromatic amines PhIP and IQ and a polyaromatic hydrocarbon B(a)P. Recently the comet assay was applied on spheroids developed by hanging drop method and genotoxic activity of direct acting compounds alkylating agent MMS, and hydrogen peroxide was assessed (Elje et al. 2019); however, no indirect genotoxic compounds were included in the study to confirm the metabolic activity of the spheroids.

In mammalian cells most of the xenobiotic metabolizing enzymes are inducible in response to the xenobiotic exposure (Denison and Whitlock 1995; Xu et al. 2005; Westerink and Schoonen 2007). Therefore, in addition to their basal expression also their inducibility is important for proper response of exposed cells and detection of genotoxic effects of indirect acting genotoxins. The inducibility of metabolic enzymes in spheroids was investigated by measuring the changes in the mRNA expression of selected genes encoding phase I (*CYP1A1*, *CYP1A2*, *CYP3A4*) and II (*UGT1A1*,

NAT1, *NAT2*, *SULT1A1* and *SULT1B1*) enzymes after the exposure to the model genotoxic compounds. The expressions of genes *CYP1A1*, *CYP1A2* and/or *CYP3A4* were up-regulated by all studied compounds except AFB1. B(a)P is metabolically activated predominantly by *CYP1A1* in combination with microsomal epoxide hydrolase that results in the formation of DNA reactive dihydrodiol epoxides (Stiborová et al. 2014; Ewa and Danuta 2017). The representatives of heterocyclic aromatic amines, PhIP and IQ, are metabolically activated preferentially by *CYP1A* to *N*-hydroxy-HAA metabolites that are further metabolized by glucuronidases, sulfotransferases and, to a lesser extent, by *N*-acetyltransferases, to produce a DNA reactive nitrenium ion (Turesky 2010). Predominant enzymes involved in AFB1 bioactivation in human liver are *CYP1A2* and subfamily *CYP3A* that lead to the formation of DNA reactive epoxide intermediate (Kamdem et al. 2006; Lee et al. 2009), however their expression was not changed in spheroids. Numerous studies demonstrated that in animals aflatoxicosis causes decrease in cytochrome P450 activity (Guerre et al. 2000) that is partly associated with decreases in *CYP* mRNA expression in AFB1 treated rabbit hepatocytes, which may explain the observed lack of the changes in mRNA expression of *CYP1A1*, *CYP1A2* and *CYP3A4*. ET causes formation of topoisomerase II-induced DNA strand breaks by inhibiting the ability of topoisomerase II to ligate cleaved DNA molecules (Bromberg et al. 2003). Its genotoxic activity does not depend on the metabolic activation; however, ET metabolism is mediated by *CYP* enzymes (Zhou et al. 2004), which explains the observed upregulation of the gene expression of phase I enzymes. Induction of the mRNA expression of *CYP1A1*, *CYP1A2* and *CYP3A4* upon exposure to indirect acting genotoxic compounds in HepG2 2D monolayer cultures has been reported in numerous studies. However, recently Shah et al. (2018) reported significantly higher activities of *CYP1A1* and *CYP1A2* in HepG2 hanging drop spheroids compared to monolayers after exposure to BaP and PhIP that was associated with induction of higher levels of micronuclei.

Changes in the expression of genes encoding the major classes of phase II enzymes (glucuronosyltransferases; UGTs, *N*-acetyltransferases; NATs and sulfotransferases; SULTs) involved in the detoxification of xenobiotic substances (Wilkening et al. 2003; Shimada 2006) were in HepG2 spheroids deregulated after the exposure to all indirect acting genotoxic compounds [B(a)P, AFB1, PhIP and IQ]. The up-regulation of the expression of *UGT1A1* that encodes glucuronosyltransferase that catalyzes conjugation of reactive species and enables their elimination was previously reported also in HepG2 monolayer cultures (Pezdiric et al. 2013). In spheroids all indirect acting genotoxins induced up-regulation of gene expression of *N*-acetyltransferases (*NAT1* and *NAT2*) and sulfotransferases (*SULT1A1* and

SULT1B1), which was not the case in HepG2 2D monolayer cultures as reported previously (Pezdiric et al. 2013). As already mentioned sulfotransferases and *N*-acetyltransferases activate *N*-hydroxy-HAA metabolites to produce a DNA reactive nitrenium ion (Turesky 2010), which explains why PhIP and IQ genotoxic activity was detected only in spheroids. The expression of phase I and II enzymes in HepG2 spheroids after the exposure to genotoxic compounds was confirmed also at the protein level. Altogether, these results show that 3D spheroids from HepG2 cells express certain phase I and phase II metabolic enzymes that are transcriptionally induced by the exposure to indirect acting genotoxic compounds.

Chang and Hughes-Fulford (2009) investigated cellular and molecular differences between HepG2 monolayers and spheroids using the whole human genome microarray and results revealed that significantly more genes related to extracellular matrix, cytoskeleton, and cell adhesion were expressed in monolayer cells. On the other hand, they showed that genes involved in liver-specific functions of xenobiotic and lipid metabolism were upregulated in spheroids of age 3–7 days (Chang and Hughes-Fulford 2009). Similarly also Terashima et al. (2015) reported that the expression of *CYP1A1* and *CYP1A2* at mRNA and protein levels was higher in 3D spheroids compared to 2D monolayer cells (Terashima et al. 2015).

Recently, Luckert et al. (2017) described that metabolic competence of HepG2 cells is not primarily the result of 3D culture but a consequence of the duration of cultivation. They cultivated HepG2 cells for 21 days in 2D monolayer and reported that the cells exhibit comparable biochemical characteristics, *CYP* activities and gene expression patterns as 3D culture systems applied under different culture conditions (collagen sandwich, Matrigel and Alvetex scaffold) (Luckert et al. 2017). However, it has to be noted that although HepG2 cells in the mentioned study had been cultivated in a form of a monolayer cultures, after 21-days in culture the cells formed 3D structures.

When comparing the levels of the phase I and phase II enzymes in HepG2 cell line to primary human hepatocytes, it has to be noted that substantially higher gene expression levels and enzyme activities are detected in the primary cells (Wilkening et al. 2003; Westerink and Schoonen 2007; Guo et al. 2011; Gerets et al. 2012). However, the rapid decline of their functionality under in vitro culture conditions (Richert et al. 2006), polymorphism and high variability in the cell quality between different donors and very restricted availability of fresh liver tissue from healthy individuals (Gomez-Lechon et al. 2003; Godoy et al. 2013; den Braver-Sewradj et al. 2016) hinder their use for routine genotoxicity testing and screening purposes.

Genotoxic stress triggers transcriptional activation of genes regulating DNA repair, cell-cycle arrest and

apoptosis (Hollander et al. 1997). It has been demonstrated that changes in the expression of tumour suppressor *TP53* and its downstream regulated DNA damage response genes such as *CDKN1A* and *GADD45a* involved in cell cycle arrest, and *MDM2* a negative regulator of *TP53* expression, can be considered as markers of genotoxic stress (Ellinger-Ziegelbauer et al. 2005; Hreljac et al. 2008; Žegura et al. 2008; Petković et al. 2011; Štraser et al. 2011; Pezdirc et al. 2013). Statistically significant up-regulation of the *TP53* gene and protein was detected only in B(a)P and AFB1 exposed spheroids. It is known that *TP53* is usually not up-regulated at the transcription level as it is in response to DNA damage predominantly activated at the protein level, through its phosphorylation by DNA damage-responsive kinases (Zhou and Elledge 2000). The western blot analysis confirmed that all tested compounds elevated the expression of the *TP53* protein. The genes involved in cell cycle arrest were up-regulated by B(a)P, AFB1, IQ and ET. B(a)P and AFB1 up-regulated the expression of both cell cycle arrest genes *CDKN1A* and *GADD45a*, IQ elevated the expression of *CDKN1A* and ET the expression of *GADD45a*. Although the exposure to PhIP induced DNA damage in spheroids, it did not affect the expressions of the DNA damage responsive genes. Similar gene expression changes were observed in HepG2 monolayer cultures after 24 h exposure to B(a)P and IQ (Pezdirc et al. 2013). However, on the contrary to this study PhIP in 2D monolayer cultures induced an increase in the expression of *CDKN1A* and *GADD45a* (Pezdirc et al. 2013). The expression of *MDM2* was at the applied experimental conditions up-regulated only by ET. In HepG2 monolayer cultures exposure to ET in addition to the up-regulation of the expressions of *MDM2* and *GADD45* upregulated also the expression of *CDKN1A* (Novak et al. 2016). The expression of *ERCC4* that is involved in nucleotide excision repair and is regulated by transcription factor AP-1 (Christmann and Kaina 2013) was not affected by the exposure to any of the genotoxic compounds.

In vitro 3D cell models provide more accurate models of tissues and organs and better reflect physiological processes in vivo compared to 2D culture system. These systems are already applied for disease studies, pharmacokinetic studies and drug development. Despite obvious advantages of 3D models over 2D models, there have been only a few attempts to use 3D cellular systems for the genotoxicity testing (Shah et al. 2018; Reisinger et al. 2018). The exception are skin in vitro 3D models that have been developed and validated as a response to the restriction of the use of animal experiments for testing cosmetics [Regulation on cosmetic products (1223/2009)]. Thus, physiologically more relevant hepatic in vitro 3D cell models with higher expression of metabolic enzymes provide an opportunity to develop a cost-effective and reliable test system for routine genotoxicity testing applicable for a wide range of chemicals and products. This would mean that with

enhanced performance of in vitro testing battery and improved in vitro experimental models fewer in vivo follow-up studies are necessary. This complies with the 3R strategy (replace, reduce, refine) to reduce the use of animals for experimental purposes. Moreover, because of the intrinsic aberrant expression of liver functions in 2D models, the 3D models will be a valuable tool for studying the mechanisms of action of genotoxic compounds.

Conclusions

We optimized the forced floating method for the production of 3D spheroids from HepG2 cells. The method proved to be simple and enabled obtaining a high number of uniform spheroids in a very short time. The background levels of mRNA expression of albumin and selected genes encoding phase I and phase II xenobiotic metabolic enzymes were in 3D cultures significantly higher than in the 2D monolayer cultures. The results of the genotoxicity testing of selected model genotoxic compounds demonstrated that 3D spheroids are compared to traditional 2D model more sensitive for detecting DNA damage induced by certain indirect acting genotoxic compounds. Genotoxicity of heterocyclic aromatic amines PhIP and IQ was detected only in the 3D cultures, whereas genotoxicity of BaP was detected at lower concentration than in 2D culture. Upon exposure to the model genotoxic compounds the 3D spheroids from HepG2 cells responded with upregulated expression of phase I and phase II metabolic enzymes that are transcriptionally induced by the exposure to indirect acting genotoxic compounds. The developed 3D HepG2 cell model can contribute to more reliable genotoxicity assessment of chemicals and may provide the bridge between in vitro and in vivo experiments. However, prior to the routine use it has to be further optimized and validated in terms of response to different classes of genotoxic compounds as well as for detection of other genotoxicity endpoints such as induction of micronuclei.

Acknowledgements The authors acknowledge the financial support from the Slovenian Research Agency [research core funding P1-0245, J1-6730 and MR-MStampar], and COST Action CA16119 (In vitro 3-D total cell guidance and fitness) and CA15132 (The comet assay as a human biomonitoring tool).

Compliance with ethical standards

Conflict of interest The authors declare that they have no conflict of interest.

References

- Altindag O, Karakoc M, Kocyigit A et al (2007) Increased DNA damage and oxidative stress in patients with rheumatoid arthritis. *Clin Biochem* 40:167–171. <https://doi.org/10.1016/j.clinbiochem.2006.10.006>

- Baebler Š, Svalina M, Petek M et al (2017) quantGenius: implementation of a decision support system for qPCR-based gene quantification. *BMC Bioinform* 18:276. <https://doi.org/10.1186/s12859-017-1688-7>
- Bromberg KD, Burgin AB, Osheroff N (2003) A two-drug model for etoposide action against human topoisomerase II α . *J Biol Chem* 278:7406–7412. <https://doi.org/10.1074/jbc.M212056200>
- Chang TT, Hughes-Fulford M (2009) Monolayer and spheroid culture of human liver hepatocellular carcinoma cell line cells demonstrate distinct global gene expression patterns and functional phenotypes. *Tissue Eng Part A* 15:559–567. <https://doi.org/10.1089/ten.tea.2007.0434>
- Christmann M, Kaina B (2013) Transcriptional regulation of human DNA repair genes following genotoxic stress: trigger mechanisms, inducible responses and genotoxic adaptation. *Nucleic Acids Res* 41:8403–8420. <https://doi.org/10.1093/nar/gkt635>
- Corvi R, Madia F (2017) In vitro genotoxicity testing—can the performance be enhanced? NC-ND license. *Food Chem Toxicol* 106:600–608. <https://doi.org/10.1016/j.fct.2016.08.024>
- den Braver-Sewradj SP, den Braver MW, Vermeulen NPE et al (2016) Inter-donor variability of phase I/phase II metabolism of three reference drugs in cryopreserved primary human hepatocytes in suspension and monolayer. *Toxicol Vitro* 33:71–79. <https://doi.org/10.1016/j.tiv.2016.02.013>
- Denison MS, Whitlock JP (1995) Xenobiotic-inducible transcription of cytochrome P450 genes. *J Biol Chem* 270:18175–18178
- Edmondson R, Broglie JJ, Adcock AF, Yang L (2014) Three-dimensional cell culture systems and their applications in drug discovery and cell-based biosensors. *Assay Drug Technol* 12:207–218. <https://doi.org/10.1089/adt.2014.573>
- Elje E, Hesler M, Rundén-Pran E et al (2019) The comet assay applied to HepG2 liver spheroids. *Mutat Res Toxicol Environ Mutagen*. <https://doi.org/10.1016/j.mrgentox.2019.03.006>
- Ellinger-Ziegelbauer H, Stuart B, Wahle B et al (2005) Comparison of the expression profiles induced by genotoxic and nongenotoxic carcinogens in rat liver. *Mutat Res Mol Mech Mutagen* 575:61–84. <https://doi.org/10.1016/j.mrfmmm.2005.02.004>
- Ewa B, Danuta M-Š (2017) Polycyclic aromatic hydrocarbons and PAH-related DNA adducts. *J Appl Genet* 58:321–330. <https://doi.org/10.1007/s13353-016-0380-3>
- Fey SJ, Wrzesinski K (2012) Determination of drug toxicity using 3D spheroids constructed from an immortal human hepatocyte cell line. *Toxicol Sci* 127:403–411. <https://doi.org/10.1093/toxsci/ikfs122>
- Gajski G, Gerić M, Žegura B et al (2016) Genotoxic potential of selected cytostatic drugs in human and zebrafish cells. *Environ Sci Pollut Res* 23:14739–14750. <https://doi.org/10.1007/s11356-015-4592-6>
- Gerets HHJ, Tilmant K, Gerin B et al (2012) Characterization of primary human hepatocytes, HepG2 cells, and HepaRG cells at the mRNA level and CYP activity in response to inducers and their predictivity for the detection of human hepatotoxins. *Cell Biol Toxicol* 28:69–87. <https://doi.org/10.1007/s10565-011-9208-4>
- Godoy P, Hewitt NJ, Albrecht U, Andersen ME, Ansari N, Bhattacharya S, Bode JG, Bolleyn J, Borner C, Böttger J, Braeuning A, Budinsky RA, Burkhardt B, Cameron NR, Camussi G, Cho CS, Choi YJ, Craig Rowlands J, Dahmen U, Damm G, Dirsch O, Donato MT, Dong J, Dooley S, Drasdo D, Eakins R, Ferreira KS, Fonsato V, Fraczek J, Gebhardt R, Gibson A, Glanemann M, Goldring CEP, Gómez-Lechón MJ, Groothuis GMM, Gustavsson L, Guyot C, Hallifax D, Hammad S, Hayward A, Häussinger D, Hellerbrand C, Hewitt P, Hoehme S, Holzhütter HG, Houston JB, Hrach J, Ito K, Jaeschke H, Keitel V, Kelm JM, Kevin Park B, Kordes C, Kullak-Ublick GA, LeCluyse EL, Lu P, Luebke-Wheeler J, Lutz A, Maltman DJ, Matz-Soja M, McMullen P, Merfort I, Messner S, Meyer C, Mwinyi J, Naisbitt DJ, Nussler AK, Olinga P, Pampaloni F, Pi J, Pluta L, Przyborski SA, Ramachandran A, Rogiers V, Rowe C, Schelcher C, Schmich K, Schwarz M, Singh B, Stelzer EHK, Stieger B, Stöber R, Sugiyama Y, Tetta C, Thasler WE, Vanhaecke T, Vinken M, Weiss TS, Widera A, Woods CG, Xu JJ, Yarborough KM, Hengstler JG (2013) Recent advances in 2D and 3D in vitro systems using primary hepatocytes, alternative hepatocyte sources and non-parenchymal liver cells and their use in investigating mechanisms of hepatotoxicity, cell signaling and ADME. *Arch Toxicol* 87(8):1315–1530. <https://doi.org/10.1007/s00204-013-1078-5>
- Gomez-Lechon M, Donato M, Castell J, Jover R (2003) Human hepatocytes as a tool for studying toxicity and drug metabolism. *Curr. Drug Metab.* 4:292–312. <https://doi.org/10.2174/1389200033489424>
- Gomez-Lechon M, Donato M, Castell J, Jover R (2004) Human hepatocytes in primary culture: the choice to investigate drug metabolism in man. *Curr Drug Metab* 5:443–462. <https://doi.org/10.2174/1389200043335414>
- Guerre P, Pineau T, Costet P et al (2000) Effects of AFB1 on CYP1A1, 1A2 and 3A6 mRNA, and P450 expression in primary culture of rabbit hepatocytes. *Toxicol Lett* 111:243–251. [https://doi.org/10.1016/S0378-4274\(99\)00181-2](https://doi.org/10.1016/S0378-4274(99)00181-2)
- Gunness P, Mueller D, Shevchenko V et al (2013) 3D organotypic cultures of human heparg cells: a tool for in vitro toxicity studies. *Toxicol Sci* 133:67–78. <https://doi.org/10.1093/toxsci/kft021>
- Guo L, Dial S, Shi L et al (2011) Similarities and differences in the expression of drug-metabolizing enzymes between human hepatic cell lines and primary human hepatocytes. *Drug Metab Dispos* 39:528–538. <https://doi.org/10.1124/dmd.110.035873>
- Hercog K, Maisanaba S, Filipič M et al (2017) Genotoxic potential of the binary mixture of cyanotoxins microcystin-LR and cylindrospermopsin. *Chemosphere* 189:319–329. <https://doi.org/10.1016/j.chemosphere.2017.09.075>
- Hoeijmakers JHJ (2009) DNA damage, aging, and cancer. *N Engl J Med* 361:1475–1485. <https://doi.org/10.1056/NEJMr0804615>
- Hollander MC, Zhan Q, Bae I, Fornace AJ (1997) Mammalian GADD34, an apoptosis- and DNA damage-inducible gene. *J Biol Chem* 272:13731–13737
- Hreljac I, Zajc I, Lah T, Filipič M (2008) Effects of model organophosphorous pesticides on DNA damage and proliferation of HepG2 cells. *Environ Mol Mutagen* 49:360–367. <https://doi.org/10.1002/em.20392>
- Hurrell T, Lilley KS, Cromarty AD (2019) Proteomic responses of HepG2 cell monolayers and 3D spheroids to selected hepatotoxins. *Toxicol Lett* 300:40–50. <https://doi.org/10.1016/j.toxle.2018.10.030>
- Kamdem LK, Meineke I, Gödtel-Armbrust U et al (2006) Dominant contribution of P450 3A4 to the hepatic carcinogenic activation of aflatoxin B₁. *Chem Res Toxicol* 19:577–586. <https://doi.org/10.1021/tx050358e>
- Le Hégarat L, Mourou A, Huet S et al (2014) Performance of comet and micronucleus assays in metabolic competent HepaRG cells to predict in vivo genotoxicity. *Toxicol Sci* 138:300–309. <https://doi.org/10.1093/toxsci/kfu004>
- LeCluyse EL (2001) Human hepatocyte culture systems for the in vitro evaluation of cytochrome P450 expression and regulation. *Eur J Pharm Sci* 13:343–368
- Lee C-M, Pohl J, Morgan ET (2009) Dual mechanisms of CYP3A protein regulation by proinflammatory cytokine stimulation in primary hepatocyte cultures. *Drug Metab Dispos* 37:865–872. <https://doi.org/10.1124/dmd.108.026187>
- Li C-L, Tian T, Nan K-J et al (2008) Survival advantages of multicellular spheroids vs monolayers of HepG2 cells in vitro. *Oncol Rep* 20:1465–1471

- Luckert C, Schulz C, Lehmann N et al (2017) Comparative analysis of 3D culture methods on human HepG2 cells. *Arch Toxicol* 91:393–406. <https://doi.org/10.1007/s00204-016-1677-z>
- Majer BJ, Mersch-Sundermann V, Darroudi F et al (2004) Genotoxic effects of dietary and lifestyle related carcinogens in human derived hepatoma (HepG2, Hep3B) cells. *Mutat Res Mol Mech Mutagen* 551:153–166. <https://doi.org/10.1016/j.mrfmm.2004.02.022>
- Mazzoleni G, Di Lorenzo AD, Steimberg AN (2009) Modelling tissues in 3D: the next future of pharmaco-toxicology and food research? *Genes Nutr* 4:13–22. <https://doi.org/10.1007/s12263-008-0107-0>
- Novak M, Žegura B, Baebler Š et al (2016) Influence of selected anticancer drugs on the induction of DNA double-strand breaks and changes in gene expression in human hepatoma HepG2 cells. *Environ Sci Pollut Res* 23:14751–14761. <https://doi.org/10.1007/s11356-015-5420-8>
- Petković J, Žegura B, Stevanović M et al (2011) DNA damage and alterations in expression of DNA damage responsive genes induced by TiO₂ nanoparticles in human hepatoma HepG2 cells. *Nanotoxicology* 5:341–353. <https://doi.org/10.3109/17435390.2010.507316>
- Pezdirc M, Žegura B, Filipič M (2013) Genotoxicity and induction of DNA damage responsive genes by food-borne heterocyclic aromatic amines in human hepatoma HepG2 cells. *Food Chem Toxicol* 59:386–394. <https://doi.org/10.1016/j.fct.2013.06.030>
- Ramaiahgari SC, Den Braver MW, Herpers B et al (2014) A 3D in vitro model of differentiated HepG2 cell spheroids with improved liver-like properties for repeated dose high-throughput toxicity studies. *Arch Toxicol* 88:1083–1095. <https://doi.org/10.1007/s00204-014-1215-9>
- Reisinger K, Blatz V, Brinkmann J et al (2018) Validation of the 3D Skin Comet assay using full thickness skin models: transferability and reproducibility. *Mutat Res Toxicol Environ Mutagen* 827:27–41. <https://doi.org/10.1016/j.MRGENTOX.2018.01.003>
- Richert L, Liguori MJ, Abadie C et al (2006) Gene expression in human hepatocytes in suspension after isolation is similar to the liver of origin, is not affected by hepatocyte cold storage and cryopreservation, but is strongly changed after hepatocyte plating. *Drug Metab Dispos* 34:870–879. <https://doi.org/10.1124/dmd.105.007708>
- Shah UK, de Mallia JO, Singh N et al (2018) A three-dimensional in vitro HepG2 cells liver spheroid model for genotoxicity studies. *Mutat Res Genet Toxicol Environ Mutagen* 825:51–58. <https://doi.org/10.1016/j.mrgentox.2017.12.005>
- Shimada T (2006) Xenobiotic-metabolizing enzymes involved in activation and detoxification of carcinogenic polycyclic aromatic hydrocarbons. *Drug Metab Pharmacokinet* 21:257–276. <https://doi.org/10.2133/dmpk.21.257>
- Singh NP, McCoy MT, Tice RR, Schneider EL (1988) A simple technique for quantitation of low levels of DNA damage in individual cells. *Exp Cell Res* 175:184–191. [https://doi.org/10.1016/0014-4827\(88\)90265-0](https://doi.org/10.1016/0014-4827(88)90265-0)
- Snykers S, De Kock J, Rogiers V, Vanhaecke T (2009) In Vitro differentiation of embryonic and adult stem cells into hepatocytes: state of the art. *Stem Cells* 27:577–605. <https://doi.org/10.1634/stemcells.2008-0963>
- Soldatow VVY, Lecluyse EEL, Griffith LLG, Rusyn I (2013) In vitro models for liver toxicity testing. *Toxicol Res (Camb)* 2:23–39. <https://doi.org/10.1039/C2TX20051A>
- Stiborová M, Moserová M, Černá V et al (2014) Cytochrome b5 and epoxide hydrolase contribute to benzo[a]pyrene-DNA adduct formation catalyzed by cytochrome P450 1A1 under low NADPH:p450 oxidoreductase conditions. *Toxicology* 318:1–12. <https://doi.org/10.1016/j.tox.2014.02.002>
- Šraser A, Filipič M, Žegura B (2011) Genotoxic effects of the cyanobacterial hepatotoxin cylindrospermopsin in the HepG2 cell line. *Arch Toxicol* 85:1617–1626. <https://doi.org/10.1007/s00204-011-0716-z>
- Takahashi Y, Hori Y, Yamamoto T et al (2015) Three-dimensional (3D) spheroid cultures improve the metabolic gene expression profiles of HepaRG cells. *Biosci Rep*. <https://doi.org/10.1042/bsr20150034>
- Terashima J, Goto S, Hattori H et al (2015) CYP1A1 and CYP1A2 expression levels are differentially regulated in three-dimensional spheroids of liver cancer cells compared to two-dimensional monolayer cultures. *Drug Metab Pharmacokinet* 30:434–440. <https://doi.org/10.1016/J.DMPK.2015.10.001>
- Tice RR, Agurell E, Anderson D et al (2000) Single cell gel/comet assay: guidelines for in vitro and in vivo genetic toxicology testing. *Environ Mol Mutagen* 35:206–221
- Tomc J, Kološa K, Žegura B et al (2018) Adipose tissue stem cell-derived hepatic progenies as an in vitro model for genotoxicity testing. *Arch Toxicol*. <https://doi.org/10.1007/s00204-018-2190-3>
- Turesky RJ (2010) Heterocyclic aromatic amines: potential human carcinogens. In: Fishbein J (ed) *Advances in molecular toxicology*. Elsevier, Amsterdam, pp 37–83
- Waldherr M, Mišik M, Ferk F et al (2018) Use of HuH6 and other human-derived hepatoma lines for the detection of genotoxins: a new hope for laboratory animals? *Arch Toxicol* 92:921–934. <https://doi.org/10.1007/s00204-017-2109-4>
- Westerink WMA, Schoonen WGEJ (2007) Cytochrome P450 enzyme levels in HepG2 cells and cryopreserved primary human hepatocytes and their induction in HepG2 cells. *Toxicol Vitro* 21:1581–1591. <https://doi.org/10.1016/J.TIV.2007.05.014>
- Wilkening S, Stahl F, Bader A (2003) Comparison of primary human hepatocytes and hepatoma cell line HepG2 with regard to their biotransformation properties. *Drug Metab Dispos* 31:1035–1042. <https://doi.org/10.1124/dmd.31.8.1035>
- Wong SF, No DY, Choi YY et al (2011) Concave microwell based size-controllable hepatosphere as a three-dimensional liver tissue model. *Biomaterials* 32:8087–8096. <https://doi.org/10.1016/j.biomaterials.2011.07.028>
- Wrzesinski K, Fey SJ (2015) From 2D to 3D—a new dimension for modelling the effect of natural products on human tissue. *Curr Pharm Des* 21:5605–5616. <https://doi.org/10.2174/1381612821666151002114227>
- Xu C, Li CY-T, Kong A-NT (2005) Induction of phase I, II and III drug metabolism/transport by xenobiotics. *Arch Pharm Res* 28:249–268. <https://doi.org/10.1007/BF02977789>
- Žegura B, Volčič M, Lah TT, Filipič M (2008) Different sensitivities of human colon adenocarcinoma (CaCo-2), astrocytoma (IPDDC-A2) and lymphoblastoid (NCNC) cell lines to microcystin-LR induced reactive oxygen species and DNA damage. *Toxicon* 52:518–525. <https://doi.org/10.1016/j.toxicon.2008.06.026>
- Zhang X, Yang S-T (2011) High-throughput 3-D cell-based proliferation and cytotoxicity assays for drug screening and bioprocess development. *J Biotechnol* 151:186–193. <https://doi.org/10.1016/j.jbiotec.2010.11.012>
- Zhou B-BS, Elledge SJ (2000) The DNA damage response: putting checkpoints in perspective. *Nature* 408:433–439. <https://doi.org/10.1038/35044005>
- Zhou S, Koh H-L, Gao Y et al (2004) Herbal bioactivation: the good, the bad and the ugly. *Life Sci* 74:935–968. <https://doi.org/10.1016/J.LFS.2003.09.035>

Publisher's Note Springer Nature remains neutral with regard to jurisdictional claims in published maps and institutional affiliations.

2.3 HepG2 Spheroids as a Biosensor-Like Cell Based System for (Geno)toxicity Assessment (Submitted)

Martina ŠTAMPAR, Sonja ŽABKAR, Metka FILIPIČ and Bojana ŽEGURA

Submitted to the International Journal of Molecular Science



1 Article

2 HepG2 spheroids as a biosensor-like cell-based 3 system for (geno)toxicity assessment

4

5 Martina ŠTAMPAR^{1,2}, Sonja ŽABKAR, Metka FILIPIČ¹ and Bojana ŽEGURA^{1,*}

6 ¹ Department of Genetic Toxicology and Cancer Biology, National Institute of Biology, Ljubljana, Slovenia;
7 martina.stampar@nib.si; sonja.zabkar@gmail.com; metka.filipic@nib.si

8 ² Jozef Stefan International Postgraduate School, Ljubljana, Slovenia

9 * Correspondence: bojana.zegura@nib.si; Tel.: +386 5 923 28 62; ORCID: 0000-0002-5731-0785 (F.L.)

10

11 **Abstract:** In the present study, hepatic 3D spheroids developed from human hepatocellular
12 carcinoma (HepG2) cell line were used as a biosensor-like system for detection of (geno)toxic effects
13 induced by chemicals. Two genotoxic agents, benzo(a)pyrene B(a)P and amino-1-methyl-6-
14 phenylimidazo[4,5-b]pyridine (PhIP) with well-known mechanisms of action were used for the
15 validation of the system. HepG2 spheroids grown for 3 days under static conditions were exposed
16 to graded doses of BaP and PhIP for 24 and 72 hours. The planimetry (spheroid surface area) was
17 used to monitor the growth of spheroids, while the viability was assessed by confocal microscopy
18 with quantitative image analysis (Live/Dead staining of cells). Further, multi-parametric flow
19 cytometric analysis was applied for simultaneous detection of specific end-effects ranging from cell
20 cycle analysis (Hoechst staining), cell proliferation (KI67 marker), and DNA double-strand breaks
21 (γ H2AX) induced by genotoxic compounds. The results showed that BaP dose-dependently reduced
22 the growth of the spheroids and affected cell proliferation by arresting HepG2 cells in S and G2
23 phase with concomitant reduction of cell number in G1 phase depending on the concentration and
24 time of exposure. Furthermore, it induced DNA double-strand breaks (dsb) after 24 and 72 hours of
25 exposure. Simultaneous staining of γ H2AX lesions and cell cycle analysis revealed that 60 % of cells
26 in G0/G1 phase had DNA dsb after BaP (10 μ M) exposure, while after prolonged exposure only 20
27 % of cells contained DNA dsb indicating efficient repair of DNA lesions. In the case of PhIP, no
28 influence on the spheroid size was noticed; however, the accumulation of cells in G2 phase was
29 noticed after both treatment times. At the same time, the evaluation of DNA damage revealed that
30 at 200 μ M PhIP 50 % of cells in G0/G1 phase had DNA dsb that was after 72-hour exposure present
31 in approximately 40 % of cells, showing lower repair capacity as in the case of BaP. Altogether, the
32 results revealed that developed approach can due to simultaneous detection of several parameters
33 provide more insight into the mechanism of action of genotoxic compounds and can thus contribute
34 to a more reliable genotoxicity assessment of chemicals as a high-content and high-throughput
35 screening tool.

36

37 **Keywords:** *in vitro* 3D cell model, HepG2, flow cytometry, cell cycle, proliferation, γ -H2AX

38

39 1. Introduction

40 During the last decades, concern has been raised about the possible adverse genotoxic effects of
41 various compounds on human health due to increased development of new chemicals and consumer
42 products, such as drugs, cosmetics, food and feed additives and similar, which are widely used in
43 our everyday life [1]. Genetic damage is considered to be an important mechanism of toxicity [2]

44 involved in the onset of diseases such as cancer, infertility, a malformation in the offspring,
45 neurodegeneration, arthritis, and other human disorders [3–5]. Presently, genotoxicity data of
46 chemicals are as recommended by the authoritative international organizations, obtained using a
47 battery of short-term genotoxicity tests, which are usually conducted on bacteria and rodent or
48 human cell lines [6]. Positive results are then confirmed in animal models, which are many times
49 unnecessary due to often misleading results obtained with *in vitro* 2D test systems. One of the key
50 elements contributing to the relatively high proportion of false positive *in vitro* results is the
51 inadequate representation of enzymes involved in the metabolism of xenobiotic compounds in cell
52 lines used for routine genotoxicity evaluation [7]. As these cells are grown in monolayer cultures they
53 do not reflect the physiological properties of tissues and are not appropriate for prediction of *in vivo*
54 behaviour [8]. Moreover, currently used animal models, mostly rats and mice, have a weak
55 correlation with humans and thus fail to predict the human outcome, are costly, and are associated
56 with several ethical issues [9]. On the other hand, primary human hepatocytes are considered as a
57 golden standard in drug development and toxicity testing [10]; however, in 2D cultures, they rapidly
58 dedifferentiate resulting in the loss of their hepatic phenotype and functionality. Besides, they have
59 limited availability, inter-donor variability, and relatively high cost, which makes them an
60 inappropriate model for routine *in vitro* genotoxicity testing [11,12]. Thus, there is an urgent need for
61 the development of reliable and physiologically relevant, human-derived *in vitro* cell models that will
62 give predictive results for human exposures to genotoxic chemicals and will enable efficient
63 screening. Recently, the Workshop on Genotoxicity Testing (IWGT) recommended to focus on the
64 development of alternative *in vitro* 3D systems with enhanced liver-like functions to provide cost-
65 effective and reliable tools for the safety assessment of chemicals that will enable high-throughput
66 screening [13] and will follow the “3R” principles (Reduce, Refine and Replace) related to the use of
67 animals for research purposes [14]. The advantage of cells grown under 3D arrangement is the fact
68 that they are surrounded by natural extra-cellular matrix (ECM), which promotes tissue specific
69 architecture, direct cell-cell and cell-extracellular matrix interactions, and thus provides *in vivo*-like
70 environment by recapitulating structures and functionality of the native tissue [15,16]. The spheroids
71 enable prolonged exposures, due to their increased stability as they retain high cell viability and
72 morphology over several weeks [13,17–23]. Due to the improved characteristics of 3D cell models
73 over traditional 2D cell cultures, the use of liver spheroids in genetic toxicology has increased
74 markedly in the last few years. So far, the liver spheroids have been applied for detection of DNA
75 strand breaks [13,23–27] and chromosomal damage [19,28–30].

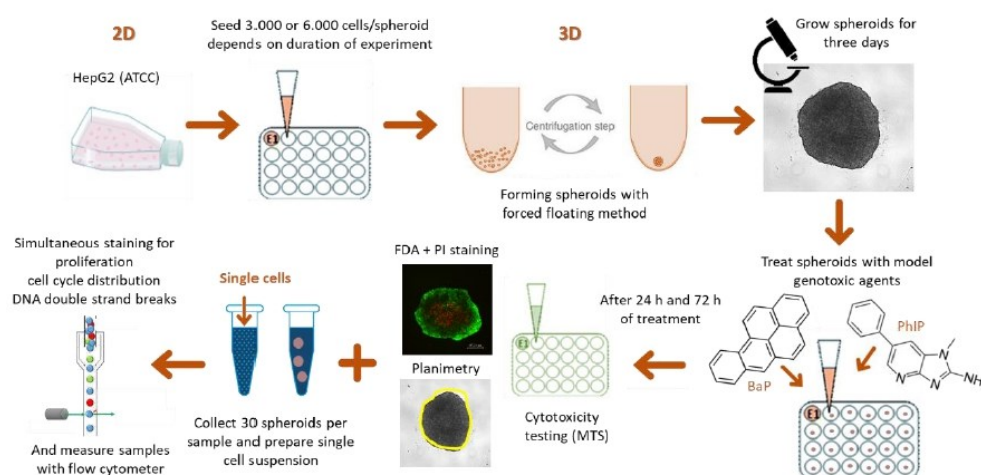
76 The threats and issues of genotoxic compounds necessitate not only a sensitive detection regimen but
77 also the employment of a rapid, broad-spectrum screening tool that can be used for high-throughput
78 detection of genotoxic agents. Therefore, in the present study, we developed a testing approach
79 utilizing *in vitro* 3D cell model combined with detection techniques based on microscopy and flow
80 cytometry. The spheroids developed from a human hepatocellular carcinoma cell line (HepG2)
81 grown under static conditions were used for detection of cytotoxic and genotoxic effects induced by
82 model indirect-acting genotoxic compounds, polycyclic aromatic hydrocarbon (BaP) and heterocyclic
83 aromatic amine (PhIP), which were used for the functional evaluation of the proposed testing
84 approach. The influence of BaP and PhIP on the spheroid growth was monitored with planimetry by
85 light microscopy, while the viability was assessed with fluorescent Live/Dead staining using FDA
86 and PI, respectively, and detected by confocal microscopy. Further, a flow cytometric approach for
87 simultaneous detection of specific lesions in the same cell ranging from cell cycle analysis (Hoechst
88 staining), cell proliferation (KI67 antibodies), and DNA double-strand breaks (γ H2AX antibodies)
89 was developed. By applying two genotoxic agents (BaP and PhIP) with well-known mechanisms of
90 action we investigated whether sensing of fluorescent signals within exposed cells corresponding to
91 specific lesions could be suited as a high-throughput screening approach for detection of (geno)toxic
92 compounds.

93

94 2. Results and discussion

95 There is an ever-increasing need for the development of fast, reliable and physiologically relevant in
96 vitro models for the safety assessment of various chemicals, and, more recently, for the screening of
97 pharmaceuticals, food and agricultural products, and environmental samples, which all emerged as
98 a major concern due to significant impact on human health. Currently, there is an ongoing trend to
99 develop standardized and robust in vitro hepatic 3D cell models, which closely resemble in vivo
100 microenvironment and can be used for toxicity assessment of critical endpoints of the above-
101 mentioned substances [2,13,26,27,31]. Moreover, it was highlighted that hepatic 3D cell models are
102 more sensitive than monolayer cultures [15,21,24,25,29,32–34]. Several studies showed that HepG2
103 spheroids represent a robust metabolically competent in vitro cell model, which can be applied for
104 the screening purposes in the (geno)toxicity assessment of various substances [24–26,35]. A huge
105 advantage of this model is the support of both acute and long-term repeated studies [23,25,29,30,36].

106 In the present study, we evaluated the sensitivity of the HepG2 spheroid model for detection of
107 cytotoxic and genotoxic activity of (geno)toxic compounds. For this purpose, we selected two model
108 indirect-acting genotoxic compounds, benzo(a)pyrene (BaP) and 2-Amino-1-methyl-6-
109 phenylimidazo[4,5-b]pyridine (PhIP), for which it is well known that they induce genotoxic effects in
110 the form of chromosomal aberrations [19,37,38] and DNA strand breaks [39,40]. To validate HepG2
111 spheroid model two approaches were used: i) three-day old spheroids were exposed to higher non-
112 cytotoxic concentrations of BaP and PhIP for 24 hours to investigate their short-term influence on the
113 cell cycle, cell proliferation and formation of DNA double-strand breaks; and ii) three-day old
114 spheroids were exposed to lower concentrations of BaP and PhIP for 72 hours to investigate the effects
115 of environmentally relevant concentrations, which are applicable for human exposure (Fig. 1). The
116 prolonged exposure allows cells to metabolize genotoxic compounds and to repair induced DNA
117 damage. Nevertheless, if DNA double-strand breaks persist in genetic material, this lesions may lead
118 to mutations, which are transmitted to the next generation of somatic cells, causing an increase in the
119 number of diseases including cancer development [41].



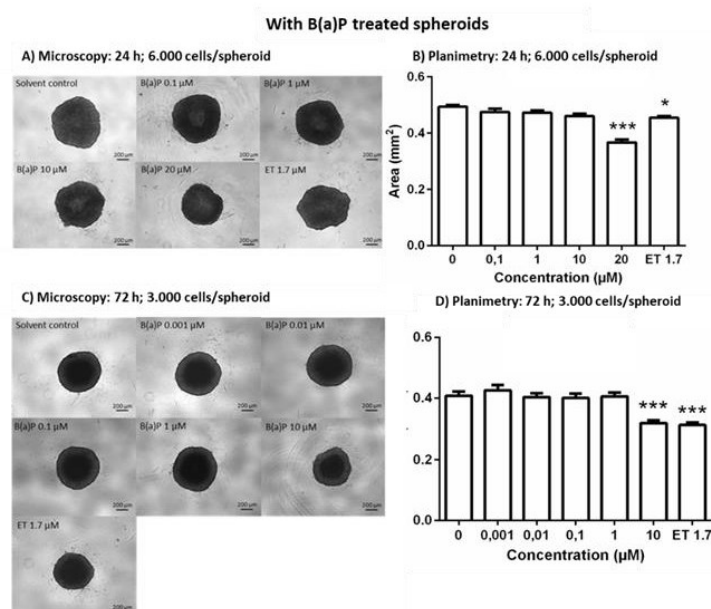
120

121 **Figure 1.** The formation of HepG2 spheroid cultures and a novel approach for testing cytotoxic and
122 genotoxic activity of (geno)toxic compounds. The HepG2 cells were seeded onto 96 microtiter plates
123 and were cultured for three days and subsequently treated with model genotoxic compounds B(a)P
124 and PhIP for additional 24 and 96 hours. After the treatment, cell viability, Live/Dead staining and
125 planimetry measurements were performed. Flow cytometric analysis was done on single-cell
126 suspension simultaneously stained for three endpoints, Hoechst for determination of the cell cycle;
127 FITC for proliferation detection and APC for detection of DNA double-strand breaks.

128 2.1. The impact of BaP and PhIP on growth and viability of HepG2 spheroids

129 The growth of spheroids was monitored after the exposure to graded concentrations of BaP for 24 h
 130 (0.1, 1, 10 in 20 μM) and 72 h (0.001, 0.01, 0.1, 1 in 10 μM) and graded concentrations of PhIP for 24 h
 131 (50, 100, 150 in 200 μM) and 72 h (25, 50, 100, 150 in 200 μM). The changes in the growth and
 132 morphology of spheroids were monitored by measuring and quantifying the average spheroid area
 133 by planimetry. After 24 hours, BaP at 20 μM statistically significantly decreased the average surface
 134 area ($0.37 \pm 0.02 \text{ mm}^2$) of spheroids (initial density of 6.000 cells/spheroid) when compared to solvent
 135 control spheroids ($0.49 \pm 0.01 \text{ mm}^2$) (Fig. 2 A-B). The positive control, etoposide (1.7 μM) decreased
 136 the average surface area to $0.46 \pm 0.02 \text{ mm}^2$. Similarly, reduced growth of spheroids with the initial
 137 density of 3.000 cells/spheroid was determined after prolonged exposure of 72 hours to BaP. The
 138 spheroid surface area significantly differed from the solvent control ($0.40 \pm 0.05 \text{ mm}^2$) at 10 μM BaP
 139 ($0.32 \pm 0.03 \text{ mm}^2$) as well as at 1.7 μM ET ($0.31 \pm 0.03 \text{ mm}^2$) (Fig. 2 C-D).

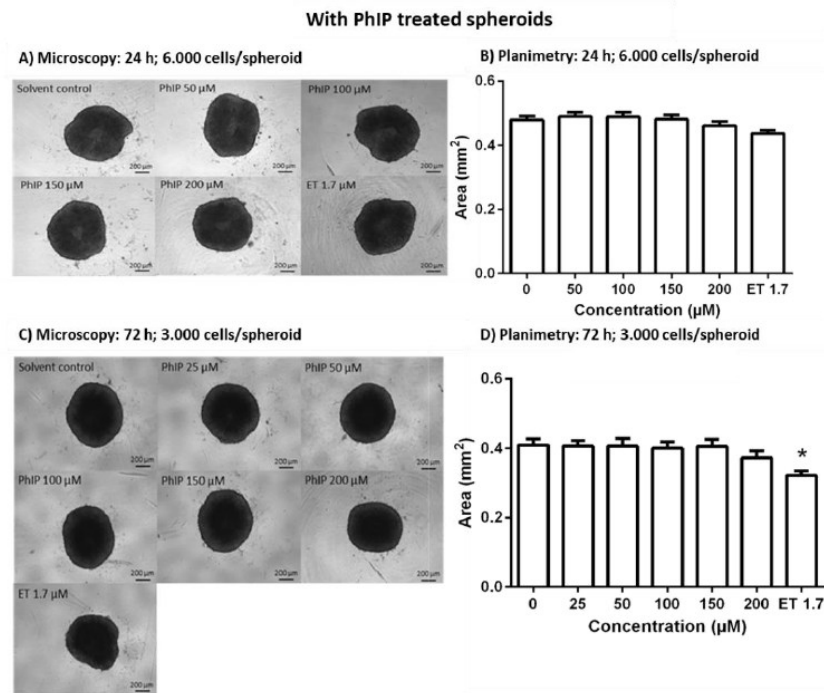
140



141

142 **Figure 2.** Planimetry of three-day-old spheroids monitored after (A-B) short-term (24 hours) and (C-
 143 D) long-term (72 hours) treatment with graded concentrations of BaP. The growth of spheroids was
 144 monitored at 10X magnification (Nikon Instruments) with the Ti Eclipse inverted microscope (Nikon).
 145 ET (1.7 μM etoposide) was a positive control. The results are presented as the mean \pm SD (N=10). The
 146 statistical analysis was conducted in Graph Pad Prism 6, by the one-way ANOVA using the Dunnett's
 147 multiple comparisons tests, * $p < 0.05$, ** $p < 0.01$, *** $p < 0.001$.

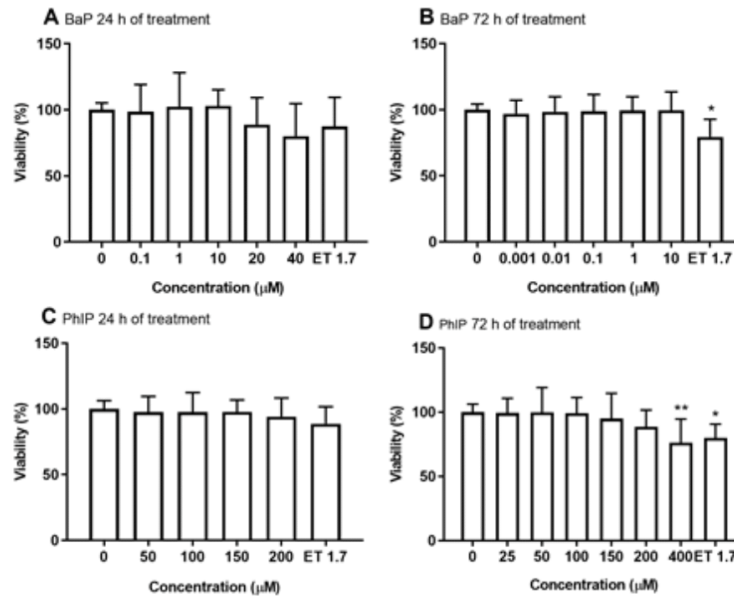
148 PhIP (50, 100, 150 and 200 μM), on the other hand, after 24 hours did not significantly influence the growth
 149 of spheroids. (Fig. 3 A-B). The average surface area of the control spheroids was $0.48 \pm 0.01 \text{ mm}^2$, while the
 150 one of the PhIP treated spheroids at 200 μM accounted for $0.46 \pm 0.03 \text{ mm}^2$ and $0.43 \pm 0.01 \text{ mm}^2$ for positive
 151 control. After prolonged (72 h) exposure of spheroids to PhIP (200 μM), a trend of reduced spheroid growth
 152 ($0.37 \pm 0.06 \text{ mm}^2$) was observed compared to solvent control ($0.41 \pm 0.05 \text{ mm}^2$) but was not statistically
 153 important (Fig. 3 C-D). The positive control (ET at 1.7 μM) significantly reduced the growth of spheroids
 154 ($0.32 \pm 0.03 \text{ mm}^2$). Similar results were reported for 21-day old HepG2/C3A spheroids grown in bioreactors
 155 under dynamic conditions that were exposed for 24 and 96 hours to BaP (40 and 4 μM , respectively) and
 156 PhIP (200 and 400, respectively) [23].



157

158 **Figure 3.** Planimetry of three-day old spheroids monitored after (A-B) short-term (24 hours) and (C-
159 D) long-term (72 hours) treatment with graded concentrations of PhIP. The growth of spheroids was
160 monitored at 10X magnification (Nikon Instruments) with the Ti Eclipse inverted microscope (Nikon).
161 ET (1.7 µM etoposide) was used as a positive control. The results are presented as the mean ± SD
162 (N=10). The statistical analysis was conducted in Graph Pad Prism 6, by the one-way ANOVA using
163 the Dunnett's multiple comparisons test, *p<0.05.

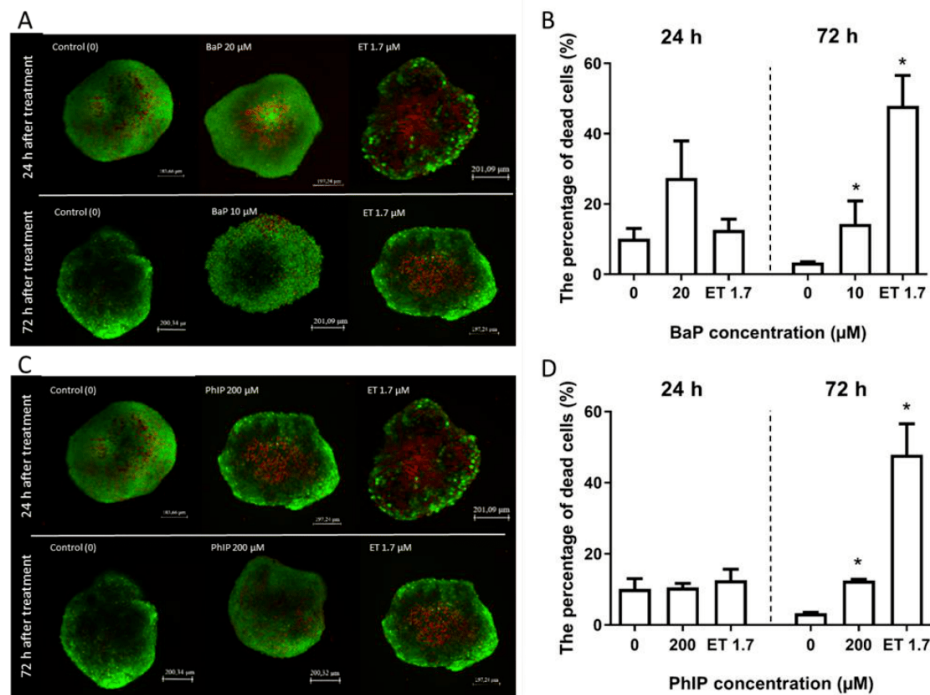
164 The impact of BaP and PhIP on spheroid's cell viability was measured with the tetrazolium-based (MTS)
165 assay (Fig. 4) and with differential staining of the whole spheroid with FDA and PI (Fig. 5). Spheroids with
166 the initial density of 6.000 and 3.000 cells/spheroid grown for 3 days were exposed to graded concentrations
167 of each compound. The MTS assay results revealed that BaP did not affect the viability of cells at applied
168 conditions (Fig. 4 A-B), which is in line with results reported by [24]. In 21-day old HepG2/C3A spheroids
169 grown in dynamic bioreactors, BaP at 40 µM and 4 µM after 24- and 96-hour exposure, respectively,
170 reduced cell viability measured by the ATP content [23], while in 10-day old HepaRG spheroids 24-hour
171 exposure to B(a)P at concentrations of up to 20 µM no effect on cell viability was reported [27]. On the other
172 hand, we showed that PhIP at 400 µM after 72-hour exposure significantly decreased cell viability in HepG2
173 spheroids for approximately 24 % (Fig. 4 D). Previously, a slight though significant decrease in cell viability
174 upon 24-hour exposure of HepG2 spheroids to PhIP (200 µM) [24] and 21-day old HepG2/C3A spheroids
175 to PhIP (400 µM) [23] was reported. In monolayer cultures, significant effects of PhIP on HepG2 cell
176 survival were also shown; however, at lower concentrations [24,38] compared to 3D cultures. A positive
177 control, etoposide (1.7 µM) after 72-hour exposure significantly reduced cell viability for approximately 20
178 % (Fig. 4 B and D).



179

180 **Figure 4.** Cell viability of HepG2 spheroids after 24 and 72 hours of exposure to graded concentrations
 181 of (A-B) BaP and (C-D) PhIP determined with the MTS assay. The results were normalized to the
 182 solvent control (0.2 % DMSO for BaP and 1 % DMSO for PhIP). Etoposide at 1.7 µM was used as a
 183 positive control. The results are given as a mean value of three independent experiments ± SD. The
 184 statistical analysis was performed by the one-way analysis of variance – ANOVA, using Dunnett’s
 185 multiple comparisons tests (*p < 0.05, ** p < 0.01).

186 Further, Live/Dead staining of the whole spheroid was conducted on spheroids treated with the highest
 187 BaP (24 h: 20 µM, 72 h: 10 µM) (Fig. 5 A-B) and PhIP (24 h: 200 µM and 72 h: 200 µM) concentration (Fig. 5
 188 C-D). After quantification of fluorescent images, where red fluorescently stained nuclei are used to estimate
 189 dead cells and green fluorescently stained cells present the total number of live cells, an increased
 190 percentage of dead cells was determined at 20 µM BaP after 24-hour exposure, but was not significantly
 191 different from the control spheroids, while significant increase compared to control was determined after
 192 96-hour exposure to 10 µM BaP. No increased red fluorescence corresponding to dead cells was notified
 193 after 24-hour exposure to PhIP, while after 96-hour exposure to 200 µM PhIP the percentage of dead cells
 194 increased significantly. The positive control, etoposide, significantly increased the percentage of dead cells
 195 (approximately 45 %) after 72 hours. Image-based analysis allows the visualisation of spheroids along the
 196 Z-axis, thus enabling the observation of cells located inside and not just on the surface of spheroids. This
 197 enables to differentiate the occurrence of dead cells within the spheroid.



198

199 **Figure 5.** The images of Live/Dead staining and the quantification of Z-stacks of spheroids recorded
 200 after 24 and 72 hours of exposure to (A-B) BaP and (C-D) PhIP. Etoposide 1.7 µM was considered as
 201 a positive control. The live spheroids were stained with FDA (green, live cells) and PI (red, dead cells).
 202 The Z-stacks were obtained using a confocal microscope at 100x-magnification and a collection of 50
 203 Z-stacks images was presented as a gallery of ‘maximum intensity projection image’. The
 204 quantification was conducted with ImagePro 10 software, where at least 20 stacks per spheroid were
 205 measured, and the percentage of dead cells in the spheroid was calculated (n=3). The statistical
 206 significance was calculated with the Student t-test, with *p<0.05.

207

208 *2.2. The impact of BaP and PhIP on cell cycle, cell proliferation and DNA damage*

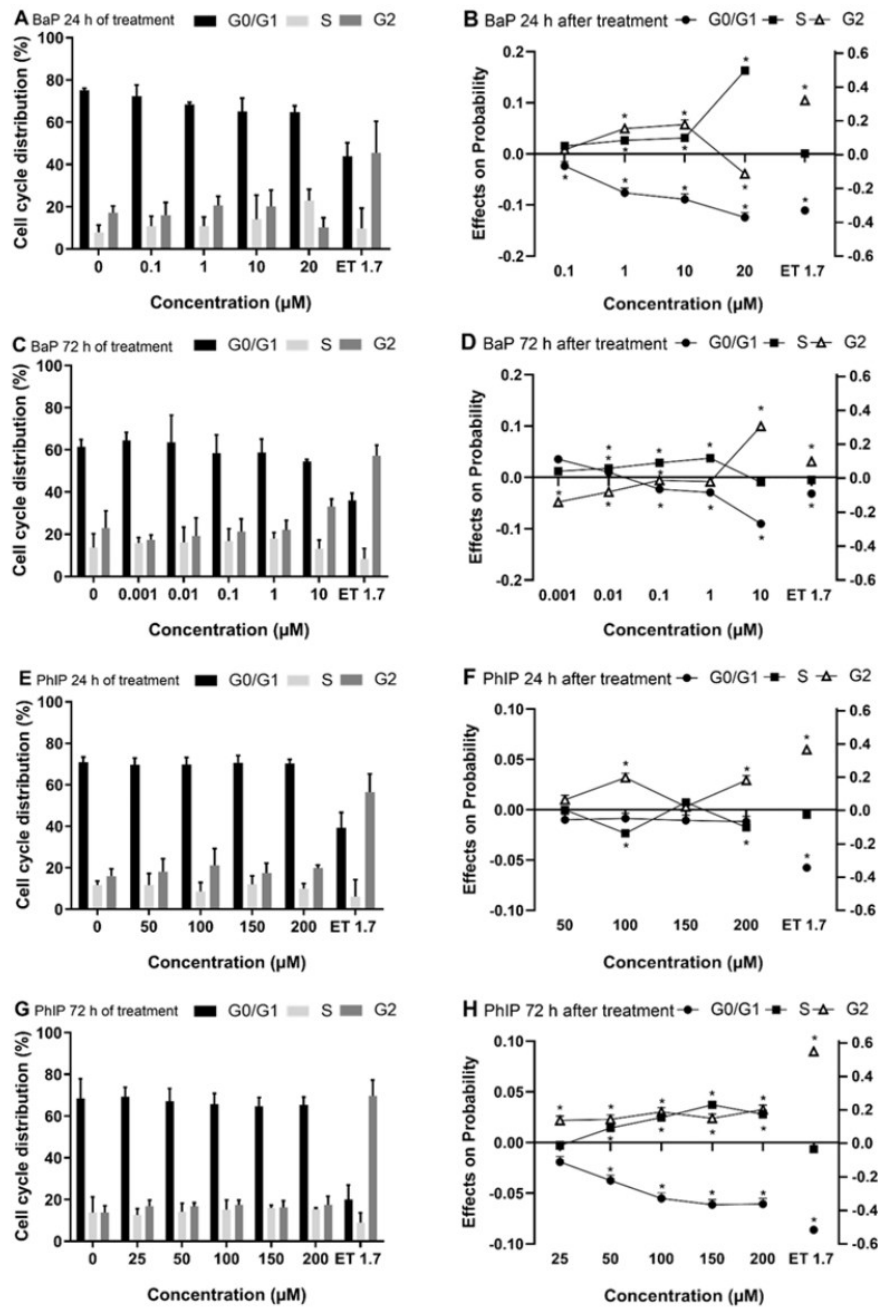
209 The impact of BaP and PhIP at two different time points (24 and 72 hours) on cell cycle, cell
 210 proliferation, and DNA double-strand break formation were studied with a new approach by
 211 simultaneous measurement of fluorescent signals of the dye Hoechst 33258 for cell cycle analysis and
 212 anti-bodies, FITC coinciding to the proliferation marker KI67, and APC coinciding to DNA double-
 213 strand breaks detected by flow cytometry. This approach enables to study several end-points at the
 214 same time in the same cell and could be used as a high-throughput screening tool for determination
 215 of (geno)toxic effects induced by various chemicals and complex mixtures.

216 The single-cell suspension from HepG2 spheroids was obtained by mechanical degradation and
 217 enzymatic digestion as described by Štampar et al., (2019). The viability of cells was determined by
 218 Trypan blue staining and the cell suspension accounted for ≥ 80 % of viable cells (data not shown).

219 The cell cycle of proliferating eukaryotic cells consists of four phases, namely G1, S, G2, and M and
 220 is regulated at several checkpoints, with the most important being G1/S and G2/M, where crucial
 221 decisions on DNA replication and the completion of the cell division are made [42]. In the case of
 222 DNA damage, the cell cycle is arrested until the damage is repaired, which causes the accumulation
 223 of cells in one of the checkpoints. If the DNA damage cannot be repaired, the cells undergo apoptosis

224 [43] or mutations can occur [44]. In HepG2 spheroids after 24-hour exposure, BaP arrested the cells
225 in S phase in a concentration-dependent manner with concomitant reduction of the cell number in
226 the G1 phase. At 20 μM BaP reduced also the number of cells in the G2/M phase (Fig. 6 A). After
227 prolonged exposure, a significant decrease of cells in G1 and concomitant significant increase of cells
228 in G2/M was noticed in HepG2 spheroids exposed to 10 μM BaP (Fig. 6 C). This is in line with
229 previous reports showing that DNA damage induced by BaP activates the S-phase and G2/M
230 checkpoints in human cell lines (e.g. HepG2, MCF7), allowing the majority of cells to survive [45–48].
231 Consequently, a part of cells re-enters the cell cycle while carrying significant amounts of residual
232 damage, which persist even when the cells complete the first and enter the second cycle, leading to a
233 new round of checkpoint kinase 1 (Chk1) activation. Activation of Chk1 holds the cell in the G2 phase
234 until ready to enter the mitotic phase. This delay allows time for DNA damage to be repaired or the
235 occurrence of cell death if DNA damage is irreparable. However, such repeated Chk1 activations are
236 leading to failure of the cells to divide correctly and increase the frequency of mitotic abnormalities
237 [49,50]. Our results, calculated by a multinomial logistic regression, confirmed that BaP arrested cells
238 in the S and G2/M phase after short and prolonged exposure, respectively (Fig. 6 B, D). However, the
239 effect on the cell cycle was lower compared to monolayer cultures as described by Stellas et al.
240 (2014)[48]. This can be ascribed to the difference in physiological attributes (both structural and
241 metabolically) between 3D and 2D cell models [51]. Furthermore, the calculated predicted
242 probabilities (see Fig. 6 B, D), which tell us the probability that a cell is in a particular phase of the
243 cell cycle at a particular concentration of the genotoxic compound, showed a clear accumulation of
244 cells in the S phase (by 16.4 percentage points) with a decrease of cells in the G1 and G2 phase (-12.4
245 and -3.9 percentage points, respectively), upon 24-hour exposure to BaP (20 μM), meaning that
246 probably the interruption of DNA synthesis had occurred, which was also reported in other studies
247 [45,46]. The arrest in DNA synthesis probably occurs because of the intra-S checkpoint, which enables
248 the recognition of the damaged DNA and time to correct it, while avoiding the irreversible errors
249 during replication [52].

250 After prolonged exposure (72h) of spheroids to BaP (10 μM), the predicted probability indicated a
251 significant decrease of cell number in G1 (by -9.0 percentage points) and a concomitant increase of
252 cells in the G2 phase (by 9.9 percentage points), clearly showing the arrest of cells in the G2/M phase
253 of the cell cycle. In the case of PhIP, the effect on the predicted probability at 24-hour exposure for
254 each phase of the cell cycle was minimal, while after prolonged exposure time (72 hours), the
255 predicted probability of the cells to be in the G1 phase started gradually to decrease in a
256 concentration-dependent manner (Fig. 6 F, H). At the same time, the predicted probability of cells to
257 be in S and G2 phase began to increase. Additional pairwise comparisons of the predicted
258 probabilities were conducted using the Bonferroni correction to account for the multiple
259 comparisons, which allowed us to identify the differences between each treatment. The pairwise
260 comparisons, presented in the supplementary Tables S1-S4, confirmed the effect of BaP on the cell
261 cycle distribution after 24 and 72 h and a negligible effect of PhIP after 24 h and a stronger effect after
262 72 h of exposure. In line with our results, is the study on HepG2 monolayer culture, where PhIP at
263 200 μM induced the accumulation of cells in S phase and decreased the number of cells in G0/G1
264 phase after 24-hour exposure [38]. Furthermore, Zhu et al. (2000)[53] also reported accumulation of
265 human lymphoblastoid TK6 cells in S phase upon short-term exposure (20 and 40 h) to PhIP in
266 particular at higher PhIP (5–10 $\mu\text{g}/\text{ml}$ corresponding to 2.3–4.5 μM) concentrations. In HepG2
267 spheroids, a positive control, etoposide, a DNA topoisomerase inhibitor, clearly arrested the cells in
268 G2 phase at both exposure times, which complies with its well-known mechanism of action [35,54].



269

270

271

272

273

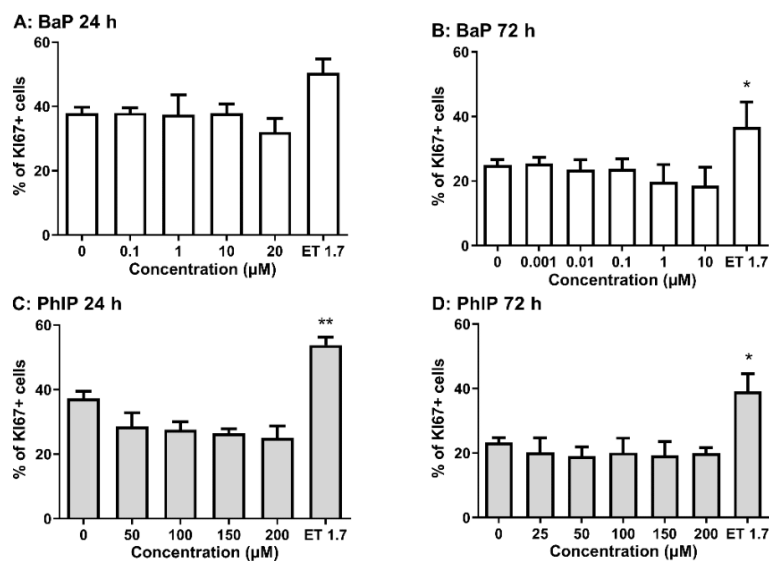
274

275

276

Figure 6. Distribution of cells across the phases of the cell cycle measured after 24 and 72 hours of exposure to BaP (A, C) and PhIP (E, G) and the predicted probabilities of BaP (B, D) and PhIP with 95 % CIs (F, H). Etoposide 1.7 μM was considered as a positive control. The cell cycle results are presented as the mean ± SD (N=3). The probabilities were calculated in Stata 15 using a multinomial logistic regression *p<0.05. The effects are shown with respect to the corresponding solvent control (marked as 0). Statistically significant differences compared to corresponding solvent control are marked with * (*p<0.05).

277 It is known that cells grown in 3D conformation have reduced proliferation [22,36], which leads to
 278 self-organization and differentiation of cells in spheroids [31,32]. Thus, we further studied the effects
 279 of BaP and PhIP on the proliferation of the same cell population from the HepG2 spheroids as
 280 evaluated for the cell cycle distribution by flow cytometric detection of anti-KI67 antibody through
 281 the fluorescent signals of FITC corresponding to the proliferation marker KI67. The Ki-67 protein is
 282 an excellent marker for determining the so-called growth fraction of a given cell population [55] since
 283 it is present in all active phases of the cell cycle (G1, S, G2, and mitosis) and is absent from the resting
 284 cells (G0). We notified that 43.2 ± 4.3 % of cells from control spheroids that were for four days in
 285 culture (3 days of spheroid formation + additional 24 hours) proliferated, while upon 24-hour
 286 exposure to BaP at 20 μM only 32.1 ± 7.4 % cells proliferated clearly showing the impact of BaP on
 287 cell proliferation. Further, we determined that only 28.1 ± 5.7 % of cells from control spheroids that
 288 were for six days in culture (3 days of spheroid formation + additional 72 hours) proliferated. BaP at
 289 1 and 10 μM reduced cell proliferation to 19.8 ± 7.6 % and 18.6 ± 9.9 %, respectively, (Fig. 7 A, B),
 290 indicating the influence of BaP on HepG2 cell division even after prolonged exposure. On the
 291 contrary, PhIP at applied exposure conditions (24 and 72 hours) did not significantly affect cell
 292 proliferation compared to control (Fig. 7 C, D); however, a trend of decreased proliferation was
 293 noticed. A decrease of approximately 7.1 % of KI67 positive cells compared to the control group was
 294 noticed after 24-hour exposure to 200 μM PhIP. In spheroids, exposed to the positive control,
 295 etoposide, the increased percentage of Ki-67 positive cells was measured (for approximately 52 %),
 296 however, this was not due to increased cell proliferation but was due to the accumulation of viable
 297 cells in G2 phase as shown in the cell cycle analysis (Fig 6 E, G).



298

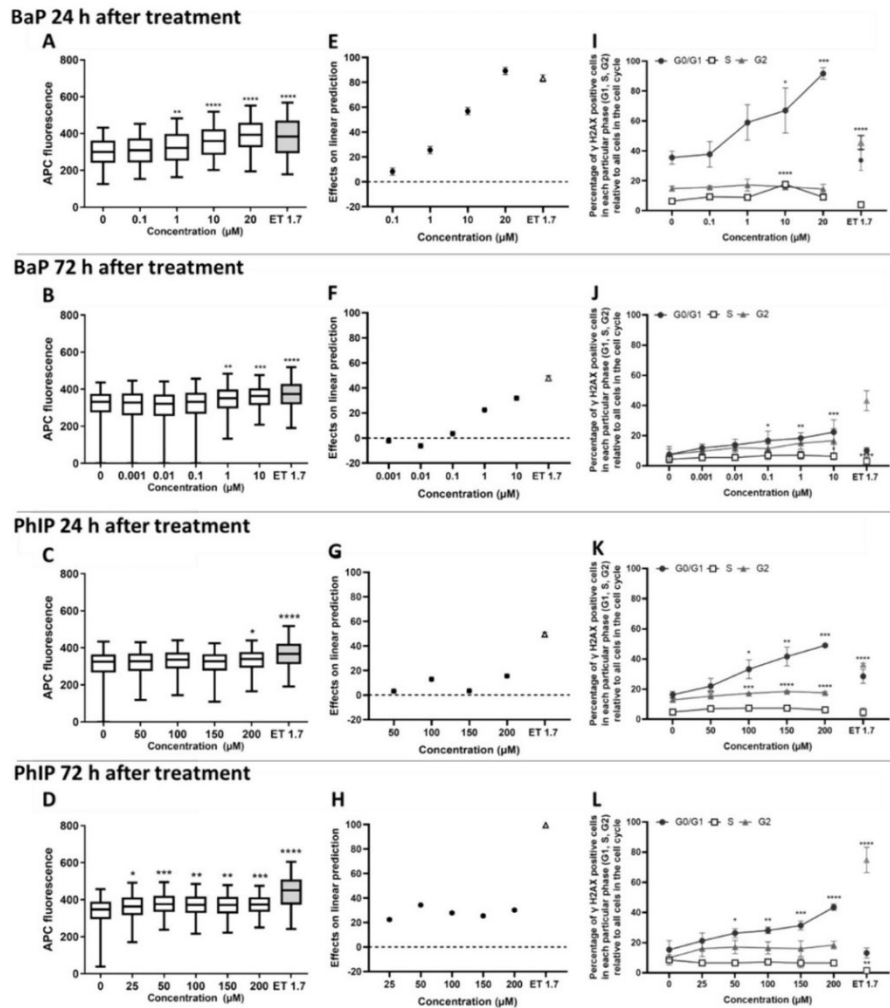
299 **Figure 7.** The percentage of KI67 positive cells (A, C) and the percentage of KI67 positive cells within
 300 the G0/G1 phase (B, D) of the cell cycle after 24 and 72 hours of exposure to graded concentrations of
 301 BaP (A, B) and PhIP (C, D). PC = 1.7 μM etoposide. The results are presented as the mean \pm SD (N=3).
 302 The statistical analysis was conducted in Graph Pad Prism 6, by the two-way ANOVA using the
 303 Bonferroni multiple comparisons test, ** $p < 0.01$.

304 The third end-point measured in the same population of cells isolated from HepG2 spheroids was
 305 phosphorylated histone H2AX (γH2AX) that was reported as a promising early and sensitive marker
 306 for DNA double-strand breaks and DNA adducts [56]. The results from our study showed that BaP
 307 after 24 and 72-hour exposure induced dose-dependent increase of DNA double-strand breaks in
 308 HepG2 spheroids, which significantly differed from control ≥ 1 μM at both exposure times (Fig. 8 A,
 309 B). This was confirmed by the calculated predicted probabilities (Fig. 8 E-F), which enabled us to

310 estimate the differences in the amount of DNA double-strand breaks between the solvent control and
311 the treated samples. Previously, using the comet assay as a detection method, BaP was shown to
312 induce DNA single-strand breaks in spheroids developed from HepG2 cells at $\geq 10 \mu\text{M}$ [24],
313 HepG2/C3A cells at $\geq 40 \mu\text{M}$ [23] and HepaRG cells at $20 \mu\text{M}$ [27] after 24 hours of exposure. Besides,
314 micronuclei formation upon BaP at $3 - 8 \mu\text{M}$ [19] was reported in 3D HepG2 hanging drop spheroids
315 [19] and the induction was 2-fold higher compared to HepG2 monolayer culture [19], revealing that
316 HepG2 spheroids are a very sensitive cell model for detection of genotoxic agents. When comparing
317 the results of all three assays we can conclude that flow cytometric analysis of γH2AX lesions proved
318 to be the most sensitive method as it detected DNA damage at the lowest BaP concentration. It is
319 known that $\gamma\text{-H2AX}$ assay is more precise and sensitive than the comet assay [57], while the
320 formation of $\gamma\text{-H2AX}$ foci was reported to correlate with the formation of micronuclei [58].
321 Furthermore, the results of the present study clearly showed that cell defence against DNA damage
322 was activated in HepG2 cells, which was indicated by the induction of cell-cycle arrest. BaP ($20 \mu\text{M}$)
323 induced DNA DSBs, which was followed by the arrest of cells in the S phase of the cells cycle (Fig. 8
324 A and 6 A). It is known that DNA DSBs induce the arrest of cells in the S-phase of DNA synthesis,
325 which occurs via a p53-independent ATM pathway [59]. Additionally, using FlowJo software we
326 conducted an advanced analysis by combining the results of cell cycle analysis and γH2AX positive
327 cells. The simultaneous staining and measurement of these two endpoints enabled us to accurately
328 detect in which cell phase the cells with DNA dsb were. Further, we calculated the proportion of
329 γH2AX positive cells in each phase of the cell cycle (G0/G1, S, G2) relative to all cells included in the
330 analysis (Fig. 8 I-L). Clear dose dependent increase in the percentage of cell with DNA dsb in G0/G1
331 phase after 24 h of exposure to BaP was determined, while after 72h much lower percentage of cells
332 with DNA dsb was detected in G0/G1 (Fig. 8 I-J). On the contrary, no important differences in the
333 amount of cells with DNA dsb were determined for the S and G2 phase when compared to control.
334 Moreover, from the results it can be seen that after 24 hours at 10 and $20 \mu\text{M}$ BaP DNA dsb were
335 detected approximately in 67 % and 92 % of cells that were in G0/G1 phase, respectively. After 72
336 hours, DNA dsb were detected in only ≈ 20 % of the cells that were exposed to $10 \mu\text{M}$ BaP. Altogether,
337 this suggests that DNA dsb induced by BaP were repaired in HepG2 spheroids. Previously, in hepatic
338 spheroids developed from HepG2/C3A cells, a subclone of HepG2 cells [60] that were grown for 21
339 days in bioreactors and were exposed to BaP for 24 ($40 \mu\text{M}$) and 96 ($4 \mu\text{M}$) hours, increased gene
340 expression of CYP1A1 was reported [23]. Similarly, in HepG2 spheroids grown for three days and
341 exposed to BaP ($40 \mu\text{M}$) for 24 hours the mRNA level of CYP1A1 and CYP1A2 [24] encoding the
342 most important phase I enzymes involved in metabolic activation of BaP [61]. In the same study, also
343 the genes encoding phase II enzymes (detoxification), namely UGT1A1 and SULTB1 were
344 upregulated [24], suggesting that BaP is metabolized in HepG2 spheroids already within 24 hours of
345 exposure.

346 The second model genotoxic compounds, PhIP significantly increased DNA dsb at ≥ 200 and $\geq 25 \mu\text{M}$
347 after 24 and 72-hour exposure, respectively (Fig. 8 C-D), which was confirmed by the linear prediction
348 (Fig. 8 G-H). Previously, PhIP was reported to induce DNA damage after 24 hours in HepaRG
349 spheroids at $40 \mu\text{M}$ [27] and HepG2 spheroids at $\geq 50 \mu\text{M}$ [24] determined with the comet assay.
350 Moreover, in 21-day old HepG2/C3A spheroids grown under dynamic clinostat conditions DNA
351 strand breaks induced by PhIP ($\geq 200 \mu\text{M}$) were determined after 24 hours with the comet assay,
352 while after prolonged exposure of 96 hours no DNA damage was detected [23]. Beside DNA strand
353 breaks, PhIP ($\geq 3 \mu\text{M}$) induced the formation of micronuclei in HepG2 spheroids as reported by [19].
354 In the present study, by analyzing the percentage of γH2AX positive cells in each phase of the cell
355 cycle (G0/G1, S, G2) relative to all measured cells in the corresponding group (Fig. 8 K-L), a dose
356 depended increase of γH2AX positive cells was determined in G0/G1 phase of PhIP exposed
357 spheroids after both exposure times. After 24-hour exposure to PhIP at 150 and $200 \mu\text{M}$, 42 % and 49
358 % of γH2AX positive cells, respectively, were detected in G0/G1 phase, while after 72 hours 31 % and
359 44 % of cells with DNA dsb were measured (Fig. 8 K-L). Similarly, as in the case of BaP also here no
360 important differences in the percentage of γH2AX positive cells in the S and G2 phase were noticed.
361 Several studies are showing that PhIP is metabolised in hepatic spheroids. Increased activities of

362 CYP1A2 enzyme [19], and upregulated mRNA expression of several phase I and II metabolic
 363 enzymes [23,24] were reported upon exposure of spheroids to PhIP. Altogether, the literature data
 364 and results obtained within the present study indicate that PhIP is metabolised and detoxified in
 365 hepatic spheroids and that DNA damage induced by PhIP is repaired as already suggested in the
 366 previous study [23]. After 24 hours, etoposide-induced DNA dsb in approximately 30 % of cells
 367 within G0/G1 and G2 phase each (Fig. 8 I-L), while after 72 hours DNA dsb were detected in more
 368 than 70 % of cells within G2 phase, while less than 10 % of cells within G0/G1 and S phase were
 369 γ H2AX positive.



370

371 **Figure 8.** Relative values of APC fluorescence corresponding to anti- γ H2AX labelled sites (A-D); the
 372 predicted probabilities of BaP and PhIP with 95 % CIs (E-H) and (I-L) after 24 and 72 hours of exposure
 373 to graded concentrations of BaP and PhIP. PC = 1.7 μ M etoposide. Significant difference between the
 374 treated sample and the solvent control (0) for γ H2AX was tested using the R software with the Mixed
 375 Effects Models (nlme) package by REML and is indicated by * $p < 0.05$, ** $p < 0.01$, *** $p < 0.001$ and
 376 **** $p < 0.0001$. The effects of probability were calculated in Stata 15 using a multinomial logistic
 377 regression * $p < 0.05$. The effects are shown with respect to the solvent control (marked as 0). The results
 378 for the proportion of γ H2AX positive cells in each phase (G0/G1, S, G2) relative to all cells in the cell

379 cycle are presented as the mean \pm SD (N=3). The statistical analysis was conducted in Graph Pad Prism
380 6, by the one-way ANOVA using the Bonferroni multiple comparisons test, $\alpha=0.05$.

381

382 **3. Materials and Methods**

383

384 *3.1. Chemicals*

385 Benzo(a)pyrene (B(a)P CAS-No. 50-32-8), minimum essential medium eagle (MEME) and its
386 supplements, fluorescein diacetate (FDA), propidium iodide (PI) and dimethylsulphoxide (DMSO)
387 were obtained from Sigma (St. Louis, MO, USA). Amino-1-methyl-6-phenylimidazo[4,5-b]pyridine
388 (PhIP; CAS-No. 105650-23-5) was obtained from Toronto Research Chemicals Inc. (Canada).
389 Etoposide (ET) was obtained from Santa Cruz Biotechnology (St. Cruz, CA, USA), while Hoechst
390 33258 dye was purchased from Invitrogen (Waltham, MA, USA). CellTiter 96® AQueous cell
391 proliferation assay (MTS) was obtained from Promega, (Madison, WI, USA). Phosphate buffered
392 saline (PBS) and ethanol were obtained from PAA Laboratories (Dartmouth, NH, USA), while Foetal
393 bovine serum (FBS), Triton X-100 from Fisher Sciences (New Jersey, USA), TRIzol® reagent and
394 trypsin-EDTA (0.25 %) were from Gibco (Praisley, Scotland, UK). Anti-H2AX pS139 (130-107-586),
395 while Anti-Ki-67-FITC (130-107-586), REA Control (I)-FITC (131-104-611) and REA Control (I)-APC
396 (131-104-615) antibodies were obtained from Miltenyi Biotec (Bergisch Gladbach, Germany).

397

398 *3.2. Cell culture, the formation of spheroids and treatment conditions*

399 The HepG2 cells (HB-8065™) provided by the ATCC-Cell bank, were cultured in MEME media
400 containing 10 % FBS, 100 IU/ml pen/strep, 1 % NEAA, 0.1 g/mL Na-pyruvate, 0.1 g/mL NaHCO₃ and
401 2 mM L-glutamine grown under standard cell culture conditions (at 37 °C, 5 % CO₂ atmosphere and
402 95 % humidity). The spheroids were prepared by the forced floating method, using a growth medium
403 supplemented with 4 % methylcellulose as described in Štampar et al. (2019)[24]. In the study, two
404 initial densities of 3000 and 6000 cells/spheroid were used and grown for 72 hours under standard
405 cell culture conditions. Afterwards, the growth media was replaced with fresh media containing
406 benzo(a)pyrene (BaP) or amino-1-methyl-6-phenylimidazo[4,5-b]pyridine (PhIP). The spheroids
407 were exposed to BaP at concentrations 0.1, 1, 10, 20 and 40 μ M for 24 h, and 0.001, 0.01, 0.1, 1, 10 μ M
408 for 72 h; and PhIP at concentrations 50, 100, 150, 200 μ M for 24 h, and 25, 50, 100, 150, 200 μ M for 72
409 h. In all experiments, solvent (0.2 and 1 % DMSO for BaP and PhIP, respectively) and appropriate
410 positive controls (PC) were included.

411

412 *3.3. Determination of cytotoxic activity by MTS assay*

413 The viability of spheroids was determined by the tetrazolium-based (MTS) assay, which was
414 performed as described in the manufacturer's protocol with slight modifications [24]. After 24 and
415 72-hour exposure of spheroids to graded concentrations of BaP and PhIP, a freshly prepared MTS:
416 PMS solution (20:1) was added to each well (one spheroid per well) and incubated for 3 hours at 37°.
417 The absorbance was measured using the spectrofluorimeter (Synergy MX, BioTek, USA) at 490 nm.
418 The experiments were performed in three independent biological replicates and each time five
419 spheroids per treatment were measured. Etoposide (1.7 μ M) was used as a PC. The difference
420 between treated groups and the solvent control was analyzed by the One-way ANOVA with the
421 posthoc multiple comparisons Dunnett's test using GraphPad Prism V6 (GraphPad Software,
422 California USA). * $p < 0.05$ was considered statistically significant.

423

424 3.4. *Monitoring of growth and morphology of spheroids*

425 The surface area of at least ten spheroids with the initial density of 6.000 cells/spheroid and 3.000
426 cells/spheroid was monitored after 72h of culturing and additional 24h (altogether 96 hours old
427 spheroids), and 72h of treatment (altogether 144 hours old spheroids), respectively, with BaP and
428 PhIP at applied concentrations. The surface area (mm²) of each spheroid was determined by
429 planimetry using the NIS elements software 4.13 V at 100x magnification (Nikon Instruments,
430 Melville, NY, USA) connected to the Ti Eclipse inverted microscope (Nikon, Japan). Growth
431 monitoring was conducted in three independent biological replicates.

432

433 3.5. *Determination of the ratio of Live/Dead cells in the spheroids by Confocal Z-stack imaging*

434 Three live spheroids were stained and monitored after 24 and 72-hour exposure to BaP (20 and 10
435 μ M, respectively) and PhIP (200 μ M) for each condition (6.000 and 3.000 cells/spheroid, respectively).
436 The cultured media was substituted with the FBS-free media with FDA stain [8 μ g/mL; live cells] and
437 incubated in the dark for 1h at 37 °C in a 5 % CO₂ atmosphere. Afterwards, the spheroids were washed
438 with PBS and stained with PI [20 μ g/mL; death cells] and incubated for additional 5 minutes. The
439 spheroids were washed again with PBS and placed in 100 μ L of fresh serum-free MEME media. The
440 Leica confocal software connected to confocal microscope Leica SP8 TCS at 100x magnification was
441 used to capture the Z-stack images of single spheroids. Etoposide (1.7 μ M) was used as a PC. Along
442 the entire thickness of the spheroid, the Z-stacks of optical sections were taken using suitable
443 excitation and emission settings for simultaneous dual-channel recordings (PI: 493/636 nm, FDA:
444 488/530 nm). At least 50 Z-stacks per spheroid were taken. The Image-Pro 10 software (Media
445 Cybernetics, USA) was used for the image analysis and the quantification of the proportion of dead
446 cells. At least 20 stacks per spheroid were quantified, and the percentage of dead cells in the spheroid
447 was calculated as a ratio between the whole spheroid area and the number of dead cells. Z-stacks of
448 spheroids were processed and analysed by the Leica confocal software (LCS) and presented as a
449 'maximum intensity projection image' gallery. The analysis provided a numerical value for the area
450 of the spheroid. The difference between the treated groups and the solvent control was analysed by
451 the Student t-test using GraphPad Prism V6 Software. * $p < 0.05$ was considered statistically
452 significant.

453

454 3.6. *Simultaneous measurement of the cell cycle, cell proliferation and gamma-H2AX positive cells by flow*
455 *cytometry*

456 The flow cytometric analysis of the cell cycle, cell proliferation, and gamma-H2AX positive cells was
457 performed on the spheroids treated with BaP and PhIP for 24 (initial density 6.000 cell/well) and 72
458 hours (initial density 3.000 cells/spheroid) of exposure as described in Štampar et al. (2020a)[36]. Flow
459 cytometry was conducted on a single-cell suspension, for which a pool of 30 spheroids per sample
460 was processed, according to Štampar et al. (2019; 2020b)[23,24]. The obtained single-cell suspension
461 was washed with PBS, fixed in ethanol, and stored at -20°C overnight until analysis (for details see
462 Hercog et al. 2019 [62]). Afterwards, fixed cells were washed in cold PBS and labelled with anti-H2AX
463 pS139-APC and anti-KI67-FITC (50-fold diluted antibodies in 1 % BSA), washed with PBS, and
464 subsequently stained with Hoechst 33258 dye (diluted in 0.1 % Triton X-100 1:500). The flow
465 cytometric measurements were conducted on a MACSQuant Analyzer 10 (Miltenyi Biotec,
466 Germany). Hoechst fluorescence related to DNA content for cell cycle analysis was detected in the
467 V1 (450/500nm) channel; FITC fluorescence, related to the proliferation marker KI67+, was detected
468 in the B1 (525/500nm) channel; and APC fluorescence, related to DNA double-strand breaks (DSBs),
469 was detected in the R1 (655-730 nm) channel. Rea-FITC and rea-APC controls (Miltenyi Biotec,
470 Germany) excluded the unspecific binding of antibodies. The experiment was repeated four times
471 independently, where 10.000 (for gamma-H2AX) and 20.000 (for proliferation and cell cycle) single

472 cells per experimental point were recorded. In all experiments, solvent (0.2 % DMSO for BaP and 1
473 % DMSO for PhIP) and appropriate positive (PC; Etoposide: 1.7 μ M) controls were included. The
474 obtained data were analysed and graphically presented in the FlowJo software V10 (Becton
475 Dickinson, New Jersey USA).

476

477 3.6.1 Statistical analysis of the results obtained by flow cytometry

478 The analysis of the frequency distributions of cells in the cell cycle (the percentage of cells in the
479 G0/G1, S, and G2 phase) was conducted by the multinomial logistic regression, and further post
480 estimation tests in Stata 15 (StataCorp LLC, USA). The multinomial logistic regression is an advanced
481 classification technique that allowed us to predict the probabilities of different possible outcomes
482 (G0/G1, S, and G2) given a set of independent variables. Specifically, it enabled us to assess the effect
483 of different concentrations of model genotoxic compounds on the cell cycle distribution. The
484 difference in the amount of KI67 positive cells in exposed and control cell populations was tested by
485 the one-way ANOVA with Dunnett's multiple comparison test, using GraphPad V6 Software. The
486 proportion of γ H2AX positive cells in each phase (G0/G1, S, G2) relative to all cells in the cell cycle
487 was determined in FlowJo software V10 (Becton Dickinson, New Jersey USA) and the statistical
488 significance was tested by the one-way ANOVA with Dunnett's multiple comparison test, using
489 GraphPad V6 Software. The statistically significant difference in the APC fluorescence between
490 treated and control groups was tested using exported .csv values in the R software with the Mixed
491 Effects Models (nlme) package by REML [63]. Furthermore, additional marginal effects were
492 calculated in Stata 15 (StataCorp LLC, USA) for an easier assessment of the results.

493

494 4. Conclusions

495 The significant increase of chemicals to which humans can be exposed calls for the development of
496 rapid and reliable research methodologies and approaches to monitor their (geno)toxic activities and
497 possible adverse human health effects. In the last few years, there is an ongoing shift for the
498 development of novel 3D cell-based systems, which can provide a better understanding of the
499 processes taking place in living cells and organs. In this context, hepatic spheroids represent an
500 alternative to an animal model that can be due to the improved structural, physiological and
501 metabolic properties exploited for broad applications, including (geno)toxicity studies. Furthermore,
502 high-throughput and high-content flow cytometry has developed into a leading technology that
503 supports many applications designed to study the nature of individual cells within homogeneous or
504 mixed cell populations. In the present study, HepG2 spheroids were used as a biosensor-like model
505 for high content screening combining confocal microscopy and quantitative image analysis, which
506 allowed us to address biological questions related to the cell viability and growth of spheroids
507 affected by time and genotoxic agents. Further, simultaneous staining of multiple endpoints in the
508 same cell ranging from DNA double-strand breaks (γ H2Ax), proliferation marker (KI67) and cell
509 cycle using specific antibodies and fluorescent signalling combined with flow cytometry enabled us
510 to track the cells with damaged DNA within the cell cycle. Validation of biosensor-like HepG2
511 spheroids by applying two genotoxic agents, benzo(a)pyrene and amino-1-methyl-6-
512 phenylimidazo[4,5-b]pyridine with well-known mechanisms of action confirmed that sensing of
513 fluorescent signals within the exposed cells corresponding to specific lesions represents a powerful
514 tool for the identification of (geno)toxic compounds. Thus, the resulting confocal imaging coupled
515 with multi-parametric flow cytometry in 3D hepatic spheroids represents an advanced biosensor-like
516 approach that can provide more insight into the mechanism of action of genotoxic compounds due
517 to the ability of simultaneous measurement of several parameters and its applicability in toxicological
518 studies as a high-content and high-throughput screening tool.

519

520 **Author Contributions:** **Conceptualization:** Bojana Žegura, Martina Štampar; **Methodology:** Martina Štampar,
 521 Sonja Žabkar, Bojana Žegura; **Software:** Martina Štampar, Barbara Breznik; **Validation:** Martina Štampar, Bojana
 522 Žegura, Sonja Žabkar; **Formal analysis:** Martina Štampar, Bojana Žegura; **Investigation:** Martina Štampar,
 523 Bojana Žegura; **Resources:** Metka Filipič, Bojana Žegura; **Data curation:** Martina Štampar, Bojana Žegura;
 524 **Writing – original draft:** Martina Štampar, Bojana Žegura; **Writing – review & editing:** Metka Filipič, ;
 525 **Visualization:** Martina Štampar, Bojana Žegura; **Supervision:** Bojana Žegura; **Project administration:** Bojana
 526 Žegura, Metka Filipič; **Funding acquisition:** Metka Filipič, Bojana Žegura.

527 **Acknowledgements:** The authors thank Klara Hercog, PhD for her technical assistance; Barbara Breznik, PhD
 528 (National Institute of Biology) for her valuable advice in confocal microscopy; and Miha Diminko, PhD (Institute
 529 for Economic Research) for his useful advice related to statistical methods and interpretations.

530 **Funding:** This work was supported by the Slovenian Research Agency [P1-0245, J1-2465 and MR-MŠtampar],
 531 and COST Action CA16119 (In vitro 3-D total cell guidance and fitness).

532 **Conflicts of Interest:** The authors declare no conflict of interest.

533

534 References

- 535 1. Corvi, R.; Madaia, F. In vitro genotoxicity testing: Can the performance be enhanced?—NC-ND
 536 license (<http://creativecommons.org/licenses/by-nc-nd/4.0/>). *Food Chem. Toxicol.* **2017**, *106*,
 537 600–608, doi:10.1016/j.fct.2016.08.024.
- 538 2. Guo, X.; Seo, J.; Li, X.; Mei, N. Genetic toxicity assessment using liver cell models: past,
 539 present, and future. *J. Toxicol. Environ. Heal. Part B* **2019**, *00*, 1–24,
 540 doi:10.1080/10937404.2019.1692744.
- 541 3. Mostafalou, S.; Abdollahi, M. The link of organophosphorus pesticides with
 542 neurodegenerative and neurodevelopmental diseases based on evidence and mechanisms.
 543 *Toxicology* **2018**, *409*, 44–52, doi:10.1016/j.tox.2018.07.014.
- 544 4. Altindag, O.; Karakoc, M.; Kocyigit, A.; Celik, H.; Soran, N. Increased DNA damage and
 545 oxidative stress in patients with rheumatoid arthritis. *Clin. Biochem.* **2007**, *40*, 167–171,
 546 doi:10.1016/j.clinbiochem.2006.10.006.
- 547 5. Hoeijmakers, J.H.J. DNA Damage, Aging, and Cancer. *N. Engl. J. Med.* **2009**, *361*, 1475–1485,
 548 doi:10.1056/NEJMra0804615.
- 549 6. Ge, J.; Chow, D.N.; Fessler, J.L.; Weingeist, D.M.; Wood, D.K.; Engelward, B.P. Micropatterned
 550 comet assay enables high throughput and sensitive DNA damage quantification. *Mutagenesis*
 551 **2015**, *30*, 11, doi:10.1093/MUTAGE/GEU063.
- 552 7. Kirkland, D.; Pfuhler, S.; Tweats, D.; Aardema, M.; Corvi, R.; Darroudi, F.; Elhajouji, A.; Glatt,
 553 H.; Hastwell, P.; Hayashi, M.; et al. How to reduce false positive results when undertaking in
 554 vitro genotoxicity testing and thus avoid unnecessary follow-up animal tests: Report of an
 555 ECVAM Workshop. *Mutat. Res. Toxicol. Environ. Mutagen.* **2007**, *628*, 31–55,
 556 doi:10.1016/J.MRGENTOX.2006.11.008.
- 557 8. Edmondson, R.; Broglie, J.J.; Adcock, A.F.; Yang, L. Three-dimensional cell culture systems
 558 and their applications in drug discovery and cell-based biosensors. *Assay Drug Dev. Technol.*

- 559 **2014**, *12*, 207–18, doi:10.1089/adt.2014.573.
- 560 9. Kirkland, D.; Aardema, M.; Henderson, L.; Müller, L. Erratum: Evaluation of the ability of a
561 battery of three in vitro genotoxicity tests to discriminate rodent carcinogens and non-
562 carcinogens I. Sensitivity, specificity and relative predictivity (*Mutation Research - Genetic*
563 *Toxicology and Environmental Mut. Res. - Genet. Toxicol. Environ. Mutagen.* **2005**, *588*,
564 70, doi:10.1016/j.mrgentox.2005.10.002.
- 565 10. LeCluyse, E.L. Human hepatocyte culture systems for the in vitro evaluation of cytochrome
566 P450 expression and regulation. *Eur. J. Pharm. Sci.* **2001**, *13*, 343–368, doi:10.1016/S0928-
567 0987(01)00135-X.
- 568 11. Gomez-Lechon, M.; Donato, M.; Castell, J.; Jover, R. Human Hepatocytes in Primary Culture:
569 The Choice to Investigate Drug Metabolism in Man. *Curr. Drug Metab.* **2004**, *5*, 443–462,
570 doi:10.2174/1389200043335414.
- 571 12. den Braver-Sewradj, S.P.; den Braver, M.W.; Vermeulen, N.P.E.; Commandeur, J.N.M.;
572 Richert, L.; Vos, J.C. Inter-donor variability of phase I/phase II metabolism of three reference
573 drugs in cryopreserved primary human hepatocytes in suspension and monolayer. *Toxicol.*
574 *Vitr.* **2016**, *33*, 71–79, doi:10.1016/j.tiv.2016.02.013.
- 575 13. Pfuhler, S.; van Benthem, J.; Curren, R.; Doak, S.H.; Dusinska, M.; Hayashi, M.; Heflich, R.H.;
576 Kidd, D.; Kirkland, D.; Luan, Y.; et al. Use of in vitro 3D tissue models in genotoxicity testing:
577 Strategic fit, validation status and way forward. Report of the working group from the 7th
578 International Workshop on Genotoxicity Testing (IWGT). *Mutat. Res. - Genet. Toxicol. Environ.*
579 *Mutagen.* **2020**, 850–851.
- 580 14. Corvi, R.; Madia, F.; Worth, A.; Whelan, M. *EURL ECVAM Strategy to Avoid and Reduce Animal*
581 *Use in Genotoxicity Testing*; European Commission, Ed.; 2013; ISBN 9789279348440.
- 582 15. Fey, S.J.; Wrzesinski, K. Determination of drug toxicity using 3D spheroids constructed from
583 an immortal human hepatocyte cell line. *Toxicol. Sci.* **2012**, *127*, 403–411,
584 doi:10.1093/toxsci/kfs122.
- 585 16. Wrzesinski, K.; Fey, S.J. After trypsinisation, 3D spheroids of C3A hepatocytes need 18 days
586 to re-establish similar levels of key physiological functions to those seen in the liver. *Toxicol.*
587 *Res. (Camb).* **2013**, *2*, 123–135, doi:10.1039/c2tx20060k.
- 588 17. Bell, C.C.; Hendriks, D.F.G.; Moro, S.M.L.; Ellis, E.; Walsh, J.; Renblom, A.; Fredriksson
589 Puigvert, L.; Dankers, A.C.A.; Jacobs, F.; Snoeys, J.; et al. Characterization of primary human
590 hepatocyte spheroids as a model system for drug-induced liver injury, liver function and
591 disease. *Sci. Rep.* **2016**, *6*, doi:10.1038/srep25187.
- 592 18. Hughes, B. Industry concern over EU hepatotoxicity guidance. *Nat. Rev. Drug Discov.* **2008**, *7*,
593 719–719, doi:10.1038/nrd2677.

- 594 19. Shah, U.K.; Mallia, J. de O.; Singh, N.; Chapman, K.E.; Doak, S.H.; Jenkins, G.J.S. A three-
595 dimensional in vitro HepG2 cells liver spheroid model for genotoxicity studies. *Mutat. Res. -*
596 *Genet. Toxicol. Environ. Mutagen.* **2018**, *825*, 51–58, doi:10.1016/j.mrgentox.2017.12.005.
- 597 20. Wrzesinski, K.; Fey, S.J. From 2D to 3D - a new dimension for modelling the effect of natural
598 products on human tissue. *Curr. Pharm. Des.* **2015**, *21*, 5605–16,
599 doi:10.2174/1381612821666151002114227.
- 600 21. Bokhari, M.; Carnachan, R.J.; Cameron, N.R.; Przyborski, S.A. Culture of HepG2 liver cells on
601 three dimensional polystyrene scaffolds enhances cell structure and function during
602 toxicological challenge. *J. Anat.* **2007**, *211*, 567–576, doi:10.1111/j.1469-7580.2007.00778.x.
- 603 22. Eilenberger, C.; Rothbauer, M.; Ehmoser, E.K.; Ertl, P.; Küpcü, S. Effect of Spheroidal Age on
604 Sorafenib Diffusivity and Toxicity in a 3D HepG2 Spheroid Model. *Sci. Rep.* **2019**, *9*,
605 doi:10.1038/s41598-019-41273-3.
- 606 23. Štampar, M.; Frandsen, H.S.; Rogowska-Wrzesinska, A.; Wrzesinski, K.; Filipič, M.; Žegura,
607 B. Hepatocellular carcinoma (HepG2/C3A) cell-based 3D model for genotoxicity testing of
608 chemicals. *Sci. Total Environ.* **2020**, 143255, doi:10.1016/j.scitotenv.2020.143255.
- 609 24. Štampar, M.; Tomc, J.; Filipič, M.; Žegura, B. Development of in vitro 3D cell model from
610 hepatocellular carcinoma (HepG2) cell line and its application for genotoxicity testing. *Arch.*
611 *Toxicol.* **2019**, *93*, 3321–3333, doi:10.1007/s00204-019-02576-6.
- 612 25. Elje, E.; Hesler, M.; Rundén-Pran, E.; Mann, P.; Mariussen, E.; Wagner, S.; Dusinska, M.; Kohl,
613 Y. The comet assay applied to HepG2 liver spheroids. *Mutat. Res. - Genet. Toxicol. Environ.*
614 *Mutagen.* **2019**, *845*, 403033, doi:10.1016/j.mrgentox.2019.03.006.
- 615 26. Elje, E.; Mariussen, E.; Moriones, O.H.; Bastús, N.G.; Puentes, V.; Kohl, Y.; Dusinska, M.;
616 Rundén-Pran, E. Hepato(Geno)toxicity assessment of nanoparticles in a hepg2 liver spheroid
617 model. *Nanomaterials* **2020**, *10*, doi:10.3390/nano10030545.
- 618 27. Mandon, M.; Huet, S.; Dubreil, E.; Fessard, V.; Le Hégarat, L. Three-dimensional HepaRG
619 spheroids as a liver model to study human genotoxicity in vitro with the single cell gel
620 electrophoresis assay. *Sci. Rep.* **2019**, *9*, doi:10.1038/s41598-019-47114-7.
- 621 28. Llewellyn, S. V.; Conway, G.E.; Shah, U.K.; Evans, S.J.; Jenkins, G.J.S.; Clift, M.J.D.; Doak, S.H.
622 Advanced 3D liver models for in vitro genotoxicity testing following long-term nanomaterial
623 exposure. *J. Vis. Exp.* **2020**, *2020*, 1–10, doi:10.3791/61141.
- 624 29. Conway, G.E.; Shah, U.K.; Llewellyn, S.; Cervena, T.; Evans, S.J.; Al Ali, A.S.; Jenkins, G.J.;
625 Clift, M.J.D.; Doak, S.H. Adaptation of the in vitro micronucleus assay for genotoxicity testing
626 using 3D liver models supporting longer-term exposure durations. *Mutagenesis* **2020**, *35*, 319–
627 330, doi:10.1093/mutage/geaa018.
- 628 30. Shah, U.-K.; Verma, J.R.; Chapman, K.E.; Wilde, E.C.; Tonkin, J.A.; Brown, M.R.; Johnson, G.E.;

- 629 Doak, S.H.; Jenkins, G.J. OUP accepted manuscript. *Mutagenesis* **2020**, 1–8,
630 doi:10.1093/mutage/geaa029.
- 631 31. Hurrell, T.; Lilley, K.S.; Cromarty, A.D. Proteomic responses of HepG2 cell monolayers and
632 3D spheroids to selected hepatotoxins. *Toxicol. Lett.* **2019**, *300*, 40–50,
633 doi:10.1016/j.toxlet.2018.10.030.
- 634 32. Ramaiahgari, S.C.; Den Braver, M.W.; Herpers, B.; Terpstra, V.; Commandeur, J.N.M.; Van De
635 Water, B.; Price, L.S. A 3D in vitro model of differentiated HepG2 cell spheroids with
636 improved liver-like properties for repeated dose high-throughput toxicity studies. *Arch.*
637 *Toxicol.* **2014**, *88*, 1083–1095, doi:10.1007/s00204-014-1215-9.
- 638 33. Ramaiahgari, S.C.; Waidyanatha, S.; Dixon, D.; DeVito, M.J.; Paules, R.S.; Ferguson, S.S. Three-
639 dimensional (3D) HepaRG spheroid model with physiologically relevant xenobiotic
640 metabolism competence and hepatocyte functionality for liver toxicity screening. *Toxicol. Sci.*
641 **2017**, *159*, 124–136, doi:10.1093/toxsci/kfx122.
- 642 34. Luckert, C.; Schulz, C.; Lehmann, N.; Thomas, M.; Hofmann, U.; Hammad, S.; Hengstler, J.G.;
643 Braeuning, A.; Lampen, A.; Hessel, S. Comparative analysis of 3D culture methods on human
644 HepG2 cells. *Arch. Toxicol.* **2016**, 1–14, doi:10.1007/s00204-016-1677-z.
- 645 35. Hercog, K.; Štampar, M.; Štern, A.; Filipič, M.; Žegura, B. Application of advanced HepG2 3D
646 cell model for studying genotoxic activity of cyanobacterial toxin cylindrospermopsin.
647 *Environ. Pollut.* **2020**, *265*, 114965, doi:10.1016/j.envpol.2020.114965.
- 648 36. Štampar, M.; Breznik, B.; Filipič, M.; Žegura, B. Characterization of In Vitro 3D Cell Model
649 Developed from Human Hepatocellular Carcinoma (HepG2) Cell Line. *Cells* **2020**, *9*, 2557,
650 doi:10.3390/cells9122557.
- 651 37. Peng, C.; Muthusamy, S.; Xia, Q.; Lal, V.; Denison, M.S.; Ng, J.C. Micronucleus formation by
652 single and mixed heavy metals/loids and PAH compounds in HepG2 cells. *Mutagenesis* **2015**,
653 *30*, 593–602, doi:10.1093/mutage/gev021.
- 654 38. Pezdirc, M.; Žegura, B.; Filipič, M. Genotoxicity and induction of DNA damage responsive
655 genes by food-borne heterocyclic aromatic amines in human hepatoma HepG2 cells. *Food*
656 *Chem. Toxicol.* **2013**, *59*, 386–394, doi:10.1016/j.fct.2013.06.030.
- 657 39. Tomc, J.; Kološa, K.; Žegura, B.; Kamenšek, U.; Breznik, B.; Turnšek, T.L.; Filipič, M. Adipose
658 tissue stem cell-derived hepatic progenies as an in vitro model for genotoxicity testing. *Arch.*
659 *Toxicol.* **2018**, 1–11, doi:10.1007/s00204-018-2190-3.
- 660 40. Stiborová, M.; Moserová, M.; Černá, V.; Indra, R.; Dračinský, M.; Šulc, M.; Henderson, C.J.;
661 Wolf, C.R.; Schmeiser, H.H.; Phillips, D.H.; et al. Cytochrome b5 and epoxide hydrolase
662 contribute to benzo[a]pyrene-DNA adduct formation catalyzed by cytochrome P450 1A1
663 under low NADPH:P450 oxidoreductase conditions. *Toxicology* **2014**, *318*, 1–12,
664 doi:10.1016/j.tox.2014.02.002.

- 665 41. Turkez, H.; Arslan, M.E.; Ozdemir, O. Genotoxicity testing: progress and prospects for the
666 next decade. *Expert Opin. Drug Metab. Toxicol.* 2017, 13, 1089–1098.
- 667 42. Bartek, J.; Lukas, J. Mammalian G1- and S-phase checkpoints in response to DNA damage.
668 *Curr. Opin. Cell Biol.* 2001, 13, 738–747.
- 669 43. Andrew Murray; Tim Hunt, W.H. The cell cycle: An introduction. *Mol. Reprod. Dev.* 1994, 39,
670 247–247, doi:10.1002/mrd.1080390223.
- 671 44. Lodish, H.; Berk, A.; Zipursky, S.L.; Matsudaira, P.; Baltimore, D.; Darnell, J. DNA Damage
672 and Repair and Their Role in Carcinogenesis. 2000.
- 673 45. Jeffy, B.D.; Chen, E.J.; Gudas, J.M.; Romagnolo, D.F. Disruption of cell cycle kinetics by
674 benzo[a]pyrene: Inverse expression patterns of BRCA-1 and p53 in MCF-7 cells arrested in S
675 and G2. *Neoplasia* 2000, 2, 460–470, doi:10.1038/sj.neo.7900104.
- 676 46. Hockley, S.L.; Arlt, V.M.; Brewer, D.; Giddings, I.; Phillips, D.H. Time- and concentration-
677 dependent changes in gene expression induced by benzo(a)pyrene in two human cell lines,
678 MCF-7 and HepG2. *BMC Genomics* 2006, 7, doi:10.1186/1471-2164-7-260.
- 679 47. Caino, M.C.; Oliva, J.L.; Jiang, H.; Penning, T.M.; Kazanietz, M.G. Benzo[a]pyrene-7,8-
680 dihydrodiol promotes checkpoint activation and G 2/M arrest in human bronchoalveolar
681 carcinoma H358 cells. *Mol. Pharmacol.* 2007, 71, 744–750, doi:10.1124/mol.106.032078.
- 682 48. Stellas, D.; Souliotis, V.L.; Bekyrou, M.; Smirlis, D.; Kirsch-Volders, M.; Degrassi, F.; Cundari,
683 E.; Kyrtopoulos, S.A. Benzo[a]pyrene-induced cell cycle arrest in HepG2 cells is associated
684 with delayed induction of mitotic instability. *Mutat. Res. - Fundam. Mol. Mech. Mutagen.* 2014,
685 769, 59–68, doi:10.1016/j.mrfmmm.2014.07.004.
- 686 49. Löffler, H.; Bochtler, T.; Fritz, B.; Tews, B.; Ho, A.D.; Lukas, J.; Bartek, J.; Krämer, A. DNA
687 damage-induced accumulation of centrosomal Chk1 contributes to its checkpoint function.
688 *Cell Cycle* 2007, 6, 2541–2548, doi:10.4161/cc.6.20.4810.
- 689 50. Wilsker, D.; Petermann, E.; Helleday, T.; Bunz, F. Essential function of Chk1 can be uncoupled
690 from DNA damage checkpoint and replication control. *Proc. Natl. Acad. Sci. U. S. A.* 2008, 105,
691 20752–20757, doi:10.1073/pnas.0806917106.
- 692 51. Wrzesinski, K.; Rogowska-Wrzesinska, A.; Kanlaya, R.; Borkowski, K.; Schwämmle, V.; Dai,
693 J.; Joensen, K.E.; Wojdyla, K.; Carvalho, V.B.; Fey, S.J. The cultural divide: Exponential growth
694 in classical 2D and metabolic equilibrium in 3D environments. *PLoS One* 2014, 9,
695 doi:10.1371/journal.pone.0106973.
- 696 52. Hamouchene, H.; Arlt, V.M.; Giddings, I.; Phillips, D.H. Influence of cell cycle on responses
697 of MCF-7 cells to benzo[a]pyrene. *BMC Genomics* 2011, 12, 333, doi:10.1186/1471-2164-12-333.
- 698 53. Zhu, H.; Boobis, A.R.; Gooderham, N.J. The food-derived carcinogen 2-amino-1-methyl-6-
699 phenylimidazo[4,5-b]pyridine activates S-phase checkpoint and apoptosis, and induces gene

- 700 mutation in human lymphoblastoid TK6 cells. *Cancer Res.* **2000**, *60*, 1283–9.
- 701 54. Bergant Loboda, K.; Janežič, M.; Štampar, M.; Žegura, B.; Filipič, M.; Perdih, A. Substituted
702 4,5'-Bithiazoles as Catalytic Inhibitors of Human DNA Topoisomerase II α . *J. Chem. Inf. Model.*
703 **2020**, *60*, 3662–3678, doi:10.1021/acs.jcim.0c00202.
- 704 55. Scholzen, T.; Gerdes, J. The Ki-67 protein: From the known and the unknown. *J. Cell. Physiol.*
705 **2000**, *182*, 311–322.
- 706 56. Kopp, B.; Vignard, J.; Mirey, G.; Fessard, V.; Zalko, D.; Le Hgarat, L.; Audebert, M.
707 Genotoxicity and mutagenicity assessment of food contaminant mixtures present in the
708 French diet. *Environ. Mol. Mutagen.* **2018**, *59*, 742–754, doi:10.1002/em.22214.
- 709 57. Kuo, L.J.; Yang, L.X. γ -H2AX- A novel biomaker for DNA double-strand breaks. *In Vivo*
710 (*Brooklyn*). **2008**, *22*, 305–310.
- 711 58. Watters, G.P.; Smart, D.J.; Harvey, J.S.; Austin, C.A. H2AX phosphorylation as a genotoxicity
712 endpoint. *Mutat. Res. - Genet. Toxicol. Environ. Mutagen.* **2009**, *679*, 50–58,
713 doi:10.1016/j.mrgentox.2009.07.007.
- 714 59. Kastan, M.B.; Lim, D.S.; Kim, S.T.; Xu, B.; Canman, C. Multiple signaling pathways involving
715 ATM. In Proceedings of the Cold Spring Harbor Symposia on Quantitative Biology; Cold
716 Spring Harbor Laboratory Press, 2000; Vol. 65, pp. 521–526.
- 717 60. Bandele, O.J.; Santillo, M.F.; Ferguson, M.; Wiesenfeld, P.L. In vitro toxicity screening of
718 chemical mixtures using HepG2/C3A cells. *Food Chem. Toxicol.* **2012**, *50*, 1653–1659,
719 doi:10.1016/j.fct.2012.02.016.
- 720 61. Arlt, V.M.; Stiborová, M.; Henderson, C.J.; Thiemann, M.; Frei, E.; Aimová, D.; Singh, R.; da
721 Costa, G.G.; Schmitz, O.J.; Farmer, P.B.; et al. Metabolic activation of benzo[a]pyrene in vitro
722 by hepatic cytochrome P450 contrasts with detoxification in vivo: Experiments with hepatic
723 cytochrome P450 reductase null mice. *Carcinogenesis* **2008**, *29*, 656–665,
724 doi:10.1093/carcin/bgn002.
- 725 62. Hercog, K.; Maisanaba, S.; Filipič, M.; Sollner-Dolenc, M.; Kač, L.; Žegura, B. Genotoxic
726 activity of bisphenol A and its analogues bisphenol S, bisphenol F and bisphenol AF and their
727 mixtures in human hepatocellular carcinoma (HepG2) cells. *Sci. Total Environ.* **2019**, *687*, 267–
728 276, doi:10.1016/j.scitotenv.2019.05.486.
- 729 63. Pinheiro, J.; Bates, D.; DebRoy, S.; Sarkar, D. R Development Core Team. 2010. nlme: Linear
730 and Nonlinear Mixed Effects Models. *R Packag. version 3* **2007**.

731



© 2020 by the authors. Submitted for possible open access publication under the terms and conditions of the Creative Commons Attribution (CC BY) license (<http://creativecommons.org/licenses/by/4.0/>).

732

2.4 Application of Advanced HepG2 3D Cell Model for Studying Genotoxic Activity of Cyanobacterial Toxin Cylindrospermopsin

Klara HERCOG, Martina ŠTAMPAR, Alja ŠTERN, Metka FILIPIČ and Bojana ŽEGURA

Environmental Pollution 2020; 265: 114965. DOI: [10.1016/j.envpol.2020.114965](https://doi.org/10.1016/j.envpol.2020.114965)



Contents lists available at ScienceDirect

Environmental Pollution

journal homepage: www.elsevier.com/locate/envpol



Application of advanced HepG2 3D cell model for studying genotoxic activity of cyanobacterial toxin cylindrospermopsin[☆]



Klara Hercog^{a, b}, Martina Štampar^{a, b}, Alja Štern^a, Metka Filipič^{a, b}, Bojana Žegura^{a, b, *}

^a Department of Genetic Toxicology and Cancer Biology, National Institute of Biology, Ljubljana, Slovenia

^b Jozef Stefan International Postgraduate School, Ljubljana, Slovenia

ARTICLE INFO

Article history:

Received 24 February 2020

Received in revised form

2 June 2020

Accepted 3 June 2020

Available online 10 June 2020

Keywords:

Cylindrospermopsin

3D cell model

Cytotoxic

Genotoxic

Cell cycle

Gene expression

ABSTRACT

Cylindrospermopsin (CYN) is an emerging cyanotoxin increasingly being found in freshwater cyanobacterial blooms worldwide. Humans and animals are exposed to CYN through the consumption of contaminated water and food as well as occupational and recreational water activities; therefore, it represents a potential health threat. It exhibits genotoxic effects in metabolically active test systems, thus it is considered as pro-genotoxic. In the present study, the advanced 3D cell model developed from human hepatocellular carcinoma (HepG2) cells was used for the evaluation of CYN cyto-/genotoxic activity. Spheroids were formed by forced floating method and were cultured for three days under static conditions prior to exposure to CYN (0.125, 0.25 and 0.5 µg/mL) for 72 h. CYN influence on spheroid growth was measured daily and cell survival was determined by MTS assay and live/dead staining. The influence on cell proliferation, cell cycle alterations and induction of DNA damage (γH2AX) was determined using flow cytometry. Further, the expression of selected genes (qPCR) involved in the metabolism of xenobiotics, proliferation, DNA damage response, apoptosis and oxidative stress was studied. Results revealed that CYN dose-dependently reduced the size of spheroids and affected cell division by arresting HepG2 cells in G1 phase of the cell cycle. No induction of DNA double strand breaks compared to control was determined at applied conditions. The analysis of gene expression revealed that CYN significantly deregulated genes encoding phase I (*CYP1A1*, *CYP1A2*, *CYP3A4*, *ALDH3A*) and II (*NAT1*, *NAT2*, *SULT1B1*, *SULT1C2*, *UGT1A1*, *UGT2B7*) enzymes as well as genes involved in cell proliferation (*PCNA*, *TOP2α*), apoptosis (*BBC3*) and DNA damage response (*GADD45a*, *CDKN1A*, *ERCC4*). The advanced 3D HepG2 cell model due to its more complex structure and improved cellular interactions provides more physiologically relevant information and more predictive data for human exposure, and can thus contribute to more reliable genotoxicity assessment of chemicals including cyanotoxins.

© 2020 Elsevier Ltd. All rights reserved.

1. Introduction

Cyanobacterial blooms are of increasing concern since their occurrence in the environment is expanding due to water eutrophication and climate change (Mantzouki et al., 2018; O'Neil et al., 2012; Visser et al., 2016). Cyanobacteria produce a wide range of secondary metabolites including highly toxic cyanotoxins that can pose threat to human and animal health. One of the emerging

cyanotoxins is cylindrospermopsin (CYN) that is produced by many cyanobacterial species including *Anabaena* sp., *Aphanizomenon* sp., *Chroococcoides ovalisporum*, *Raphidiopsis raciborskii*, *Lyngbya wollei*, *Oscillatoria* sp., *Raphidiopsis* sp., *Umezakia natans* etc (Rzymiski and Poniedzialek, 2014). Its producers are mainly native to subtropical areas (de la Cruz et al., 2013), but CYN has recently been identified also in inland waters of North America and Europe (Sukenic et al., 2012; Svirčev et al., 2019) as well as in reservoirs for urban water supply (Buratti et al., 2017; Miller et al., 2017; Poniedzialek et al., 2012), indicating that species producing the toxin are spreading to temperate regions.

Humans may be exposed to CYN through several routes, where dermal and inhalation exposure may occur with professional (e.g. fishing), recreational (sports) or domestic (e.g. showering) use of contaminated water. The most frequent way of human exposure, is

[☆] This paper has been recommended for acceptance by Wen Chen.

* Corresponding author. Department of Genetic Toxicology and Cancer Biology, National Institute of Biology, Ljubljana, Slovenia.

E-mail addresses: klara.hercog@nib.si (K. Hercog), martina.stampar@nib.si (M. Štampar), alja.stern@nib.si (A. Štern), metka.filipic@nib.si (M. Filipič), bojana.zegura@nib.si (B. Žegura).

2

K. Hercog et al. / Environmental Pollution 265 (2020) 114965

the oral route, which occurs through the ingestion of contaminated drinking water or accidental swallowing of water during recreational activities. In the environment, the concentrations of CYN in surface waters can reach up to several tens of $\mu\text{g/L}$ (Mohamed and Al-Shehri, 2013; Moreira et al., 2017), while during the blooming season the concentrations of CYN can reach concentrations such as 589 $\mu\text{g/L}$ (Saker and Eaglesham, 1999) and up to 800 $\mu\text{g/L}$ (Shaw et al., 2000).

CYN is a polyketide-derived alkaloid with a guanidine moiety combined with a hydroxymethyluracil group attached to its tricyclic carbon skeleton (Ohtani et al., 1992). The primary target organs of CYN toxicity are the liver and kidney; however, also other organs (e.g. spleen, thymus, lung, heart, and lymphocytes) can be affected (Falconer and Humpage, 2006). CYN displays a wide range of toxic effects, with protein synthesis inhibition (Froschio et al., 2001) being the main known mechanism of action. An interplay between the hydroxyl and guanidine functional groups appears to be the key for CYNs toxicity (Evans et al., 2019); however, detailed information of its molecular mode of action remains unclear. In addition to being hepatotoxic (Runnegar et al., 2002) and generally cytotoxic, it is developmentally toxic (Berry et al., 2009), immunotoxic (Moosova et al., 2019; Poniedziatek et al., 2014), dermatotoxic, and there are indications of its endocrine disrupting (Liu et al., 2018; Young et al., 2008) and neurotoxic activity (for review see: Hinojosa et al., 2019).

At the molecular level, CYN is inhibiting glutathione synthesis (Runnegar et al., 1994, 1995) resulting in generation of reactive oxygen species and lipid peroxidation (Evans et al., 2019; Liebel et al., 2011; Poniedziatek et al., 2015). Its genotoxic activity is manifested in the form of DNA strand breaks (Humpage et al., 2005; Sieroslawska and Rymuszka, 2015; Straser et al., 2013b, 2013a; Żegura et al., 2011a, 2011b) and chromosomal damage (Bazin et al., 2010; Hercog et al., 2017; Humpage et al., 2000; Sieroslawska and Rymuszka, 2015; Straser et al., 2011; Żegura et al., 2011a, 2011b). CYN is considered to be pro-genotoxic, meaning that metabolic activation is required for its cytotoxic and/or genotoxic effects; however, the exact metabolic pathway remains unclear. Numerous indirect evidences are showing that various isoforms of cytochrome P450 (CYP450) family are involved in its metabolic activation (Bazin et al., 2010; Froschio et al., 2003; Hercog et al., 2017; Humpage et al., 2005; Kittler et al., 2016; Straser et al., 2013c, 2013a, 2011; Żegura et al., 2011a, 2011b), while not much literature data exists on the involvement of phase II enzymes in CYN detoxification.

Recently US Environmental Protection Agency (EPA, 2015) and European Food Safety Agency (Testai et al., 2017) published documents prioritizing the identification of CYN adverse health effects, thus there is an urgent need to elucidate its molecular mechanisms of action in detail.

In the present study, cytotoxic and genotoxic activity of CYN was studied in three dimensional (3D) *in vitro* cell model (spheroids) developed from human hepatocellular carcinoma cell line (HepG2). Compared to the traditional two dimensional (2D) cell cultures, cell line derived hepatospheres possess improved cell-cell and cell-matrix interactions, resulting in higher cell differentiation, cell morphology and cytoskeleton architecture that more closely resemble *in vivo* cellular functions (Fey and Wrzesinski, 2012; Godoy et al., 2013; Zhang et al., 2016). Primary liver cells are considered the best approximation to *in vivo* situation; however, spheroids formed from hepatocyte cell lines appear equally useful for determination of cytotoxic effects *in vitro*, while the classical 2D cultured cell models show significantly lower correlation (Fey and Wrzesinski, 2012). Another advantage of 3D cell models is that they allow prolonged exposures due to their higher stability as they retain cell viability, morphology, and functionality over a period of several weeks (Bell et al., 2016).

The spheroids obtained from HepG2 cells show increased level

of liver-specific functions and expression of markers of differentiated and polarized hepatocytes (Kelm et al., 2003; Luckert et al., 2017; Mueller et al., 2011; Ramaiahgari et al., 2014). In HepG2 spheroids bile canaliculi-like structures are formed (Kelm et al., 2003; Ramaiahgari et al., 2014) and thus spheroids possess functional bile transport (Luckert et al., 2017; Mueller et al., 2011). Moreover, gene expression patterns including liver-specific genes and genes involved in xenobiotic metabolism are markedly different compared to monolayer cultures (Chang and Hughes-Fulford, 2009; Hurrell et al., 2019; Luckert et al., 2017; Stampar et al., 2019).

In our study, the HepG2 spheroids were exposed to non-cytotoxic concentrations of CYN and the influence on spheroid growth, cell division, and DNA damage was studied with microscopy and flow cytometry. To explore molecular mechanisms underlying CYN induced cellular effects, deregulation of the expression of selected genes involved in metabolism of xenobiotics (phase I and II), DNA damage response, cell proliferation, apoptosis and oxidative stress upon exposure of 3D spheroids to CYN was analysed using the qPCR.

2. Materials and methods

2.1. Chemicals

Cylindrospermopsin (CYN) was obtained from Enzo Life Sciences GmbH (Lausen, Switzerland). A 0.5 mg/mL stock solution of CYN was prepared in 50% methanol and stored at $-20\text{ }^{\circ}\text{C}$. Minimum essential medium eagle (MEME) and its supplements, benzo(a) pyrene (BaP), fluorescein diacetate (FDA) and propidium iodide (PI) were obtained from Sigma (St. Louis, MO, USA), while the etoposide (ET) was from Santa Cruz Biotechnology (St. Cruz, CA, USA). Hoechst 33258 dye was purchased from Invitrogen (Waltham, MA, USA). Methanol and phosphate buffered saline (PBS) were from PAA Laboratories (Dartmouth, NH, USA). Foetal bovine serum (FBS), trypsin-EDTA (0.25%) and TRIzol® reagent were from Gibco (Praisley, Scotland, UK). Triton X-100 was from Fisher Sciences (New Jersey, USA). CellTiter 96® Aqueous cell proliferation assay (MTS) was from Promega, (Madison, WI, USA). qPCR reagents (High capacity cDNA Transcription Kit, TaqMan Gene Expression Assays, TATAA PreAmp Grand Master Mix (2x), and TaqMan Universal PCR Master Mix) were from Applied Biosystems (Foster City, CA, USA). Anti-H2AX pS139 (130-107-586) and Anti-Ki-67-FITC (130-107-586) antibodies were from Miltenyi Biotec (Bergisch Gladbach, Germany).

2.2. Cell culture and spheroids formation

HepG2 cells (ATCC, HB-8065™) were cultured at $37\text{ }^{\circ}\text{C}$ and 5% CO_2 in MEME medium supplemented with 1% non-essential amino acids, 2.2 g/L NaHCO_3 , 2 mM L-glutamine, 1 mM sodium pyruvate, 100 IU/mL penicillin/streptomycin and 10% FBS.

The spheroids were prepared by the forced floating method according to (Stampar et al., 2019) with minor modifications. Briefly, the cells (5000 cells/well) in growth media supplemented with 4% methylcellulose were centrifuged at 900 g for 1.5 h at $28\text{ }^{\circ}\text{C}$ in 96-well U-bottom low attachment plate to form spheroids. Subsequently they were cultured for 3 days at $37\text{ }^{\circ}\text{C}$ and 5% CO_2 prior treatment. Afterwards, the growth media was replaced with fresh media containing cylindrospermopsin (CYN) at concentrations 0.125, 0.25 and 0.5 $\mu\text{g/mL}$ and the spheroids were incubated for additional 72 h. In all experiments, untreated (growth media), solvent (0.05% methanol) and appropriate positive (PC) controls were included.

2.3. Monitoring of growth and morphology of spheroids

Five spheroids per treatment were monitored over 72 h of cultivation. The surface area of each spheroid in each treatment condition was measured every 24 h and the image of each spheroid was captured using NIS elements software 4.13 v (Nikon Instruments, Melville, NY, USA) connected with Ti Eclipse inverted microscope (Nikon, Japan). Spheroid growth was monitored in three independent parallels. Etoposide [1 µg/mL] was used as a PC. The difference between treated spheroids and solvent control was analysed by the Two-way ANOVA with Fisher's LSD test using GraphPad Prism V6 for Windows (GraphPad Software, California USA). $p < 0.05$ was considered statistically significant.

2.4. Cell viability test

The tetrazolium-based (MTS) assay was performed according to the manufacturer's protocol with minor modifications (Stampar et al., 2019). Briefly, after 72 h exposure to CYN, a freshly prepared MTS:PMS solution (20:1) was added to each well corresponding to one spheroid. After 3 h of incubation, the absorbance was measured at 490 nm using the spectrofluorimeter (Synergy MX, BioTek, USA). The experiment was repeated three times independently and each time eight spheroids per treatment were included. Etoposide [30 µg/mL] was used as a PC. The difference between treated groups and the solvent control was analysed by the One-way ANOVA using GraphPad Prism Software. $p < 0.05$ was considered statistically significant.

2.5. Confocal z-stack imaging of life/dead stained spheroids

After 72 h of CYN exposure, the culture media was replaced with FBS-free media with FDA stain [8 µg/mL] and incubated in darkness for 1 h. Afterwards, PI [20 µg/mL] was added and incubated for additional 5 min. Z-stack images of single spheroids were taken using the confocal microscope Leica SP8 TCS at 100x magnification. Etoposide [1 µg/mL] was used as a PC. The image analysis and the quantification of the ratio of dead cells was performed using the Image-Pro 10 software (Media Cybernetics, USA). At least 40 Z-stack images per spheroid were recorded through the entire volume of the spheroid using excitation and emission settings for simultaneous dual channel recordings and at least three spheroids per treatment point were included in the analysis. The difference between treated groups and the solvent control was analysed by the One-way ANOVA using GraphPad Software. $p < 0.05$ was considered statistically significant.

2.6. Flow cytometric analyses of cell cycle, cell proliferation and gamma-H2AX formation

For the analyses of the cell cycle, cell proliferation and gamma-H2AX formation single-cell suspension was prepared with enzymatic digestion and mechanical degradation according to (Stampar et al., 2019) with modifications. After the exposure, 30 spheroids per treatment were collected in a tube, washed in PBS and incubated in trypsin-EDTA (0.25%, Gibco) for 4 min. Next, the spheroids were disintegrated into a single-cell suspension using 200 µL pipet tips. The obtained single cells were washed in PBS, fixed in ethanol and stored at -20 °C until analysis (for details see (Hercog et al., 2019)). Fixed cells were washed in cold PBS and labelled for simultaneous detection of three endpoints. First, they were labelled with anti-H2AX pS139-APC and anti-Ki67-FITC (50-fold diluted antibodies in 1% BSA), washed with PBS, and subsequently stained with Hoechst 33342 dye (diluted in 0.1% Triton X-100 1:500). Flow cytometric analyses were carried out on a MACSQuant Analyzer 10

(Miltenyi Biotec, Germany). APC fluorescence, corresponding to DNA double strand breaks (DSBs), was detected in R1 (655–730 nm) channel; FITC fluorescence, corresponding to the proliferation marker Ki67+, was detected in the B1 (525/50 nm) channel and Hoechst fluorescence corresponding to DNA content for cell cycle analysis was detected in V1 (450/50 nm) channel. Unspecific binding of antibodies was excluded based on reagent and reagent-APC controls (Miltenyi Biotec, Germany). The experiment was repeated three times independently where each time 10^4 single cells per experimental point were recorded. Etoposide [1 µg/mL] was used as a PC.

Flow cytometry data were analysed and graphically presented in the FlowJo software V10 (Becton Dickinson, New Jersey USA). The comparison of the cell cycle distribution of cells in the solvent control and treated samples was done by two-way ANOVA with Fisher's LSD test, while the significance of Ki67 positive cells was tested by one-way ANOVA with Dunnett's multiple comparison test both using GraphPad Software. The statistical significance in the change of APC fluorescence was tested using exported.csv values in the R software with Linear and Nonlinear Mixed Effects Models (nlme) package (Pinheiro et al., 2007).

2.7. The qPCR analyses of the expression of selected genes

The expression of selected genes was determined in spheroids exposed to the highest concentration of CYN [0.5 µg/mL], solvent control and B(a)P [30 µM] as a PC. Total mRNA was isolated from a pool of 32 spheroids per treatment, using TRIzol reagent, according to manufacturer's instructions. The mRNA concentration and quality were spectrophotometrically determined using NanoDrop 1000 (Thermo Fischer Scientific, Wilmington, USA). 1 µg of total isolated mRNA per sample was reverse transcribed using The High capacity cDNA Transcription Kit. The experiment was repeated in three parallels with two technical repetitions. The BioMark™ HD System to perform real-time quantitative PCR (qPCR) analysis on the 48.48 Dynamic Array™ was employed to analyse the level of expression of selected genes (Table 1) according to the manufacturer's instructions. The relative quantification of gene deregulation was performed with the QuantGenious web-based tool (Baebler et al., 2017) comparing the Ct values of reference (GAPDH and HPRT1) and target genes using the standard curve. Relative gene expression ≥ 1.5 -fold or ≤ 0.66 compared to control was considered as up- or down-regulation, respectively. The significance of the difference between treated groups and the solvent control was analysed by two tailed Student's t-test with Welch's correction using GraphPad Software.

3. Results and discussion

In the last decade, the toxicity and genotoxicity and potential carcinogenicity of CYN has been extensively studied using traditional monolayer (2D) cell culture models *in vitro*. However, 2D cultures are associated with inherent weaknesses, which reduce their reliability for predicting of the effects *in vivo* in whole organisms. Recently we developed *in vitro* 3D cell model from HepG2 cells by the forced floating method (Stampar et al., 2019) that was in the present study used for studying the cyto-/genotoxic effects and the underlying molecular mechanisms of toxin activity.

3.1. The effects of CYN on HepG2 spheroid morphology and cell viability

The exposure of HepG2 spheroids to CYN for 72 h caused dose-dependent decrease of spheroid's growth (Fig. 1C). At the end of exposure the average surface area of control spheroids cultivated in

4

K. Hercog et al. / Environmental Pollution 265 (2020) 114965

Table 1
Genes included in the gene expression analyses.

	Gene symbol	Full Gene Name	Taqman Gene Expression Assay
Housekeeping gene	<i>GAPDH</i>	Glyceraldehyde-3-Phosphate Dehydrogenase	Hs02758991_g1
	<i>HPRT1</i>	Hypoxanthine Phosphoribosyltransferase 1	Hs02800695_m1
Metabolism of xenobiotics	<i>CYP1A1</i>	Cytochrome P450 Family 1 Subfamily A Member 1	Hs01054797_g1
	<i>CYP1A2</i>	Cytochrome P450 Family 1 Subfamily A Member 2	Hs00167927_m1
	<i>CYP3A4</i>	Cytochrome P450 Family 3 Subfamily A Member 4	Hs02514989_s1
	<i>ALDH3A1</i>	Aldehyde Dehydrogenase 3 Family Member A1	Hs00964880_m1
	<i>AHR</i>	Aryl Hydrocarbon Receptor	Hs00169233_m1
	<i>NAT1</i>	N-Acetyltransferase 1	Hs02511243_s1
	<i>NAT2</i>	N-Acetyltransferase 2	Hs01854954_s1
	<i>SULT1B1</i>	Sulfotransferase Family 1 B Member 1	Hs00234899_m1
	<i>SULT1C2</i>	Sulfotransferase Family 1C Member 2	Hs00602560_m1
	<i>UGT1A1</i>	UDP Glucuronosyltransferase Family 1 Member A1	Hs02511055_s1
	<i>UGT2B7</i>	UDP Glucuronosyltransferase Family 2 Member B7	Hs00426592_m1
Oxidative stress	<i>HIF-1α</i>	Hypoxia Inducible Factor 1 Subunit Alpha	Hs00153153_m1
DNA damage response and cell cycle arrest	<i>CDKN1A</i>	Cyclin Dependent Kinase Inhibitor 1 A	Hs00355782_m1
	<i>GADD45α</i>	Growth Arrest And DNA Damage Inducible Alpha	Hs00169255_m1
	<i>ERCC4</i>	ERCC Excision Repair 4, Endonuclease Catalytic Subunit	Hs00193342_m1
	<i>CCND1</i>	Cyclin D1	Hs00765553_m1
Proliferation	<i>MKI67</i>	Marker Of Proliferation Ki-67	Hs01032443_m1
	<i>PCNA</i>	Proliferating Cell Nuclear Antigen	Hs00427214_g1
	<i>TOP2 α</i>	DNA Topoisomerase II Alpha	Hs01032137_m1
Apoptosis	<i>BBC3</i>	BCL2 Binding Component 3	Hs00248075_m1

medium with solvent (0.05% methanol) was 0.451 ± 0.040 mm², while the surface area of spheroids exposed to 0.5 μ g/mL CYN was 1.433 ± 0.039 mm². When the spheroid growth was normalized to its size at the treatment point (time 0), the measurements revealed that after 72 h CYN inhibited spheroid growth for 8% on average when compared to the solvent control ($p = 0.0003$) (Fig. 1A and C). Etoposide, the positive control, after 72-h exposure decreased the spheroid area for 31% on average compared to solvent control ($p < 0.0001$). CYN affected the surface and the integrity of spheroids, which was less compact than that of control ones (Fig. 1B). The loosened and detached cells on the surface were viable (Fig. 2). Sasu et al. (2018) described similar effects of CYN (1.04 μ g/mL) on the surface of spheroids developed from liver stem cells HL1-hT1. The surface of control spheroids was generally smooth, while in CYN treated spheroids it was ruffled and disintegrated. Previously, Straser et al. (2013b) reported CYN induced morphological changes in HepG2 cells cultured in a monolayer. In cells exposed to CYN, formation of a compact monolayer of cells was reduced and a less firm attachment of cells to the surface of the culture plates and to each other was reported, which is in line with our observations on the surface of the spheroids. There are several indications that CYN affects the cytoskeleton of cells (reviewed in Mathe et al., 2017), which results in changed cell morphology and intracellular bonds, which may explain the observed effects.

The exposure of the spheroids to CYN for 72 h did not significantly reduce the viability of cells. No difference between cells from CYN treated and control spheroids was observed with the tetrazolium-based (MTS) assay (Fig. 3A), while the live/dead staining of the whole spheroid showed a trend of dose dependent increase in the ratio of dead cells that was however not statistically significant (Fig. 3B). The positive control, etoposide significantly reduced cell viability (Fig. 3). Contrary to these results, under the same exposure conditions, in 2D HepG2 cultures, CYN reduced cell viability for approximately 50% (Straser et al., 2013b). Higher cell survival in 3D compared to 2D HepG2 cultures has been observed also after the exposure to two heterocyclic aromatic amines PhIP and IQ, a polycyclic aromatic hydrocarbon B(a)P, and a mycotoxin AFB1, (Stampar et al., 2019). Li (2008) reported that HepG2 cells cultured in 3D are more resistant to drug-induced apoptosis and the same phenomenon has been observed in several studies where cells cultured in 3D showed higher resistance to anticancer drugs

than cells cultured in 2D, irrespective of the compound's mechanism of action (Karlsson et al., 2012; Loessner et al., 2010; Patra et al., 2016). Similar pattern of chemoresistance as developed in 3D spheroids is observed also *in vivo* (Sodek et al., 2009). Lower sensitivity of 3D culture vs. 2D can result from the differences in i) physical and physiological characteristics (interactions between neighbouring cells and extracellular matrix influencing cellular decision-making process); ii) presence and spatial arrangement of membrane receptors; iii) gene expression levels; iv) cell stages and v) drug accessibility and local pH (reviewed in Edmondson et al., 2014). The difference in CYN cytotoxic effects obtained in 3D vs. 2D models is in line with higher resistance of 3D models towards cytotoxic compounds.

3.2. The effects of CYN on cell cycle, cell proliferation and DNA damage

The effects of CYN on cell cycle, cell proliferation and DNA damage was determined by flow cytometry with simultaneous measurement of the fluorescent signals of Hoechst 33342 for cell cycle determination, FITC corresponding to proliferation marker Ki67 and APC corresponding to DNA DSBs. The effect of CYN on the cell cycle was observed at concentrations ≥ 0.25 μ g/mL (Fig. 4A). Compared to solvent control, the number of cells in G0/G1 phase was increased together with the reduction of the number of cells in S phase. The proliferation marker Ki67 was equally present in the cells of treated and control spheroids (Fig. 4B). However, the simultaneous staining with Hoescht and anti-Ki67 antibody enabled us to analyse the distribution of Ki67 positive cells across the cell cycle phases (Fig. 4D) and therefore to distinguish between cells in G0 and G1 phase (Kim and Sederstrom, 2015) since Ki67 is not present in G0 phase. The ratio of Ki67 positive cells in G0/G1 phase was similar in the control and CYN treated groups (approximately 55%) (Fig. 4C), which means that the increased number of cells in G0/G1 after CYN exposure was not due to the increased number of non-proliferating cells (G0), but represents G1 cell cycle arrest (Fig. 4A). In etoposide (PC) exposed spheroids 68% of cells in G0/G1 cells were Ki67 negative (Fig. 4C), meaning that less cells were dividing.

In G1 phase of the cell cycle, crucial decisions on DNA replication and completing the cell division are made in cells. Genotoxic stress

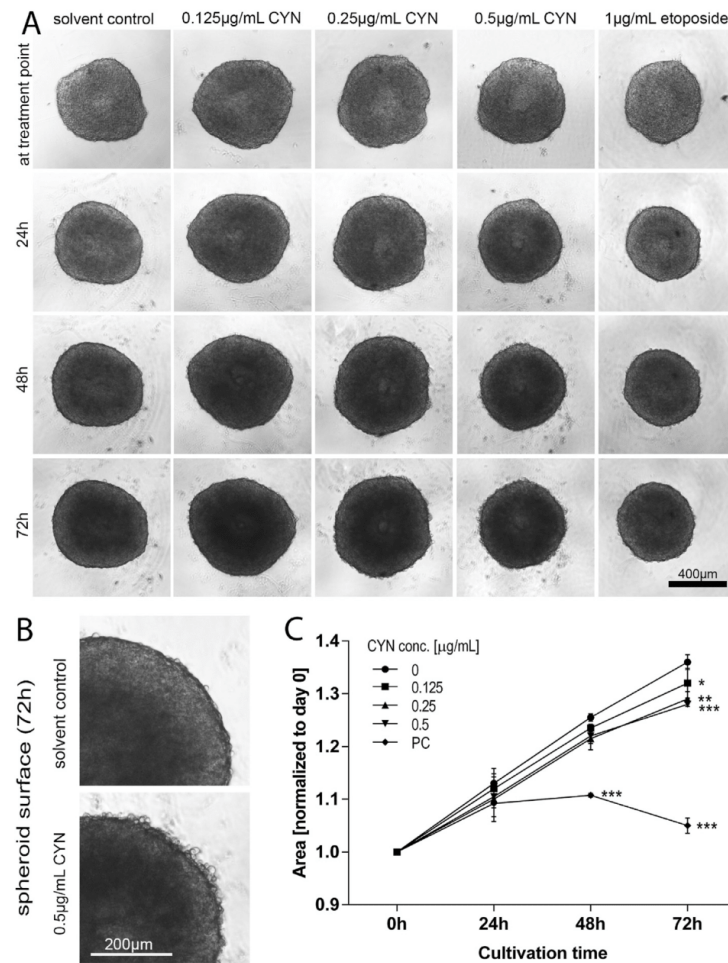


Fig. 1. A: Monitoring of the spheroids at different times of exposure to CYN (0.125, 0.25 and 0.5 µg/mL) and controls. For each treatment, a representative image sequence of the same spheroid is shown. The scale (400 µm) corresponds to all images; B: The surface of spheroid cultivated in the medium with solvent [0.05% methanol] and CYN [0.5 µg/mL] treated for 72 h; C: The area of spheroids at different times of cultivation and exposure to CYN and PC (ET [1 µg/mL]).

of various sources leads to activation of p53 protein which regulates the transcription of genes involved in G1/S cell-cycle arrest, including the cyclin-dependent kinase inhibitor 1 (p21) (Bartek and Lukas, 2001).

CYN [1 µg/mL] induced cell cycle arrest at G0/G1 phase was observed also in human lymphocytes (Poniedziatek et al., 2014). On the contrary, Straser et al. (2013b) reported that in the HepG2 monolayer culture 72 h exposure to CYN [0.5 µg/mL] decreased the number of cells in G0/G1 phase and caused S-phase cell cycle arrest. In the same study CYN induced DNA DSBs were observed (Straser et al., 2013b), while the results from the present study showed no increase of γH2AX positive cells corresponding to DNA DSBs in HepG2 spheroids (Fig. 4E). The S-phase DNA synthesis arrest is specifically related to DSBs via the p53-independent ATM pathway (Kastan and Lim, 2000). This explains why the cells in spheroids exposed to CYN were not arrested in S phase as has been previously

observed by Straser et al. (2013b). These results suggest differences in the mechanisms of action of CYN in 2D and 3D models. In HepaRG cells exposed to CYN, Huguet et al. (2019) reported cell cycle alternations with G2/M arrest and the induction of γH2AX, but at concentrations at which the cell viability was reduced to 50% [≥ 1.3 µg/mL] and 10% [5.2 µg/mL]. The DNA DSBs observed at such high cytotoxicity may not reflect genotoxic activity but correspond to degradation of DNA in the process of apoptosis or necrosis (Müller et al., 1999).

3.3. The effects of CYN on the expression of selected genes

To elucidate the molecular mechanisms involved in CYN induced toxicity and genotoxicity we analysed changes in the transcription of selected genes involved in metabolic transformation, oxidative stress, DNA damage response, proliferation

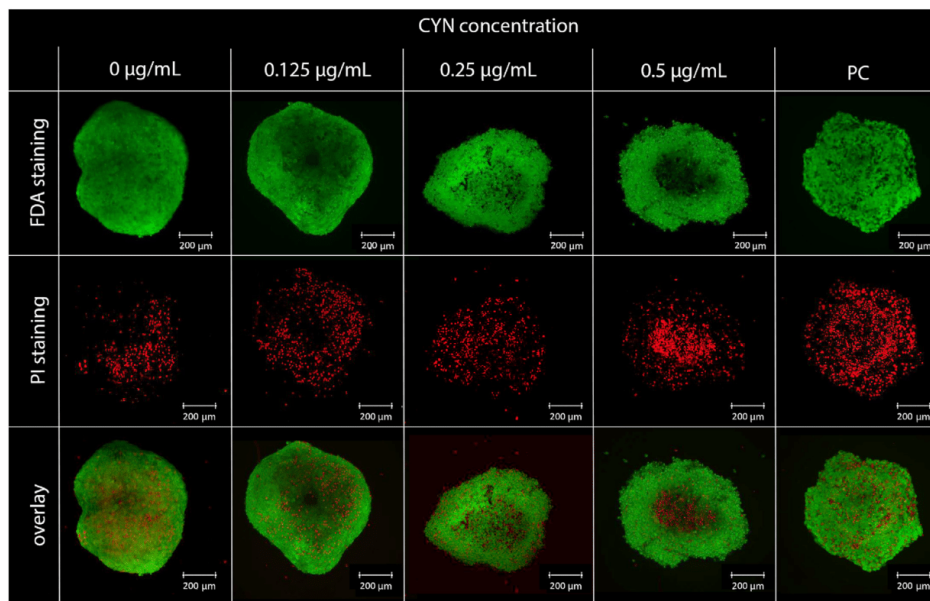


Fig. 2. Images of control and CYN (0.125, 0.25 and 0.5 µg/mL) treated spheroids stained with FDA (green, live cells) and PI (red, dead cells). Etoposide (1 µg/mL) was used as a positive control. The images were obtained using a confocal microscope at 100 \times -magnification. (For interpretation of the references to colour in this figure legend, the reader is referred to the Web version of this article.)

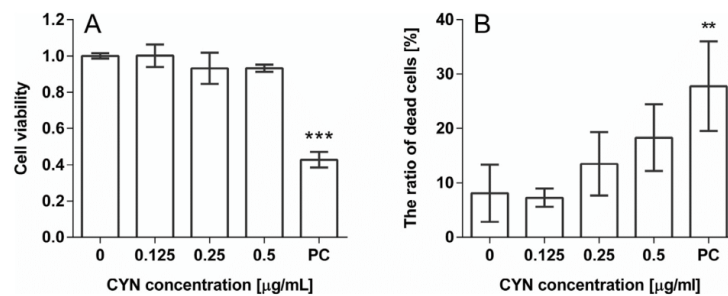


Fig. 3. The effect of CYN (0.125, 0.25 and 0.5 µg/mL) on the viability of HepG2 cells in spheroids after 72 h exposure. A: Viability determined with the MTS assay. B: The ratio of dead cells determined with live/dead staining of whole spheroid (confocal microscopy). PC = 30 µg/mL etoposide. Significant difference between treated spheroids and solvent control (0) one-way ANOVA) is indicated by ** $p < 0.01$ and *** $p < 0.001$.

and apoptosis (Table 2). Nowadays, CYN is generally recognized as pro-genotoxic compound, which requires metabolic activation by cytochrome P-450 (CYP450) enzymes to cause genotoxic effects (Straser et al., 2011). The cytochrome P450 (CYP) enzymes are membrane-bound hemoproteins that play a pivotal role in the detoxification of xenobiotics, cellular metabolism and homeostasis. Induction or inhibition of CYP enzymes is a principal mechanism for metabolism-based drug-drug interactions. CYP enzymes can be transcriptionally activated by various xenobiotics and endogenous substrates through receptor-dependent mechanisms and consequently CYP-mediated biotransformation may result in metabolic activation of environmental chemicals to reactive carcinogenic products (Manikandan and Nagini, 2017). In metabolically incompetent *in vitro* models, CYN does not induce genotoxic effects

(Fessard and Bernard, 2003; Lankoff et al., 2007; Puerto et al., 2018), while in metabolically active models CYP450 inhibitors reduce toxic effects of CYN *in vitro* (Bazin et al., 2010; Humpage et al., 2005; Kittler et al., 2016) and *in vivo* (Froschio et al., 2003). The HepG2 spheroids used in the present study have been shown to be metabolically competent and sensitive for detecting the effects of indirect genotoxic compounds (Stampar et al., 2019). CYN upregulated the expression of *CYP1A1* (13.2-fold) and *CYP3A4* (2.45-fold), suggesting their role in the activation of the toxin, while the transcription of *CYP1A2* was not significantly affected. Another phase I enzyme *ALDH3A1*, a member of aldehyde dehydrogenase 3 family, which oxidizes various aldehydes to the corresponding acids (Lindahl, 1992), was also strongly upregulated (30.7-fold). Moreover, the transcription of *AHR*, the main nuclear factor in the

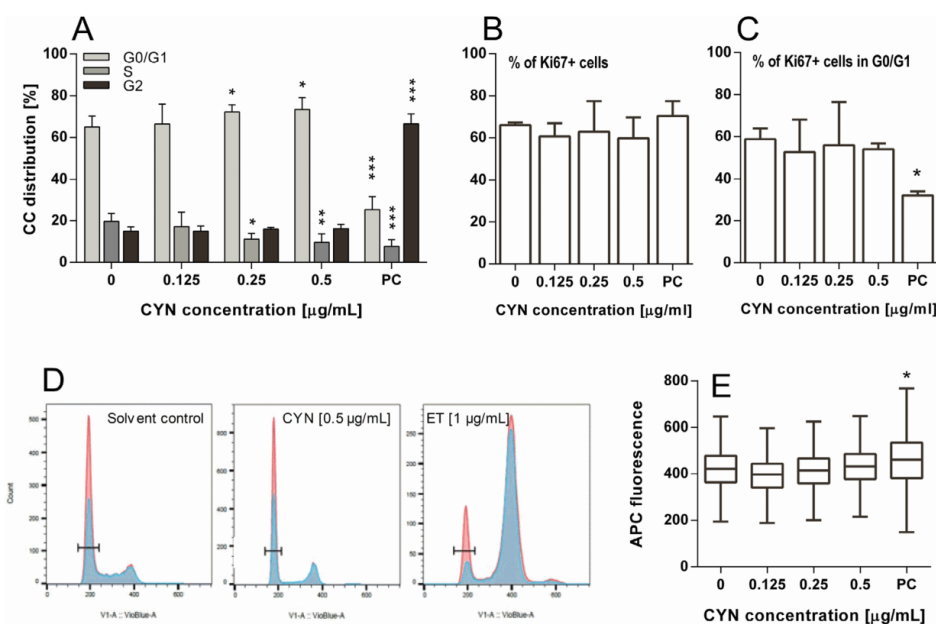


Fig. 4. A: Distribution of cells across different phases of cell cycle (CC) after exposure to CYN; B: Percentage of Ki67 positive cells after exposure to CYN; C: Percentage of Ki67 positive cells within G0/G1 phase of cell cycle after exposure to CYN; D: Representative overlays of simultaneous staining with Hoechst for cell cycle (red) and anti-Ki67 antibody (blue); E: relative values of APC fluorescence corresponding to anti- γ H2AX labelled sites after exposure to CYN. PC = 1 µg/mL etoposide. Significant difference between treated sample and solvent control (0) for cell cycle (two-way ANOVA with Fisher's LSD test), Ki67 (one-way ANOVA with Dunnett's multiple comparison) and γ H2AX (R nlme package) is indicated by * $p < 0.05$, ** $p < 0.01$ and *** $p < 0.001$. (For interpretation of the references to colour in this figure legend, the reader is referred to the Web version of this article.)

Table 2

Relative expression of selected genes after the exposure of HepG2 spheroids to CYN [0.5 µg/mL] for 72 h. BaP [10 µM] treatment was included as PC.

function	gene	CYN [0.5 µg/mL]			BaP [10 µM]			
		Average	SD	p-value	average	SD	p-value	
metabolism of xenobiotics	<i>CYP1A1</i>	13.16	2.24	0.00155	340.91	21.51	0.00002	***
	<i>CYP1A2</i>	0.86	0.03	0.00421	11.93	1.74	0.00089	***
	<i>CYP3A4</i>	2.45	0.69	0.04072	2.00	0.46	0.03709	*
	<i>ALDH3A1</i>	30.74	9.50	0.01144	270.28	103.16	0.02099	*
	<i>AHR</i>	4.85	0.38	0.00014	2.15	0.18	0.00076	***
	<i>NAT1</i>	5.36	0.41	0.00011	2.85	0.10	0.00001	***
	<i>NAT2</i>	0.61	0.33	0.168972	4.69	2.68	0.12311	*
	<i>SULT1B1</i>	2.56	1.91	0.31259	2.65	1.63	0.22543	
	<i>SULT1C2</i>	2.32	0.02	0.00000	1.51	0.12	0.00412	**
	<i>UGT1A1</i>	12.69	1.97	0.00111	61.73	4.81	0.00006	***
oxidative stress	<i>UGT2B7</i>	2.43	0.09	0.00003	11.82	0.64	0.00002	***
	<i>HIF1α</i>	2.13	0.26	0.00331	1.88	0.08	0.00011	***
DNA damage response and cell cycle arrest	<i>CDKN1A</i>	10.58	0.54	0.00001	22.02	3.17	0.00072	***
	<i>GADD45α</i>	32.74	5.11	0.00093	4.76	0.59	0.00082	***
	<i>ERCC4</i>	5.27	0.31	0.00004	1.90	0.11	0.00033	***
proliferation	<i>CCND1</i>	1.46	0.08	0.00119	1.96	0.21	0.00303	**
	<i>PCNA</i>	0.47	0.03	0.00001	1.82	0.08	0.00016	***
	<i>TOP2α</i>	0.40	0.03	0.00001	0.49	0.06	0.00024	***
	<i>MKI67</i>	0.73	0.08	0.01061	0.42	0.05	0.00006	***
apoptosis	<i>BBC3</i>	4.75	0.85	0.00334	3.34	0.33	0.00055	***

regulation of CYPs and ALDHs (Omicinski et al., 2011), was upregulated (4.85-fold), indicating that aryl hydrocarbon receptor (AHR) mediated induction of the transcription of phase I enzymes. CYN upregulated the mRNA level of all studied phase II enzymes, with the exception of *NAT2*, which was downregulated (-1.64-fold). The highest relative expression was observed for *UGT1A1* (12.7-fold) and *NAT1* (5.4-fold), while *SULT1A1*, *SULT1C2*, and

UGT2B7 were approximately 2.4-fold upregulated. The results are in line with previously reported deregulation of the expression of genes encoding metabolic enzymes in HepG2 monolayer culture exposed to 0.5 µg/mL CYN for up to 24-h (Hercog et al., 2017; Straser et al., 2013c, 2011). CYN upregulated the expression of *CYP1A1* also in human peripheral blood lymphocytes (Zegura et al., 2011a, 2011b). Recently, strong downregulation of genes encoding

enzymes involved in the metabolism of xenobiotics was detected in the differentiated HepaRG monolayer culture exposed to CYN ($\geq 0.2 \mu\text{g/mL}$) for 24 h together with reduced activity of cytochromes P450, including CYP3A4 ($\geq 0.66 \mu\text{g/mL}$) (Huguet et al., 2019). These data are contrary to our results; however, also to other published data (Bazin et al., 2010; Frosco et al., 2003; Hercog et al., 2017; Humpage et al., 2005; Kittler et al., 2016; Štraser et al., 2013c, 2011; Žegura et al., 2011a, 2011b). Up to date, there are no literature data describing deregulation of the enzymes SUL1B1, SUL1C2, and JGT2B7 following cell exposure to CYN. Our study demonstrated potential involvement of enzymes encoded by these genes in CYN detoxification. From the obtained data we can conclude that in the 3D HepG2 cells model CYN upregulated the expression of metabolic genes especially those involved in detoxification (phase II) to a higher extent than previously reported in 2D cultures, further supporting the evidence that there are differences in metabolic pathways between 2D and 3D cell cultures. More efficient metabolism of CYN in 3D spheroids not only through the activation phase but also through the detoxification is in alignment with its reduced cytotoxic and genotoxic effects as well as lower effects on proliferation in 3D spheroids compared to 2D cultures, which is described above.

One of the CYN mechanisms of action is generation of reactive oxygen species (ROS) and induction of oxidative stress (Evans et al., 2019; Liebel et al., 2011; Poniedzialek et al., 2015; Runnegar et al., 1994, 1995), which corresponds to the upregulation of *HIF1A* (2.13-fold) in the present study. The *HIF1A* gene is constitutively expressed at low levels; however, its expression is often significantly upregulated in response to hypoxia and may also be upregulated by ROS (Yeo, 2019).

Despite no increase in γH2AX positive cells was observed under the conditions applied in the present study, the genes involved in DNA damage response were highly upregulated, showing genotoxic activity of CYN in HepG2 spheroids. The up-regulation of DNA damage responsive genes *CDKN1A*, *GADD45a*, *MDM2*, and *ERCC4* upon CYN exposure has already been described in HepG2 monolayer cultures (Bain et al., 2007; Hercog et al., 2017; Štraser et al., 2013c, 2011), human peripheral blood lymphocytes (Žegura et al., 2011a, 2011b) and human dermal fibroblasts (Bain et al., 2007).

DNA damage is followed by rapid induction of the GADD45 protein family members resulting in cell cycle arrest. Afterwards, the cell undergo apoptosis or DNA repair mechanisms in which GADD45 proteins play an active role (Tamura et al., 2012). The GADD45-mediated cell cycle arrest is induced primarily via the CDK1/Cyclin B1 complex, which is responsible for the G2/M checkpoint. However, through interaction with p21 (encoded by *CDKN1A*), GADD45 proteins modulate G1/S transition (reviewed in Tamura et al., 2012), which was also observed in the present study. Likewise, *ERCC4* is also induced by genotoxic stress, especially chemicals causing covalent helix-distorting adducts. *ERCC4* acts as an essential element of DNA nucleotide excision repair (NER) pathway (Manandhar et al., 2015). The upregulation of *GADD45a* (32.7-fold), *CDKN1A* (10.6-fold) and *ERCC4* (5.27-fold) together with cell-cycle arrest discussed above is an indication of DNA damaging effects of CYN in HepG2 spheroids. The positive control, benzo(a)pyrene, a well-known indirectly acting genotoxic compound at concentration of $10 \mu\text{M}$ induced similar deregulation of DNA damage responsive genes as CYN that was, used at 8.3-times lower concentrations ($0.5 \mu\text{g/mL}$ corresponds to $1.2 \mu\text{M}$) (Table 2).

The *CCND1* encodes the cyclin D1 protein, which binds to cyclin-dependent kinases 4 and 6 and regulates progression from G1 into S phase of the cell cycle (reviewed in Bertoli et al., 2015). Elevated expression of cyclin D1 has been reported in many human tumours and correlates to increased cell proliferation and differentiation due to shortened G1/S transition (Snoj et al., 2009). In our study,

upregulation of the expression of *CCND1*, although statistically significant was less than 1.5-fold that is considered as biologically irrelevant. The lack of upregulation of the expression of *CCND1* is in line with the observed G1 cell cycle arrest. Although no significant reduction of the proliferation marker Ki67 measured using flow cytometry and qPCR (at the mRNA level) was observed, down-regulation of *PCNA* (-2.13 -fold) and *TOP2 α* (-2.5 -fold) by CYN indicated the toxin's negative impact on the cell proliferation. Proliferating Cell Nuclear Antigen (PCNA) is a protein associated with DNA polymerase alpha; thus it plays a critical role in DNA synthesis and is highly abundant in cells during the G1/S phase of the cell cycle, while in quiescent and senescent cells the levels of PCNA mRNA and protein are low (Kelman, 1997). Topoisomerase II alpha (TOP2 α) is a protein essential for DNA condensation before its replication and the segregation of chromosomes in mitotic cells (Colozza et al., 2005). The expression of TOP2 α is cell cycle-dependent and its elevated protein as well as mRNA levels are recognized as a marker of cell proliferation (Neubauer et al., 2016). Several authors reported reduced cell proliferation upon exposure to CYN. It significantly decreased the mitotic index and cell proliferation in CHO-K1 cells (Lankoff et al., 2007), proliferation of T-lymphocytes was significantly reduced after exposure to CYN at $1 \mu\text{g/mL}$ (Poniedzialek et al., 2014) and in 2D HepG2 culture CYN ($0.5 \mu\text{g/mL}$, ≥ 24 h) reduced proliferation measured as the ratio of Ki67 positive cells by immunostaining (Štraser et al., 2013b). Moreover, negative impact of CYN on proliferation was observed at the gene transcription level in HepG2 (Štraser et al., 2013c) as well as in HepaRG (Huguet et al., 2019) monolayer cultures. Therefore, it can be concluded that CYN is inhibiting cell proliferation in variety of 2D *in vitro* models as well as in the 3D HepG2 model as shown by the present study.

Finally, we analysed the influence of CYN on the apoptosis by measuring the expression of *BBC3*. The *BBC3* gene encodes the Bcl-2-binding component 3 also known as 'p53 upregulated modulator of apoptosis (PUMA). This pro-apoptotic protein interacts with anti-apoptotic Bcl-2 family members resulting in mitochondria induced apoptosis and cell death through the caspase cascade. The expression of *BBC3* is regulated on the transcription level by p53 and not by post-translational modifications (Nakano and Vousden, 2001). In the present study, *BBC3* was upregulated (4.75-fold) after 72 h exposure to $0.5 \mu\text{g/mL}$ CYN, suggesting that in HepG2 spheroids one of the mechanisms of CYN action is the induction of apoptosis. There are several reports that CYN induces apoptosis in CHO-K1 cells (Fessard and Bernard, 2003; Gácsi et al., 2009; Lankoff et al., 2007), primary human lymphocytes (Pichardo et al., 2017; Poniedzialek et al., 2014) and primary rodent hepatocytes (López-Alonso et al., 2013). However, other authors are reporting less conclusive results (Štraser et al., 2013c) or even no apoptotic effects in hepatic HepG2 (Štraser et al., 2013a) and HepaRG cells (Huguet et al., 2019) nor in human lymphocytes (Bojana Žegura et al., 2011a, 2011b).

The results represent relative mRNA expression normalized to solvent control.

4. Conclusions

In experimental toxicology, a lot of effort has recently been focused on the development and use of advanced *in vitro* models to reduce, replace and refine animal experiments. Compared to the classical 2D cultures, 3D cell models *in vitro* resemble cell organization of tissues and organs and thus better mimic *in vivo* micro-environment, which is an important aspect in cellular responses and cell survival after exposure to various compounds. In the present study, the advanced 3D cell model *in vitro* (spheroids) from HepG2 cells was used for studying the adverse effects of

cyanobacterial toxin cylindrospermopsin for the first time. The toxin affected the growth and the shape of HepG2 cells in spheroids. The formation of γ H2AX positive cells corresponding to DNA double strand breaks was not detected; however, at the same time, strong up-regulation of DNA damage responsive genes *CDKN1A*, *GADD45 α* , and *ERCC4* was observed confirming the genotoxic activity of CYN. The cell cycle status was altered after the exposure to CYN and several genes involved in cell cycle regulation were deregulated, indicating that the TP53-pathway was importantly involved in cell cycle arrest induced by CYN. Further, phase I and phase II metabolic enzymes that are transcriptionally induced by the exposure to indirect-acting genotoxic compounds were up-regulated, which confirmed that metabolism plays an important role in CYN activation and its toxic and genotoxic activity, where genes such as *CYP1A1*, *CYP3A4*, *ALDH3A1* as well as their main transcription factor *AHR* play a significant role. Even more importantly, results on the mRNA induction of phase II enzymes *NAT1*, *SULT1B1*, *SULT1C2*, *UGT1A1*, and *UGT2B7* suggested their involvement in CYN detoxification pathways. The developed 3D HepG2 cell model can contribute to more reliable genotoxicity assessment of chemical compounds, including cyanobacterial toxins, due to its higher physiological relevance for human exposure.

Author contribution

Klara Hercog: Conceptualization, Methodology, Software, Validation, Formal analysis, Investigation, Data Curation, Writing - Original Draft, Visualization; Martina Stampar: Methodology, Software, Validation, Formal analysis, Investigation, Writing - Review & Editing, Visualization; Alja Stern: Methodology, Software, Validation, Formal analysis, Investigation, Writing - Review & Editing, Visualization; Metka Filipič: Resources, Writing - Review & Editing, Supervision, Project administration, Funding acquisition; Bojana Žegura: Conceptualization, Methodology, Formal analysis, Investigation, Resources, Writing - Original Draft, Visualization, Supervision, Project administration, Funding acquisition.

Declaration of competing interests

The authors declare that they have no known competing financial interests or personal relationships that could have appeared to influence the work reported in this paper.

Acknowledgements

The authors acknowledge the financial support from the Slovenian Research Agency [research core funding P1-0245 and grants to young researchers MR-KHercog and MR-MStampar], and COST Actions CA16119 (In vitro 3-D total cell guidance and fitness) and ES1105 (Cyanobacterial blooms and toxins in water resources: Occurrence, impacts and management).

References

- Baebler, S., Svalina, M., Petek, M., Stare, K., Rotter, A., Pompe-Novak, M., Gruden, K., 2017. QuantGenius: implementation of a decision support system for qPCR-based gene quantification. *BMC Bioinf.* 18 <https://doi.org/10.1186/s12859-017-1688-7>.
- Bain, P., Shaw, C., Patel, B., 2007. Induction of p53-regulated gene expression in human cell lines exposed to the cyanobacterial toxin cylindrospermopsin. *J. Toxicol. Environ. Health Part A Curr. Issues* 70, 1687–1693. <https://doi.org/10.1080/15287390701434877>.
- Bartek, J., Lukas, J., 2001. Mammalian G1- and S-phase checkpoints in response to DNA damage. *Curr. Opin. Cell Biol.* 13, 738–747. [https://doi.org/10.1016/S0955-0674\(00\)0280-5](https://doi.org/10.1016/S0955-0674(00)0280-5).
- Basu, A., Dydowiczová, A., Čtveráková, L., Jaša, L., Troško, J.E., Bláha, L., Babica, P., 2018. Assessment of hepatotoxic potential of cyanobacterial toxins using 3D in vitro model of adult human liver stem cells. *Environ. Sci. Technol.* 52, 10078–10088. <https://doi.org/10.1021/acs.est.8b02291>.
- Bazin, E., Mourot, A., Humpage, A.R., Fessard, V., 2010. Genotoxicity of a freshwater cyanotoxin, cylindrospermopsin, in two human cell lines: caco-2 and HepaRG. *Environ. Mol. Mutagen.* 51, 251–259. <https://doi.org/10.1002/em.20539>.
- Bell, C.C., Hendriks, D.F.G., Moro, S.M.L., Ellis, E., Walsh, J., Renblom, A., Fredriksson Puigvert, L., Dankers, A.C.A., Jacobs, F., Snoeys, J., Sison-Young, R.L., Jenkins, R.E., Nordling, Å., Mkrtchian, S., Park, B.K., Kitteringham, N.R., Goldring, C.E.P., Lauschke, V.M., Ingelman-Sundberg, M., 2016. Characterization of primary human hepatocyte spheroids as a model system for drug-induced liver injury, liver function and disease. *Sci. Rep.* 6, 1–13. <https://doi.org/10.1038/srep25187>.
- Berry, J.P., Gibbs, P.D.L., Schmale, M.C., Saker, M.L., 2009. Toxicity of cylindrospermopsin, and other apparent metabolites from *Cylindrospermopsis raciborskii* and *Aphanizomenon ovalisporum*, to the zebrafish (*Danio rerio*) embryo. *Toxicol.* 53, 289–299. <https://doi.org/10.1016/j.toxicol.2008.11.016>.
- Bertoli, C., Skotheim, J.M., Bruin, R.A.M. De, 2015. Control of cell cycle transcription during G1 and S phases. *Nat. Rev. Mol. Cell Biol.* 14, 518–528. <https://doi.org/10.1038/nrm3629> (Control).
- Buratti, F.M., Manganelli, M., Vichi, S., Stefanelli, M., Scardala, S., Testai, E., Funari, E., 2017. Cyanotoxins: producing organisms, occurrence, toxicity, mechanism of action and human health toxicological risk evaluation. *Arch. Toxicol.* 91, 1049–1130. <https://doi.org/10.1007/s00204-016-1913-6>.
- Chang, T.T., Hughes-Fulford, M., 2009. Monolayer and spheroid culture of human liver hepatocellular carcinoma cell line cells demonstrate distinct global gene expression patterns and functional phenotypes. *Tissue Eng.* 15, 559–567. <https://doi.org/10.1089/ten.tea.2007.0434>.
- Colozza, M., Azambuja, E., Cardoso, F., Sotiriou, C., Larsimont, D., Piccart, M.J., 2005. Proliferative markers as prognostic and predictive tools in early breast cancer: where are we now? *Ann. Oncol.* 16, 1723–1739. <https://doi.org/10.1093/annonc/mdj352>.
- de la Cruz, A.A., Hiskia, A., Kaloudis, T., Chernoff, N., Hill, D., Antoniou, M.G., He, X., Loftin, K., O'Shea, K., Zhao, C., Pelaez, M., Han, C., Lynch, T.J., Dionysiou, D.D., 2013. A review on cylindrospermopsin: the global occurrence, detection, toxicity and degradation of a potent cyanotoxin. *Environ. Sci. Process. Impacts* 15, 1979–2003. <https://doi.org/10.1039/c3em00353a>.
- Edmondson, R., Broglie, J.J., Adcock, A.F., Yang, L., 2014. Three-dimensional cell culture systems and their applications in drug discovery and cell-based biosensors. *Assay Drug Dev. Technol.* 12, 207–218. <https://doi.org/10.1089/adt.2014.573>.
- Epa, 2015. Drinking Water Health Advisory for the Cyanobacterial Toxin Cylindrospermopsin. *Epa-820R15 101*.
- Evans, D.M., Hughes, J., Jones, L.F., Murphy, P.J., Falfushynska, H., Horyn, O., Sokolova, I.M., Christensen, J., Coles, S.J., Rzymiski, P., 2019. Elucidating cylindrospermopsin toxicity via synthetic analogues: an in vitro approach. *Chemosphere* 234, 139–147. <https://doi.org/10.1016/j.chemosphere.2019.06.021>.
- Falconer, I.R., Humpage, A.R., 2006. Cyanobacterial (blue-green algal) toxins in water supplies: Cylindrospermopsins. *Environ. Toxicol.* 21, 299–304. <https://doi.org/10.1002/tox.20194>.
- Fessard, V., Bernard, C., 2003. Cell alterations but no DNA strand breaks induced in vitro by cylindrospermopsin in CHO K1 cells. *Environ. Toxicol.* 18, 353–359. <https://doi.org/10.1002/tox.10136>.
- Fey, S.J., Wrzesinski, K., 2012. Determination of drug toxicity using 3D spheroids constructed from an immortal human hepatocyte cell line. *Toxicol. Sci.* 127, 403–411. <https://doi.org/10.1093/toxsci/ktf122>.
- Frosio, S.M., Humpage, A.R., Burcham, P.C., Falconer, I.R., 2003. Cylindrospermopsin-induced protein synthesis inhibition and its dissociation from acute toxicity in mouse hepatocytes. *Environ. Toxicol.* 18, 243–251. <https://doi.org/10.1002/tox.10121>.
- Frosio, S.M., Humpage, A.R., Burcham, P.C., Falconer, I.R., 2001. Cell-free protein synthesis inhibition assay for the cyanobacterial toxin cylindrospermopsin. *Environ. Toxicol.* 16, 408–412.
- Gácsi, M., Antal, O., Vasas, G., Máthé, C., Borbély, G., Saker, M.L., Gyori, J., Farkas, A., Vehovszky, Á., Bánfalvi, G., 2009. Comparative study of cyanotoxins affecting cytoskeletal and chromatin structures in CHO-K1 cells. *Toxicol. Vitro* 23, 710–718. <https://doi.org/10.1016/j.tiv.2009.02.006>.
- Godoy, P., Hewitt, N.J., Albrecht, U., Andersen, M.E., Ansari, N., Bhattacharya, S., Bode, J.G., Bolley, J., Borner, C., Böttger, J., Braeuning, A., Budinsky, R.A., Burkhardt, B., Cameron, N.R., Camussi, G., Cho, C.-S., Choi, Y.-J., Craig Rowlands, J., Dahmen, U., Damm, G., Dirsch, O., Donato, M.T., Dong, J., Dooley, J., Drasdo, D., Eakins, R., Ferreira, K.S., Fonsato, V., Fraczek, J., Gebhardt, R., Gibson, A., Glanemann, M., Goldring, C.E.P., Gómez-Lechón, M.J., Groothuis, G.M.M., Gustavsson, L., Guyot, C., Hallifax, D., Hammad, S., Hayward, A., Häussinger, D., Hellerbrand, C., Hewitt, P., Hoehme, S., Holzhütter, H.-G., Houston, J.B., Hrach, J., Ito, K., Jaeschke, H., Keitel, V., Kelm, J.M., Kevin Park, B., Kordes, C., Kullak-Ublick, G.A., LeCluyse, E.L., Lu, P., Luebke-Wheeler, J., Lutz, A., Maltman, D.J., Matz-Soja, M., McMullen, P., Merfort, I., Messner, S., Meyer, C., Mwinji, J., Naisbitt, D.J., Nussler, A.K., Olinga, P., Pampaloni, F., Pi, J., Pluta, L., Przyborski, S.A., Ramachandran, A., Rogiers, V., Rowe, C., Schelcher, C., Schmich, K., Schwarz, M., Singh, B., Stelzer, E.H.K., Stieger, B., Stöber, R., Sugiyama, Y., Tetta, C., Thasler, W.E., Vanhaecke, T., Vinken, M., Weiss, T.S., Widera, A., Woods, C.G., Xu, J.J., Yarborough, K.M., Hengstler, J.G., 2013. Recent advances in 2D and 3D in vitro systems using primary hepatocytes, alternative hepatocyte sources and non-parenchymal liver cells and their use in investigating mechanisms of hepatotoxicity, cell signaling and ADME. *Arch. Toxicol.* 87, 1315–1530. <https://doi.org/10.1007/s00204-013-1078-5>.

- Herczeg, K., Maisanaba, S., Filipić, M., Jos, A., Cameán, A.M., Žegura, B., 2017. Genotoxic potential of the binary mixture of cyanotoxins microcystin-LR and cylindrospermopsin. *Chemosphere* 189, 319–329. <https://doi.org/10.1016/j.chemosphere.2017.09.075>.
- Herczeg, K., Maisanaba, S., Filipić, M., Sollner-Dolenc, M., Kač, L., Žegura, B., 2019. Genotoxic activity of bisphenol A and its analogues bisphenol S, bisphenol F and bisphenol AF and their mixtures in human hepatocellular carcinoma (HepG2) cells. *Sci. Total Environ.* 687, 267–276. <https://doi.org/10.1016/j.scitotenv.2019.05.486>.
- hinojosa, M.G., Gutiérrez-Praena, D., Prieto, A.I., Guzmán-Guillén, R., Jos, A., Cameán, A.M., 2019. Neurotoxicity induced by microcystins and cylindrospermopsin: a review. *Sci. Total Environ.* 668, 547–565. <https://doi.org/10.1016/j.scitotenv.2019.02.426>.
- Huguet, A., Lanceleur, R., Quenault, H., Le Hégarat, L., Fessard, V., 2019. Identification of key pathways involved in the toxic response of the cyanobacterial toxin cylindrospermopsin in human hepatic HepaRG cells. *Toxicol. Vitro* 58, 69–77. <https://doi.org/10.1016/j.tiv.2019.03.023>.
- humpage, A.R., Fenech, M., Thomas, P., Falconer, I.R., 2000. Micronucleus induction and chromosome loss in transformed human white cells indicate clastogenic and aneugenic action of the cyanobacterial toxin, cylindrospermopsin. *Mutat. Res. Genet. Toxicol. Environ. Mutagen* 472, 155–161. [https://doi.org/10.1016/S1383-5718\(00\)00144-3](https://doi.org/10.1016/S1383-5718(00)00144-3).
- humpage, A.R., Fontaine, F., Proscio, S., Burcham, P., Falconer, I.R., 2005. Cylindrospermopsin genotoxicity and cytotoxicity: role of cytochrome P-450 and oxidative stress. *J. Toxicol. Environ. Health Part A* 68, 739–753. <https://doi.org/10.1080/15287390590925465>.
- turrell, T., Lilley, K.S., Cromarty, A.D., 2019. Proteomic responses of HepG2 cell monolayers and 3D spheroids to selected hepatotoxins. *Toxicol. Lett.* 300, 40–50. <https://doi.org/10.1016/j.toxlet.2018.10.030>.
- Carlsson, H., Fryknäs, M., Larsson, R., Nygren, P., 2012. Loss of cancer drug activity in colon cancer HCT-116 cells during spheroid formation in a new 3-D spheroid cell culture system. *Exp. Cell Res.* 318, 1577–1585. <https://doi.org/10.1016/j.yexcr.2012.03.026>.
- Gastan, M.B., Lim, D.S., 2000. The many substrates and functions of ATM. *Nat. Rev. Mol. Cell Biol.* 1, 179–186. <https://doi.org/10.1038/35043058>.
- Celm, J.M., Timmins, N.E., Brown, C.J., Fussenegger, M., Nielsen, L.K., 2003. Method for generation of homogeneous multicellular tumor spheroids applicable to a wide variety of cell types. *Biotechnol. Bioeng.* 83, 173–180. <https://doi.org/10.1002/bit.10655>.
- Celman, Z., 1997. PCNA: structure, functions and interactions. *Oncogene* 14, 629–640. <https://doi.org/10.1038/sj.onc.1200886>.
- Kim, K.H., Sederstrom, J.M., 2015. Assaying cell cycle status using flow cytometry. *Curr. Protoc. Mol. Biol.* 2015, 28. <https://doi.org/10.1002/0471142727.mb2806s111>, 61–28.6.11.
- Gittler, K., Hurtaud-Pessel, D., Maul, R., Kolrep, F., Fessard, V., 2016. In vitro metabolism of the cyanotoxin cylindrospermopsin in HepaRG cells and liver tissue fractions. *Toxicol. Vitro* 10, 47–50. <https://doi.org/10.1016/j.toxicol.2015.11.007>.
- ankoff, A., Wojcik, A., Lisowska, H., Bialczyk, J., Dziga, D., Carmichael, W.W., 2007. No induction of structural chromosomal aberrations in cylindrospermopsin-treated CHO-K1 cells without and with metabolic activation. *Toxicol. Environ. Health* 50, 1105–1115. <https://doi.org/10.1016/j.toxicol.2007.07.021>.
- Li, 2008. Survival advantages of multicellular spheroids vs. monolayers of HepG2 cells in vitro. *Oncol. Rep.* 1465–1471. <https://doi.org/10.3892/or.00000167>.
- Jebel, S., Oliveira Ribeiro, C.A., Silva, R.C., Ramsdorf, W.A., Cestari, M.M., Magalhães, V.F., Garcia, J.R.E., Esquivel, B.M., Filipak Neto, F., 2011. Cellular responses of Prochilodus lineatus hepatocytes after cylindrospermopsin exposure. *Toxicol. Vitro* 25, 1493–1500. <https://doi.org/10.1016/j.tiv.2011.05.010>.
- Indahl, R., 1992. Aldehyde dehydrogenases and their role in carcinogenesis. *Crit. Rev. Biochem. Mol. Biol.* 27, 283–335. <https://doi.org/10.3109/10409239209082565>.
- Ju, J., Hernández, S.E., Swift, S., Singhal, N., 2018. Estrogenic activity of cylindrospermopsin and anatoxin-a and their oxidative products by FcIL-B*/H2O2. *Water Res.* 132, 309–319. <https://doi.org/10.1016/j.watres.2018.01.018>.
- Joessner, D., Stok, K.S., Lutolf, M.P., Huttmacher, D.W., Clements, J.A., Rizzi, S.C., 2010. Bioengineered 3D platform to explore cell-ECM interactions and drug resistance of epithelial ovarian cancer cells. *Biomaterials* 31, 8494–8506. <https://doi.org/10.1016/j.biomaterials.2010.07.064>.
- Jópez-Alonso, H., Rubiolo, J.A., Vega, F., Vieytes, M.R., Botana, L.M., 2013. Protein synthesis inhibition and oxidative stress induced by cylindrospermopsin elicit apoptosis in primary rat hepatocytes. *Chem. Res. Toxicol.* 26, 203–212. <https://doi.org/10.1021/tx3003438>.
- Juckert, C., Schulz, C., Lehmann, N., Thomas, M., Hofmann, U., Hammad, S., Hengstler, J.G., Braeuning, A., Lampen, A., Hessel, S., 2017. Comparative analysis of 3D culture methods on human HepG2 cells. *Arch. Toxicol.* 91, 393–406. <https://doi.org/10.1007/s00204-016-1677-z>.
- Manandhar, M., Boulware, K.S., Wood, R.D., 2015. The ERCC1 and ERCC4 (XPF) genes and gene products. *Gene* 569, 153–161. <https://doi.org/10.1016/j.gene.2015.06.026>.
- Manikandan, P., Nagini, S., 2017. Cytochrome P450 structure, function and clinical significance: a review. *Curr. Drug Targets* 19, 38–54. <https://doi.org/10.2174/1389450118666170125144557>.
- Mantzouki, E., Lüring, M., Fastner, G., de Senarpont Domis, L., Wilk-Woźniak, E., Korevieniė, J., Seelen, L., Teurlinckx, S., Verstijnen, Y., Krztoń, W., Walusiak, E., Karosienė, J., Kasperovienė, J., Savadova, K., Vitonytė, I., Cillero-Castro, C., Budzynska, A., Goldyn, R., Kozak, A., Rosińska, J., Szląg-Wasielewska, E., Domek, P., Jakubowska-Krepska, N., Kwasizur, K., Messyas, B., Pelechata, A., Pelechaty, M., Kokocinski, M., García-Murcia, A., Real, M., Romans, E., Noguero-Ribes, J., Duque, D.P., Fernández-Morán, E., Karakaya, N., Häggqvist, K., Demir, N., Beklioglu, M., Filiz, N., Levi, E.E., Iskin, U., Bezirci, G., Tavşanoğlu, Ü.N., Özhan, K., Gkeli, S., Panou, M., Fakioglu, Ö., Avagianos, C., Kaloudis, T., Celik, K., Yilmaz, M., Marcé, R., Catalán, N., Bravo, A.G., Buck, M., Colom-Montero, W., Mustonen, K., Pierson, D., Yang, Y., Raposeiro, P.M., Gonçalves, V., Antoniou, M.G., Tsiarta, N., McCarthy, V., Perello, V.C., Feldmann, T., Laas, A., Panksep, K., Tuvikene, L., Gagala, I., Mankiewicz-Boczek, J., Yağci, M.A., Çınar, Ş., Çapkin, K., Yağci, A., Cesur, M., Bilgin, F., Bulut, C., Uysal, R., Obertegger, U., Boscaini, A., Flaim, G., Salmasso, N., Cerasino, L., Richardson, J., Visser, P.M., Verspagen, J.M.H., Karan, T., Soyulu, E.N., Maraşoğlu, F., Napiórkowska-Krzebietke, A., Ochocka, A., Pasztaleniec, A., Antão-Geraldes, A.M., Vasconcelos, V., Morais, J., Vale, M., Köker, L., Akçaalan, R., Albay, M., Spoljarić Maronić, D., Stević, F., Zuna Pfeiffer, T., Fonvielle, J., Straile, D., Rothhaupt, K.O., Hansson, L.A., Urrutia-Cordero, P., Blaha, L., Geris, R., Fránková, M., Kočer, M.A.T., Alp, M.T., Remec-Rekar, S., Elersek, T., Triantis, T., Zervou, S.K., Hiskia, A., Haande, S., Skjelbred, B., Madrecka, B., Nemova, H., Drastichova, I., Chomova, L., Edwards, C., Sevindik, T.O., Tunca, H., Önem, B., Aleksovski, B., Krstić, S., Uvelič, I.B., Nawrocka, L., Salmi, P., Machado-Vieira, D., De Oliveira, A.G., Delgado-Martín, J., García, D., Cereijo, J.L., Gomá, J., Trapote, M.C., Vegas-Vilarrubia, T., Obrador, B., Grabowska, M., Karpowicz, M., Chmura, D., Úbeda, B., Gálvez, J.A., Özen, A., Christoffersen, K.S., Warming, T.P., Kobos, J., Mazur-Marzec, H., Pérez-Martínez, C., Ramos-Rodríguez, A., Arvola, L., Alcaraz-Párraga, P., Toporowska, M., Pawlik-Skowronska, B., Niedźwiecki, M., Peczuła, W., Leira, M., Hernández, A., Moreno-Ostos, E., Blanco, J.M., Rodríguez, V., Montes-Pérez, J.J., Palomino, R.L., Rodríguez-Pérez, E., Cárballera, R., Camacho, A., Picazo, A., Rochera, C., Santamans, A.C., Ferriol, C., Romo, S., Soria, J.M., Dunalska, J., Sienska, J., Szymański, D., Kruk, M., Kostrzewska-Szlakowska, I., Jasser, I., Žutinić, P., Gligora Udovic, M., Plenković-Moraj, A., Frač, M., Bankowska-Sobczak, A., Wasilewicz, M., Ozkan, K., Maliaka, V., Kangro, K., Grossart, H.P., Paerl, H.W., Carey, C.C., Ibelings, B.W., 2018. Temperature effects explain continental scale distribution of cyanobacterial toxins. *Toxins* 10, 1–24. <https://doi.org/10.3390/toxins10040156>.
- Mathe, C., M-Hamvas, M., Garda, T., Beyer, D., Vasas, G., 2017. Cellular effects of cylindrospermopsin (cyanobacterial alkaloid toxin) and its potential medical consequences. *Curr. Med. Chem.* 24, 91–109. <https://doi.org/10.2174/0929867323666161028153814>.
- Miller, T.R., Beversdorf, L.J., Weirich, C.A., Bartlett, S.L., 2017. Cyanobacterial toxins of the Laurentian great lakes, their toxicological effects, and numerical limits in drinking water. *Mar. Drugs* 15, 1–51. <https://doi.org/10.3390/md15060160>.
- Mohamed, Z.A., Al-Shehri, A.M., 2013. Assessment of cylindrospermopsin toxin in an arid Saudi lake containing dense cyanobacterial bloom. *Environ. Monit. Assess.* 185, 2157–2166. <https://doi.org/10.1007/s10661-012-2696-8>.
- Moosova, Z., Pekarova, M., Sindlerova, I.S., Vasicek, O., Kubala, L., Blaha, L., Adamovsky, O., 2019. Immunomodulatory effects of cyanobacterial toxin cylindrospermopsin on innate immune cells. *Chemosphere* 439–446. <https://doi.org/10.1016/j.chemosphere.2019.03.143>.
- Moreira, C., Mendes, R., Azevedo, J., Vasconcelos, V., Antunes, A., 2017. First occurrence of cylindrospermopsin in Portugal: a contribution to its continuous global dispersal. *Toxicol. Environ. Health* 50, 87–90. <https://doi.org/10.1016/j.toxicol.2017.02.024>.
- Mueller, D., Koetemann, A., Noor, F., 2011. Organotypic cultures of HepG2 cells for in vitro toxicity studies. *J. Bioeng. Biomed. Sci.* <https://doi.org/10.4172/2155-9538.s2-002.01>.
- Müller, L., Kikuchi, Y., Probst, G., Schechtman, L., Shimada, H., Sofuni, T., Tweats, D., 1999. ICH-Harmonised guidances on genotoxicity testing of pharmaceuticals: evolution, reasoning and impact. *Mutat. Res. Rev. Mutat. Res.* 436, 195–225. [https://doi.org/10.1016/S1383-5742\(99\)00004-6](https://doi.org/10.1016/S1383-5742(99)00004-6).
- Nakano, K., Vousden, K.H., 2001. PUMA, a novel proapoptotic gene, is induced by p53. *Mol. Cell.* 7, 683–694. [https://doi.org/10.1016/S1097-2765\(01\)00214-3](https://doi.org/10.1016/S1097-2765(01)00214-3).
- Neubauer, E., Wirtz, R.M., Kaemmerer, D., Athelou, M., Schmidt, L., Sänger, J., Lupp, A., 2016. Comparative evaluation of three proliferation markers, Ki-67, TOP2A, and RacGAP1, in bronchopulmonary neuroendocrine neoplasms: issues and prospects. *Oncotarget* 7, 41959–41973. <https://doi.org/10.18632/oncotarget.9747>.
- O'Neil, J.M., Davis, T.W., Burford, M.A., Gobler, C.J., 2012. The rise of harmful cyanobacteria blooms: the potential roles of eutrophication and climate change. *Harmful Algae* 14, 313–334. <https://doi.org/10.1016/j.hal.2011.10.027>.
- Ohtani, I., Moore, R.E., Runnegar, M.T.C., 1992. Cylindrospermopsin - a potent hepatotoxin from the blue-green-alga cylindrospermopsis-raciborskii. *J. Am. Chem. Soc.* 114, 7941–7942.
- Omicinski, C.J., Vanden Heuvel, J.P., Perdew, G.H., Peters, J.M., 2011. Xenobiotic metabolism, disposition, and regulation by receptors: from biochemical phenomenon to predictors of major toxicities. *Toxicol. Sci.* 120 <https://doi.org/10.1093/toxsci/120.3.338>.
- Patra, B., Peng, C.C., Liao, W.H., Lee, C.H., Tung, Y.C., 2016. Drug testing and flow cytometry analysis on a large number of uniform sized tumor spheroids using a microfluidic device. *Sci. Rep.* 6, 1–12. <https://doi.org/10.1038/srep21061>.
- Pichardo, S., Cameán, A.M., Jos, A., 2017. In Vitro Toxicological Assessment of Cylindrospermopsin: A Review. *Toxins (Basel)*. <https://doi.org/10.3390/toxins9120402>.
- Pinheiro, J., Bates, D., DebRoy, S., Sarkar, D., 2007. R development core team. 2010. *Nlme: linear and nonlinear mixed effects models. R Packag version 3.1–97*.
- Poniedziałek, B., Rzymiski, P., Karczewski, J., 2015. The role of the enzymatic antioxidant system in cylindrospermopsin-induced toxicity in human lymphocytes.

- Toxicol. *Vitro* 29, 926–932. <https://doi.org/10.1016/j.tiv.2015.03.023>.
- Poniedziatek, B., Rzymiski, P., Kokociński, M., 2012. Cylindrospermopsin: water-linked potential threat to human health in Europe. *Environ. Toxicol. Pharmacol.* 34, 651–660. <https://doi.org/10.1016/j.etap.2012.08.005>.
- Poniedziatek, B., Rzymiski, P., Wiktorowicz, K., 2014. Toxicity of cylindrospermopsin in human lymphocytes: proliferation, viability and cell cycle studies. *Toxicol. Vitro* 28, 968–974. <https://doi.org/10.1016/j.tiv.2014.04.015>.
- Puerto, M., Prieto, A.I., Maisanaba, S., Gutiérrez-Praena, D., Mellado-García, P., Jos, Á., Cameán, A.M., 2018. Mutagenic and genotoxic potential of pure Cylindrospermopsin by a battery of in vitro tests. *Food Chem. Toxicol.* 121, 413–422. <https://doi.org/10.1016/j.fct.2018.09.013>.
- Ramaiahgari, S.C., Den Braver, M.W., Herpers, B., Terpstra, V., Commandeur, J.N.M., Van De Water, B., Price, L.S., 2014. A 3D in vitro model of differentiated HepG2 cell spheroids with improved liver-like properties for repeated dose high-throughput toxicity studies. *Arch. Toxicol.* 88, 1083–1095. <https://doi.org/10.1007/s00204-014-1215-9>.
- Runnegar, M., Kong, S., Zhong, Y., 1994. The role of glutathione in the toxicity of a novel cyanobacterial alkaloid cylindrospermopsin in cultured rat hepatocytes. *Biochem. Biophys. Res. Commun.* <https://doi.org/10.1006/bbrc.1994.1694>.
- Runnegar, M.T., Kong, S.M., Zhong, Y.Z., Lu, S.C., 1995. Inhibition of reduced glutathione synthesis by cyanobacterial alkaloid cylindrospermopsin in cultured rat hepatocytes. *Biochem. Pharmacol.* 49, 219–225. [https://doi.org/10.1016/S0006-2952\(94\)00466-8](https://doi.org/10.1016/S0006-2952(94)00466-8).
- Runnegar, M.T., Xie, C., Snider, B.B., Wallace, G.A., Weinreb, S.M., Kuhlenkamp, J., 2002. In vitro hepatotoxicity of the cyanobacterial alkaloid cylindrospermopsin and related synthetic analogues. *Toxicol. Sci.* 67, 81–87. <https://doi.org/10.1093/toxsci/67.1.81>.
- Rzymiski, P., Poniedziatek, B., 2014. In search of environmental role of cylindrospermopsin: a review on global distribution and ecology of its producers. *Water Res.* 66, 320–337. <https://doi.org/10.1016/j.watres.2014.08.029>.
- Saker, M.L., Eaglesham, G.K., 1999. The accumulation of cylindrospermopsin from the cyanobacterium *Cylindrospermopsis raciborskii* in tissues of the Redclaw crayfish *Cherax quadricarinatus*. *Toxicol.* 37, 1065–1077. [https://doi.org/10.1016/S0041-0101\(98\)00240-2](https://doi.org/10.1016/S0041-0101(98)00240-2).
- Shaw, G.R., Seawright, A.A., Moore, M.R., Lam, P.K.S., 2000. Cylindrospermopsin, a cyanobacterial alkaloid: evaluation of its toxicologic activity. *Ther. Drug Monit.* 22, 89–92. <https://doi.org/10.1097/00007691-200002000-00019>.
- Sieroslawska, A., Rymuszka, A., 2015. Cylindrospermopsin induces oxidative stress and genotoxic effects in the fish CLC cell line. *J. Appl. Toxicol.* 35, 426–433. <https://doi.org/10.1002/jat.3040>.
- Snoj, N., Dinh, P., Bedard, P., Sotiriou, C., 2009. Molecular biology of breast cancer. *Molecular Pathology: the Molecular Basis of Human Disease*. Elsevier Inc., pp. 501–517. <https://doi.org/10.1016/B978-0-12-374419-7.00025-1>.
- Sodek, K.L., Ringuelet, M.J., Brown, T.J., 2009. Compact spheroid formation by ovarian cancer cells is associated with contractile behavior and an invasive phenotype. *Int. J. Canc.* 124, 2060–2070. <https://doi.org/10.1002/ijc.24188>.
- Stampar, M., Tomec, J., Filipić, M., Žegura, B., 2019. Development of in vitro 3D cell model from hepatocellular carcinoma (HepG2) cell line and its application for genotoxicity testing. *Arch. Toxicol.* <https://doi.org/10.1007/s00204-019-02576-6>.
- Straser, A., Filipić, M., Gorenc, I., Žegura, B., 2013a. The influence of cylindrospermopsin on oxidative DNA damage and apoptosis induction in HepG2 cells. *Chemosphere* 92, 24–30. <https://doi.org/10.1016/j.chemosphere.2013.03.023>.
- Straser, A., Filipić, M., Novak, M., Žegura, B., 2013b. Double strand breaks and cell-cycle arrest induced by the cyanobacterial toxin cylindrospermopsin in HepG2 cells. *Mar. Drugs* 11, 3077–3090. <https://doi.org/10.3390/md11083077>.
- Straser, A., Filipić, M., Žegura, B., 2013c. Cylindrospermopsin induced transcriptional responses in human hepatoma HepG2 cells. *Toxicol. Vitro* 27, 1809–1819. <https://doi.org/10.1016/j.tiv.2013.05.012>.
- Straser, A., Filipić, M., Žegura, B., 2011. Genotoxic effects of the cyanobacterial hepatotoxin cylindrospermopsin in the HepG2 cell line. *Arch. Toxicol.* 85, 1617–1626. <https://doi.org/10.1007/s00204-011-0716-z>.
- Sukenik, A., Hadas, O., Kaplan, A., Quesada, A., 2012. Invasion of Nostocales (cyanobacteria) to subtropical and temperate freshwater lakes - physiological, regional, and global driving forces. *Front. Microbiol.* 3, 1–9. <https://doi.org/10.3389/fmicb.2012.00086>.
- Svirčev, Z., Lalić, D., Bojadžija Savić, G., Tokodi, N., Drobač Backović, D., Chen, L., Meriluoto, J., Codd, G.A., 2019. Global Geographical and Historical Overview of Cyanotoxin Distribution and Cyanobacterial Poisonings. *Archives of Toxicology*. Springer Berlin Heidelberg. <https://doi.org/10.1007/s00204-019-02524-4>.
- Tamura, R.E., de Vasconcelos, J.F., Sarkar, D., Libermann, T.A., Fisher, P.B., Zerbini, L.F., 2012. GADD45 proteins: central players in tumorigenesis. *Curr. Mol. Med.* 12, 634–651. <https://doi.org/10.2174/156652412800619978>.
- Testai, E., Buratti, F.M., Funari, E., Manganello, M., Vichi, S., Arnich, N., Biré, R., Fessard, V., Sialehaamo, A., 2017. Review and analysis of occurrence, exposure and toxicity of cyanobacteria toxins in food. *EFSA Support. Publ.* 13 <https://doi.org/10.2903/sp.efsa.2016.en-998>.
- Visser, P.M., Verspagen, J.M.H., Sandrini, G., Stal, L.J., Matthijs, H.C.P., Davis, T.W., Paerl, H.W., Huisman, J., 2016. How rising CO2 and global warming may stimulate harmful cyanobacterial blooms. *Harmful Algae* 54, 145–159. <https://doi.org/10.1016/j.hal.2015.12.006>.
- Yeo, E.J., 2019. Hypoxia and aging. *Exp. Mol. Med.* 51 <https://doi.org/10.1038/s12276-019-0233-3>.
- Young, F.M., Micklem, J., Humpage, A.R., 2008. Effects of blue-green algal toxin cylindrospermopsin (CYN) on human granulosa cells in vitro. *Reprod. Toxicol.* 25, 374–380. <https://doi.org/10.1016/j.reprotox.2008.02.006>.
- Žegura, B., Gajski, G., Straser, A., Garaj-Vrhovac, V., 2011a. Cylindrospermopsin induced DNA damage and alteration in the expression of genes involved in the response to DNA damage, apoptosis and oxidative stress. *Toxicol.* 58, 471–479. <https://doi.org/10.1016/j.toxicol.2011.08.005>.
- Žegura, B., Gajski, G., Straser, A., Garaj-Vrhovac, V., Filipić, M., 2011b. Microcystin-LR induced DNA damage in human peripheral blood lymphocytes. *Mutat. Res. Genet. Toxicol. Environ. Mutagen.* 726, 116–122. <https://doi.org/10.1016/j.mrgentox.2011.10.002>.
- Zhang, Y., Shi, K., Liu, J., Deng, J., Qin, B., Zhu, G., Zhou, Y., 2016. Meteorological and hydrological conditions driving the formation and disappearance of black blooms, an ecological disaster phenomena of eutrophication and algal blooms. *Sci. Total Environ.* 569 (570), 1517–1529. <https://doi.org/10.1016/j.scitotenv.2016.06.244>.

2.5 A Toolbox for Separation of Spheroids into Core and Rim Fractions or Viable Single Cell Suspension and their Downstream Applications

Helle SEDIGHI FRANDBSEN, Martina ŠTAMPAR, Joel Mario VEJ-NIELSEN, Bojana ŽEGURA and Adelina ROGOWSKA-WRZESINSKA

Accepted in Springer Protocols 2020. DOI: 10.1007/978-1-0716-1246-0.

Springer Protocols

Method for spheroids disassemble into core and rim for downstream applications such as flow cytometry, comet assay, transcriptomics, proteomics and lipidomics.

--Manuscript Draft--

Manuscript Number:	
Full Title:	Method for spheroids disassemble into core and rim for downstream applications such as flow cytometry, comet assay, transcriptomics, proteomics and lipidomics.
Article Type:	Protocol Chapters
Corresponding Author:	Adelina Rogowska-Wrzesinska, PhD University of Southern Denmark Odense, DENMARK
Corresponding Author Secondary Information:	
Corresponding Author's Institution:	University of Southern Denmark
Corresponding Author's Secondary Institution:	University of Southern Denmark: Syddansk Universitet
First Author:	Helle Sedighi Frandsen
First Author Secondary Information:	
Order of Authors:	Helle Sedighi Frandsen Martina Štampar Joel Mario Vej-Nielsen Bojana Žegura Adelina Rogowska-Wrzesinska, PhD
Order of Authors Secondary Information:	
Funding Information:	
Abstract:	Cells cultured in a monolayer have been a central tool in molecular and cell biology, toxicology, biochemistry etc. Therefore, most methods for adherent cells in cell biology are tailored to this format of cell culturing. Limitations and disadvantages of monolayer cultures, however, have resulted in the ongoing development of advanced cell culturing techniques. One such technique is culturing cells as multicellular spheroids, that had been shown to mimic the physiological conditions found in vivo more accurately. This chapter presents a novel method for separation of the spheroid rim and core in mature spheroids (>21 days) for further analysis using advanced molecular biology techniques such as flow cytometry, viability estimations, comet assay, transcriptomics, proteomics and lipidomic. This fast and gentle disassembly of intact spheroids into rim and core fractions, and further into viable single cell suspension provides an opportunity to bridge the gap from 3D cell culture to current state-of-the-art analysis methods.

Method for spheroids disassemble into core and rim for downstream applications such as flow cytometry, comet assay, transcriptomics, proteomics and lipidomics.

Helle Sedighi Frandsen¹, Martina Štampar², Joel Mario Vej-Nielsen¹, Bojana Žegura², Adelina Rogowska-Wrzesinska^{1*}

¹ Institute for Biochemistry and Molecular Biology, University of Southern Denmark, Odense, Denmark

² Department of Genetic Toxicology and Cancer Biology, National Institute of Biology, Ljubljana; Slovenia

* Corresponding author: Adelina Rogowska-Wrzesinska, Institute for Biochemistry and Molecular Biology, University of Southern Denmark, Campusvej 55, 5230 Odense M, Denmark, adelinar@bmb.sdu.dk

running title: **Core and Rim**

Abstract

Cells cultured in a monolayer have been a central tool in molecular and cell biology, toxicology, biochemistry etc. Therefore, most methods for adherent cells in cell biology are tailored to this format of cell culturing. Limitations and disadvantages of monolayer cultures, however, have resulted in the ongoing development of advanced cell culturing techniques. One such technique is culturing cells as multicellular spheroids, that had been shown to mimic the physiological conditions found *in vivo* more accurately. This chapter presents a novel method for separation of the spheroid rim and core in mature spheroids (>21 days) for further analysis using advanced molecular biology techniques such as flow cytometry, viability estimations, comet assay, transcriptomics, proteomics and lipidomic. This fast and gentle disassembly of intact spheroids into rim and core fractions, and further into viable single cell suspension provides an opportunity to bridge the gap from 3D cell culture to current state-of-the-art analysis methods.

Key words (5-10 keywords): 3D cell culture, HepG2/C3A, spheroids, rim and core, flow cytometry, comet assay, transcriptomics, proteomics, lipidomic

1 Introduction

For more than a century monolayer (2D) cultures have been used as a valuable model for cell-based *in vitro* studies. Recently several limitations, such as the loss of tissue-specific architecture, mechanical and biochemical identity and cell-to-cell communication, have been increasingly recognized as a significant drawback of such systems [1]. At the same time, three-dimensional (3D) cell cultures have emerged as a new approach providing environment physiologically more relevant and data with more predictive power for *in vivo* conditions [2]. Cells in the 3D culture differ morphologically and physiologically from cells in monolayer cultures and provide a more accurate insight into the responses to stimuli, drug metabolism and general cell function [3]. Creation of multicellular spheroids or organoids is one of the ways for providing 3-dimensional microenvironment for cells grown in cell cultures. Three main zones can be observed in those multilayer cell aggregates: an outer proliferating rime, viable non-proliferating zone and an inner core that contains cell remnants. Cells from different zones within the spheroid have different morphology [4]. It is currently understood that these zones are formed in response to the exposure of cells to different micro-environment factors such as access to nutrients, CO₂ and oxygen levels [5] [6]. In cancer research, the zones of spheroids are thought to represent the behaviour of cells in larger tumours, where a necrotic core appears at the centre of tissue mass. The different physiological states of cells mimic the cellular heterogeneity of solid *in vivo* tumours [7].

The availability of accurate, robust and cost-effective *in vitro* assays for 3D cell cultures is an increasingly important challenge for applications in basic research, toxicity testing and safety assessment [3]. The existing 3D cell models vary widely due to the diverse requirements of different cell lines and applications, and each model has its own advantages and limitations [8] [9]. The methods described in this chapter are applicable to

spheroids obtained with a scaffold independent system and had been tested on HepG2/C3A spheroids cultured for 21-days.

The protocol provides an efficient method for disassembly of spheroids into the core and rim fractions and to obtain a single cell suspension. This new approach allows for the application of a wide variety of existing techniques enabling us studying the biological processes taking place in the inner and outer fraction of the spheroid. Within this protocol we provide guidelines for how to prepare samples from spheroids core and rim for downstream applications techniques such as comet assay, flow cytometry, transcriptomics, proteomics and lipidomic. **Figure 1** presents the summary of methods described.

2 Materials

A sterile laminar flow hood, humidified incubator with 5 % CO₂ at 37 °C and a centrifuge are required in several steps of the protocol.

2.1 Separation of spheroids into core and rim fractions and single cell suspension in sections

Materials from this section are used in protocols described in 3.1

1. Eppendorf tubes 1.5 mL
2. 0.5 % Trypsin/EDTA
3. Hanks Balanced Salt Solution without calcium and magnesium (HBSS)
4. Cut P1000 tip (*Note 1*) and cut P200 pipette tip (*Note 2*)
5. Foetal Bovine Serum (FBS)

3 Methods

This chapter utilises spheroids created using AggreWell plates (STEMCELL Technologies UK), rotary bioreactors and the CelVivo bio array matrix (BAM) system (CelVivo Denmark) as described before by Fey and Wrzesinski [10] and by Wrzesinski et al. in this issue. It can also be applied to multicellular spheroids and organoids created with other systems. All handling is performed at room temperature, all liquids are preheated to 37 °C unless otherwise stated.

3.1 Spheroid disassembly

This protocol presents a technique to separate the inner core and outer rim fractions of intact spheroids, and subsequently single cell suspensions either from intact spheroid or core/rim fraction. **Figure 2** shows the overview over the workflow of spheroid formation and disassembly.

3.1.1 Single cell suspension from spheroid

Preparing a single cell suspension is a critical step, when spheroids had been grown for several weeks and tight connections between cells have been formed. Spheroid disassembly, enzymatic digestion and mechanical dissociation are the major steps leading to the degradation of the intracellular connections and to the isolation of viable single cells.

1. Harvest desired number of spheroids at specific age (suggested at 21 days) and transfer them to an Eppendorf tube with 200 µl HBSS (*Note 3*).
2. Create diluted trypsin/EDTA solution (0.05%) by mixing 9 ml cool HBSS into a 15 ml falcon tube with 1 ml trypsin/EDTA 0.5% (*Note 4*).
3. Transfer an appropriate number of spheroids to an Eppendorf tube containing 200 µl of 0.05 % trypsin/EDTA in HBSS.
4. Incubate spheroids for 8 minutes at 37 °C (this refers to the spheroids of the age of 21 days) (*Note 5*).

5. Gently aspirate the spheroids using a P200 pipette (uncut tip). Repeat approximately 50 times or until the spheroid breaks into smaller fragments.
6. Add 200 μ l of FBS to deactivate/quench the trypsin.
7. Aspirate the solution into the pipette tip for additional 5 times to create a single cell suspension.
8. After obtaining a single cell suspension examine viability of cells using i.e. trypan blue staining (section 3.2.1.1).

3.1.2 Separation of spheroids into core and rim fractions

This protocol can only be performed on spheroids with a mature core, for system described in this article the core will be mature after approximately 21 days of culturing.

1. Prepare diluted trypsin solution (0.05 %) (step 3.1.1.2) (*Note 4*).
2. Collect the spheroids from the bioreactor and transfer them to a petri dish (35 mm) containing 3 ml growth media, use a cut pipette tip in all steps unless indicated otherwise (*Note 2, 6 and 7*).
3. Select one spheroid at a time and transfer to an Eppendorf tube containing 200 μ l HBSS.
4. After few seconds transfer the spheroid to a new Eppendorf tube containing 200 μ l 0.05% trypsin/EDTA.
5. Incubate at 37 °C for 4 minutes (the time depends on spheroid size and compactness).
6. Aspirate the spheroid while still in trypsin/EDTA solution, aspirate and drain 30 times until rim peels off (*Note 8*).
7. Immediately transfer the core to an Eppendorf tube containing 200 μ l FBS.
8. Add 200 μ l of FBS to the Eppendorf tube with the spheroid rim.

3.1.3 Single cell suspension from core and rim

To generate single cell suspensions from each spheroid part, first perform the separation of spheroids into core and rim fractions (section 3.1.2 step 1-6), then follow this procedure

1. Transfer the core to a new Eppendorf tube containing 200 μ l 0.05 % trypsin/EDTA and incubate it for additional 2 minutes at room temperature.
2. After incubation, resuspend spheroid core 10 times with a cut P200 pipette tip (*Note 9*) until single cell suspension is obtained. Add 100 μ l of FBS.
3. Keep the spheroid rim in the original tube.
4. Resuspend it with a cut P200 pipette tip 5 times to obtain a single cell solution (*Note 10*). Add 100 μ l FBS.
5. Centrifuge both spheroid parts (core/rim) for 5 minutes at 140 g at 37 °C.
6. Remove supernatant and resuspend cells in a solution of choice or snap freeze cells for later analysis.

3.2 Applications

This section presents how samples created with the above protocols can be used to analyse cells for viability and by comet assay, flow cytometry, transcriptomics, proteomics and lipidomic.

3.2.1 Cell viability

Estimating cell viability is an essential tool to evaluate the cell culture population. All viability estimations highlighted in this chapter, require disassembly of the spheroid. As such, sterile conditions are not necessary as the cells are subsequently not cultured. Table 1 summarises commonly used viability methods with their strengths and weaknesses highlighted.

TABLE 1: BENEFITS AND SHORTCOMINGS OF THREE FREQUENTLY USED VIABILITY ASSAYS.

	Advantages	Disadvantages
Trypan blue staining	Quantify number of cells Fast (automated)	Quickly overstains Chance of induced cell death Hard to discriminate live/dead

ATP assay	Works directly on intact spheroids, rim/core fraction and single cells (low probability of induced cell death) Evaluates entire spheroid	No exact estimation of the number of dead cells Slow (40 min, incubation) Can over/underestimate ATP since amount is not the same in core and rim Requires sophisticated equipment (luminometer)
Flow cytometry and propidium iodide staining	Quantify number of cells Fast Semi-Automated High number of cells evaluated in short time, giving more reliable results	Possibility of induced cell death Possibility to overstain Requires sophisticated equipment (flow cytometer)

3.2.1.1 Trypan blue staining

This protocol was adopted from [11]. The single cell suspension can also be used in automated cell counters.

1. Prepare a 0.2% solution of trypan blue, in HBSS with calcium and magnesium in an Eppendorf tube.
2. Prepare single cell suspension from spheroid(s) of interest as described in sections 3.1.1 or 3.1.3. (Note 11).
3. Transfer and mix single cell suspension with staining solution to attain a final concentration of 0.2% trypan blue (Note 12).
4. Use a haemocytometer and light microscopy to quantify the amount of dead and live cells in sample (Note 13).

3.2.1.2 ATP assay

ATP is present in all living cells and the amount of ATP within the spheroid can be used as an indicator of the relative number of viable cells. For more detailed protocol for conducting ATP assay for measurement of viability in spheroids follow the procedure as described before by Fey and Wrzesinski [12] and Wrzesinski et

al., in this issue. As the assay utilises cell lysis to release ATP from the cells, it can be applied directly on intact spheroids as well as spheroid fractions and single cell suspension.

1. Mix CellTiter-Glo reagents and leave on a shaker for 5 minutes at room temperature at 300 rpm.
2. Harvest spheroids from a bioreactor and transfer them to a petri dish containing growth media (*Note 14*).
3. Prepare an appropriate ATP standard for the size of the spheroids-of-interest. As spheroids grow during the experiment the standard may need to be adapted throughout the experiment (*Note 15*)
4. Add samples, ATP standards and negative control (blank) to a 96 well plate, in triplicates.
5. Add CellTiter-Glo reagents to each well with content and mix gently by pipetting.
6. Facilitate thorough cell lysis by additional pipetting in wells containing spheroids and confirm complete spheroid destruction (only single cells visible) prior to incubation period by light microscopy.
7. Wrap the plate in aluminium foil and incubate for 40 minutes on shaker at 300 rpm at room temperature.
8. Determine luminescence signal of samples using plate reader.

3.2.1.3 Flow cytometry using propidium iodide

Viability can be estimated by combining spheroid disassembly with propidium iodide staining [13].

1. To analyse spheroids by flow cytometer, the single cell suspension must be prepared from the spheroids (whole or core/rim) as described in sections 3.1.1 or 3.1.3.
2. Mix cells with a solution of 10 µg/ml propidium iodide (PI) at a ratio of 1:1.
3. Load cells on flow cytometer.
4. Estimate viability based on 10.000 events.

3.2.2 Comet assay

The comet assay (single cell gel electrophoresis) is a simple and sensitive technique for detecting DNA damage, caused by compounds of interest. With this method, different types of strand breaks can be observed such as DNA double-strand breaks (DSB) and single-strand breaks (SSB), alkali labile sites (ALS) like apurinic/apyrimidinic (AP) sites, DNA–DNA and DNA–protein cross-links, and SSB associated with incomplete excision repair. The protocol is presented as described previously by Zegura and Filipic [14].

1. Prepare a viable single cell suspension by following the procedure described in sections 3.1.1 or 3.1.3.
2. Evaluate viability of the cell suspension (section 3.2.1). The comet assay can be performed up to 25 % decrease of viability.
3. Mix 30 μ L single cell suspension with 70 μ L 1% low melting point (LMP) agarose.
4. Transfer 70 μ L of the mixture of LMP and cell suspension to fully frosted slides (or slides covered with 0.5% NMP) covered with a layer of 1% NMP (normal melting point) agarose.
5. Add lysis buffer (0.1 M EDTA, 2.5 M NaOH, pH 10, 0.01 M Tris and 1% Triton X-100) to the slides and incubate for 1 h at 4 °C in darkness (*Note 16*).
6. Perform DNA denaturation for 20 minutes in alkaline solution (300 mM NaOH, 1m M EDTA, pH 13) at 4°C to allow DNA unwinding and subsequently conduct the electrophoresis for 20 minutes at 0.7–1 V/cm (*Note 17*). Neutralize the nuclei in neutralisation buffer (0.4 M Tris buffer; pH 7.5) for 15 minutes in darkness.
7. Stain the gels with Gelred or similar stain (e.g. acridine orange).
8. Analyse the comets using a fluorescence microscope and the image analysis software (e.g. Comet IV from Instem, UK).
9. The experiment should be carried out on at least 5 spheroids each considered as a separate unit and at least 50 nuclei should be analysed from each spheroid.

3.2.3 Flow cytometry

Flow cytometry is a powerful technology in cell biology as it allows high-throughput analysis of large number of cells. It is a technique that utilises fluorescent dyes to quantify and identify cellular components and cell types. In flow cytometry, cells treated with one or more fluorochrome(s) undergo monochromatic excitations by one or more laser(s) and the resulting fluorescence is collected by detectors in the machine [15]. The technique can effectively be applied to the 3D cell culture model as it can be disassembled into the highly homogenous viable single cell suspension. This makes the tool ideal to keep track of cellular populations within the spheroid.

1. In order to analyse spheroids by flow cytometer, the viable single cell suspension must be prepared first as described in sections 3.1.1 – 3.1.3.
2. Prepare a staining solution by mixing fluorochromes of interest (table 2) (Note 18).
3. Mix single cell suspension with staining solution and incubate in the dark for appropriate time (Note 19 and 20).
4. If you use multicolour staining each dye can contribute to the signal on several detectors. Therefore, it is essential to perform the calibration of the lasers prior to starting an experiment especially when applying a new cell line.
5. Run cell suspension through a strainer in order to remove larger cellular aggregates and to prevent clogging of the tubes in the flow cytometer.
6. Load cells on flow cytometer in an approximate concentration of 10^6 cells/ml.

Table 2: Examples of flow cytometry applications used in cell culturing, adapted from [16].

Flow cytometry application	Source of fluorescence
Quantifying cells in specific cell cycle phases	Anti-Ki67, anti-PCNA, Hoechst 33342, 7AAD & Chromomycin A3

Measure level of active proliferation	Bromodeoxy uridine (BrdU) and conjugated anti BrdU dye Carboxyfluoroscein succinimidly ester (CFSE)
Quantifying cell viability	Fluorescent diacetate (FDA), propidium iodide (PI) & Hoechst 33342
Identifying differentiation states and quantifying amount of differentiation	Conjugated antibodies for differentiation markers
Quantifying cell types in co-cultures	Endogenous fluorescence in reporter cell lines
Identifying or isolating cell types in immunology	Conjugated antibodies for lineage markers
Measuring cell activation and signaling	Calcium indicators: Indo-1 & fluo-3
Measuring specific antigen response	Biotinylated MHC multimers, in combination with fluorescent streptavidin
Identifying mechanism of cell death	JC-1, anti-APO 2.7, fluorogenic caspase substrates & anti-annexin-V
Measuring phagocytosis	pH sensitive-fluorescently tagged biomolecules or bacteria
Perform generational tracking	Carboxyfluoroscein succinimidly ester (CFSE)
Measure level of protein expression	Inducible expression of fluorescent protein

3.2.4 Omics

Omics analysis have developed immensely in the last 10 years and are highly used technologies aiming to collectively characterize and quantify pools of biological molecules, subsequently translating into function and dynamics of an organism. Due to the heterogeneity of cells within spheroids, the rim and core separation protocol could be performed prior to omics analysis to increase information output.

3.2.4.1 Washing and freezing of samples

It is important to perform extensive washing after collecting the spheroids to avoid contaminating the sample with growth media components such as foetal calf serum which can interfere with the final results.

1. Transfer intact spheroids or spheroid core and rim (prepared as in 3.1.2) into separate Eppendorf tubes.
2. Remove growth media or any other solutions and gently wash with 500 μ l HBSS.
3. For proteomics and lipidomic experiments repeat the washing step five times to remove contaminating FBS proteins and lipids.
4. Remove all liquid after the final wash step using for an example a gel loading tip.
5. Add RNA stabilisation and storage solution such as RNAlater for samples destined for transcriptomics or store samples without any liquid for later proteomics and lipidomics analysis.
6. Snap freeze samples in liquid nitrogen and store at -80°C (*Note 21*).

3.2.4.2 Sample preparation for transcriptomic

High-throughput quantitative, real-time, reverse-transcription PCR (QPCR) is the method of choice for measuring the relative level of expression of selected gene transcripts in a given tissue or cell type, and after pharmacologic or genotypic manipulation [17]. The presented protocol had been described in detail by Buh et al. and Štampar et al. [18] [19] previously. A short summary of the protocol follows below.

1. Prepare spheroids or spheroid core and rim according to the protocols from section 3.2.4.1 and 3.1.2, respectively (*Note 22*).
2. Each sample for transcriptomic analysis should contain at least 1 μ g of RNA.
3. Isolate total mRNA using TRIzol Gibco BRL (Paisley, Scotland) or similar.
4. Measure the concentration and the purity of the isolated RNA (*Note 23*).
5. Transfer 1 μ g of total RNA from each sample to a fresh Eppendorf tube.
6. Apply the cDNA High Capacity Archive Kit (Biosystems, New Jersey, USA) or similar, to generate cDNA from each sample (reverse transcription).
7. Select TaqMan probes for genes of interest and carry out the pre-amplification of genes with the PreAmp GrandMasterMix (TATAA Biocenter AB, Göteborg, Sweden) or similar.

8. Prepare TaqMan Universal PCR Master Mix and add the mixture to each sample.
9. To evaluate the performance of a primer set and to eliminate the effect of the inhibition a serial of 10-fold dilutions of each target gene should be performed.
10. Perform qPCR on 48.48 Dynamic Array™ IFC method (BioMark HD machine system, Fluidigm, UK) or on a classic Q-PCR on 384 plate (VIA Real-Time PCR System machine, Applied Biosystems™) or similar equipment.
11. Analyse data using the relative quantification according to solvent control (*Note 24*)

3.2.4.3 Sample processing for proteomics

Proteomics using mass spectrometry enables to quantification and identification of thousands of proteins in one experiment. This protocol presents a method of how to prepare samples from spheroids for bottom-up label free LC-MS using a one-pot buffer [21] and filter aided sample preparation [22]. This protocol is selected due to its speed and applicability to handling a high number of samples [23].

1. Prepare spheroids or spheroid core and rim according to the protocols from section 3.2.4.1 and 3.1.2, respectively.
2. Thaw the frozen samples on ice.
3. Add lysis buffer (50 mM TEAB, 1% SDC, 10 mM TCEP 40 mM chloroacetamide, protease and phosphatase inhibitors) so that the final protein concentration is within 1-5 µg/µl.
4. Disintegrate cells by pipetting using a regular P200 pipette tip (*Note 25*).
5. Heat samples for 10 minutes (80 °C), vortex for one minute and sonicate to lyse cells, fragment nucleic acids and inactivate enzymes (*Note 26*).
6. Determine protein concentration in the sample using e.g. amino acids analysis [24] or ProStain™ Protein Quantification Kit (ActiveMotif) or any other method compatible with the lysis buffer.

7. Transfer 100 µg protein to spin filter (Vivacon 500, Sartorius), dilute samples to equal total volume of buffer and mix gently by pipetting.
8. Centrifuge at 14,000 g for 15 minutes., wash with 100 µl 50 mM ammonium bicarbonate (ABC), centrifuge at 14,000 g for 15 minutes and repeat wash for a total of three washes (*Note 27*).
9. Transfer the filters to a fresh low-binding Eppendorf tubes, add 1 µg trypsin and dilute sample in ABC to a volume of 50 µl. Incubate samples at 37 °C overnight (*Note 28*)
10. Centrifuge at 14,000 g for 10 minutes, add 1 µg trypsin diluted in 50 µl ABC and incubate for four hours at 37 °C.
11. Centrifuge filter at 14,000 g for 10 minutes, add 100 µl ABC to filters, centrifuge filters at 14,000 g for 10 minutes, lyophilize peptides and store at –20 °C.
12. Resuspend samples in 2% acetonitrile/0.1% trifluoroacetic acid, quantify the amount of peptides with e.g. amino acid analysis [24] and analyse 1 µg peptide using LC-MS/MS

3.2.4.4 Sample preparation for lipidomics

Quantification and identification of several hundred of lipids in biological samples is achieved using mass spectrometry combined with liquid chromatography LC-MS [25]. We present a simple method for lipid extraction from intact spheroids and core and rim spheroid fractions. Here we present a brief summary of the protocol published by Matyash et al. [26]. All steps of the protocol should be performed in a laminar flow hood due to harmful vapours from the chemicals used.

1. Collect spheroids or spheroids rim and core as described in 3.2.4.1. and 3.1.2 respectively.
2. Add 100 µl PBS and thaw the samples on ice (*Note 29*).
3. Disintegrate spheroids by repeated pipetting with a normal pipette tip.
4. Sonicate spheroid homogenates (*Note 30*), determine protein content (*Note 31*) and transfer equivalent of 200 µg protein to an Eppendorf tube.
5. Add internal standards (*Note 32*) and vortex samples for 10 minutes.

6. Add 300 μL methanol, vortex for 10 minutes, add 500 μL methyl-tert-butyl ether, vortex for 10 minutes, add 250 μL H₂O and centrifuge at 1,2000 g for 10 minutes
7. Collect upper organic layer in glass vial, repeat step 5 and collect organic layer in same glass vial.
8. Lyophilize lipids and store at $-20\text{ }^{\circ}\text{C}$ with argon gas to void oxidation of lipids.
9. Resuspend sample in 30 μL chloroform/methanol (1:1, 10 mM ammonium acetate) and analyse using LC-MS/MS.

4 Notes

1: Cut the bottom end of pipette tip P1000 to create a larger opening of approximately 2 mm in diameter, keep the tip sterile.

2: Cut the bottom end of pipette tip P200 so the diameter of the opening is larger than the spheroid (approximately 1.5 mm in diameter for 21 days old spheroids), keep the tip sterile.

3: The number of harvested spheroids depends on which method you intend to perform subsequently. Single cell suspension from an intact spheroid can be obtained at any spheroid age.

4: Thaw trypsin at $4\text{ }^{\circ}\text{C}$ to limit auto digestion.

5: Incubation time depends on the size and compactness of the spheroids. Optimize incubation time of the protocol for each spheroid type. Too long exposure to trypsin may damage the cell membrane and cause cell death.

6: Leave the petri dish with spheroids in a sterile incubator at $37\text{ }^{\circ}\text{C}$ with humidified 0.5% CO₂ atmosphere, whenever it is not being used. Spheroids should not be kept in the petri dish for prolonged periods of time. Collection should be carried out in sterile conditions.

7: Cut P200 pipette tip is needed as the diameter of spheroids is too large to make it through the original opening.

8: Start with gentle resuspensions and gradually get more vigorous. The rim will look like a light and transparent sheet and the inner core will be a small dark compact lump of cells.

9: After 10 resuspensions, no visible pieces of core should be present. Keep in mind that core is more compact, therefore longer time or more resuspension is needed.

10: In this step, you will get the single cell suspension of the rim, while the core is still incubating in trypsin.

11: Be aware that the cells can lose membrane integrity during disassembly to single cell suspension if incubation in trypsin is not properly adjusted.

12: Single cell suspension should be prepared immediately before trypan blue staining, as cells are being treated harshly and can die outside of the bioreactor.

13: Evaluate viability immediately after mixing staining solution and cell suspension as trypan blue will eventually penetrate the cell membrane of even live cells.

14: Ensure that after collection the spheroids are kept in growth media in a humidified incubator until analysed.

15: It is preferable to analyse a single spheroid per well as the signal can be too high for the plate reader for larger spheroids.

16: The method should be adapted to optimal conditions for every cell type. Perform all the following steps of the protocol at 4°C in the dark to prevent additional DNA damage occurring during the assay.

17: Always use identical settings to obtain comparable and reproducible results.

18: If needed exclude unspecific binding with isotopic controls.

19: Incubation is carried out in the dark as to avoid photo bleaching; the incubation time depends on characteristics of antibodies.

20: If you use multicolour staining each dye can contribute to the signal on several detectors. Therefore, it is essential to perform the calibration of the lasers prior to starting an experiment especially when applying a new cell line.

21: For experiments where several time points are analysed, all samples can be stored frozen and subsequent sample preparation can be performed in parallel.

22: A pool of at least 25 spheroids or at least 35 parts of each fraction - core and rim at the age of 21 days is sufficient to obtain a desired amount of mRNA.

23: For reliable results obtained with qPCR, it is essential to check the purity and degradation (gel-electrophoresis) as well as the concentration of isolated mRNA (NanoDrop 1000 Spectrophotometer) before starting the experiment.

24: Freely available program such as QuantGenious [20] can be used.

25: Add as low volume of buffer as possible to keep a high protein concentration; however enough buffer to stop processes if necessary. Five spheroids aged 21 days can be properly dissolved in 100 μ l buffer.

26: Cycle between 15 seconds of sonication and 30 seconds pause to avoid overheating of the sample.

27: If some samples do not fully pass through the filter, increase the number of washes.

28: If you intend to digest another amount of protein maintain a ratio of 1:100 of trypsin to protein.

29: Use as low volume of liquid as possible; however enough to dissolve it. For this protocol 100 μ l is sufficient to dissolve 5x 21-days old spheroids.

30: Cycle between 15 seconds of sonication and 30 seconds pause to avoid overheating of the sample.

31: Lipid content is not measured directly but is assumed to be relative to the protein concentration. Each 21-day old spheroid should contain at least 200 µg protein.

32: The internal standard should contain lipid species that are to be identified in the samples. Use as low concentration of the standard as possible to avoid losing peaks of interest. Include a lipid standard for each class of interest as the internal standard.

Acknowledgements

The authors acknowledge the financial support from the Sino Danish Research and Education Center for PhD project for HSF and JMVN , Slovenian Research Agency [research core funding - J, and grant to young researchers MR-MStampar P1-0245], and COST Actions CA16119 (In vitro 3-D total cell guidance and fitness).

References

- [1] Pampaloni F, Reynaud EG, Stelzer EH (2007) The third dimension bridges the gap between cell culture and live tissue. *Nat Rev Mol Cell Biol.* 8(10):839-845. doi:10.1038/nrm2236
- [2] Edmondson R, Broglie JJ, Adcock AF, Yang L (2014) Three-dimensional cell culture systems and their applications in drug discovery and cell-based biosensors. *Assay Drug Dev Technol.* doi:10.1089/adt.2014.573
- [3] Antoni D, Burckel H, Josset E, Noel G (2015) Three-dimensional cell culture: a breakthrough in vivo. *Int J Mol Sci.* doi:10.3390/ijms16035517
- [4] Wrzesinski K, Rogowska-Wrzesinska A, Kanlaya R et al (2014) The cultural divide: exponential growth in classical 2D and metabolic equilibrium in 3D environments. *PLoS One.* doi:10.1371/journal.pone.0106973

- [5] Mehta G, Hsiao AY, Ingram M et al (2012) Opportunities and challenges for use of tumor spheroids as models to test drug delivery and efficacy. *J Control Release*. doi:10.1016/j.jconrel.2012.04.045
- [6] Asthana A, Kisaalita WS (2012) Microtissue size and hypoxia in HTS with 3D cultures. *Drug Discov Today*. doi:10.1016/j.drudis.2012.03.004
- [7] Zanoni M, Piccinini F, Arienti C et al (2016) 3D tumor spheroid models for in vitro therapeutic screening: a systematic approach to enhance the biological relevance of data obtained *Sci Rep*. doi:10.1038/srep19103
- [8] Breslin S, O'Driscoll L (2013) Three-dimensional cell culture: the missing link in drug discovery. *Drug Discov Today*. doi:10.1016/j.drudis.2012.10.003
- [9] Godoy P, Hewitt NJ, Albrecht U et al (2013) Recent advances in 2D and 3D in vitro systems using primary hepatocytes, alternative hepatocyte sources and non-parenchymal liver cells and their use in investigating mechanisms of hepatotoxicity, cell signaling and ADME. *Arch Toxicol*. doi:10.1007/s00204-013-1078-5
- [10] Fey SJ, Wrzesinski K (2012) Determination of drug toxicity using 3D spheroids constructed from an immortal human hepatocyte cell line. *Toxicol Sci*. doi:10.1093/toxsci/kfs122
- [11] Strober W (2001) Trypan blue exclusion test of cell viability. *Curr Protoc Immunol*. doi:10.1002/0471142735.ima03bs21
- [12] Fey SJ, Wrzesinski, K (2013) Determination of Acute Lethal and Chronic Lethal Dose Thresholds of Valproic Acid Using 3D Spheroids Constructed from the Immortal Human. *Valproic Acid*.
- [13] Wigg AJ, Phillips JW, Wheatland L, Berry MN (2003) Assessment of cell concentration and viability of isolated hepatocytes using flow cytometry. *Anal Biochem*. doi:10.1016/s0003-2697(03)00057-5

- [14] Zegura B, Filipic M (2004) Application of In Vitro Comet Assay for Genotoxicity Testing. *Methods In Pharmacology and Toxicology*
- [15] Tung JW, Heydari K, Tirouvanziam R et al (2007) Modern flow cytometry: a practical approach. *Clin Lab Med.* doi:10.1016/j.cll.2007.05.001
- [16] McKinnon KM (2018) Flow Cytometry: An Overview. *Curr Protoc Immunol.* doi:10.1002/cpim.40
- [17] Bookout AL, Mangelsdorf DJ (2003) Quantitative real-time PCR protocol for analysis of nuclear receptor signaling pathways. *Nucl Recept Signal.* doi:10.1621/nrs.01012
- [18] Buh Gasparic M, Cankar K, Zel J, Gruden K (2008) Comparison of different real-time PCR chemistries and their suitability for detection and quantification of genetically modified organisms. *BMC Biotechnol.* doi:10.1186/1472-6750-8-26
- [19] Štampar M, Tomc J, Filipič M, Žegura B (2019) Development of in vitro 3D cell model from hepatocellular carcinoma (HepG2) cell line and its application for genotoxicity testing. *Arch Toxicol.* doi:10.1007/s00204-019-02576-6
- [20] Baebler Š, Svalina M, Petek M et al (2017) quantGenius: implementation of a decision support system for qPCR-based gene quantification. *BMC Bioinformatics.* doi:10.1186/s12859-017-1688-7
- [21] Kovalchuk SI, Jensen ON, Rogowska-Wrzesinska A (2019) FlashPack: Fast and Simple Preparation of Ultrahigh-performance Capillary Columns for LC-MS. *Mol Cell Proteomics.* doi:10.1074/mcp.TIR118.000953
- [22] Wiśniewski JR, Zougman A, Nagaraj N, Mann M (2009) Universal sample preparation method for proteome analysis. *Nat Methods.* doi:10.1038/nmeth.1322
- [23] Wang WQ, Jensen ON, Møller IM, Hebelstrup KH, Rogowska-Wrzesinska A (2015) Evaluation of sample preparation methods for mass spectrometry-based proteomic analysis of barley leaves. *Plant Methods.* doi:10.1186/s13007-018-0341-4

- [24] Højrup P (2015) Analysis of Peptides and Conjugates by Amino Acid Analysis. *Methods Mol Biol.* doi:10.1007/978-1-4939-2999-3_8
- [25] Lydic TA, Goo YH (2018) Lipidomics unveils the complexity of the lipidome in metabolic diseases. *Clin Transl Med.* doi:10.1186/s40169-018-0182-9
- [26] Matyash V, Liebisch G, Kurzchalia TV et al (2008) Lipid extraction by methyl-tert-butyl ether for high-throughput lipidomics. *J Lipid Res.* doi:10.1194/jlr.D700041-JLR200

Figure Captions

Figure 1

Overview over the methods presented in this manuscript. Step 1 –spheroid processing and separation into core and rim or single cell suspension; Step 2 – evaluation of cell population by measuring cell viability; Step 3 – analysis by comet assay, flow cytometry, transcriptomics, proteomics and lipidomic.

Figure 2

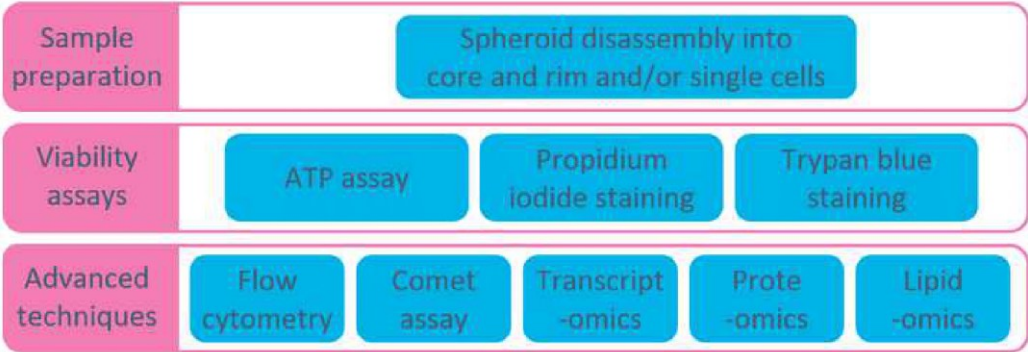
Overview over the spheroid disassembly workflow steps with key processes indicated.

Figure 3

Separation of 32 days old HEPG2/C3A spheroids into core and rim structures. A) three individual intact spheroids aged 32 days; B) one spheroid disassembled into rim (arrow) and core fractions. Scale bar equals 1 mm.

Figure1

[Click here to access/download;Figure;Core and Rim - Figure 1.tif](#)



2.5 A Toolbox for Separation of Spheroids into Core and Rim Fractions or Viable Single Cell Suspension and their Downstream Applications 109

Figure2

[Click here to access/download;Figure;Core and Rim - Figure 2.tif](#)

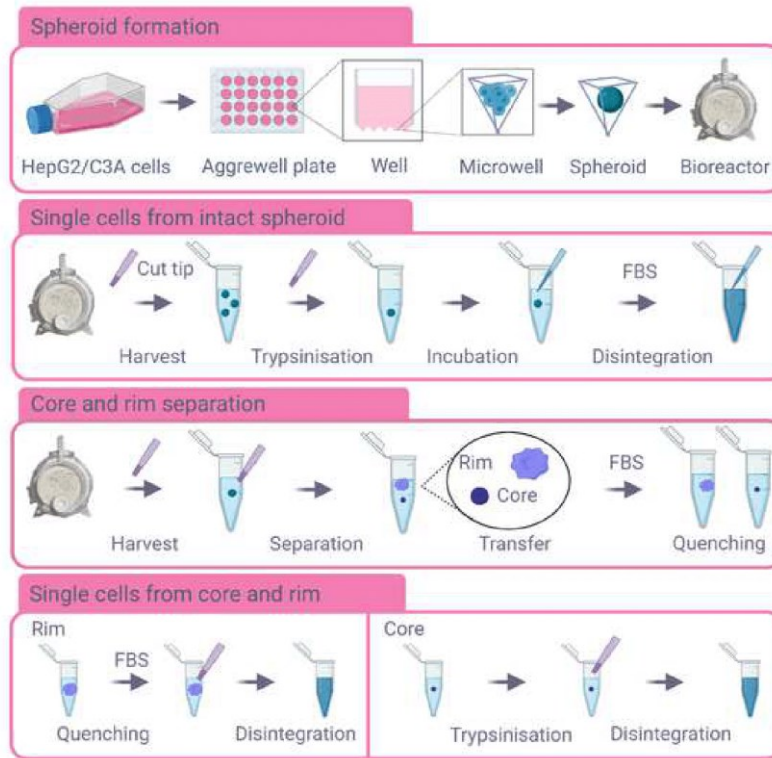
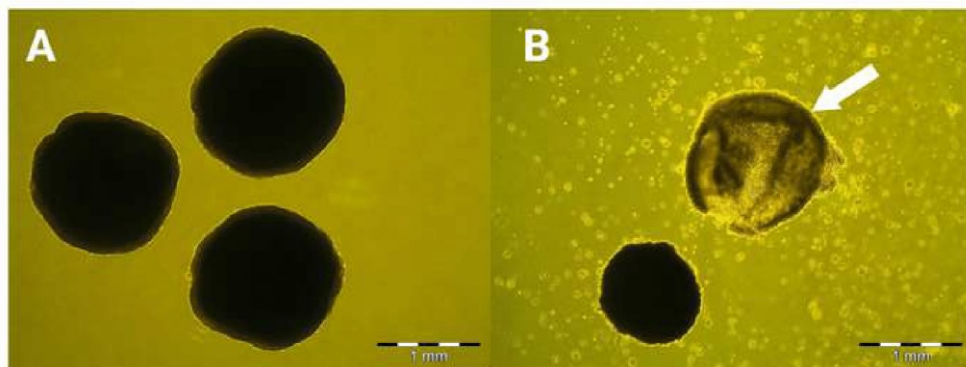


Figure3

[Click here to access/download;Figure;Core and Rim - Figure 3.tif](#)



2.6 Hepatocellular Carcinoma (HepG2/C3A) Cell-Based 3D Model for Genotoxicity Testing of Chemicals

Martina ŠTAMPAR, Helle SEDIGHI FRANDSEN, Adelina ROGOWSKA-WRZESINSKA, Krzysztof WRZESINSKI, Metka FILIPIČ and Bojana ŽEGURA

Science of the Total Environment 2020; 755: 143255. DOI: 10.1016/j.scitotenv.2020.1432



Hepatocellular carcinoma (HepG2/C3A) cell-based 3D model for genotoxicity testing of chemicals



Martina Štampar^{a,b}, Helle Sedighi Frandsen^c, Adelina Rogowska-Wrzesinska^c, Krzysztof Wrzesinski^d, Metka Filipič^a, Bojana Žegura^{a,*}

^a Department of Genetic Toxicology and Cancer Biology, National Institute of Biology, Ljubljana, Slovenia

^b Jozef Stefan International Postgraduate School, Ljubljana, Slovenia

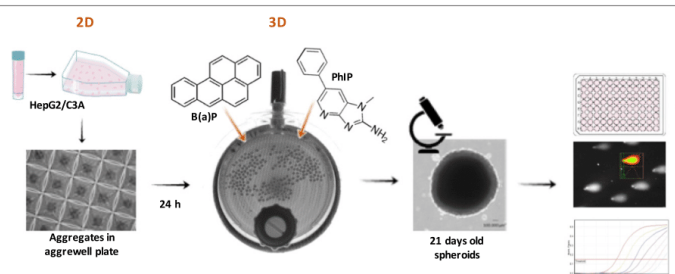
^c Department of Biochemistry and Molecular Biology, University of Southern Denmark, Odense, Denmark

^d CelVivo ApS 3D Structures, Blommenslyst, Denmark

HIGHLIGHTS

- Hepatic 3D cell models have more complex structure and improved metabolic capacity compared to 2D.
- HepG2/C3A 3D model provide physiologically more relevant information for human exposure.
- Hepatic 3D cell model can contribute to trustworthy risk assessment genotoxic compounds.
- Dynamic HepG2/C3A 3D model enables prolonged exposures to low doses of xenobiotics.
- Comet assay was successfully implemented to the dynamic HepG2/C3A 3D cell model.

GRAPHICAL ABSTRACT



ARTICLE INFO

Article history:

Received 21 September 2020

Received in revised form 22 October 2020

Accepted 24 October 2020

Available online 3 November 2020

Editor: Henner Hollert

Keywords:

In vitro 3D cell model

21-day old spheroids

Cytotoxic

Genotoxic

Gene expression

ABSTRACT

The major weakness of the current *in vitro* genotoxicity test systems is the inability of the indicator cells to express metabolic enzymes needed for the activation and detoxification of genotoxic compounds, which consequently can lead to misleading results. Thus, there is a significant emphasis on developing hepatic cell models, including advanced *in vitro* three-dimensional (3D) cell-based systems, which better imitate *in vivo* cell behaviour and offer more accurate and predictive data for human exposures. In this study, we developed an approach for genotoxicity testing with 21-day old spheroids formed from human hepatocellular carcinoma cells (HepG2/C3A) using the dynamic clinostat bioreactor system (CelVivo BAM/bioreactor) under controlled conditions. The spheroids were exposed to indirect-acting genotoxic compounds, polycyclic aromatic hydrocarbon [PAH; benzo (a) pyrene B(a)P], and heterocyclic aromatic amine [PhIP] at non-cytotoxic concentrations for 24 and 96 h. The results showed that both environmental pollutants B(a)P and PhIP significantly increased the level of DNA strand breaks assessed by the comet assay. Further, the mRNA level of selected genes encoding metabolic enzymes from phase I and II, and DNA damage responsive genes was determined (qPCR). The 21-day old spheroids showed higher basal expression of genes encoding metabolic enzymes compared to monolayer culture. In spheroids, B(a)P or PhIP induced compound-specific up-regulation of genes implicated in their metabolism, and deregulation of genes implicated in DNA damage and immediate-early response. The study demonstrated that this model utilizing HepG2/C3A spheroids grown under dynamic clinostat conditions represents a very sensitive

* Corresponding author at: National Institute of Biology, Department of Genetic Toxicology and Cancer Biology, Večna pot 111, 1000 Ljubljana, Slovenia.

E-mail addresses: martina.stampar@nib.si (M. Štampar), helle@bmb.sdu.dk (H. Sedighi Frandsen), adelinar@bmb.sdu.dk (A. Rogowska-Wrzesinska), kwr@celvivo.com (K. Wrzesinski), metka.filipic@nib.si (M. Filipič), bojana.zegura@nib.si (B. Žegura).

and promising *in vitro* model for genotoxicity and environmental studies and can thus significantly contribute to a more reliable assessment of genotoxic activities of pure chemicals, and complex environmental samples even at very low for environmental exposure relevant concentrations.

© 2020 The Author(s). Published by Elsevier B.V. This is an open access article under the CC BY-NC-ND license (<http://creativecommons.org/licenses/by-nc-nd/4.0/>).

1. Introduction

Cell-based assays play an important role in the drug development process and safety assessment of chemicals and drugs as a fast, cost-effective and straightforward approach to reduce animal testing (Burden et al., 2015; Pfuhrer et al., 2020; Schechtman, 2002). Genotoxicity testing is an essential element of the safety assessment of nearly all types of compounds on the market. It is also a very important issue when evaluating the possible adverse health effects of complex environmental samples to which humans can be exposed in their everyday life, to avoid unforeseen genotoxic effects on human health and the environment as well (Dix et al., 2007). The testing begins with a series of *in vitro* bacterial and mammalian cell-based assays, and in case of positive results, it is followed by *in vivo* testing in rodents. However, *in vitro* genotoxicity tests with mammalian cells are prone to misleading results. One of the crucial elements contributing to a relatively high percentage of *in vitro* misleading results is an insufficient representation of enzymes implicated in the metabolism of genotoxic compounds in cell lines used for routine genotoxicity testing (Kirkland et al., 2007). Over the last two decades, test systems with human hepatocellular carcinoma-derived cell lines such as HepG2 with the retained activity of specific metabolic enzymes *in vitro* have been introduced to the routine genotoxicity testing (Shah et al., 2018; Yang et al., 2018). Traditionally, *in vitro* test systems are based on monolayer [two-dimensional (2D)] cell cultures, which are associated with inherent limitations (Edmondson et al., 2014; Wrzesinski and Fey, 2015). The most important is the lack of multiple biological functions such as cell-to-cell and cell-to-matrix contacts. These result in reduced cell differentiation, modified cell signalling pathways, and the reduced expression and activities of several hepatic enzymes implicated in the metabolism of xenobiotic substances (phase I and II enzymes) (Aucamp et al., 2017; Edmondson et al., 2014; Hurrell et al., 2019).

Furthermore, 2D cell cultures do not adequately mimic the natural cell microenvironment represented by surrounding extracellular matrix and nearby cells. The 3R's strategy (reduce, replace, refine), focus on the reduction and optimization of the use of animals for *in vivo* testing (Corvi and Madia, 2017; Pfuhrer et al., 2009). To follow this strategy it is essential to develop alternative *in vitro* cell-based systems, which more realistically resemble *in vivo* cell behaviour and microenvironment and thus ensure additional predictive data compared to 2D conditions.

The hepatic 3D cell models exhibit a greater level of liver-specific functions, including metabolic enzyme activities. Furthermore, the cell morphology and their biochemical properties are more similar to *in vivo* tissues (Aucamp et al., 2017; Loessner et al., 2010). Spheroids represent a very promising 3D cell model that can be cultured under static or dynamic conditions, using many techniques, ranging from hanging drop cultures, spinner flasks, non-adhesive surfaces, micro-moulding, NASA rotary system (developed by National Aeronautics and Space Administration), bioreactors, and many more (Basu et al., 2020; Breslin and O'Driscoll, 2013; Lin et al., 2008), each offering numerous advantages and disadvantages.

In addition to mechanistic studies (Elje et al., 2019; Mandon et al., 2019; Štampar et al., 2019), 3D models have also proven to be a very useful tool in environmental toxicology, including effect-based monitoring of various environmental natural and man-made pollutants (Basu et al., 2018; Hercog et al., 2020). The 3D models allow long-term repeat dose studies (Wong et al., 2011) enabling the exposure to

lower concentrations of pollutants that are relevant for the environment and thus, real human exposure.

In the present study, the spheroids were developed using the advanced dynamic clinostat micro-tissue culturing technique, which applies rotating bioreactors, which provide better resemblance to *in vivo* conditions than 2D cell cultures (Fey and Wrzesinski, 2012; Wojdyla et al., 2016; Wrzesinski and Fey, 2015). The rotation of bioreactors causes the flow of growth media around the spheroids, resulting in higher diffusion of oxygen and nutrients into the spheroids and preventing the generation of a necrotic core (Fey and Wrzesinski, 2012; Gong et al., 2015; Lin et al., 2008). During prolonged culturing of several weeks, the spheroids develop structures with characteristics resembling tissues and stable physiological functionality such as bile canaliculi-like structures and sinusoid-like channels (Wrzesinski and Fey, 2013). Due to the advanced morphology and biochemical properties, the spheroids grown under dynamic conditions provide more predictive data for human exposure in comparison to classically cultured (2D) immortal or primary human hepatocytes and therefore represent an alternative approach for animal studies (Wrzesinski and Fey, 2013, 2015). Moreover, a dynamic clinostat micro-tissue culturing technique enables the formation of up to three hundred spheroids in one bioreactor at the same time (Fey and Wrzesinski, 2012) and thereby offers a simple high-throughput system for culturing uniform spheroids, where several down-stream techniques can be applied and various endpoint measured on the same population of spheroids that is particularly suitable in the environmental contamination studies.

This study aimed to develop an approach for genotoxicity testing of chemicals using 21-day old spheroids formed from human hepatocellular carcinoma (HepG2/C3A) cells utilizing the dynamic bioreactor (CelVivo BAM/bioreactor) system (Fig. 1). The age of 21 days was selected, since after this time the spheroids reach maturity and provide metabolically competent cell model (Fey and Wrzesinski, 2012; Wrzesinski et al., 2013; Wrzesinski and Fey, 2013). For the spheroid formation, the hepatocellular HepG2/C3A cell line (HepG2 cell subclone) was chosen due to its strong contact-inhibited growth characteristics, high transferrin and albumin production, alpha-fetoprotein synthesis, and the ability to grow in media containing a physiological level of glucose (Iyer et al., 2010; Sun et al., 2014; Tamta et al., 2012; Wrzesinski et al., 2013). When cultured in the form of spheroids HepG2/C3A cells have several advantages over other cell lines, such as reduced proliferation, the reestablishment of crucial functions (cholesterol and urea synthesis, cellular organization and expression of cytochrome P450) and can be utilised for studying long-term repeated dose exposures (Nibourg et al., 2012; Ramaiahgari et al., 2014; Wrzesinski and Fey, 2013). In addition, the HepG2/C3A spheroids have epigenetic markers that are present in the liver but are lost when cultured under 2D conditions (Tvardovskiy et al., 2015). However, recovery of physiological functions when grown in 3D is not limited to HepG2/C3A but is also seen with other cell lines, such as HepaRG, HepG2 and many others (Mandon et al., 2019; Štampar et al., 2019; Wrzesinski and Fey, 2013, 2015; Young and Young, 2019). The response of 21-day old HepG2/C3A spheroids for detection of indirect-acting genotoxic chemicals were tested with two model genotoxic compounds; benzo(a)pyrene (B(a)P) and 2-Amino-1-methyl-6-phenylimidazo(4,5-b)pyridine (PhIP) that are ubiquitously found in the environment and thus represent a risk for human health. Environmental pollution is a wide-reaching problem associated with the health of the ecosystem and humans, as well as global climate change (Hartig et al., 2014). Human

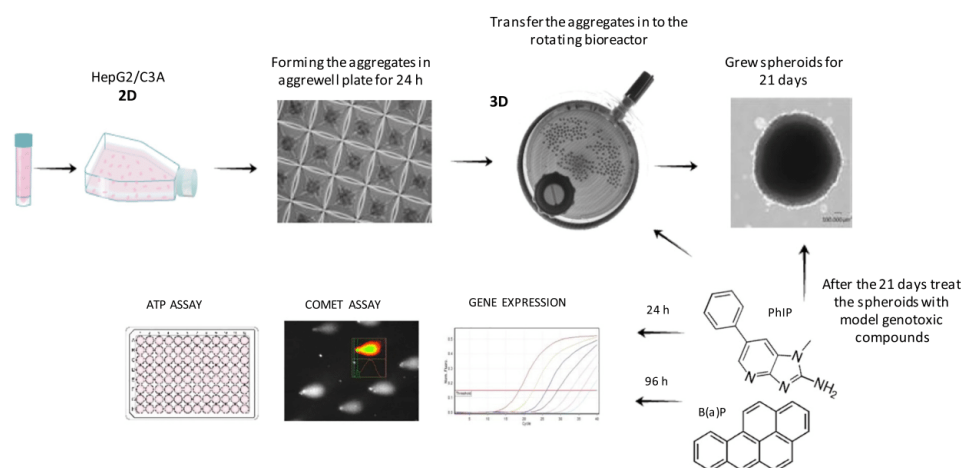


Fig. 1. The formation of the 3D HepG2/C3A spheroid cultures and treatment approach for genotoxicity assessment. First, the HepG2/C3A cells were seeded in the AggreWell™ plates and were left for 24 h at 37 °C. After that, the aggregates were transferred to the pre-wetted bioreactors. Spheroids were cultivated for 21 days until treated with B(a)P and PhIP for 24 and 96 h. After the treatment different end-point measurements were performed (cell viability, DNA damage and gene expression).

exposure to B(a)P is inevitable and is associated with pollution of the natural environment (water, air, soil), as well as with the intake of food, mainly grilled, charcoal-broiled, and smoked meat and fish (Baan et al., 2009). The second indirect-acting genotoxic chemical used in the present study belongs to the group of heterocyclic aromatic amines (HAAs) (Skog et al., 1998) and occurs in almost all types of food of animal origin (meat and fish) heated at high temperatures (Baird et al., 2005). PhIP has been detected not only in products of animal origin, but also in wine, beer (Manabe et al., 1993), and smoked cheese (Naccari et al., 2009), meaning that humans can be exposed to PhIP in their everyday environment due to their lifestyle. Moreover, it can occur in rainwater and cigarette smoke condensate (Naccari et al., 2009).

In the present study, the spheroids were exposed to BaP or PhIP for 24 and 96 h, and DNA damage was studied with the comet assay, which detects DNA lesions in the form of DNA strand breaks. To explore the metabolic competence of the spheroid model, the basal and induced mRNA level of genes, encoding selected enzymes implicated in xenobiotic metabolism induction, was determined. Besides, the effects of the tested compounds on deregulation of selected genes involved in the response to DNA damage and immediate-early response related to carcinogenesis were investigated.

2. Materials and methods

2.1. Chemicals

Dulbecco's Modified Eagle's Medium with 1 g Glucose/L (DMEM), GlutaMAX, Hanks' buffered saline solution and Trypsin-EDTA (10×; 0.50%) were from Gibco (Carlsbad, CA). Normal (NMP) and low (LMP) melting point agaroses, TRIzol® reagent and Trypan Blue (15250-061) were from Gibco (Praisley, Scotland, UK). Foetal calf serum (FCS), dimethylsulphoxide (DMSO), DEPC-treated water (w4502), non-essential amino acids (NEAA), penicillin/streptomycin (pen/strep), and benzo(a)pyrene (B(a)P; CAS-No. 50-32-8) were purchased from Sigma (St. Louis, USA). Cell-Titer-Glo luminescent cell viability assay (G7571) was obtained from Promega (Madison, USA). Amino-1-methyl-6-phenylimidazo[4,5-b] pyridine (PhIP; CAS-No. 105650-23-5) was from Toronto Research Chemicals Inc. (Canada). Methanol, ethanol,

and phosphate-buffered saline (PBS) were from PAA Laboratories (Dartmouth, NH, USA). GelRed solution was from Biotium (Fremont, CA) and Triton X-100 from Fisher Sciences (New Jersey, USA). TaqMan Gene Expression Assays, the high capacity cDNA kit, and TaqMan Universal PCR Master Mix (4440038) were purchased from Applied Biosystems (New Jersey, USA). The PreAmp GrandMasterMix (TA05-50) was from TATAA Biocenter AB (Göteborg, Sweden). GE 48.48 Dynamic Array Sample and Assay loading Reagent Kit – 10 IFCs (85000821), and 48.48 Dynamic Array: Gene expression chip were obtained from Fluidigm (South San Francisco, USA). The B(a)P (9.9 mM) and PhIP (20 mM) stock solutions were prepared in DMSO and stored at –20 °C.

2.2. Cell culture

The immortalized human hepatocellular carcinoma cell line, HepG2/C3A, was bought at American Type Culture Collection (ATCC, CRL-10741). Cells were grown at standard culture conditions as described by Wrzesinski and Fey (2013) in DMEM (31885-023) supplemented with 10% FCS (Sigma F7524), 0.5% pen/strep (15140-122), 1% NEAA (11140-035), 1% GlutaMAX (35050-038), at 37 °C, 5% CO₂ atmosphere (Wrzesinski and Fey, 2013). HepG2/C3A cells were used between passage 6 and 9 and were regularly checked for mycoplasma (MycoAlert™ kit; Lonza, Walkersville, MD, USA).

2.3. Development of 3D spheroids and culture conditions

The spheroids made of HepG2/C3A cells were created using AggreWell™ 400 plates (Stemcell Technologies, 27845) as described by Wrzesinski and Fey (2013). In brief, the plates were first prewashed with the DMEM growth medium. Subsequently, the air bubbles were cleared away from the well surfaces by prefilling the plates with growth medium (0.5 ml) and centrifuging for 3 min at 3000g. Subsequently, 1.2×10^6 cells were added to the well resulting in 1000 cells per spheroid initially. The plates were centrifuged for 3 min at 100g and left overnight for spheroid formation. After the formation of spheroids, they were detached from the AggreWell™ plate by washing the well with growth medium pre-warmed to 37 °C and subsequently collected into a Petri-dish, and their quality was examined by microscopy (Olympus IX81, 4x). Cell aggregates, unlike the major population, if

any, have been removed to facilitate uniformity and the remaining spheroids were transferred, with cut p200 pipette tips, into the pre-equilibrated bioreactors (CelVivo BAM/bioreactor), which was subsequently filled with growth medium. The spheroids were cultured at 37 °C and 5% CO₂ for 21 days, replacing medium accordingly to 48/48/72 hour schedule (Fey and Wrzesinski, 2012). The day of the transfer of cell aggregates from AggreWell™ plates into the bioreactors is defined as day 0 (Wrzesinski and Fey, 2013). Optimal growth conditions were achieved by rotating bioreactors at appropriate speeds using the 16 axels BioArray Matrix drive BAM v4 (CelVivo, Blommenslyst) (Wojdyla et al., 2016).

2.4. Treatment of HepG2/C3A spheroids with model genotoxic compounds

After the spheroid cultures were matured for 21 days in bioreactors, spheroids have been divided into experimental subpopulation (50 spheroids in each bioreactor). The spheroids were treated with indirect-acting genotoxic compounds, namely polycyclic aromatic hydrocarbon benzo(a)pyrene (B(a)P) and heterocyclic aromatic amine amino-1-methyl-6-phenylimidazo[4,5-b]pyridine (PhIP) for 24 and 96 h. The spheroid size corresponded to approximately 9 million cells or 1.5 mg protein after 24 h of exposure and approximately 7 million cells or 1 mg protein after 96 h of exposure. The protein content was calculated from the standard curve (planimetry standardised table historical data) correlating the protein content and spheroid size. To initiate the chemical treatment, the rotation of bioreactors was terminated for a short time to allow the spheroids to descend to the bottom of the bioreactor. The media was replaced with fresh media containing B(a)P or PhIP. The concentrations of B(a)P and PhIP in the treatment media were adjusted to doses resulting in spheroids exposure to 0.15 and 0.011 µg B(a)P/µg cellular protein (corresponding to 40 and 4 µM) for 24 (short term) and 96 h (long term), respectively or 0.34 and 0.68 µg PhIP/µg cellular protein (corresponding to 200 and 400 µM) for 24-hour exposure and 0.246 µg PhIP/µg protein (corresponding to 100 µM) for 96-h. The dose is given as µg of chemical per µg of cellular protein (µg/µg P). The unit was converted from the concentration (mM) to the dose (e.g., mg compound per mg cellular protein) based on the size of spheroids (Fey and Wrzesinski, 2012; Piccinini et al., 2015; Wrzesinski and Fey, 2015). The doses of genotoxins were selected according to previous studies with 2D models of HepG2 cells (Gajski et al., 2016; Pezdirc et al., 2013). The solvent (medium containing DMSO) and negative (growth medium) controls were included in all experiments. The final solvent dose was adjusted to be the same as the amount of the solvent in the exposure conditions. The experiments were performed in three independent repetitions and several spheroids were used for each time point and dose. The number of spheroids depended on the end-point evaluated.

2.5. Measurement of the surface area of spheroids (planimetry)

Spheroids were cultivated under dynamic clinostat conditions for 21 days, as described previously. Before and after the treatment, the quality, compactness, size, and roundness of at least 15 spheroids were documented at 4× magnification by light microscopy (Olympus IX81 motorized microscope). The images of spheroids were taken with the Olympus DP71 camera and analysed with Olympus AnalySiS Docu program (Soft Imaging System) where the spheroid area was measured in µm². This procedure was described in details by Fey and Wrzesinski in 2012.

2.6. Viability of spheroids after the treatment with genotoxic compounds – ATP assay

The 21-day old spheroids were treated with indirect-acting model genotoxins, B(a)P and PhIP, for 24 (short term) and 96 h (long term) in rotating bioreactors. In each bioreactor, 50 spheroids were grown.

The viability of cells in spheroids was assessed after the treatment by measuring the ATP content of spheroids referring to the manufacturer's protocol (CellTiter-Glo, Cat. no. G7571) with minor modifications described by Wrzesinski and Fey (2013). Briefly, five spheroids from each treatment were collected at specific time points and each transferred to a well of microtiter plates (Nunc, 165306). The final volume of the growth medium was 100 µl, and spheroids were lysed by shaking in the darkness (40 min). Luminescence was determined using the FluoStar Omega® luminometer (BMG Labtech, Germany). Three independent experiments were performed. Data were normalized to the reference ATP standard curve, to the untreated control, and the surface area of each spheroid (determined with planimetry). Statistical relevance between solvent control and treated groups was calculated by unpaired parametric *t*-test with Welch's correction (**p* < 0.05).

2.7. DNA damage induced by genotoxic compounds – comet assay

After the treatment, a suspension of viable single cells was obtained by the combination of enzymatic digestion and mechanical degradation. Each spheroid was put in trypsin-EDTA (0.05%; 3 min) and afterwards, using cut pipette tips, disassembled into a suspension of single cells. The viability of the single cells was immediately evaluated by staining with Trypan Blue (0.4%). The comet assay was conducted according to Štraser et al. (2011) with modifications by Štampar et al. (2019). The images were captured with the fluorescence microscope Eclipse 800 (Nikon, Japan) with a Basler camera and analysed using Comet IV image analysis software (Perceptive Instruments, UK). Each spheroid represented one unit, and at least four spheroids were investigated per experimental point. In each spheroid, 50 randomly captured nuclei were analysed, and experiments were repeated three times independently. The results are shown as % of tail DNA. Statistic calculations were done by one-way ANOVA using Dunnett's Multiple Comparison test to test the differences in % of tail DNA of treatments vs control, and to compare the treated groups to solvent control (**p* < 0.01).

2.8. Gene expression analysis

The expression of studied genes involved in the metabolism of xenobiotics, immediate-early response and response to DNA damage were determined by quantitative real-time PCR (qPCR) on gene expression 48.48 Dynamic Array™ IFC (Fluidigm, US). The basal mRNA level of studied liver-specific and metabolic genes was determined in HepG2/C3A monolayers (2D) cultured for 48 h and in spheroids (3D) cultured for 22 and 25 days in bioreactors under dynamic conditions. Further, the expression of studied metabolic genes and genes encoding response to DNA damage and immediate-early response were evaluated in 21-day old spheroids exposed to B(a)P (0.15 µg/µg P and 0.011 µg/µg P for 24 and 96 h, respectively) or PhIP (0.34, 0.68 µg/µg P and 0.25 µg/µg P for 24 and 96 h, respectively). From the pool of 25 spheroids for each genotoxic compound and control, the mRNA was isolated using TRIzol Gibco BRL. The mRNA concentration and the purity were assessed using NanoDrop 1000 Spectrophotometer (Thermo Fischer Scientific, Wilmington, USA), while degradation was checked by gel-electrophoresis (BioRad Power PAC 3000 and UVP Chem Studio PLUS, Analytik Jena AG, US). Reverse transcription of total mRNA (1 µg) per sample was performed using the cDNA High Capacity Archive Kit. Quantification of studied genes was determined with qPCR on 48.48 Dynamic Array™ IFC method where TaqMan Universal PCR Master Mix and pre-amplified (TATAA PreAmp GrandMasterMix) Taqman Gene Expression Assays listed in Table 1 were applied. All genes were pre-amplified. To eliminate the effects of inhibition and to evaluate the performance of the primer set, a serial of 5-fold dilutions of each target gene was analysed. The qPCR experiments were run on 48.48 Dynamic Array™ IFC chips for gene expression on the BioMark HD machine system (Fluidigm, UK). The program QuantGenious was used for data processing using the relative quantification regarding solvent control (Baebler

Table 1
The list of Taqman gene expression assays.

	Gene symbol	Entire gene name	Assay ID	
Cellular function	Reference genes	<i>GAPDH</i>	Human Endogenous Control	
		<i>HPRT1</i>	Hypoxanthine phosphoribosyl transferase 1	
DNA-damage response genes		<i>TP53</i>	Tumour protein P53	
		<i>MDM2</i>	Oncogene, E3 ubiquitin-protein ligase	
		<i>GADD45α</i>	Growth arrest and DNA damage-inducible gene, alpha	
		<i>CDKN1A</i>	Cyclin dependent kinase inhibitor 1A0	
		<i>ERCC4</i>	Excision repair cross-complementing rodent repair deficiency, complementation group 4	
Immediate-early response genes		<i>JUNB</i>	JunB proto-oncogene, AP-1 transcription factor subunit	
		<i>MYC</i>	V-myc avian myelocytomatosis viral oncogene homolog	
		<i>CYP1A1</i>	Cytochrome P450 family 1 subfamily A member 1	
Genes involved in metabolism		<i>CYP1A2</i>	Cytochrome P450 family 1 subfamily A member 2	
		<i>CYP3A4</i>	Cytochrome P450 family 3 subfamilies A member 4	
		<i>UGT1A1</i>	UDP glucuronosyltransferase 1 family, polypeptide A1	
		<i>UGT2B7</i>	UDP glucuronosyltransferase family 2 member B7	
		<i>NAT1</i>	N-acetyltransferase 1	
		<i>NAT2</i>	N-acetyltransferase 2	
		<i>SULT1B1</i>	Sulfotransferase family 1B member 1	
		<i>SULT1C2</i>	Sulfotransferase family 1C member	
	Hepatic markers		<i>ALDH3A1</i>	Aldehyde dehydrogenase 3 family member A1
			<i>ALB</i>	Albumin

et al., 2017). If the difference was higher/lower than 1.5-fold, than the expression was considered as up/down-regulation (relative expression >1.5 or <0.66 fold change, respectively). The inverse value of the relative expression (1/RE) was calculated, to acquire a fold change from the relative expression for down-regulated genes (RE < 1). The expression of each gene was assessed in duplicates and three experiments were done independently. Statistical analysis was done by the multiple unpaired *t*-tests with the Sidak-Bonferroni method (**p* < 0.05).

3. Results and discussion

In vitro 3D cell cultures are experimental models increasingly used in preclinical studies, pharmacology, and toxicology. Recently, they have been applied also for studying the adverse effects of natural toxins and complex environmental samples and proved to be a very sensitive model (Basu et al., 2018; Flampouri et al., 2019; Hercog et al., 2020).

In genetic toxicology, the use of 3D culture models is still in its infancy, but at a recent International Workshop on Genotoxicity Testing (IWGT), their use for genotoxicity testing was recognized as very promising (Pfuhrer et al., 2020). However, for the use in routine genotoxicity testing, further development and validation is needed (Pfuhrer et al., 2020). In the present study, we established and validated a genotoxicity test system with 21-day old spheroids developed from the HepG2/C3A cell line that enables short-term and long-term exposure to xenobiotic pollutants under controlled dynamic clinostat conditions. One of the very important and crucial issues in genotoxicity studies is that the applied model enables long-term and repeated exposures to low doses of studied compounds, which is very important for the risk assessment of environmental contaminants. Namely in the environment, animals and humans can be continuously and/or repeatedly exposed to very low concentrations of various compounds.

3.1. The influence of model genotoxic compounds on HepG2/C3A spheroid growth and viability of cells

To determine the influence of B(a)P and PhIP on the growth of 21-day old spheroids, the surface area (planimetry) of at least 15 spheroids per experimental point was measured after 24 and 96 h of exposure (Fig. 2). The average surface area of spheroids exposed to B(a)P was affected after 24 h (0.15 µg/µg P) and 96 h (0.01 µg/µg P) exposure. After 24 hour and 96 hour exposure, the surface area was $0.97 \pm 0.19 \text{ mm}^2$ and $0.98 \pm 0.07 \text{ mm}^2$, respectively, while the surface area of the control

group was $1.23 \pm 0.11 \text{ mm}^2$ and $1.14 \pm 0.23 \text{ mm}^2$, respectively. The results of PhIP exposure revealed that the heterocyclic aromatic amine (HAA) affected the growth of HepG2/C3A spheroids only after short (24 h) exposure. The surface area of spheroids exposed to PhIP at the dose of 0.34 and 0.68 µg/µg P was $1.20 \pm 0.10 \text{ mm}^2$ and $1.17 \pm 0.07 \text{ mm}^2$, respectively, while the average control surface area was $1.27 \pm 0.11 \text{ mm}^2$ and $1.23 \pm 0.11 \text{ mm}^2$, respectively, after a short exposure. After 96 hour exposure to 0.246 µg/µg P of PhIP, the surface area was $1.16 \pm 0.13 \text{ mm}^2$ and in control group $1.14 \pm 0.23 \text{ mm}^2$.

The effect of B(a)P and PhIP on the viability of HepG2/C3A spheroids was determined by measuring ATP content. The results showed that B(a)P and PhIP after 24 h at higher dose, reduced ATP content for 16.5% and 24.4% on average, respectively, while PhIP at lower dose did not affect the cell viability (Fig. 3A). After 96 h of exposure B(a)P or PhIP did not decrease the ATP content (Fig. 3B). As the reduction of ATP content at applied doses was less than 30%, which is considered as non-cytotoxic effect (Žegura et al., 2009), no significant disturbances of mitochondrial functions were expected; therefore, these doses were used for further experiments.

Recently it was described that cell viability of HepG2 spheroids cultured for 3 days under static conditions, exposed to B(a)P (up to 40 µM) for 24 h was not affected in their cell viability measured by MTS assay, while PhIP ($\geq 200 \text{ µM}$) decreased cell viability by approximately 20% on average (Štampar et al., 2019). Similarly, in 10-day old HepaRG spheroids after 24 h of exposure, B(a)P at concentrations of up to 20 µM did not decrease cell survival, while cytotoxic effects were described for PhIP ($\geq 320 \text{ µM}$) (Mandon et al., 2019).

3.2. The influence of model genotoxic compounds on DNA damage induction determined with the comet assay

Comet assay was recently applied in various hepatic 3D cell models (Elje et al., 2019; Mandon et al., 2019; Štampar et al., 2019), and here we successfully implemented the method on 21-day old HepG2/C3A spheroids grown under dynamic clinostat conditions. The spheroids were treated with B(a)P and PhIP for 24 and 96 h, and first, the method for obtaining the viable single-cell suspension was optimized. Before conducting the comet assay, the viability of single-cell suspension was determined by Trypan blue staining, and it was higher than 80% (data not shown). Results showed that B(a)P (0.15 µg/µg P) and PhIP (0.34 µg/µg P and 0.68 µg/µg P) after 24 h of treatment induced statistically significant increase in the amount of DNA strand breaks (Fig. 4A

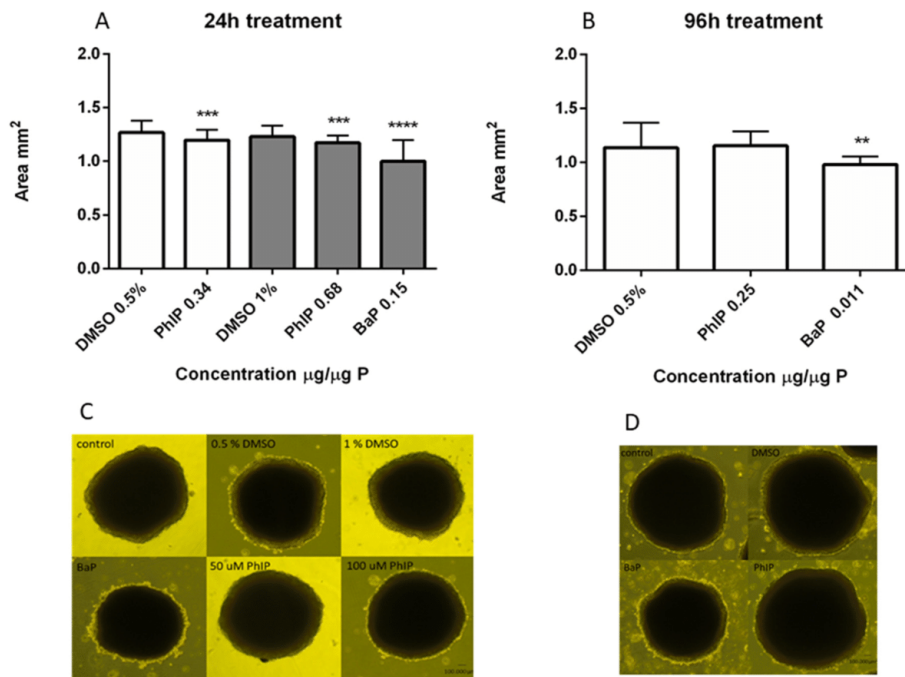


Fig. 2. The average surface area \pm SD (mm²) of control and exposed spheroids after 24 h (A) and 96 h (B) determined with planimetry. The % of the solvent in different treatments after 24 h was adjusted to the 0.5% at a lower dose of PhIP (white columns) and the 1% at the higher dose of PhIP and B(a)P (grey columns). The experiments were repeated three times independently and each time at least five spheroids were measured. The % of the solvent after 96 h was adjusted to 0.5%. The images of representative spheroids after 24 h (C) and 96 h exposure (D) are shown. The images were captured using the Olympus IX81 microscope and an Olympus DP71 camera at 4 \times magnification. Statistics analysis was conducted in Graph Pad Prism 6 (unpaired parametric *t*-test with Welch's correction).

and B). Similar results have been reported for HepG2 spheroids grown under static conditions that were exposed to B(a)P ($\geq 10 \mu\text{M}$) and PhIP ($\geq 50 \mu\text{M}$) for 24 h (Štampar et al., 2019). In line with our results, induction of DNA damage has also been observed in HepaRG spheroids exposed to B(a)P at $\geq 20 \mu\text{M}$ and PhIP at $\geq 40 \mu\text{M}$ as well as other pro-

genotoxic compounds including cyclophosphamide, 7,12-dimethylbenz[*a*]anthracene, 2-acetylaminofluorene and acrylamide with the exception of 2-amino-3-methylimidazo[4,5-*f*]quinolone (Mandon et al., 2019). Comet assay on HepG2 spheroids has also been applied to assess genotoxicity of the direct-acting compounds methyl

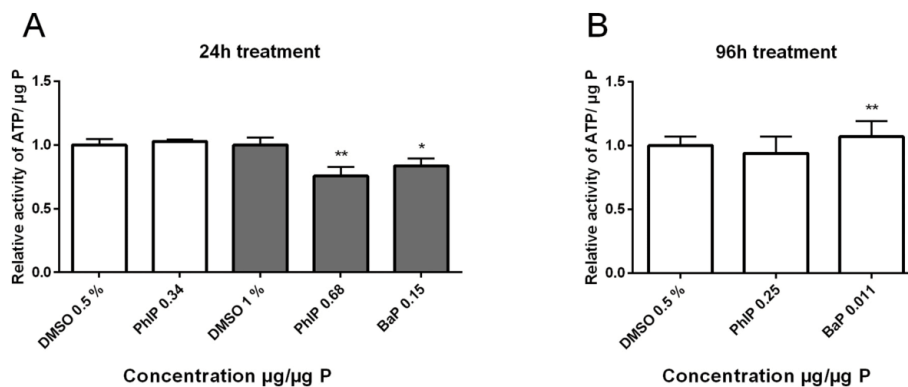


Fig. 3. The relative ATP content in HepG2/C3A spheroids (3D) after 24 (A) and 96 (B) hour treatment to B(a)P and PhIP determined with the ATP assay. Three independent experiments were performed and each time five spheroids from each bioreactor were collected at specific time points. The % of the solvent in different treatments after 24 h was adjusted to the 0.5% at a lower dose of PhIP (white columns) and to the 1% at the higher dose of PhIP and B(a)P (grey columns). The % of the solvent after 96 h was adjusted to 0.5%. Results are presented as relative ATP/ $\mu\text{g protein}$ \pm SD normalized to corresponding solvent control. The statistical analysis was conducted in Graph Pad Prism 6 (unpaired parametric *t*-test with Welch's correction).

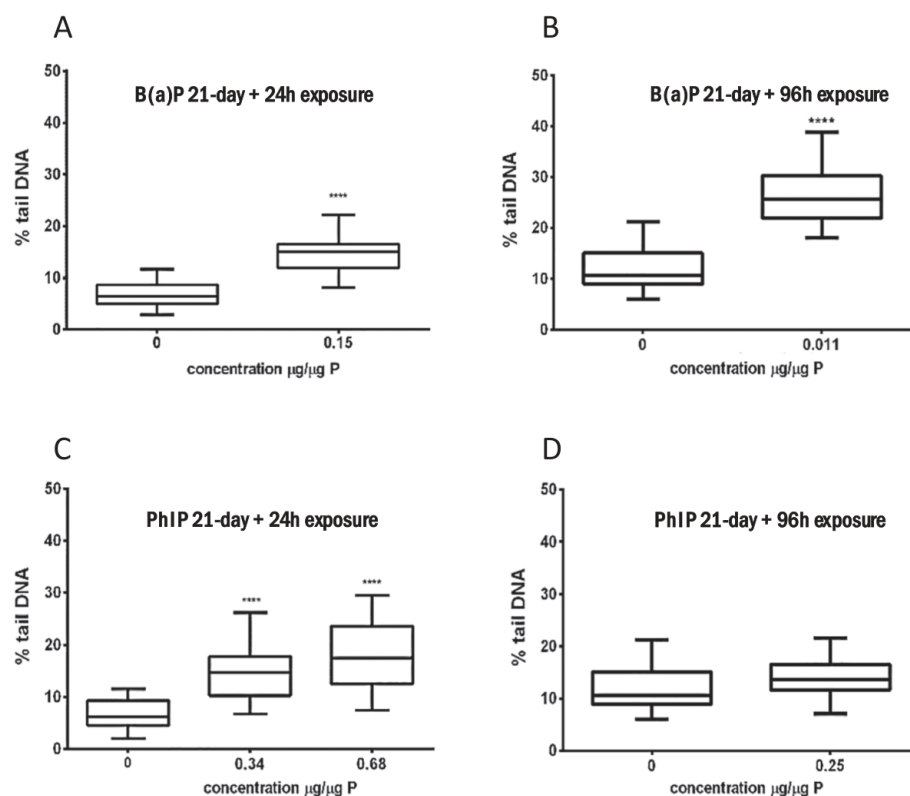


Fig. 4. Determination of DNA damage after the exposure of HepG2/C3A spheroids to indirect-acting model genotoxic compounds B(a)P and PhIP and solvent control (0) for 24 and 96 h by the comet assay (% tail DNA). Fifty nuclei were measured per experimental point and presented in box-plots. Three independent experiments were performed. (One-way ANOVA, Dunnett's test; **** $p < 0.001$).

methane sulfonate and hydrogen peroxide by Elje et al. (2019). After prolonged exposure (96 h) of HepG2/C3A spheroids to B(a)P, DNA damage was observed at approximately 10-times lower doses (0.011 $\mu\text{g}/\mu\text{g P}$) compared to doses used for 24 hour exposure (Fig. 4D), indicating high sensitivity of the system for detecting B(a)P genotoxicity. On the contrary, PhIP did not induce DNA damage in HepG2/C3A spheroids (Fig. 4C) after prolonged exposure to doses of 0.246 $\mu\text{g}/\mu\text{g P}$. The explanation for the observed effect can be the metabolism of PhIP after prolonged exposure and/or repair of DNA damage within 96 h of exposure as HepG2/C3A spheroids have been shown to have a very high level of DNA repair enzymes (Wrzesinski et al., 2014). It is also possible that the used dose of PhIP was too low to induce DNA damage although it was only 25% lower than the dose used for 24 hour exposure (0.246 $\mu\text{g}/\mu\text{g P}$ vs. 0.34 $\mu\text{g}/\mu\text{g P}$, respectively).

3.3. Gene expression

3.3.1. Basal mRNA expression in 3D compared to 2D monolayer system

The basal mRNA expression of studied liver-specific and phase I and phase II metabolic enzymes was determined in HepG2/C3A spheroids cultivated for 22 days (21 days plus additional 24 h) and 25 days (21 days plus additional 96 h). In HepG2/C3A monolayer cultures (2D), mRNA expression was determined after 2 days (1 day plus additional 24 h) of cell cultivation. The mRNA expressions of *albumin* (1.4-fold and 2.2-fold, respectively), *ALDH3A1* (3.5-fold and 1.6-fold,

respectively) and metabolic enzymes of phase I, *CYP3A4* (1.1-fold and 3.2-fold, respectively), *CYP1A1* (3.5-fold and 2.5-fold, respectively), and phase II, *UGT2B7* (2.2-fold and 1.6-fold, respectively) and *SULT1C2* (3.4-fold and 5.9-fold, respectively), were up-regulated after 22 days and 25 days of cultivation compared to the 2D system cultured for 2 days (Fig. 5). The obtained results are in line with observations described by Stampar et al. (2019), and Shah et al. (2018) who demonstrated that HepG2 spheroids grown under static conditions expressed higher mRNA levels of metabolic enzymes, which is a crucial physiological function of hepatocytes *in vivo* (Snykers et al., 2009). Similarly, higher mRNA levels of genes encoding phase I and II drug-metabolizing enzymes (Ramaiahgari et al., 2014; Whitlock, 1999), nuclear receptors and xenobiotic transcription factors (Hurrell et al., 2019; Ramaiahgari et al., 2014, 2017) as well as a time-dependent increase of *albumin* (Ramaiahgari et al., 2014) was described in HepG2 spheroids, when compared to monolayer cultures. We have noticed that the basal mRNA levels of *UGT1A1* (0.5-fold and 0.6-fold, respectively) and *NAT2* (0.2-fold and 0.26-fold, respectively) were expressed to a lower extent in the dynamic clinostat 3D HepG2/C3A cell system compared to 2D cell culture (Fig. 5), while the expressions of *SULT1B1* (1.3-fold and 1.09-fold, respectively) and *NAT1* (0.85-fold and 1.15-fold, respectively) were not biologically importantly deregulated. Previously, Chang and Hughes-Fulford (2009) showed that the expression of metabolic and synthetic functional genes changes differently with the time of cultivation in 3 to 7-day old HepG2 spheroids when compared

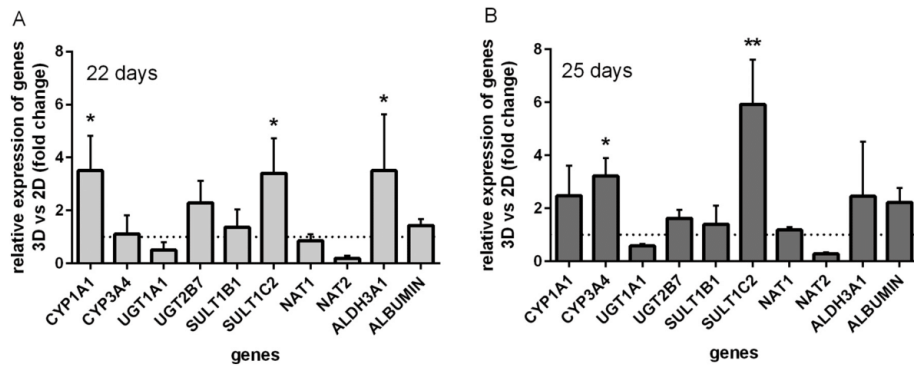


Fig. 5. Relative basal mRNA expression in 3D HepG2/C3A spheroids cultured under dynamic conditions for 22 (A) and 25 (B) days compared to 2-day old monolayer cultures. Data are presented as an average \pm SD (N = 3). The dotted line denotes the expression of the corresponding gene in monolayer culture (1-fold change). A significant variance in mRNA expression in 3D compared to 2D cultures was assessed with the one-way ANOVA using multiple comparisons (Dunnnett's) (* $p < 0.05$, ** $p < 0.01$).

to monolayer cultures. Therefore, our results are not surprising since the expression of genes in spheroids changes over time.

3.3.2. The impact of model genotoxic compounds on mRNA level in HepG2/C3A spheroids

Further, the changes in the transcription of studied genes involved in the metabolism (phase I and II), immediate early response and response to DNA damage were analysed after the exposure to genotoxic compounds. Relative mRNA level of the studied genes in treated groups compared to solvent controls are shown in Figs. 6 and 7.

Most of the xenobiotic-metabolizing enzymes are inducible (Braeuning et al., 2009; Denison and Whitlock, 1995; Mitchell and

Warszawsky, 2003). Therefore, induction of the mRNA level of studied genes encoding phase I (CYP3A4, CYP1A1, CYP1A2, and ALDH3A1) and II (UGT1A1, UGT2B7, SULT1C2, SULT1B1, NAT2, NAT1) enzymes was investigated after the treatment of spheroids to B(a)P and PhIP for 24 or 96 h. B(a)P is primarily metabolized in the liver by human cytochromes (CYP1A1/CYP1B1) and epoxide hydrolase to carcinogenic intermediates that covalently bind to DNA to start the carcinogenic process (Melendez-Colon et al., 1999; Nebert et al., 2004; Qin and Meng, 2010; Whitlock, 1999). In HepG2/C3A spheroids, B(a)P after 24 h up-regulated the expression of CYP3A4 (12.3-fold), CYP1A1 (295.6-fold), CYP1A2 (3.9-fold), UGT1A1 (13.6-fold), UGT2B7 (14.7-fold), NAT2 (4.0-fold), NAT1 (8.0-fold) and ALDH3A1 (345.9-fold). This is in line

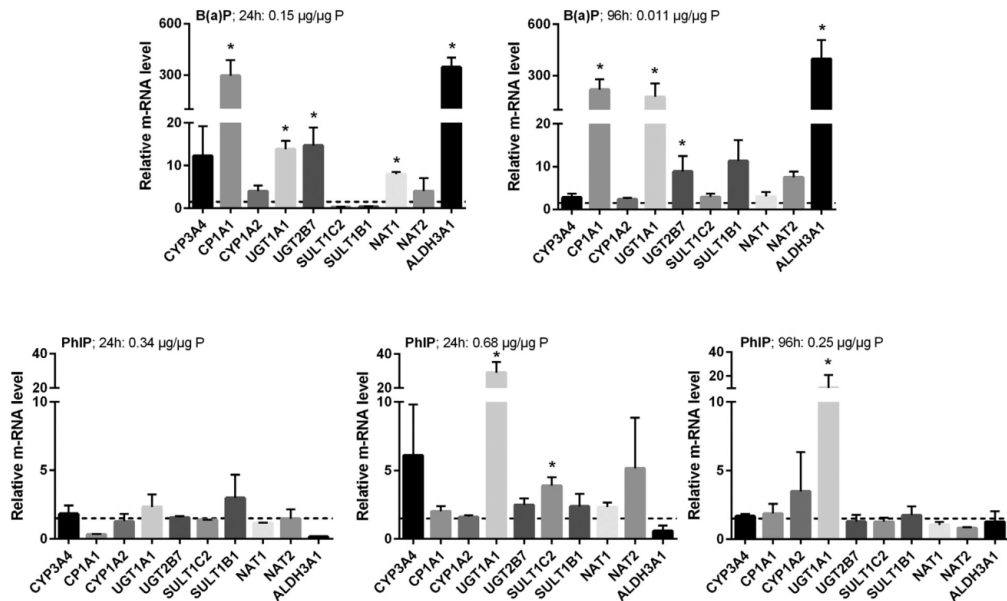


Fig. 6. The mRNA level of selected genes involved in the metabolism after 24 and 96 h of exposure of 21-day old HepG2/C3A spheroids to genotoxic compounds, B(a)P and PhIP. The dotted line denotes biologically significant differences in gene expression (1.5-fold change). The expression of each gene was assessed in duplicates and three independent experiments were performed. The statistical analysis between exposed and control groups was done by the multiple t -test analysis using the Sidak-Bonferroni method (* $p < 0.05$). An up-/down-regulation of ≥ 1.5 and ≤ 0.66 -fold change, respectively, compared to the corresponding solvent control was considered a positive response.

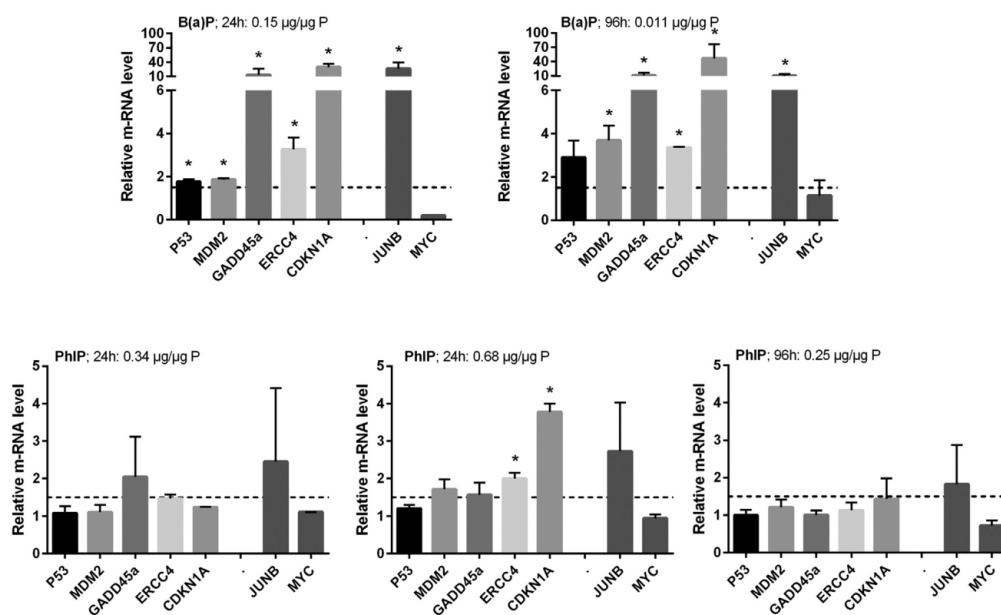


Fig. 7. The mRNA expression of studied genes involved in DNA damage response and the immediate-early response in 21-day old HepG2/C3A spheroids after 24 and 96 h of exposure to model genotoxic compounds. The dotted line denotes biologically significant differences in gene expression (1.5-fold change). The expression of each gene was assessed in duplicates and three experiments were done independently. The statistical variance was tested using the multiple *t*-tests and the Sidak-Bonferroni method (**p* < 0.05). An up-/down-regulation of ≥ 1.5 and ≤ 0.66 -fold change, respectively, compared to the control, was considered as a positive response.

with previous findings demonstrating that B(a)P in HepG2 monolayer cultures up-regulated genes encoding important cytochromes (*CYP1A1*, *CYP1A2*, and *CYP3A4*) (Bartosiewicz et al., 2001; Ewa and Danuta, 2017; Lee et al., 2006, 2009; Stiborová et al., 2014). Glucuronosyltransferases (UGTs), *N*-acetyltransferases (NATs) and sulfotransferases (SULT) belonging to phase II enzymes, act on the oxidized products generated from phase I and thus represent an important detoxification pathway (Gamage et al., 2006; Li et al., 2008). B(a)P up-regulated *UGT1A1* (13.8-fold), *UGT2B7* (14.6-fold), *NAT1* (7.9-fold) and *NAT2* (5.7-fold) and down-regulated *SULT1C2* (0.28-fold) and *SULT1B1* (0.36-fold). The up-regulation of *UGT1A1* by B(a)P has previously been observed in HepG2 cell monolayer cultures (Pezdiric et al., 2013) and in HepG2 spheroid cultures (Štampar et al., 2019). On the contrary, *NAT2* was not deregulated in HepG2 monolayer cultures (Pezdiric et al., 2013) and HepG2 spheroids (Štampar et al., 2019), while in the latter cell model *NAT1* was upregulated (Štampar et al., 2019).

PhIP is metabolized to a DNA-binding product by CYP1A2- and CYP1A1-catalyzed *N*-hydroxylation (Wilkening et al., 2003), while the major PhIP detoxification pathway is considered UGT-mediated glucuronidation and sulfotransferation and to a lesser extent *N*-acetyltransferation (Turesky, 2011; Turesky and Le Marchand, 2011). However, *O*-esterification of *N*-hydroxy-derivatives catalyzed by *N*-acetyltransferases (NATs) and sulfotransferases (SULTs) also produces *N*-acetoxy HAA derivatives, which after heterocyclic cleavage produces DNA reactive nitrenium ion (Turesky, 2011). The 24-hour exposure of HepG2/C3A spheroids to PhIP was performed at two doses, 0.34 µg/µg P and 0.68 µg/µg P. At the lower dose PhIP up-regulated *CYP3A4* (1.8-fold), *UGT1A1* (2.3-fold) and *SULT1B1* (3.0-fold) and down-regulated *CYP1A1* (0.32-fold) and *ALDH3A1* (0.16-fold). In contrast, at 0.68 µg/µg P PhIP up-regulated phase I metabolic genes *CYP3A4* (6.1-fold), *CYP1A1* (6.0-fold) and *CYP1A2* (1.6-fold), and phase II metabolic genes *UGT1A1* (29.1-fold), *UGT2B7* (2.5-fold), *SULT1B1* (2.4-fold), *SULT1C2*

(3.9-fold), *NAT1* (2.3-fold) and *NAT2* (5.2-fold), while *ALDH3A1* (0.74-fold) was not importantly deregulated. Similar metabolic gene deregulation by PhIP was described in metabolically competent HepaRG cells, where increased mRNA and activity levels of *CYP1A1*, *CYP1A2* and *CYP1B1* were described by Dumont et al. (2010). Presumably, this is the consequence of the activation of the aryl hydrocarbon receptor (AHR), the key nuclear factor in the regulation of CYPs and ALDHs (Omiecinski et al., 2011). Also in HepG2 monolayer cultures, PhIP up-regulated genes encoding phase I (*CYP1A1* and *CYP1A2*) (Pezdiric et al., 2013; Viegas et al., 2012) and phase II (*NAT2* and *UGT1A1*) (Pezdiric et al., 2013) metabolism, while *SULT1A1* was not expressed in HepG2 cells under the tested experimental conditions. The results of our study clearly demonstrate that in HepG2/C3A spheroids *SULTs* were expressed at the mRNA level and were up-regulated upon PhIP exposure.

After 96 hour exposure, B(a)P up-regulated all studied genes involved in metabolism; *CYP3A4* (2.8-fold), *CYP1A1* (218.8-fold), *CYP1A2* (2.4-fold), *UGT1A1* (176.2-fold), *UGT2B7* (8.8-fold), *NAT1* (3.0-fold), *NAT2* (7.5-fold), *SULT1C2* (2.9-fold), *SULT1B1* (11.3-fold) and *ALDH3A1* (397.6-fold). The up-regulation of some of these genes was after 96 h exposure more pronounced than after 24 h exposure to a higher dose. In PhIP (0.25 µg/µg P) exposed HepG2/C3A spheroids, *CYP1A2* (3.47-fold) and *UGT1A1* (10.35-fold) were up-regulated to a higher extent than after 24-hour exposure to 0.34 µg/µg P of PhIP (Fig. 6), while the expressions of other studied genes were not significantly different from their expressions in control spheroids. This may indicate that PhIP (0.25 µg/µg P) has been efficiently metabolized and detoxified during 96 h of exposure, which stopped upregulation of the expression of CYPs, SULTs, and NATs or the exposure dose was not high enough to up-regulate the expression of these enzymes.

The cellular response to the exposure to genotoxic chemicals depends on the cellular defence, particularly, DNA damage repair

mechanisms (Dumont et al., 2010). DNA damage triggers the activation of p53 network, where tumour suppressor p53 plays an essential role in controlling cellular proliferation in the context of DNA damage by activating the transcription of many crucial genes involved in cell cycle arrest and DNA repair, apoptosis, differentiation and senescence (Vogelstein et al., 2000). The cyclin-dependent kinase inhibitor 1A gene (*CDKN1A*) that encodes p21 is a p53-dependent key regulator of cell fate by triggering cell cycle arrest in G1 phase under multiple stress conditions including DNA damage (Warfel and El-Deiry, 2013). It is directly involved in DNA repair, including nucleotide excision repair (NER) (Cazzalini et al., 2010). The *GADD45α* is another gene that is regulated by p53 and is implicated in the regulation of several cellular functions, such as DNA damage and repair, cell cycle checkpoint, signalling transduction and maintenance of genomic stability (Tamura et al., 2012). It controls the cell cycle G2-M checkpoint, the DNA repair process and apoptosis (Wang et al., 1999). MDM2 protein, a product of a proto-oncogene, is under non-stressed conditions the negative regulation of *TP53* (Michael and Oren, 2002). It enhances the tumorigenicity of the cells and promotes survival of the cells and the progression of the cell cycle (Deb, 2003). The *ERCC4* gene has a vital role in DNA damage repair processes and in maintaining genomic stability. It is activated by DNA damaging compounds that induce covalent helix-distorting adducts and plays a central role in DNA NER (Manandhar et al., 2015). An important cellular response to carcinogens is also gene regulation via the transcription factor, the activator protein 1 (AP-1) that is composed of JUN and FOS protein dimers, known as homologs of retroviral oncoproteins. JUN-B is implicated in many essential cell processes, including differentiation, proliferation, and tumorigenesis (Hess et al., 2004). Another oncogene that is considered as a critical regulator of cell proliferation is *MYC*. Its deregulation is associated with the genesis of most human tumours (Adhikary and Eilers, 2005). The immediate-early response genes (*MYC* and *JUN*), which coordinate the expression of further genes required for subsequent cell cycle progression (Kohn, 1999), enable ligands of AHR to act as influential tumour promoters and carcinogens (Marlowe and Puga, 2005). Transcriptomic analyses revealed that in HepG2/C3A spheroids, exposure to B(a)P for 24 and 96 h caused transcriptional activation of *TP53* (1.8-fold and 2.9-fold, respectively), and its down-stream regulated genes *CDKN1A* (29.5-fold and 46.5-fold, respectively), *GADD45α* (13.5-fold and 10.4-fold, respectively) and *MDM2* (1.9-fold and 3.7-fold, respectively) as well as *ERCC4* (3.3-fold and 3.2-fold, respectively). Higher levels of the expressions of *TP53* and *CDKN1A* after prolonged exposure (96 h) correlate with the more pronounced increase of DNA damage after prolonged exposure. In HepG2 cells grown in monolayer, 24 hour exposure to B(a)P up-regulated the mRNA level of *CDKN1A* and *GADD45α*, whereas the expression of *TP53* was not affected, while *MDM2* was down-regulated (Pezdiric et al., 2013). In 21-day old spheroids at both 24 and 96 h of exposure, B(a)P up-regulated the expression of *JUNB* (26.4-fold and 9.5-fold, respectively), while *MYC* was significantly down-regulated (0.2-fold) after 24 h. Modifications in the expression of growth-related genes associated with the exposure to xenobiotics may be associated to tumorigenesis in target organs, for this reason, the significantly induced expression of *JUNB* by B(a)P may implicate the process of B(a)P induced carcinogenesis (Goldsworthy et al., 1994; Mehta, 1995). Altogether, the results showed that all genes associated with DNA damage response were greatly upregulated upon exposure to B(a)P at all applied conditions, which correlate with its genotoxic activity.

The heterocyclic aromatic amine PhIP after 24 hour exposure at dose 0.34 µg/µg P slightly, but not significantly upregulated only the expression of *GADD45α* (2.0-fold) and *JUNB* (2.45-fold). The higher dose of PhIP (0.68 µg/µg P) upregulated the expression of *CDKN1A1* (3.8-fold), *MDM2* (1.71-fold), *ERCC4* (2.0-fold) and *JUNB* (2.7-fold). The upregulation of *GADD45α* after exposure to PhIP was also described in HepG2

monolayer cultures (Pezdiric et al., 2013). After 96 h of exposure, no significant mRNA deregulation of genes involved in the response to DNA damage was observed, except for *JUNB* gene (1.8-fold), which belongs to immediate-early response genes (Fig. 7). These findings support the results obtained with the comet assay, where PhIP induced increased DNA strand break formation after 24 h but not after 96 hour exposure. These results imply the lower genotoxic potential of PhIP compared to BaP, as well as a different mechanism of action.

4. Conclusions

In recent years, considerable efforts have been brought to the development of a wide range of *in vitro* 3D cell models. These have shown promising results for their usage in drug discovery, stem cell research, cancer cell biology, and recently also in genetic and environmental toxicology to reduce disparities between the traditional 2D cell models and whole-animal systems. Moreover, *in vitro* 3D cell models can be used to fulfil the 3R (reduce, refine and replace) strategy to avoid unnecessary animal experiments with inaccurate predictions for humans due to species variability.

We optimized the comet assay method to determine the genotoxic activity of indirect-acting genotoxic compounds in 21-day old HepG2/C3A spheroids cultured in bioreactors under dynamic clinostat conditions and studied the effects of genotoxic compounds on the expression of genes encoding xenobiotic metabolic enzymes and enzymes involved in DNA damage and immediate-early response. The dynamic clinostat culturing conditions that allow growth and generation of a high amount of uniform spheroids for a prolonged time without the addition of extracellular matrix enable a constant supply of nutrients entering the spheroid. The formed spheroids enable long-term exposure studies where low for human exposure relevant doses of chemicals including complex environmental mixtures can be applied. Based on the results of our study, 21-day old HepG2/C3A spheroids proved to be metabolically competent; the basal levels of mRNA of the studied genes encoding phase I and phase II metabolic enzymes were significantly higher in 3D cultures compared to 2D cultures. The 3D spheroids also responded to the exposure to indirect-acting model environmental pollutants, benzo(a)pyrene [B(a)P], and 2-amino-1-methyl-6-phenylimidazo(4,5-b)pyridine [PhIP] with compound-specific mRNA deregulation of those genes. The genotoxic activity of B(a)P and PhIP was confirmed in HepG2/C3A spheroids after short and prolonged exposure. Both compounds induced increased DNA strand break formation and compound-specific deregulation of the expression of DNA damage and immediate-early responsive genes. Our study demonstrated that high viability of HepG2/C3A spheroids and the dynamic 3D model enables their use for prolonged exposure studies, which is of great importance for detecting and predicting the genotoxic effects relevant for chronic human exposure to a low dose of genotoxic compounds, which can be found in the human environment. Therefore, the HepG2/C3A 3D cell model cultured under dynamic conditions, as a result of more complex structure and better metabolic capacity, represents a very sensitive system and can provide more physiologically important information and more predictive information for human health risk assessment and therefore, can contribute to more trustworthy genotoxicity assessment of chemicals and complex environmental samples.

Funding

This research was funded by grants P1-0245, J1-2465 and grant to young researchers MR-MŠtampar of the Slovenian Research Agency ARRS, and COST Action CA16119 (*In vitro* 3-D total cell guidance and fitness). HSF was supported by a PhD grant from Sino Danish Centre for Education and Research.

2.6 Hepatocellular Carcinoma (HepG2/C3A) Cell-Based 3D Model for Genotoxicity Testing of Chemicals

121

M. Štampar, H. Sedighi Frandsen, A. Rogowska-Wrzęsinska et al.

Science of the Total Environment xxx (xxxx) xxx

CRedit authorship contribution statement

Martina Štampar: Conceptualization, Methodology, Software, Validation, Formal analysis, Investigation, Data curation, Writing - original draft, Visualization. **Helle Sedighi Frandsen:** Methodology, Software, Validation, Investigation, Data curation, Writing - review & editing, Visualization. **Adelina Rogowska-Wrzęsinska:** Conceptualization, Methodology, Formal analysis, Investigation, Resources, Writing - review & editing, Funding acquisition. **Krzysztof Wrześinski:** Methodology, Writing - review & editing. **Metka Filipič:** Resources, Writing - review & editing, Supervision, Project administration, Funding acquisition. **Bojana Žegura:** Conceptualization, Methodology, Validation, Formal analysis, Investigation, Resources, Data curation, Writing - original draft, Visualization, Supervision, Project administration, Funding acquisition.

Declaration of competing interest

The authors declare that they have no known competing financial interests or personal relationships that could have appeared to influence the work reported in this paper.

References

Aadhikary, S., Eilers, M., 2005. Transcriptional regulation and transformation by Myc proteins. *Nat. Rev. Mol. Cell Biol.* <https://doi.org/10.1038/nrm1703>.

Aucamp, J., Calitz, C., Bronkhorst, A.J., Wrześinski, K., Hamman, S., Gouws, C., Pretorius, P.J., 2017. Cell-free DNA in a three-dimensional spheroid cell culture model: a preliminary study. *Int. J. Biochem. Cell Biol.* 89, 182–192. <https://doi.org/10.1016/j.biocel.2017.06.014>.

Baan, R., Grosse, Y., Straif, K., Secretan, B., El Ghissassi, F., Bouvard, V., Benbrahim-Tallaa, L., Guha, N., Freeman, C., Galichet, L., Coglian, V., 2009. A review of human carcinogens-part F: chemical agents and related occupations. *Lancet Oncol.* [https://doi.org/10.1016/s1470-2045\(09\)70358-4](https://doi.org/10.1016/s1470-2045(09)70358-4).

Baebler, S., Svalina, M., Petek, M., Stare, K., Rotter, A., Pompe-Novak, M., Gruden, K., 2017. quantGenius: implementation of a decision support system for qPCR-based gene quantification. *BMC Bioinformatics* 18, 276. <https://doi.org/10.1186/s12859-017-1688-7>.

Baird, W.M., Hooven, L.A., Mahadevan, B., 2005. Carcinogenic polycyclic aromatic hydrocarbon-DNA adducts and mechanism of action. *Environ. Mol. Mutagen.* <https://doi.org/10.1002/em.20095>.

Bartosiewicz, M., Penn, S., Buckpitt, A., 2001. Applications of gene arrays in environmental toxicology: fingerprints of gene regulation associated with cadmium chloride, benzo (a)pyrene, and trichloroethylene. *Environ. Health Perspect.* 109, 71–74. <https://doi.org/10.1289/ehp.0110971>.

Basu, A., Dydowiczová, A., Čtveráčková, L., Jaša, L., Troško, J.E., Bláha, L., Babica, P., 2018. Assessment of hepatotoxic potential of cyanobacterial toxins using 3D in vitro model of adult human liver stem cells. *Environ. Sci. Technol.* 52, 10078–10088. <https://doi.org/10.1021/acs.est.8b02291>.

Basu, A., Dydowiczová, A., Troško, J.E., Bláha, L., Babica, P., 2020. Ready to go 3D? A semi-automated protocol for microwell spheroid arrays to increase scalability and throughput of 3D cell culture testing. *Toxicol. Mech. Methods* (0), 1–43. <https://doi.org/10.1080/15376516.2020.1800881>.

Braeuning, A., Sanna, R., Huelsenken, J., Schwarz, M., 2009. Inducibility of drug-metabolizing enzymes by xenobiotics in mice with liver-specific knockout of *ctmnb1*. *Drug Metab. Dispos.* 37, 1138–1145. <https://doi.org/10.1124/dmd.108.026179>.

Breslin, S., O'Driscoll, L., 2013. Three-dimensional cell culture: the missing link in drug discovery. *Drug Discov. Today* 18, 240–249. <https://doi.org/10.1016/j.drudis.2012.10.003>.

Burden, N., Chapman, K., Sewell, F., Robinson, V., 2015. Pioneering better science through the 3Rs: an introduction to the National Centre for the Replacement, Refinement, and Reduction of Animals in Research (NC3Rs). *J. Am. Assoc. Lab. Anim. Sci.* 54, 198–208.

Cazzalini, O., Scovassi, A.L., Savio, M., Stivala, L.A., Prosperi, E., 2010. Multiple roles of the cell cycle inhibitor p21(CDKN1A) in the DNA damage response. *Mutat. Res.* 704, 12–20. <https://doi.org/10.1016/j.mrrev.2010.01.009>.

Chang, T.T., Hughes-Fulford, M., 2009. Monolayer and spheroid culture of human liver hepatocellular carcinoma cell line cells demonstrate distinct global gene expression patterns and functional phenotypes. *Tissue Eng. Part A* 15, 559–567. <https://doi.org/10.1089/ten.tea.2007.0434>.

Corvi, R., Madaia, F., 2017. In vitro genotoxicity testing—can the performance be enhanced? *Food Chem. Toxicol.* 106, 600–608. <https://doi.org/10.1016/j.fct.2016.08.024>.

Deb, S.P., 2003. Cell cycle regulatory functions of the human oncoprotein MDM2. *Mol. Cancer Res.* 1, 1009–1016.

Denison, M.S., Whitlock, J.P., 1995. Xenobiotic-inducible transcription of cytochrome P450 genes. *J. Biol. Chem.* <https://doi.org/10.1074/jbc.270.31.18175>.

Dix, D.J., Houck, K.A., Martin, M.T., Richard, A.M., Setzer, R.W., Kavlock, R.J., 2007. The toxcast program for prioritizing toxicity testing of environmental chemicals. *Toxicol. Sci.* 95, 5–12. <https://doi.org/10.1093/toxsci/kfl103>.

Dumont, J., Jossé, R., Lambert, C., Anthérieu, S., Laurent, V., Loyer, P., Robin, M.A., Guillouzo, A., 2010. Preferential induction of the AhR gene battery in HepaRG cells after a single or repeated exposure to heterocyclic aromatic amines. *Toxicol. Appl. Pharmacol.* 249, 91–100. <https://doi.org/10.1016/j.taap.2010.08.027>.

Edmondson, R., Broglie, J.J., Adcock, A.F., Yang, L., 2014. Three-dimensional cell culture systems and their applications in drug discovery and cell-based biosensors. *Assay Drug Dev. Technol.* 12, 207–218. <https://doi.org/10.1089/adt.2014.573>.

Elje, E., Hesler, M., Rundén-Pran, E., Mann, P., Mariussen, E., Wagner, S., Dusinska, M., Kohl, Y., 2019. The comet assay applied to HepG2 liver spheroids. *Mutat. Res. - Genet. Toxicol. Environ. Mutagen.* 845, 403033. <https://doi.org/10.1016/j.mrgentox.2019.03.006>.

Ewa, B., Danuta, M.Ś., 2017. Polycyclic aromatic hydrocarbons and PAH-related DNA adducts. *J. Appl. Genet.* <https://doi.org/10.1007/s13353-016-0380-3>.

Fey, S.J., Wrześinski, K., 2012. Determination of drug toxicity using 3D spheroids constructed from an immortal human hepatocyte cell line. *Toxicol. Sci.* 127, 403–411. <https://doi.org/10.1093/toxsci/kfs122>.

Flampouri, E., Imar, S., Oconnell, K., Singh, B., 2019. Spheroid-3D and monolayer-2D intestinal electrochemical biosensor for toxicity/viability testing: applications in drug screening, food safety, and environmental pollutant analysis. *ACS Sensors* 4, 660–669. <https://doi.org/10.1021/acssensors.8b01490>.

Gajski, G., Gerić, M., Žegura, B., Novak, M., Nunić, J., Bajrektarević, D., Garaj-Vrhovac, V., Filipič, M., 2016. Genotoxic potential of selected cytostatic drugs in human and zebrafish cells. *Environ. Sci. Pollut. Res.* 23, 14739–14750. <https://doi.org/10.1007/s11356-015-4592-6>.

Gamage, N., Barnett, A., Hempel, N., Duggleby, R.G., Windmill, K.F., Martin, J.L., McManus, M.E., 2006. Human sulfoxtransferases and their role in chemical metabolism. *Toxicol. Sci.* <https://doi.org/10.1093/toxsci/kfj061>.

Goldsworthy, T.L., Goldsworthy, S.M., Sprankle, C.S., Butterworth, B.E., 1994. Expression of *myc*, *fos* and *Ha-ras* associated with chemically induced cell proliferation in the rat liver. *Cell Prolif.* 27, 269–278. <https://doi.org/10.1111/j.1365-2184.1994.tb01424.x>.

Gong, X., Lin, C., Cheng, J., Su, J., Zhao, H., Liu, T., Wen, X., Zhao, P., 2015. Generation of multicellular tumor spheroids with microwell-based agarose scaffolds for drug testing. *PLoS One* 10, e0130348. <https://doi.org/10.1371/journal.pone.0130348>.

Hartig, T., Mitchell, R., De Vries, S., Frumkin, H., 2014. Nature and health. Annual Review of Public Health. Annual Reviews Inc., pp. 207–228. <https://doi.org/10.1146/annurev-publhealth-032013-182443>.

Hercog, K., Štampar, M., Štern, A., Filipič, M., Žegura, B., 2020. Application of advanced HepG2 3D cell model for studying genotoxic activity of cyanobacterial toxin cylindrospermopsin. *Environ. Pollut.* 265, 114965. <https://doi.org/10.1016/j.envpol.2020.114965>.

Hess, J., Angel, P., Schorpp-Kistner, M., 2004. AP-1 subunits: quarrel and harmony among siblings. *J. Cell Sci.* 117, 5965–5973. <https://doi.org/10.1242/jcs.01589>.

Hurrell, T., Lilley, K.S., Cromarty, A.D., 2019. Proteomic responses of HepG2 cell monolayers and 3D spheroids to selected hepatotoxins. *Toxicol. Lett.* 300, 40–50. <https://doi.org/10.1016/j.toxlet.2018.10.030>.

Iyer, V.V., Yang, H., Ierapetritou, M.G., Roth, C.M., 2010. Effects of glucose and insulin on HepG2-C3A cell metabolism. *Biotechnol. Bioeng.* 107, 347–356. <https://doi.org/10.1002/bit.22799>.

Kirkland, D., Pflüher, S., Tweats, D., Aardema, M., Corvi, R., Darroufi, F., Elhajouji, A., Glatt, H., Hastwell, P., Hayashi, M., Kasper, P., Kirchner, S., Lynch, A., Marzin, D., Maurici, D., Meunier, J.-R., Müller, L., Nohynek, G., Parry, J., Parry, E., Thybaud, V., Tice, R., van Benthem, J., Vanparys, P., White, P., 2007. How to reduce false positive results when undertaking in vitro genotoxicity testing and thus avoid unnecessary follow-up animal tests: report of an ECVAM Workshop. *Mutat. Res. Toxicol. Environ. Mutagen.* 628, 31–55. <https://doi.org/10.1016/j.MRGENTOX.2006.11.008>.

Kohn, K.W., 1999. Molecular interaction map of the mammalian cell cycle control and DNA repair systems. *Mol. Biol. Cell* 10, 2703–2734. <https://doi.org/10.1091/mbc.10.8.2703>.

Lee, C.M., Chen, S.Y., Lee, Y.C.G., Huang, C.Y.F., Chen, Y.M.A., 2006. Benzo(a)pyrene and glycine N-methyltransferase interactions: gene expression profiles of the liver detoxification pathway. *Toxicol. Appl. Pharmacol.* 214, 126–135. <https://doi.org/10.1016/j.taap.2005.12.020>.

Lee, J., Lilly, G.D., Doty, R.C., Podsiadlo, P., Kotov, N.A., 2009. In vitro toxicity testing of nanoparticles in 3D cell culture. *Small* 5, 1212–1221. <https://doi.org/10.1002/smll.200801788>.

Li, Y., Lindsay, J., Wang, L.-L., Zhou, S.-F., 2008. Structure, function and polymorphism of human cytosolic sulfoxtransferases. *Curr. Drug Metab.* 9, 99–105. <https://doi.org/10.2174/138920008783571819>.

Lin, Rwei-Zeng, Lin, Rwei-Zhen, Chang, H.-Y., 2008. Recent advances in three-dimensional multicellular spheroid culture for biomedical research. *Biotechnol. J.* 3, 1172–1184. <https://doi.org/10.1002/biot.200700228>.

Loessner, D., Stok, K.S., Lutolf, M.P., Hutmacher, D.W., Clements, J.A., Rizzi, S.C., 2010. Bioengineered 3D platform to explore cell-ECM interactions and drug resistance of epithelial ovarian cancer cells. *Biomaterials* 31, 8494–8506. <https://doi.org/10.1016/j.biomaterials.2010.07.064>.

Manabe, S., Kurihara, N., Wada, O., Izumikawa, S., Asakuno, K., Morita, M., 1993. Detection of a carcinogen, 2-amino-1-methyl-6-phenylimidazo[4,5-b]pyridine, in airborne particles and diesel-exhaust particles. *Environ. Pollut.* 80, 281–286. [https://doi.org/10.1016/0269-7491\(93\)90049-T](https://doi.org/10.1016/0269-7491(93)90049-T).

Manandhar, M., Boulware, K.S., Wood, R.D., 2015. The ERCC1 and ERCC4 (XPB) genes and gene products. *Gene.* <https://doi.org/10.1016/j.gene.2015.06.026>.

Mandon, M., Huet, S., Dubreil, E., Fessard, V., Le Hégarat, L., 2019. Three-dimensional HepaRG spheroids as a liver model to study human genotoxicity in vitro with the single cell gel electrophoresis assay. *Sci. Rep.* 9. <https://doi.org/10.1038/s41598-019-47114-7>.

- Marlowe, J.L., Puga, A., 2005. Aryl hydrocarbon receptor, cell cycle regulation, toxicity, and tumorigenesis. *J. Cell. Biochem.* 96, 1174–1184. <https://doi.org/10.1002/jcb.20656>.
- Mehta, R., 1995. The potential for the use of cell proliferation and oncogene expression as intermediate markers during liver carcinogenesis. *Cancer Lett.* 93, 85–102. [https://doi.org/10.1016/0304-3835\(95\)03790-4](https://doi.org/10.1016/0304-3835(95)03790-4).
- Melendez-Colon, V.J., Luch, A., Seidel, A., Baird, W.M., 1999. Cancer initiation by polycyclic aromatic hydrocarbons results from formation of stable DNA adducts rather than apurinic sites. *Carcinogenesis* 20, 1885–1891. <https://doi.org/10.1093/carcin/20.10.1885>.
- Michael, D., Oren, M., 2002. The p53 and Mdm2 families in cancer. *Curr. Opin. Genet. Dev.* 12, 53–59. [https://doi.org/10.1016/S0959-437X\(01\)00264-7](https://doi.org/10.1016/S0959-437X(01)00264-7).
- Mitchell, K.R., Warshawsky, D., 2003. Xenobiotic inducible regions of the human arylamine N-acetyltransferase 1 and 2 genes. *Toxicol. Lett.* 139, 11–23. [https://doi.org/10.1016/S0378-4274\(02\)00437-X](https://doi.org/10.1016/S0378-4274(02)00437-X).
- Naccari, C., Galceran, M.T., Moyano, E., Cristani, M., Siracusa, L., Trombetta, D., 2009. Presence of heterocyclic aromatic amines (HAS) in smoked "Provola" cheese from Calabria (Italy). *Food Chem. Toxicol.* 47, 321–327. <https://doi.org/10.1016/j.fct.2008.11.018>.
- Nebert, D.W., Dalton, T.P., Okey, A.B., Gonzalez, F.J., 2004. Role of aryl hydrocarbon receptor-mediated induction of the CYP1 enzymes in environmental toxicity and cancer. *J. Biol. Chem.* <https://doi.org/10.1074/jbc.R400004200>.
- Nibourg, G.A.A., Chamuleau, R.A.F.M., Van Gulik, T.M., Hoekstra, R., 2012. Proliferative human cell sources applied as biocomponent in bioartificial livers: a review. *Expert. Opin. Biol. Ther.* <https://doi.org/10.1517/14712598.2012.685714>.
- Omicinski, C.J., Vanden Heuvel, J.P., Perdew, G.H., Peters, J.M., 2011. Xenobiotic metabolism, disposition, and regulation by receptors: from biochemical phenomenon to predictors of major toxicities. *Toxicol. Sci.* 120 (Suppl. 1), S49–S75. <https://doi.org/10.1093/toxsci/kfq338>.
- Pezdiric, M., Žegura, B., Filipić, M., 2013. Genotoxicity and induction of DNA damage responsive genes by food-borne heterocyclic aromatic amines in human hepatoma HepG2 cells. *Food Chem. Toxicol.* 59, 386–394. <https://doi.org/10.1016/j.fct.2013.06.030>.
- Pfuhler, S., Kirkland, D., Kasper, P., Hayashi, M., Vanparys, P., Carmichael, P., Dertinger, S., Eastmond, D., Elhajouji, A., Krul, C., Rothfuss, A., Schoening, G., Smith, A., Speit, G., Thomas, C., van Benthem, J., Corvi, R., 2009. Reduction of use of animals in regulatory genotoxicity testing: identification and implementation opportunities-report from an ECVAM workshop. *Mutat. Res. - Genet. Toxicol. Environ. Mutagen.* 680, 31–42. <https://doi.org/10.1016/j.mrgentox.2009.09.002>.
- Pfuhler, S., van Benthem, J., Curran, R., Doak, S.H., Dusinska, M., Hayashi, M., Helfrich, R.H., Kidd, D., Kirkland, D., Luan, Y., Ouedraogo, G., Reisinger, K., Sofuni, T., van Acker, F., Yang, Y., Corvi, R., 2020. Use of in vitro 3D tissue models in genotoxicity testing: Strategic fit, validation status and way forward. Report of the Working Group From the 7th International Workshop on Genotoxicity Testing (IWGT). *Mutagen. Mutat. Res. - Genet. Toxicol. Environ.* <https://doi.org/10.1016/j.mrgentox.2020.503135>.
- Piccinini, F., Tesel, A., Arienti, C., Bevilacqua, A., 2015. Cancer multicellular spheroids: volume assessment from a single 2D projection. *Comput. Methods Prog. Biomed.* 118, 95–106. <https://doi.org/10.1016/j.cmpb.2014.12.003>.
- Qin, G., Meng, Z., 2010. Sulfur dioxide and benzo(a)pyrene modulates CYP1A and tumor-related gene expression in rat liver. *Environ. Toxicol.* 25, 169–179. <https://doi.org/10.1002/tox.20484>.
- Ramaiahgari, S.C., Den Braver, M.W., Herpers, B., Terpstra, V., Commandeur, J.N.M., Van De Water, B., Price, L.S., 2014. A 3D in vitro model of differentiated HepG2 cell spheroids with improved liver-like properties for repeated dose high-throughput toxicity studies. *Arch. Toxicol.* 88, 1083–1095. <https://doi.org/10.1007/s00204-014-1215-9>.
- Ramaiahgari, S.C., Waidyanatha, S., Dixon, D., DeVito, M.J., Pauls, R.S., Ferguson, S.S., 2017. Three-dimensional (3D) HepaRG spheroid model with physiologically relevant xenobiotic metabolism competence and hepatocyte functionality for liver toxicity screening. *Toxicol. Sci.* 159, 124–136. <https://doi.org/10.1093/toxsci/kfx122>.
- Schechtman, L.M., 2002. Implementation of the 3Rs (refinement, reduction, and replacement): validation and regulatory acceptance considerations for alternative toxicological test methods. *ILAR J.* 43, S85–S94. <https://doi.org/10.1093/ilar.43.suppl.1.s85>.
- Shah, U.-K., Mallia, J. de O., Singh, N., Chapman, K.E., Doak, S.H., Jenkins, G.J.S., 2018. A three-dimensional in vitro HepG2 cells liver spheroid model for genotoxicity studies. *Mutat. Res. Toxicol. Environ. Mutagen.* 825, 51–58. <https://doi.org/10.1016/j.MRGENTOX.2017.12.005>.
- Skog, K., Solyakov, A., Arvidsson, P., Jägerstad, M., 1998. Analysis of nonpolar heterocyclic amines in cooked foods and meat extracts using gas chromatography-mass spectrometry. *J. Chromatogr. A* 803, 227–233. [https://doi.org/10.1016/S0021-9673\(97\)01266-1](https://doi.org/10.1016/S0021-9673(97)01266-1).
- Snykers, S., De Kock, J., Rogiers, V., Vanhaecke, T., 2009. In vitro differentiation of embryonic and adult stem cells into hepatocytes: state of the art. *Stem Cells* 27, 577–605. <https://doi.org/10.1634/stemcells.2008-0963>.
- Štampar, M., Tomc, J., Filipić, M., Žegura, B., 2019. Development of in vitro 3D cell model from hepatocellular carcinoma (HepG2) cell line and its application for genotoxicity testing. *Arch. Toxicol.* 93, 3321–3333. <https://doi.org/10.1007/s00204-019-02576-6>.
- Stiborová, M., Moserová, M., Černá, V., Indra, R., Dračinský, M., Šulc, M., Henderson, C.J., Wolf, C.R., Schmeiser, H.H., Phillips, D.H., Frei, E., Aert, V.M., 2014. Cytochrome b5 and epoxide hydrolase contribute to benzo(a)pyrene-DNA adduct formation catalyzed by cytochrome P450 1A1 under low NADPH:P450 oxidoreductase conditions. *Toxicology* 318, 1–12. <https://doi.org/10.1016/j.tox.2014.02.002>.
- Štraser, A., Filipić, M., Žegura, B., 2011. Genotoxic effects of the cyanobacterial hepatotoxin cylindrospermopsin in the HepG2 cell line. *Arch. Toxicol.* 85, 1617–1626. <https://doi.org/10.1007/s00204-011-0716-z>.
- Sun, H., Wei, Y., Deng, H., Xiong, Q., Li, M., Lahiri, J., Fang, Y., 2014. Label-free cell phenotypic profiling decodes the composition and signaling of an endogenous ATP-sensitive potassium channel. *Sci. Rep.* 4. <https://doi.org/10.1038/srep04934>.
- Tamta, H., Pawar, R.S., Wamer, W.G., Grundel, E., Krynitsky, A.J., Rader, J.L., 2012. Comparison of metabolism-mediated effects of pyrrolizidine alkaloids in a HepG2/C3A cell-S9 co-incubation system and quantification of their glutathione conjugates. *Xenobiotica* 42, 1038–1048. <https://doi.org/10.3109/00498254.2012.679978>.
- Tamura, R.E., de Vasconcellos, J.F., Sarkar, D., Libermann, T.A., Fisher, P.B., Zerbini, L.F., 2012. GADD45 proteins: central players in tumorigenesis. *Curr. Mol. Med.* 12, 634–651. <https://doi.org/10.2174/156652412800619978>.
- Turesky, R.J., 2011. Heterocyclic aromatic amines: potential human carcinogens. *Curr. Cancer Res.* 6, 95–112. https://doi.org/10.1007/978-1-61737-995-6_5.
- Turesky, R.J., Le Marchand, L., 2011. Metabolism and biomarkers of heterocyclic aromatic amines in molecular epidemiology studies: lessons learned from aromatic amines. *Chem. Res. Toxicol.* 24, 1169–1214. <https://doi.org/10.1021/tx200135v>.
- Tvardovskiy, A., Wrzesinski, K., Sidoli, S., Fey, S.J., Rogowska-Wrzesinska, A., Jensen, O.N., 2015. Top-down and middle-down protein analysis reveals that intact and clipped human histones differ in post-translational modification patterns. *Mol. Cell. Proteomics* 14, 3142–3153. <https://doi.org/10.1074/mcp.M115.048975>.
- Viegas, O., Žegura, B., Pezdiric, M., Novak, M., Ferreira, I.M.P.L.V.O., Pinho, O., Filipić, M., 2012. Protective effects of xanthohumol against the genotoxicity of heterocyclic aromatic amines MelQx and PhIP in bacteria and in human hepatoma (HepG2) cells. *Food Chem. Toxicol.* 50, 949–955. <https://doi.org/10.1016/j.fct.2011.11.031>.
- Vogelstein, B., Lane, D., Levine, A.J., 2000. Surfing the p53 network. *Nature* 408, 307–310. <https://doi.org/10.1038/35042675>.
- Wang, X.W., Zhan, Q., Coursen, J.D., Khan, M.A., Kontny, H.U., Yu, L., Hollander, M.C., O'Connor, P.M., Fornace, A.J., Harris, C.C., 1999. GADD45 induction of a G2/M cell cycle checkpoint. *Proc. Natl. Acad. Sci. U. S. A.* 96, 3706–3711. <https://doi.org/10.1073/pnas.96.7.3706>.
- Warfel, N.A., El-Deiry, W.S., 2013. P21WAF1 and tumorigenesis: 20 years after. *Curr. Opin. Oncol.* <https://doi.org/10.1097/CCO.0b013e32835b639e>.
- Whitlock, J.P., 1999. Induction of cytochrome P4501A1. *Ann. Rev. Pharmacol. Toxicol.* 39, 103–125. <https://doi.org/10.1146/annurev.pharmtox.39.1.103>.
- Wilkening, S., Stahll, F., Augustinus, B., 2003. HepG2 with regard to their biotransformation properties. *Drug Metab. Dispos.* 31, 1035–1042.
- Wojdyła, K., Wrzesinski, K., Williamson, J., Fey, S.J., Rogowska-Wrzesinska, A., 2016. Acetaminophen-induced: S-nitrosylation and S-sulfenylation signalling in 3D cultured hepatocarcinoma cell spheroids. *Toxicol. Res. (Camb.)* 5, 905–920. <https://doi.org/10.1039/c5tx00469a>.
- Wong, S.F., No, D.Y., Choi, Y.Y., Kim, D.S., Chung, B.G., Lee, S.H., 2011. Concave microwell based size-controllable hepatosphere as a three-dimensional liver tissue model. *Biomaterials* 32, 8087–8096. <https://doi.org/10.1016/j.biomaterials.2011.07.028>.
- Wrzesinski, K., Fey, S.J., 2013. After trypsinisation, 3D spheroids of C3A hepatocytes need 18 days to re-establish similar levels of key physiological functions to those seen in the liver. *Toxicol. Res. (Camb.)* 2, 123–135. <https://doi.org/10.1039/c2tx20060k>.
- Wrzesinski, K., Fey, S.J., 2015. From 2D to 3D - a new dimension for modelling the effect of natural products on human tissue. *Curr. Pharm. Des.* 21, 5605–5616. <https://doi.org/10.2174/1381612821666151002114227>.
- Wrzesinski, K., Magnone, M.C., Hansen, L.V., Kruse, M.E., Bergauer, T., Bobadilla, M., Gubler, M., Mizrahi, J., Zhang, K., Andreasen, C.M., Joensen, K.E., Andersen, S.M., Olesen, J.B., Schaffalitzky de Muckadell, O.B., Fey, S.J., 2013. HepG2/C3A 3D spheroids exhibit stable physiological functionality for at least 24 days after recovering from trypsinisation. *Toxicol. Res. (Camb.)* 2, 163. <https://doi.org/10.1039/c3tx20086h>.
- Wrzesinski, K., Rogowska-Wrzesinska, A., Kanlaya, R., Borkowski, K., Schwämme, V., Dai, J., Joensen, K.E., Wojdyła, K., Carvalho, V.B., Fey, S.J., 2014. The cultural divide: exponential growth in classical 2D and metabolic equilibrium in 3D environments. *PLoS One* 9, <https://doi.org/10.1371/journal.pone.0106973>.
- Yang, Y., Tang, X., Hao, F., Ma, Z., Wang, Y., Wang, L., Gao, Y., 2018. Bavachin induces apoptosis through mitochondrial regulated ER stress pathway in HepG2 cells. *Biol. Pharm. Bull.* 41, 198–207. <https://doi.org/10.1248/bpb.17-00672>.
- Young, C.K.J., Young, M.J., 2019. Comparison of HepaRG cells following growth in proliferative and differentiated culture conditions reveals distinct bioenergetic profiles. *Cell Cycle* 18, 476–499. <https://doi.org/10.1080/15384101.2019.1578133>.
- Žegura, B., Heath, E., Černoša, A., Filipić, M., 2009. Combination of in vitro bioassays for the determination of cytotoxic and genotoxic potential of wastewater, surface water and drinking water samples. *Chemosphere* 75, 1453–1460. <https://doi.org/10.1016/j.chemosphere.2009.02.041>.

Chapter 3

Discussion and Conclusions

In the last decade, the safety testing of chemicals and products has been at the forefront of the European legislation and the EU REACH initiative. In the field of genotoxicity, the 3R strategy has stimulated a contemporary trend against the use of *in vivo* models. The strategy supports the reduction, replacement and refinement of animal models in preclinical testing. For this reason, the development and implementation of alternative models are strongly encouraged. In this perspective, hepatocellular 3D *in vitro* cell-based models are gaining importance as they more accurately imitate *in vivo* cell behavior and provide more predictive results for *in vivo* conditions compared to traditional 2D monolayer cultures. In the doctoral dissertation, we have provided the missing data on the validation of 3D models with a comprehensive and innovative toxicological approach for testing the genotoxic activity of chemicals and environmental pollutants.

Firstly, we developed and optimized the forced floating method for the assembly of 3D spheroids from HepG2 cells (Štampar et al., 2019). The method has been proved to be simple and enables to obtain a high number of uniform spheroids in a very short period. The formed 3D cell models revealed increased liver-specific functions and proved a stronger physiological relevance relating to the gene expression of metabolic enzymes and hepatic markers compared to 2D monolayers. These properties indicate differentiation into more metabolically competent cells. Therefore, in our research, the hepatocellular 3D spheroids were used as an improved *in vitro* model for the assessment of the cytotoxic and genotoxic activity of chemicals and environmental pollutants which humans can be exposed to in their everyday life, in order to put in place appropriate safety measures aimed at avoiding unforeseen effects on human health and the environment. Despite the urgent need to establish reliable and sensitive models with higher predictability regarding the consequences of human exposure, which was highlighted in the Workshop on Genotoxicity Testing (IWGT), for routine use, the 3D models need to be thoroughly characterized and subsequently standardized to allow the comparability and reproducibility of results. In our study, we characterized the hepatocellular 3D model by monitoring its growth, morphology, and cell viability over the time of cultivation (Štampar et al., 2020a). Flow cytometry was used to analyze the changes in the cell cycle distribution (Hoechst staining) and the effect of the time of cultivation on the proliferation of cells (KI67 proliferation marker), which were isolated from the spheroids. The obtained results show that the applied hepatocellular 3D cell model has improved metabolic capacity and can better reflect *in vivo* conditions compared to traditional HepG2 2D monolayer cultures. Based on the obtained results, we confirmed our first and second hypotheses.

Secondly, the bibliometric analysis of the research field, showed a considerably increased use of hepatocellular 3D cell models for various toxicological endpoints, such as: the micronucleus test to detect chromosomal damage (Shah et al., 2018); the comet assay,

which can provide an early prediction of genotoxic insult (Dusinska and Collins 2008; Elje et al. 2019, 2020; Mandon et al. 2019; Pfuhrer et al. 2020; Štampar et al. 2019); and the detection of double-strand breaks (γ H2AX) with flow cytometry (Hercog et al., 2020), which correlate with the micronuclei test and can predict cancer development. In our study we therefore applied the above mentioned hepatocellular 3D *in vitro* model grown under static conditions to assess the toxic and genotoxic effects of indirect-acting compounds (B(a)P, AFB1, PhIP and IQ), which required metabolic activation, and direct-acting (ET) model genotoxic agents by measuring the induction of DNA damage using the comet assay. Moreover, genotoxicity was tested by the determination of double-strand breaks (γ H2AX) when exposing HepG2 spheroids to B(a)P and PhIP for short (24 h) and prolonged (72 h) periods of time. Furthermore, the HepG2 3D cell model was also applied to detect the cytotoxic and genotoxic effects of the cyanobacterial toxin cylindrospermopsin (CYN). The obtained results showed increased sensitivity of the HepG2 3D cell model for the detection of indirect-acting genotoxic compounds compared to the 2D cell model, higher metabolic activity, and properties enabling long-term exposure studies. With these findings, we can partially confirm the fourth hypothesis.

Finally, the culturing of spheroids under dynamic conditions is a very promising approach offering better similarity to *in vivo* conditions than monolayer cultures (Fey and Wrzesinski 2012; Wrzesinski and Fey 2015; Wojdyla et al. 2016). The spheroids are grown for several weeks in bioreactors, the rotation of which generates a flow of the media around the spheroids, resulting in a higher diffusion of nutrients and oxygen into the spheroids and preventing the formation of a necrotic core (Fey & Wrzesinski, 2012; Gong et al., 2015; Lin et al., 2008). In our study, the toxicity and genotoxicity of two model genotoxic compounds, B(a)P and PhIP, was studied on a dynamic system (rotating bioreactors) by exposing 21-day-old HepG2/C3A spheroids to both compounds for short and prolonged periods of time by using the ATP assay, the comet assay, planimetry, and gene expression (qPCR) analyses (Štampar et al., 2020b). The advanced 3D cell model revealed improved characteristics of hepatic cells and can therefore provide more relevant and predictive information for human risk assessment compared to 2D conditions. With the presented results, we can confirm our third and partially our fourth hypothesis.

We believe that these new findings will contribute to the development of more accurate models for genotoxicity testing giving more predictive results that will significantly contribute to the measures for the prevention and reduction of the impact of genotoxic pollutants on human health and other organisms in the environment. Importantly, the test system also, offers an alternative to animal models, which is in accordance with the 3R policy aimed at reducing *in vivo* testing.

Appendix A

Supplementary Material of Included Publications

A.1 Supplementary Material of Publication 2.1

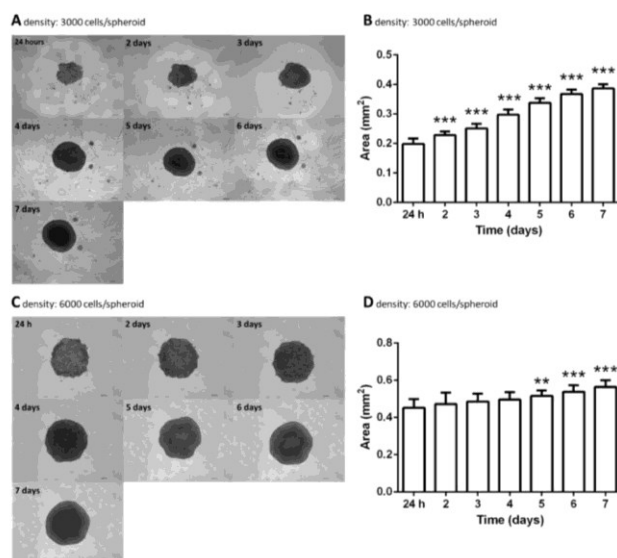


Figure S1. The growth and morphology of spheroids (planimetry) monitored during 7 days of cultivation. The surface area of spheroid size was measured every 24 h (A–B: initial density of 3000 cells/spheroid and C–D: initial density of 6000 cells/spheroid). The images were taken using an inverted microscope at 40 \times magnification (N = 3). Results are presented as the mean \pm SD (N = 10). The statistical analysis was performed in GraphPad Prism 6, by the one-way ANOVA using the Dunnett's multiple comparisons tests, ** $p < 0.01$, *** $p < 0.001$.

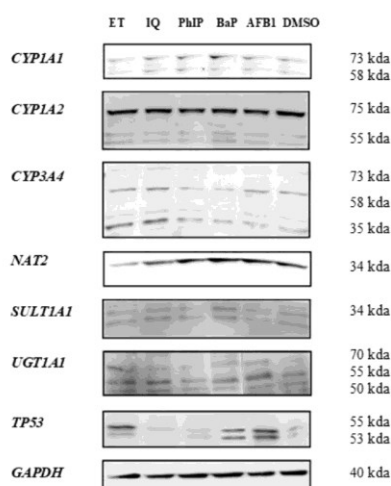
A.2 Supplementary Material of Publication 2.2

Supporting Tables and Figures

Supporting Table S1.: The planimetry of formed spheroids after 24, 48, 72 and 96 h. The planimetry of 5 spheroids per endpoint was measured by using the microscope Nikon Eclipse Ti at 40x magnification. Data represent average area \pm SD.

Cells/well (96 u- bottom well)	24 h		48 h		72 h		96 h	
	average area (mm ²)	SD (mm ²)						
500	0.022	0.003	0.019	0.006	0.028	0.009	0.044	0.006
1000	0.051	0.010	0.052	0.011	0.063	0.009	0.079	0.008
3000	0.112	0.015	0.115	0.009	0.135	0.013	0.157	0.016
6000	0.218	0.015	0.220	0.023	0.236	0.027	0.255	0.031
10000	0.278	0.027	0.284	0.011	0.296	0.004	0.316	0.036

Protein expression



Supporting Figure S1.: The expression of selected proteins (CYP1A1, CYP1A2, CYP3A4, NAT2, SULT1A1, UGT1A1, TP53 and GAPDH used as internal control) in spheroids after the exposure (24h) to B(a)P (40 μ M), AFBI (40 μ M), PhIP (200 μ M), IQ (250 μ M) and ET (10 μ g/mL), and solvent control (DMSO).

A.3 Supplementary Material of Publication 2.3

Table S1: Comparative analysis of BaP treated samples for 24h at different concentration levels, where the same letter represents no statistically different predicted probabilities (%).

Prediction	Predicted probability	Std. Err.	Groups
G1			
DMSO	0.757	0.003	
BAP01	0.734	0.002	
BAP1	0.681	0.003	E
BAP10	0.669	0.003	E
BAP20	0.633	0.003	
ET	0.428	0.002	
S			
DMSO	0.086	0.002	A
BAP01	0.102	0.001	
BAP1	0.113	0.002	B
BAP10	0.118	0.002	B
BAP20	0.250	0.002	
ET	0.094	0.001	A
G2			
DMSO	0.156	0.002	C
BAP01	0.164	0.002	C
BAP1	0.206	0.002	D
BAP10	0.214	0.003	D
BAP20	0.117	0.002	B
ET	0.478	0.002	

Table S2: Comparative analysis of BaP treated samples for 72h at different concentration levels, where the same letter represents no statistically different predicted probabilities (%).

Prediction	Predicted probability	Std. Err.	Groups
G1			
DMSO	0.630	0.001	
BAP0.001	0.666	0.002	
BAP0.01	0.640	0.002	
BAP0.1	0.607	0.002	F
BAP1	0.601	0.001	F
BAP10	0.540	0.002	E
ET	0.367	0.002	
S			
DMSO	0.141	0.001	
BAP0.001	0.153	0.001	A
BAP0.01	0.159	0.001	A
BAP0.1	0.169	0.001	
BAP1	0.178	0.001	B
BAP10	0.131	0.002	
ET	0.086	0.001	
G2			
DMSO	0.229	0.001	D
BAP0.001	0.181	0.001	B
BAP0.01	0.201	0.001	
BAP0.1	0.223	0.001	CD
BAP1	0.221	0.001	C
BAP10	0.328	0.002	
ET	0.547	0.002	E

Table S3: Comparative analysis of PhIP treated samples for 24h at different concentration levels, where the same letter represents no statistically different predicted probabilities (%).

Prediction	Predicted probability	Std. Err.	Groups
G1			
DMSO	0.715	0.001	
PhIP 50	0.705	0.002	E
PhIP 100	0.706	0.001	E
PhIP 150	0.704	0.002	E
PhIP 200	0.703	0.002	E
ET	0.372	0.002	
S			
DMSO	0.116	0.001	B
PhIP 50	0.116	0.001	B
PhIP 100	0.093	0.001	A
PhIP 150	0.123	0.001	
PhIP 200	0.099	0.001	
ET	0.092	0.001	A
G2			
DMSO	0.169	0.001	C
PhIP 50	0.179	0.001	
PhIP 100	0.201	0.001	D
PhIP 150	0.172	0.001	C
PhIP 200	0.198	0.001	D
ET	0.536	0.002	

Table S4: Comparative analysis of PhIP treated samples for 72h at different concentration levels, where the same letter represents no statistically different predicted probabilities (%).

Prediction	Predicted probability	Std. Err.	Groups
G1			
DMSO	0.725	0.002	
PhIP 25	0.706	0.002	
PhIP 50	0.687	0.002	
PhIP 100	0.670	0.002	G
PhIP 150	0.663	0.001	G
PhIP 200	0.664	0.002	G
ET	0.209	0.001	
S			
DMSO	0.128	0.001	A
PhIP 25	0.125	0.001	A
PhIP 50	0.143	0.001	B
PhIP 100	0.153	0.001	CD
PhIP 150	0.166	0.001	E
PhIP 200	0.156	0.001	D
ET	0.095	0.001	
G2			
DMSO	0.147	0.001	BC
PhIP 25	0.169	0.001	E
PhIP 50	0.170	0.001	E
PhIP 100	0.177	0.001	F
PhIP 150	0.171	0.001	E
PhIP 200	0.180	0.001	F
ET	0.696	0.002	

References

- Antoni, D., Burckel, H., Josset, E., & Noel, G. (2015). Three-dimensional cell culture: A breakthrough in vivo. *International Journal of Molecular Sciences*, *16*(3), 5517–5527. <https://doi.org/10.3390/ijms16035517>
- Asthana, A., & Kisaalita, W. S. (2012). Microtissue size and hypoxia in HTS with 3D cultures. In *Drug Discovery Today* (Vol. 17, Issues 15–16, pp. 810–817). Elsevier Ltd. <https://doi.org/10.1016/j.drudis.2012.03.004>
- Aucamp, J., Calitz, C., Bronkhorst, A. J., Wrzesinski, K., Hamman, S., Gouws, C., & Pretorius, P. J. (2017). Cell-free DNA in a three-dimensional spheroid cell culture model: A preliminary study. *International Journal of Biochemistry and Cell Biology*, *89*(June), 182–192. <https://doi.org/10.1016/j.biocel.2017.06.014>
- Augustyniak, J., Bertero, A., Coccini, T., Baderna, D., Buzanska, L., & Caloni, F. (2019). Organoids are promising tools for species-specific in vitro toxicological studies. In *Journal of Applied Toxicology* (Vol. 39, Issue 12, pp. 1610–1622). John Wiley and Sons Ltd. <https://doi.org/10.1002/jat.3815>
- Bahinski, N., Daneshian, A., De Wever, M., Fritsche, B., Goldberg, E., Hansmann, A., Hartung, J., Haycock, T., Hogberg, J., Hoelting, H., Kelm, L., Kadereit, J., Mcvey, S., Landsiedel, E., Leist, R., Lübberstedt, M., Noor, M., Pellevoisin, F., Petersohn, C., ... Zurich, K. (2014). *State-of-the-art of 3D cultures (organs-on-a-chip) in safety testing and pathophysiology*. 441–477. <https://doi.org/10.14573/altex.1406111>
- Basu, A., Dydowiczová, A., Trosko, J. E., Bláha, L., & Babica, P. (2020). Ready to go 3D? A semi-automated protocol for microwell spheroid arrays to increase scalability and throughput of 3D cell culture testing. *Toxicology Mechanisms and Methods*, *0*(0), 1–43. <https://doi.org/10.1080/15376516.2020.1800881>
- Bazou, D., Coakley, W. T., Hayes, A. J., & Jackson, S. K. (2008). Long-term viability and proliferation of alginate-encapsulated 3-D HepG2 aggregates formed in an ultrasound trap. *Toxicology in Vitro*, *22*(5), 1321–1331. <https://doi.org/10.1016/j.tiv.2008.03.014>
- Bell, C. C., Hendriks, D. F. G., Moro, S. M. L., Ellis, E., Walsh, J., Renblom, A., Fredriksson Puigvert, L., Dankers, A. C. A., Jacobs, F., Snoeys, J., Sison-Young, R. L., Jenkins, R. E., Nordling, Å., Mkrtchian, S., Park, B. K., Kitteringham, N. R., Goldring, C. E. P., Lauschke, V. M., & Ingelman-Sundberg, M. (2016). Characterization of primary human hepatocyte spheroids as a model system for drug-induced liver injury, liver function and disease. *Scientific Reports*, *6*.

<https://doi.org/10.1038/srep25187>

- Breslin, S., & O'Driscoll, L. (2013). Three-dimensional cell culture: The missing link in drug discovery. *Drug Discovery Today*, 18(5–6), 240–249. <https://doi.org/10.1016/j.drudis.2012.10.003>
- Cai, S., Shen, Y., Zou, Y., Sun, P., Wei, W., Zhao, J., & Zhang, C. (2018). Engineering highly sensitive whole-cell mercury biosensors based on positive feedback loops from quorum-sensing systems. *Analyst*, 143(3), 630–634. <https://doi.org/10.1039/c7an00587c>
- Castell, J. V., Jover, R., Martínez-Jiménez, C. P., & Gómez-Lechón, M. J. (2006). Hepatocyte cell lines: Their use, scope and limitations in drug metabolism studies. In *Expert Opinion on Drug Metabolism and Toxicology* (Vol. 2, Issue 2, pp. 183–212). Expert Opin Drug Metab Toxicol. <https://doi.org/10.1517/17425255.2.2.183>
- Chang, T. T., & Hughes-Fulford, M. (2009). Monolayer and spheroid culture of human liver hepatocellular carcinoma cell line cells demonstrate distinct global gene expression patterns and functional phenotypes. *Tissue Engineering - Part A*, 15(3), 559–567. <https://doi.org/10.1089/ten.tea.2007.0434>
- Claxton, L. D., de A. Umbuzeiro, G., & DeMarini, D. M. (2010). The *Salmonella* Mutagenicity Assay: The Stethoscope of Genetic Toxicology for the 21st Century. *Environmental Health Perspectives*, 118(11), 1515–1522. <https://doi.org/10.1289/ehp.1002336>
- Corvi, R., & Madia, F. (2017). In vitro genotoxicity testing—Can the performance be enhanced? *Food and Chemical Toxicology*, 106, 600–608. <https://doi.org/10.1016/j.fct.2016.08.024>
- Corvi, R., Madia, F., Worth, A., & Whelan, M. (2013). *EURL ECVAM Strategy to Avoid and Reduce Animal Use in Genotoxicity Testing* (European Commission (ed.)). <https://doi.org/10.2788/43865>
- Dominko, M., & Verbič, M. (2019). The Economics of Subjective Well-Being: A Bibliometric Analysis. *Journal of Happiness Studies*, 20(6), 1973–1994. <https://doi.org/10.1007/s10902-018-0022-z>
- Donato, M. T., Tolosa, L., & Gómez-Lechón, M. J. (2015). Culture and functional characterization of human hepatoma HepG2 cells. In *Protocols in In Vitro Hepatocyte Research* (pp. 77–93). Springer New York. https://doi.org/10.1007/978-1-4939-2074-7_5
- Drewitz, M., Helbling, M., Fried, N., Bieri, M., Moritz, W., Lichtenberg, J., & Kelm, J. M. (2011). Towards automated production and drug sensitivity testing using scaffold-free spherical tumor microtissues. *Biotechnology Journal*, 6(12), 1488–1496. <https://doi.org/10.1002/biot.201100290>
- Duret, C., Gerbal-Chaloin, S., Ramos, J., Fabre, J.-M., Jacquet, E., Navarro, F., Blanc,

- P., Sa-Cunha, A., Maurel, P., & Daujat-Chavanieu, M. (2007). Isolation, Characterization, and Differentiation to Hepatocyte-Like Cells of Nonparenchymal Epithelial Cells from Adult Human Liver. *Stem Cells*, *25*(7), 1779–1790. <https://doi.org/10.1634/stemcells.2006-0664>
- Dusinska, M., & Collins, A. R. (2008). The comet assay in human biomonitoring: gene-environment interactions. *Mutagenesis*, *23*(3), 191–205. <https://doi.org/10.1093/mutage/gen007>
- Dvorak, Z. (2016). Opportunities and challenges in using human hepatocytes in cytochromes P450 induction assays. *Expert Opinion on Drug Metabolism and Toxicology*, *12*(2), 169–174. <https://doi.org/10.1517/17425255.2016.1125881>
- Edmondson, R., Broglie, J. J., Adcock, A. F., & Yang, L. (2014). Three-dimensional cell culture systems and their applications in drug discovery and cell-based biosensors. In *Assay and Drug Development Technologies* (Vol. 12, Issue 4, pp. 207–218). Mary Ann Liebert Inc. <https://doi.org/10.1089/adt.2014.573>
- Elje, E., Hesler, M., Rundén-Pran, E., Mann, P., Mariussen, E., Wagner, S., Dusinska, M., & Kohl, Y. (2019). The comet assay applied to HepG2 liver spheroids. *Mutation Research - Genetic Toxicology and Environmental Mutagenesis*, *845*(November 2018), 403033. <https://doi.org/10.1016/j.mrgentox.2019.03.006>
- Elje, E., Mariussen, E., Moriones, O. H., Bastús, N. G., Puentes, V., Kohl, Y., Dusinska, M., & Rundén-Pran, E. (2020). Hepato(Geno)toxicity assessment of nanoparticles in a hepg2 liver spheroid model. *Nanomaterials*, *10*(3). <https://doi.org/10.3390/nano10030545>
- Fey, S. J., & Wrzesinski, K. (2012). Determination of drug toxicity using 3D spheroids constructed from an immortal human hepatocyte cell line. *Toxicological Sciences*, *127*(2), 403–411. <https://doi.org/10.1093/toxsci/kfs122>
- Fowler, P., Smith, R., Smith, K., Young, J., Jeffrey, L., Kirkland, D., Pfuhler, S., & Carmichael, P. (2012). Reduction of misleading (“ false”) positive results in mammalian cell genotoxicity assays. II. Importance of accurate toxicity measurement. *Mutation Research - Genetic Toxicology and Environmental Mutagenesis*, *747*(1), 104–117. <https://doi.org/10.1016/j.mrgentox.2012.04.013>
- Gaskell, H., Sharma, P., Colley, H. E., Murdoch, C., Williams, D. P., & Webb, S. D. (2016). Characterization of a functional C3A liver spheroid model. *Toxicology Research*, *5*(4), 1053–1065. <https://doi.org/10.1039/C6TX00101G>
- Gerets, H. H. J., Tilmant, K., Gerin, B., Chanteux, H., Depelchin, B. O., Dhalluin, S., & Atienzar, F. A. (2012). Characterization of primary human hepatocytes, HepG2 cells, and HepaRG cells at the mRNA level and CYP activity in response to inducers and their predictivity for the detection of human hepatotoxins. *Cell Biology and Toxicology*, *28*(2), 69–87. <https://doi.org/10.1007/s10565-011-9208-4>
- Godoy, P., Hewitt, N. J., Albrecht, U., Andersen, M. E., Ansari, N., Bhattacharya, S.,

- Bode, J. G., Bolleyn, J., Borner, C., Böttger, J., Braeuning, A., Budinsky, R. A., Burkhardt, B., Cameron, N. R., Camussi, G., Cho, C. S., Choi, Y. J., Craig Rowlands, J., Dahmen, U., ... Hengstler, J. G. (2013). Recent advances in 2D and 3D in vitro systems using primary hepatocytes, alternative hepatocyte sources and non-parenchymal liver cells and their use in investigating mechanisms of hepatotoxicity, cell signaling and ADME. In *Archives of Toxicology* (Vol. 87, Issue 8, pp. 1315–1530). <https://doi.org/10.1007/s00204-013-1078-5>
- Gong, X., Lin, C., Cheng, J., Su, J., Zhao, H., Liu, T., Wen, X., & Zhao, P. (2015). Generation of Multicellular Tumor Spheroids with Microwell-Based Agarose Scaffolds for Drug Testing. *PLOS ONE*, *10*(6), e0130348. <https://doi.org/10.1371/journal.pone.0130348>
- Goodwin, T. J., Prewett, T. L., Wolf, D. A., & Spaulding, G. F. (1993). Reduced shear stress: A major component in the ability of mammalian tissues to form three-dimensional assemblies in simulated microgravity. *Journal of Cellular Biochemistry*, *51*(3), 301–311. <https://doi.org/10.1002/jcb.240510309>
- Guillouzo, A., Corlu, A., Aninat, C., Glaise, D., Morel, F., & Guguen-Guillouzo, C. (2007). The human hepatoma HepaRG cells: A highly differentiated model for studies of liver metabolism and toxicity of xenobiotics. *Chemico-Biological Interactions*, *168*(1), 66–73. <https://doi.org/10.1016/j.cbi.2006.12.003>
- Guo, X., Seo, J., Li, X., & Mei, N. (2019). Genetic toxicity assessment using liver cell models: past, present, and future. *Journal of Toxicology and Environmental Health, Part B*, *00*(00), 1–24. <https://doi.org/10.1080/10937404.2019.1692744>
- Gupta, N., Renugopalakrishnan, V., Liepmann, D., Paulmurugan, R., & Malhotra, B. D. (2019). Cell-based biosensors: Recent trends, challenges and future perspectives. In *Biosensors and Bioelectronics* (Vol. 141, p. 111435). Elsevier Ltd. <https://doi.org/10.1016/j.bios.2019.111435>
- Harris, A. J., Dial, S. L., & Casciano, D. A. (2004). Comparison of basal gene expression profiles and effects of hepatocarcinogens on gene expression in cultured primary human hepatocytes and HepG2 cells. *Mutation Research/Fundamental and Molecular Mechanisms of Mutagenesis*, *549*(1–2), 79–99. <https://doi.org/10.1016/j.mrfmmm.2003.11.014>
- Harrison, R. G., Greenman, M. J., Mall, F. P., & Jackson, C. M. (1907). Observations of the living developing nerve fiber. *The Anatomical Record*, *1*(5), 116–128. <https://doi.org/10.1002/ar.1090010503>
- Hercog, K., Štampar, M., Štern, A., Filipič, M., & Žegura, B. (2020). Application of advanced HepG2 3D cell model for studying genotoxic activity of cyanobacterial toxin cylindrospermopsin. *Environmental Pollution*, *265*, 114965. <https://doi.org/10.1016/j.envpol.2020.114965>
- Hinson, J. A., Roberts, D. W., & James, L. P. (2010). Mechanisms of acetaminophen-

- induced liver necrosis. In *Handbook of Experimental Pharmacology* (Vol. 196, Issue 196, pp. 369–405). Handb Exp Pharmacol. https://doi.org/10.1007/978-3-642-00663-0_12
- Hoffman, R. M. (1993). To do tissue culture in two or three dimensions? that is the question. *Stem Cells*, *11*(2), 105–111. <https://doi.org/10.1002/stem.5530110205>
- Hurrell, T., Lilley, K. S., & Cromarty, A. D. (2019). Proteomic responses of HepG2 cell monolayers and 3D spheroids to selected hepatotoxins. *Toxicology Letters*, *300*, 40–50. <https://doi.org/10.1016/j.toxlet.2018.10.030>
- Ishikawa, T., Kajimoto, Y., Sun, W., Nakagawa, H., Inoue, Y., Ikegami, Y., Miyatake, S. I., & Kuroiwa, T. (2013). Role of Nrf2 in cancer photodynamic therapy: Regulation of human ABC transporter ABCG2. In *Journal of Pharmaceutical Sciences* (Vol. 102, Issue 9, pp. 3058–3069). John Wiley and Sons Inc. <https://doi.org/10.1002/jps.23563>
- Ivascu, A., & Kubbies, M. (2006). Rapid generation of single-tumor spheroids for high-throughput cell function and toxicity analysis. *Journal of Biomolecular Screening*, *11*(8), 922–932. <https://doi.org/10.1177/1087057106292763>
- Jacobs, M. N., Colacci, A., Corvi, R., Vaccari, M., Aguila, M. C., Corvaro, M., Delrue, N., Desaulniers, D., Ertych, N., Jacobs, A., Luijten, M., Madia, F., Nishikawa, A., Ogawa, K., Ohmori, K., Paparella, M., Sharma, A. K., & Vasseur, P. (2020). Chemical carcinogen safety testing: OECD expert group international consensus on the development of an integrated approach for the testing and assessment of chemical non-genotoxic carcinogens. *Archives of Toxicology*, *94*(8), 2899–2923. <https://doi.org/10.1007/s00204-020-02784-5>
- Jennen, D. G. J., Magkoufopoulou, C., Ketelslegers, H. B., van Herwijnen, M. H. M., Kleinjans, J. C. S., & van Delft, J. H. M. (2010). Comparison of HepG2 and HepaRG by whole-genome gene expression analysis for the purpose of chemical hazard identification. *Toxicological Sciences*, *115*(1), 66–79. <https://doi.org/10.1093/toxsci/kfq026>
- Jong, B. K. (2005). Three-dimensional tissue culture models in cancer biology. In *Seminars in Cancer Biology* (Vol. 15, Issue 5 SPEC. ISS., pp. 365–377). Academic Press. <https://doi.org/10.1016/j.semcancer.2005.05.002>
- Kammerer, S., & Küpper, J.-H. (2018). Human hepatocyte systems for in vitro toxicology analysis. *Journal of Cellular Biotechnology*, *3*(2), 85–93. <https://doi.org/10.3233/jcb-179012>
- Kelm, J. M., Timmins, N. E., Brown, C. J., Fussenegger, M., & Nielsen, L. K. (2003). Method for generation of homogeneous multicellular tumor spheroids applicable to a wide variety of cell types. *Biotechnology and Bioengineering*, *83*(2), 173–180. <https://doi.org/10.1002/bit.10655>
- Kim, J. Bin. (2005). Three-dimensional tissue culture models in cancer biology. *Seminars in Cancer Biology*, *15*(5), 365–377. <https://doi.org/10.1016/j.semcancer.2005.05.002>

- Kirkland, D., Aardema, M., Henderson, L., & Müller, L. (2005). Evaluation of the ability of a battery of three in vitro genotoxicity tests to discriminate rodent carcinogens and non-carcinogens: I. Sensitivity, specificity and relative predictivity. *Mutation Research - Genetic Toxicology and Environmental Mutagenesis*, *584*(1–2), 1–256. <https://doi.org/10.1016/j.mrgentox.2005.02.004>
- Kirkland, D., Aardema, M., Müller, L., & Hayashi, M. (2006). Evaluation of the ability of a battery of three in vitro genotoxicity tests to discriminate rodent carcinogens and non-carcinogens. *Mutation Research/Genetic Toxicology and Environmental Mutagenesis*, *608*(1), 29–42. <https://doi.org/10.1016/j.mrgentox.2006.04.017>
- Kirkland, D., Pfuhrer, S., Tweats, D., Aardema, M., Corvi, R., Darroudi, F., Elhajouji, A., Glatt, H., Hastwell, P., Hayashi, M., Kasper, P., Kirchner, S., Lynch, A., Marzin, D., Maurici, D., Meunier, J.-R., Müller, L., Nohynek, G., Parry, J., ... White, P. (2007). How to reduce false positive results when undertaking in vitro genotoxicity testing and thus avoid unnecessary follow-up animal tests: Report of an ECVAM Workshop. *Mutation Research/Genetic Toxicology and Environmental Mutagenesis*, *628*(1), 31–55. <https://doi.org/10.1016/J.MRGENTOX.2006.11.008>
- Kirkland, D., & Speit, G. (2008). Evaluation of the ability of a battery of three in vitro genotoxicity tests to discriminate rodent carcinogens and non-carcinogens. III. Appropriate follow-up testing in vivo. *Mutation Research - Genetic Toxicology and Environmental Mutagenesis*, *654*(2), 114–132. <https://doi.org/10.1016/j.mrgentox.2008.05.002>
- Kyffin, J. A., Sharma, P., Leedale, J., Colley, H. E., Murdoch, C., Mistry, P., & Webb, S. D. (2018). Impact of cell types and culture methods on the functionality of in vitro liver systems – A review of cell systems for hepatotoxicity assessment. In *Toxicology in Vitro* (Vol. 48, pp. 262–275). Elsevier Ltd. <https://doi.org/10.1016/j.tiv.2018.01.023>
- LeCluyse, E. L. (2001). Human hepatocyte culture systems for the in vitro evaluation of cytochrome P450 expression and regulation. In *European Journal of Pharmaceutical Sciences* (Vol. 13, Issue 4, pp. 343–368). [https://doi.org/10.1016/S0928-0987\(01\)00135-X](https://doi.org/10.1016/S0928-0987(01)00135-X)
- Lee, Y. R., & Park, S. Y. (2015). P53 expression in hepatocellular carcinoma: influence on the radiotherapeutic response of the hepatocellular carcinoma. In *Clinical and molecular hepatology* (Vol. 21, Issue 3, pp. 230–231). Korean Association for the Study of the Liver. <https://doi.org/10.3350/cmh.2015.21.3.230>
- Lin, R.-Z., Lin, R.-Z., & Chang, H.-Y. (2008). Recent advances in three-dimensional multicellular spheroid culture for biomedical research. *Biotechnology Journal*, *3*(9–10), 1172–1184. <https://doi.org/10.1002/biot.200700228>
- Loessner, D., Stok, K. S., Lutolf, M. P., Hutmacher, D. W., Clements, J. A., & Rizzi, S. C. (2010). Bioengineered 3D platform to explore cell–ECM interactions and drug resistance of epithelial ovarian cancer cells. *Biomaterials*, *31*(32), 8494–8506.

<https://doi.org/10.1016/j.biomaterials.2010.07.064>

- Lübberstedt, M., Müller-Vieira, U., Mayer, M., Biemel, K. M., Knöspel, F., Knobloch, D., Nüssler, A. K., Gerlach, J. C., & Zeilinger, K. (2011). HepaRG human hepatic cell line utility as a surrogate for primary human hepatocytes in drug metabolism assessment in vitro. *Journal of Pharmacological and Toxicological Methods*, *63*(1), 59–68. <https://doi.org/10.1016/j.vascn.2010.04.013>
- Mackowiak, B., & Wang, H. (2016). Mechanisms of xenobiotic receptor activation: Direct vs. indirect. *Biochimica et Biophysica Acta - Gene Regulatory Mechanisms*, *1859*(9), 1130–1140. <https://doi.org/10.1016/j.bbagr.2016.02.006>
- Mandon, M., Huet, S., Dubreil, E., Fessard, V., & Le Hégarat, L. (2019). Three-dimensional HepaRG spheroids as a liver model to study human genotoxicity in vitro with the single cell gel electrophoresis assay. *Scientific Reports*, *9*(1). <https://doi.org/10.1038/s41598-019-47114-7>
- Mehta, G., Hsiao, A. Y., Ingram, M., Luker, G. D., & Takayama, S. (2012). Opportunities and challenges for use of tumor spheroids as models to test drug delivery and efficacy. *Journal of Controlled Release*, *164*(2), 192–204. <https://doi.org/10.1016/j.jconrel.2012.04.045>
- Nakamura, K., Kato, N., Aizawa, K., Mizutani, R., Yamauchi, J., & Tanoue, A. (2011). Expression of albumin and cytochrome P450 enzymes in hepG2 cells cultured with a nanotechnology-based culture plate with microfabricated scaffold. *Journal of Toxicological Sciences*, *36*(5), 625–633. <https://doi.org/10.2131/jts.36.625>
- Nelson, L. J., Morgan, K., Treskes, P., Samuel, K., Henderson, C. J., LeBled, C., Homer, N., Grant, M. H., Hayes, P. C., & Plevris, J. N. (2017). Human Hepatic HepaRG Cells Maintain an Organotypic Phenotype with High Intrinsic CYP450 Activity/Metabolism and Significantly Outperform Standard HepG2/C3A Cells for Pharmaceutical and Therapeutic Applications. *Basic and Clinical Pharmacology and Toxicology*, *120*(1), 30–37. <https://doi.org/10.1111/bcpt.12631>
- Otto, M., Hansen, S. H., Dalgaard, L., Dubois, J., & Badolo, L. (2008). Development of an in vitro assay for the investigation of metabolism-induced drug hepatotoxicity. *Cell Biology and Toxicology*, *24*(1), 87–99. <https://doi.org/10.1007/s10565-007-9018-x>
- Pan, Y., Hu, N., Wei, X., Gong, L., Zhang, B., Wan, H., & Wang, P. (2019). 3D cell-based biosensor for cell viability and drug assessment by 3D electric cell/matrigel-substrate impedance sensing. *Biosensors and Bioelectronics*, *130*(September), 344–351. <https://doi.org/10.1016/j.bios.2018.09.046>
- Park, Y. C., Lee, S., & Cho, M. H. (2014). The simplest flowchart stating the mechanisms for organic xenobiotics-induced toxicity: Can it possibly be accepted as a “central dogma” for toxic mechanisms? *Toxicological Research*, *30*(3), 179–184. <https://doi.org/10.5487/TR.2014.30.3.179>
- Patel, D. K., & Jyoti Sen, D. (2013). Xenobiotics: An Essential Precursor for Living

- System. *American Journal of Advanced Drug Delivery*, 262–270.
- Patterson, A. D., Gonzalez, F. J., & Idle, J. R. (2010). Xenobiotic metabolism: A view through the metabolometer. In *Chemical Research in Toxicology* (Vol. 23, Issue 5, pp. 851–860). <https://doi.org/10.1021/tx100020p>
- Pfuhler, S., Kirkland, D., Kasper, P., Hayashi, M., Vanparys, P., Carmichael, P., Dertinger, S., Eastmond, D., Elhajouji, A., Krul, C., Rothfuss, A., Schoening, G., Smith, A., Speit, G., Thomas, C., van Benthem, J., & Corvi, R. (2009). Reduction of use of animals in regulatory genotoxicity testing: Identification and implementation opportunities-Report from an ECVAM workshop. *Mutation Research - Genetic Toxicology and Environmental Mutagenesis*, 680(1–2), 31–42. <https://doi.org/10.1016/j.mrgentox.2009.09.002>
- Pfuhler, S., van Benthem, J., Curren, R., Doak, S. H., Dusinska, M., Hayashi, M., Heflich, R. H., Kidd, D., Kirkland, D., Luan, Y., Ouedraogo, G., Reisinger, K., Sofuni, T., van Acker, F., Yang, Y., & Corvi, R. (2020). Use of in vitro 3D tissue models in genotoxicity testing: Strategic fit, validation status and way forward. Report of the working group from the 7th International Workshop on Genotoxicity Testing (IWGT). In *Mutation Research - Genetic Toxicology and Environmental Mutagenesis* (Vols. 850–851). Elsevier B.V. <https://doi.org/10.1016/j.mrgentox.2020.503135>
- Ravi, M., Paramesh, V., Kaviya, S. R., Anuradha, E., & Paul Solomon, F. D. (2015). 3D cell culture systems: Advantages and applications. *Journal of Cellular Physiology*, 230(1), 16–26. <https://doi.org/10.1002/jcp.24683>
- Reprocell USA. (2020). *The effect of changing the growth environment*. <https://www.reprocell.com/downloads/1537371086fig-2-2D-culture.png>
- Saleh, F. A., & Genever, P. G. (2011). Turning round: multipotent stromal cells, a three-dimensional revolution? *Cytotherapy*, 13(8), 903–912. <https://doi.org/10.3109/14653249.2011.586998>
- Shah, U. K., Mallia, J. de O., Singh, N., Chapman, K. E., Doak, S. H., & Jenkins, G. J. S. (2018). A three-dimensional in vitro HepG2 cells liver spheroid model for genotoxicity studies. *Mutation Research/Genetic Toxicology and Environmental Mutagenesis*, 825, 51–58. <https://doi.org/10.1016/J.MRGENTOX.2017.12.005>
- Smith, S. J., Wilson, M., Ward, J. H., Rahman, C. V., Peet, A. C., Macarthur, D. C., Rose, F. R. A. J., Grundy, R. G., & Rahman, R. (2012). Recapitulation of Tumor Heterogeneity and Molecular Signatures in a 3D Brain Cancer Model with Decreased Sensitivity to Histone Deacetylase Inhibition. *PLoS ONE*, 7(12), e52335. <https://doi.org/10.1371/journal.pone.0052335>
- Soldatow, V. Y., Lecluyse, E. L., Griffith, L. G., & Rusyn, I. (2013). In vitro models for liver toxicity testing. In *Toxicology Research* (Vol. 2, Issue 1, pp. 23–39). Royal Society of Chemistry. <https://doi.org/10.1039/c2tx20051a>
- Štampar, M., Tomc, J., Filipič, M., & Žegura, B. (2019). Development of in vitro 3D cell

- model from hepatocellular carcinoma (HepG2) cell line and its application for genotoxicity testing. *Archives of Toxicology*, *93*(11), 3321–3333. <https://doi.org/10.1007/s00204-019-02576-6>
- Štampar, M., Breznik, B., Filipič, M., & Žegura, B. (2020a). Characterization of In Vitro 3D Cell Model Developed from Human Hepatocellular Carcinoma (HepG2) Cell Line. *Cells*, *9*(12), 2557. <https://doi.org/10.3390/cells9122557>
- Štampar, M., Frandsen, H. S., Rogowska-Wrzesinska, A., Wrzesinski, K., Filipič, M., & Žegura, B. (2020b). Hepatocellular carcinoma (HepG2/C3A) cell-based 3D model for genotoxicity testing of chemicals. *Science of The Total Environment*, *755*(2021), 143255. <https://doi.org/10.1016/j.scitotenv.2020.143255>
- Stenger, D. A., Gross, G. W., Keefer, E. W., Shaffer, K. M., Andreadis, J. D., Ma, W., & Pancrazio, J. J. (2001). Detection of physiologically active compounds using cell-based biosensors. *Trends in Biotechnology*, *19*(8), 304–309. [https://doi.org/10.1016/S0167-7799\(01\)01690-0](https://doi.org/10.1016/S0167-7799(01)01690-0)
- Tibbitt, M. W., & Anseth, K. S. (2009). Hydrogels as extracellular matrix mimics for 3D cell culture. In *Biotechnology and Bioengineering* (Vol. 103, Issue 4, pp. 655–663). NIH Public Access. <https://doi.org/10.1002/bit.22361>
- van Eck, N. J., & Waltman, L. (2010). Software survey: VOSviewer, a computer program for bibliometric mapping. *Scientometrics*, *84*(2), 523–538. <https://doi.org/10.1007/s11192-009-0146-3>
- Waldherr, M., Lundt, N., Klaas, M., Betzold, S., Wurdack, M., Baumann, V., Estrecho, E., Nalitov, A., Cherotchenko, E., Cai, H., Ostrovskaya, E. A., Kavokin, A. V., Tongay, S., Klemmt, S., Höfling, S., & Schneider, C. (2018). Observation of bosonic condensation in a hybrid monolayer MoSe₂-GaAs microcavity. *Nature Communications*, *9*(1). <https://doi.org/10.1038/s41467-018-05532-7>
- Watson, C., Ge, J., Cohen, J., Pyrgiotakis, G., Engelward, B. P., & Demokritou, P. (2014). High-throughput screening platform for engineered nanoparticle-mediated genotoxicity using comet chip technology. *ACS Nano*, *8*(3), 2118–2133. <https://doi.org/10.1021/nm404871p>
- Wilkening, S., Stahl, F., & Bader, A. (2003). Comparison of primary human hepatocytes and hepatoma cell line HepG2 with regard to their biotransformation properties. *Drug Metabolism and Disposition*, *31*(8), 1035–1042. <https://doi.org/10.1124/dmd.31.8.1035>
- Wrzesinski, K., & Fey, S. J. (2013). After trypsinisation, 3D spheroids of C3A hepatocytes need 18 days to re-establish similar levels of key physiological functions to those seen in the liver. *Toxicology Research*, *2*(2), 123–135. <https://doi.org/10.1039/c2tx20060k>
- Wrzesinski, K., & Fey, S. J. (2015). From 2D to 3D - a new dimension for modelling the effect of natural products on human tissue. *Current Pharmaceutical Design*, *21*, 5605–5616. <https://doi.org/10.2174/1381612821666151002114227>

- Wrzesinski, K., Rogowska-Wrzesinska, A., Kanlaya, R., Borkowski, K., Schwämmle, V., Dai, J., Joensen, K. E., Wojdyla, K., Carvalho, V. B., & Fey, S. J. (2014). The cultural divide: Exponential growth in classical 2D and metabolic equilibrium in 3D environments. *PLoS ONE*, *9*(9). <https://doi.org/10.1371/journal.pone.0106973>
- Zou, L., Wu, C., Wang, Q., Zhou, J., Su, K., Li, H., Hu, N., & Wang, P. (2016). An improved sensitive assay for the detection of PSP toxins with neuroblastoma cell-based impedance biosensor. *Biosensors and Bioelectronics*, *67*, 458–464. <https://doi.org/10.1016/j.bios.2014.09.005>

Bibliography

Publications Related to the Thesis

- Hercog, K., Štampar, M., Štern, A., Filipič, M., & Žegura, B. (2020). Application of advanced HepG2 3D cell model for studying genotoxic activity of cyanobacterial toxin cylindrospermopsin. *Environmental Pollution*, 114965. <https://doi.org/10.1016/j.envpol.2020.114965>
- Štampar, M., Breznik, B., Filipič, M., Žegura, B. (2020). Characterization of In vitro 3D cell model developed from human hepatocellular carcinoma (HepG2) cell line. *Cells*, 9(10), 1-19. <https://doi.org/10.3390/cells9122557>
- Štampar, M., Frandsen, H. S., Rogowska-Wrzesinska, A., Wrzesinski, K., Filipič, M., & Žegura, B. (2020). Hepatocellular carcinoma (HepG2/C3A) cell-based 3D model for genotoxicity testing of chemicals. *Science of The Total Environment*, 755(2021), 143255. <https://doi.org/10.1016/j.scitotenv.2020.143255>
- Štampar, M., Tomc, J., Filipič, M., & Žegura, B. (2019). Development of in vitro 3D cell model from hepatocellular carcinoma (HepG2) cell line and its application for genotoxicity testing. *Archives of Toxicology*, 93(11), 3321-3333. <https://doi.org/10.1007/s00204-019-02576-6>
- Frandsen, H. S., Štampar, M., Vej-Nielsen, J. M., Žegura, B., Rogowska-Wrzesinska, A. (2020). Methods for spheroid disassemble into core and rim for downstream applications such as flow cytometry, comet assay, transcriptomics, proteomics and lipidomics. Accepted in Springer Protocols. DOI: 10.1007/978-1-0716-1246-0

Other Publications

- Loboda, K. B., Valjavec, K., Štampar, M., Wolber, G., Žegura, B., Filipič, M., ... & Perdih, A. (2020). Design and synthesis of 3, 5-substituted 1, 2, 4-oxadiazoles as catalytic inhibitors of human DNA topoisomerase II α . *Bioorganic Chemistry*, 103828. <https://doi.org/10.1016/j.bioorg.2020.103828>
- Loboda, K. B., Janežič, M., Štampar, M., Žegura, B., Filipič, M., & Perdih, A. (2020). Substituted 4, 5'-Bithiazoles as Catalytic Inhibitors of Human DNA Topoisomerase II α . *Journal of chemical information and modeling*, 60(7), 3662. <https://doi.org/10.1021/acs.jcim.0c00202>
- Bergant, K., Janežič, M., Valjavec, K., Sosič, I., Pajk, S., Štampar, M., ... & Perdih, A. (2019). Structure-guided optimization of 4, 6-substituted-1, 3, 5-triazin-2 (1H)-ones as catalytic inhibitors of human DNA topoisomerase II α . *European Journal of Medicinal Chemistry*, 175, 330-348. <https://doi.org/10.1016/j.ejmech.2019.04.055>
- Díez-Quijada, L., Hercog, K., Štampar, M., Filipič, M., Cameán, A. M., Jos, Á., & Žegura, B. (2020). Genotoxic Effects of Cylindrospermopsin, Microcystin-LR and Their Binary Mixture in Human Hepatocellular Carcinoma (HepG2) Cell Line. *Toxins*, 12(12), 778. <https://doi.org/10.3390/toxins1212077>

Biography

The author of this thesis, Martina Štampar, was born on 7th April 1991 in Murska Sobota. She finished Primary school Ivana Cankarja Ljutomer and High school Franca Miklošiča Ljutomer. In 2010, she enrolled at the Biotechnical Faculty of the University of Ljubljana to acquire a bachelor's degree in Microbiology. She graduated in 2013. In 2014, she enrolled in the master's study program Biotechnology at the Biotechnical Faculty, University of Ljubljana. She defended her master's thesis, entitled Development of a method for determining competition during swarming of *Bacillus subtilis* strains in September 2016. The master's thesis was written under the supervision of Prof. Dr. Ines Mandić-Mulec and Assist. Prof. Dr. Barbara Kraigher.

In October 2016, she enrolled in the PhD program Ecotechnologies at the Jožef Stefan International Postgraduate School and started her PhD research as a young researcher at the Department of Genetic Toxicology and Cancer Biology at the National Institute of Biology under the supervision of Assist. Prof. Dr. Bojana Žegura. She spent part of her PhD training abroad, at the University of Southern Denmark at the Department of Biochemistry and Molecular Biology. There, she worked under the mentorship of Prof. Dr. Adelina Rogowska-Wrzesinska, and this collaboration resulted in joint publications.

She presented her work at international conferences and meetings, such as the Conference on Translational Oncology, CellFit Workshops and annual meetings. As a PhD candidate, she attended several workshops, such as the Workshop on 3D cell culture models: lung, intestine and skin tissues (Adolphe Merkle Institute, Fribourg, Switzerland), 2nd CellFit Training School "Add a new dimension to cell culture", A practical full immersion course on the 3D matrix (Ponte di Legno, Italy) and The extracellular vesicles paradigm of intra and intercellular communication (Athens, Greece). She has been involved in international projects, such as The European Cooperation in Science and Technology COST action 16119: *In vitro* 3-D total cell guidance and fitness, where she is a substitute member of management committee.

She was also involved in other scientific related topics, such as scientific writing, communication and promotion of science, and protection of intellectual property with a patent. She is regularly involved in activities promoting the institute and presentations of scientific work to children and the public.